Application of the polar loop technique to UHF SSB transmitters

Smith, C. N.

Award date:
1986

Awarding institution:
University of Bath

APPLICATION OF THE POLAR LOOP TECHNIQUE TO UHF SSB TRANSMITTERS

submitted by C.N. Smith

for the degree of Ph.D.

of the University of Bath

1986

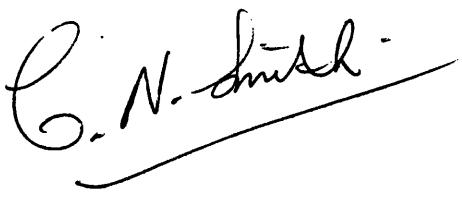

ProQuest LLC
789 East Eisenhower Parkway
P.O. Box 1346
Ann Arbor, MI 48106-1346

CONTENTS

ACKNOWLEDGEMENTS

The author gratefully acknowledges the support of the University of Bath which funded this research.

Particular thanks are due to the following:-

Mr. V. Petrovic of the School of Electrical Engineering, University of Bath, who supervised the work and provided considerable help, guidance and encouragement throughout.

Mr. E. Kaya, fellow postgraduate at the University of Bath, who provided the computer simulation results presented in this thesis.

Mrs. Hazel Gott, who skilfully typed the script.

SUMMARY

Conventional single sideband (SSB) radio transmitters suffer from two major drawbacks, these being: low efficiency, which results in the wasteful use of primary power, and poor linearity, which gives rise to the generation of spurious outputs in adjacent channels. The latter effect is normally considered to be the most serious, and consequently the RF amplifiers used are usually biassed at high quiescent current for best linearity, but at the expense of efficiency.

A novel solution to these problems is known as the Polar Loop Technique. In this arrangement, an SSB transmitter may utilise highly efficient but non-linear RF amplifiers, yet still achieve excellent linearity by the application of large amounts of negative feedback. The feedback is applied by resolving the input and output RF signals into polar coordinate form, that is, signals proportional to instantaneous amplitude and phase. Since these are baseband signals, they have bandwidths very much less than that of the RF circuits. This means that a large amount of feedback can be applied to them without encountering the stability problems which beset direct RF feedback.

This thesis is concerned with the application of the Polar Loop principle to the ultra high frequency (UHF) land mobile radio bands at 450 and 950MHz. The early chapters cover theoretical aspects of the technique both in general, and with particular reference to UHF operation. The levels of spurious outputs and noise sidebands are quantified, and

the effect on these levels of the feedback loops, and of non-ideal behaviour in the system, are examined.

The main body of the work encompasses the design, implementation and evaluation of practical UHF polar loop transmitters. It is shown that in practice, the main performance limitation is in the polar resolving process.

The final chapter is concluded with a suggestion for using cartesian rather than polar coordinate resolving, in order to overcome the drawbacks of the latter.

CHAPTER ONE

SINGLE SIDEBAND MODULATION

1.1 INTRODUCTION

Throughout the developed world, land mobile radio is one of the fastest growing areas of the telecommunications industry. In the 1970s, the annual growth rate has consistently been between 10 and 15% (1, 2), and shows no signs of abating. To accommodate this growth, more spectrum must be made available, and more efficient use must be made of the existing allocation.

In the past, improved spectrum utilisation has been obtained by successive halving of the channel spacings, from its original value of 200KHz, down to the present day spacings of 12.5KHz in the 80 and 170MHz VHF bands, and 25KHz in the 450 and 950MHz UHF bands. The mode of modulation has remained the same, being AM or FM at VHF and FM only at UHF. More recently, cellular radio schemes have been introduced, such as that in Chicago (3). These exploit the fact that the same channel may be 're-used' many times simultaneously, by separating the users spatially with a cell structure. When a mobile user traverses from one cell to another, his message is automatically re-routed through a different channel. Although such schemes can clearly make a valuable contribution to relieving spectrum congestion in the mobile radio service, this can only be temporary. A recent prediction has indicated that despite using cellular schemes, the present spectrum allocation will reach saturation by the

end of the century (4).

It is believed that more spectrum may be allocated to mobile radio with the demise of VHF 405 line TV in Band III. If this does prove to be the case, then the vast amount of extra spectrum (40MHz) available, would dramatically ease the problem in the short term. In the longer term however, improved efficiency must be sought, which inevitably means a further reduction in channel spacing.

The most spectrally efficient mode of modulation is Single Sideband (SSB), invented by J.R. Carson of the Bell Telephone Laboratories, in 1915 (5). In conventional AM or FM double sideband systems, there is considerable redundancy, since both sidebands convey the same information and the carrier component conveys no information at all. An SSB signal, however, comprises just one sideband, suppressing the other sideband and the carrier. For speech communication, the transmitted signal need only be 3KHz wide, making channelling at 5KHz entirely feasible. Since the 1930s, this system has been used almost exclusively for long range communication in the HF band, but not at higher frequencies. If SSB was implemented in the mobile radio bands, there would be an immediate increase in the number of channels by a factor of 2.5 at VHF and 5 at UHF. So far, this opportunity has not been taken up. To explain why this should be, the following Section examines some of the problems which are encountered in implementing an SSB mobile radio system at VHF and UHF frequencies.

1.2 SINGLE SIDEBAND MODULATION FOR VHF AND UHF MOBILE RADIO COMMUNICATION

The use of Single Sideband (SSB) in the VHF and UHF frequency bands has for many years been recognised by radio amateurs as a viable and extremely attractive alternative to double sideband systems such as AM or FM (6). Its benefits, such as greater range for a given power, improved signal to noise ratio, and better spectrum utilisation, have led to the widespread adoption of SSB by amateur radio enthusiasts, at frequencies as high as 1.3GHz.

In the professional land mobile radio service however, the situation is rather different, with only limited use made of SSB in the United States, and none at all in the UK. The reluctance to move to this spectrally more efficient mode has in the past been due largely to the problems associated with implementing SSB in a mobile situation at VHF and above. The factors which are continually cited as the main problem areas are:-

(i) Local oscillator frequency stability.

(ii) Doppler shift.

(iii) Rapid multipath fading.

(iv) Lack of capture effect compared with FM (impact on re-use distance).

(v) Sensitivity to ignition interference.

(vi) Circuit complexity (practicability of hand portables).

(vii) Transmitter limitations.

Considering each of these aspects in turn, a differential frequency error between the transmit and receive local oscillators in an SSB system, will result in a corresponding frequency shift of the recovered baseband spectrum. For a speech signal, this error should be kept below 20Hz if the intelligibility is not to be impaired (7). At VHF, such stability is difficult to achieve, representing 0.2ppm at 100MHz for example. Most temperature compensated crystal oscillators are little better than 1ppm over the commercial temperature range. Associated with this problem is doppler shift, when either or both ends of the link is made mobile. At a vehicle speed of 100Km/hr, a signal at 450MHz would be doppler shifted by 45Hz, and at 950MHz by 95Hz. Fortunately, both of these difficulties can be overcome by transmitting a reference, or pilot, component with the sideband, and using this at the receiver for AFC or phase locking. Three variations of this technique have been proposed, and each has been proven to work well in practice: Pilot carrier, by Philips Research (8), Pilot tone in-band, by Bath University (9) and Pilot tone above band, by Stanford University (10). The principle involved is that any frequency shift will effect both sideband and pilot equally, thus when the pilot is used to synchronise the demodulation, the recovered baseband will have zero net frequency shift.

The third major problem is multipath fading. In an urban, mobile environment, multipath propagation leads to rapid fluctuation in the received signal strength, as the moving receiver encounters the peaks and nulls of the field

pattern. The fading rate can be quite high, up to 90Hz at 450MHz and 190Hz at 950MHz, for a vehicle travelling at 100Km/hr (11). Although vehicle speeds are seldom this high in an urban setting, the fading is non-sinusoidal, and so contains spectral components above the fading rate. It has been shown, however, that this effect can be rendered largely unobtrusive by a combination of fast acting feedback and feedforward AGC (12). This is in contrast to FM systems which suffer from the subjectively disturbing effect of noise bursts during fades, due to their capture effect. In practice, it has been demonstrated that the presence of multipath fading renders an FM system no better than an SSB system in terms of its frequency re-use distance (13).

The susceptibility of an SSB receiver to ignition interference has in the past been shown to be worse than for an FM receiver, especially at low signal levels (14, 15). However, more recent trials have shown just the opposite (16). It is believed that this is due to the fact that the later equipment derived its AGC solely from the pilot carrier. The AGC therefore received very little energy from the ignition impulses.

The circuit complexity of an SSB equipment is undoubtedly greater than its AM or FM counterpart. It has nevertheless been proved possible to produce practical VHF hand portable SSB tranceivers incorporating all of the features described, although with a cost penalty (17). One of the main increases in complexity was due to the transmitter, with its multiplicity of frequency conversions. A simpler transmitter architecture would obviously help here.

The final aspect to be considered is the performance of conventional SSB transmitters. In comparative tests on the adjacent channel performance of VHF SSB, AM and FM radios, Flett (18) reported that the dominant cause of interference was the adjacent channel radiation of the transmitters.

In summary, all of the receiver or system problems associated with using SSB for mobile radio at VHF and above, would appear to have been solved, or are soluble. It remains to examine in detail the transmitter limitations and these are covered in Section 1.3.

1.3 LIMITATIONS OF CONVENTIONAL SSB RADIO TRANSMITTERS

For a mobile or handportable radio application, equipments should be compact and rugged, and should be efficient in their consumption of primary power. The first two requirements make the use of solid-state electronics mandatory, whilst the third implies that the transmitters output amplifier, which is inevitably the largest consumer of power, should be as efficient as possible in its conversion of d.c. to RF energy.

Conventional RF power amplifiers intended for the transmission of amplitude modulated signals, such as SSB, suffer from two major drawbacks: poor linearity and low efficiency, where the latter is usually the result of attempting to improve the former. In a speech communications system, amplifier distortion will have an adverse effect on

speech quality and, far more seriously, will cause interference to users of adjacent channels. Consider the general expression for the non-linear transfer function of an amplifier:-

$$V_{out} = k_1V_{in} + k_2V_{in}^2 + k_3V_{in}^3 + k_4V_{in}^4 + \ldots k_nV_{in}^n \quad (1.1)$$

where: V_{in}, V_{out} are input and output voltages,
k_{1-n} are constants.

If the input signal consists of two equal tones at frequencies f_1 and f_2, the effect of the transfer function given by equation 1.1 is to produce additional components at the output. It can be shown (18) that the even order terms produce components at multiples of f_1 and f_2, which are easily removed by filtering. The odd order terms however, produce components of the form $(af_1 - bf_2)$ which fall close to the wanted output and cannot easily be filtered out. Figure 1.1 shows the typical spectrum of the intermodulation distortion.

Designers of practical amplifiers try to minimise the level of intermodulation products by operating the active devices with a bias current (class A or AB) such that the operating point is moved to a more linear region of the transfer characteristic. Unfortunately, this also reduces the efficiency. The level of third order intermodulation products for a class AB solid state amplifier is usually in the range -20 to -30dB below the wanted output (20, 21), and the corresponding efficiencies are typically 15 to 30%. The distortion level can be improved by operating the amplifier

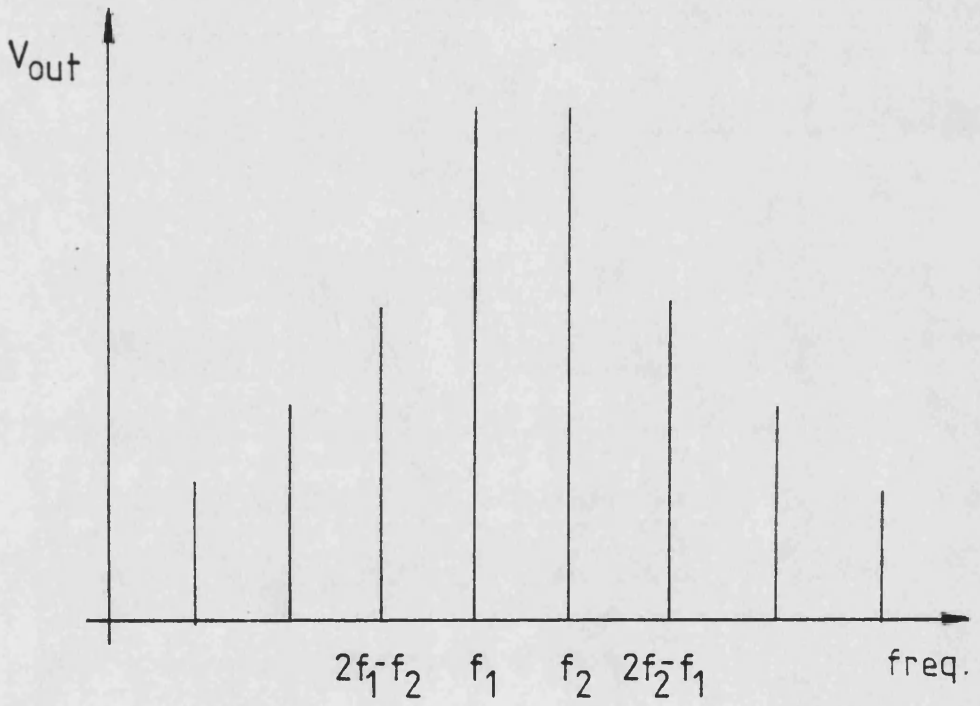

Figure 1.1 : Intermodulation Distortion Spectrum produced by a Non-linear Amplifier

at reduced power (back-off), but the efficiency would be degraded still further.

If a class C amplifier is used, in order to achieve the best efficiency, the intermodulation distortion becomes much worse. When operated with a peak envelope power of 80% of its saturated level, a typical solid state class C amplifier will produce third order products at -12dB relative to the tone level (22). Reducing the power improves this to a minimum of -18dB at 50%, below which the distortion worsens again.

A second form of distortion which afflicts RF power amplifiers is phase distortion due to AM to PM conversion. This occurs as a result of changes in the amplifier capacitance with signal amplitude. In a bipolar transistor amplifier, the main contribution is from the collector-base junction, which is reverse biassed and thus acts as a varactor diode. Depending on the Q-factor of the associated tuned circuit, the capacitance change will cause a phase displacement of the signal in sympathy with the amplitude modulation. To quantify this effect, consider the expression derived in Appendix A for the approximate level of phase shift in a tuned circuit as a function of capacitance:-

$$\frac{d\phi}{dC} = \frac{-\pi Q}{4C} \text{ rad/F} \qquad (1.2)$$

where ϕ = phase shift (r)

C = total capacitance (F)

Q = loaded Q-factor.

Taking an example of a typical UHF amplifier stage:

Let $Q = 5$

$C = 10pF$

$$\therefore \frac{d\phi}{dC} = 3 \cdot 9.10^{11} \text{ rad/F}$$

$$= 22^{o}/pF.$$

Thus, if the capacitance changed by only 10% (i.e. 1pF) as a result of envelope modulation of the signal, the peak phase deviation would be $\pm 11^{o}$. Making the narrowband approximation that a phase modulated signal has only one significant pair of sidebands for small deviations, this phase shift corresponds to sidebands at -20dB relative to the wanted output. Clearly then, the effect of AM to PM conversion can be as great, or greater, than the effect of amplitude non-linearity.

At present there is no formal commitment to the introduction of SSB into the Land Mobile Radio Service. Consequently there are no specifications laid down for SSB equipments, in terms of adjacent channel protection. However, the CCIR has made a recommendation that for any transmission up to 10W PEP, in the frequency range 30-960MHz, all spurious emissions should be at least 55dB below the wanted output (23). Likewise, the Department of Trade and Industry in the UK, sets the limit of spurious radiation at -55dB for amplitude or angle modulated signals for the Private Mobile Radio Service (24, 25). Since there is no reason to suppose that SSB would be treated any more leniently if adopted, the above value should be treated as a target specification. This requirement

would clearly preclude the use of conventional RF 'linear' amplifiers. A means must be found therefore of substantially improving the linearity of RF amplifiers, preferably to the extent that efficient class C amplifiers may be used, and at frequencies up to UHF. The following Chapter addresses this problem.

CHAPTER TWO

TECHNIQUES FOR IMPROVING RF AMPLIFIERS

2.1 INTRODUCTION

Techniques for improving the linearity of RF amplifiers fall into three main categories:-

(i) Predistortion.

This involves inserting a compensating non-linearity into the signal path, ahead of the amplifier to be linearised. The signal is thus 'predistorted' before being applied to the amplifier.

(ii) Feedforward.

In this technique an error, or distortion, signal is derived by comparing input and output, which is then separately amplified before being added in antiphase to the main amplifier output.

(iii) Feedback.

Like feedforward, an error signal is obtained, but in this case it is fed back to the input, to be amplified by the main (distorting) amplifier.

2.2 PREDISTORTION

Predistortion linearisation takes the form shown in Figure 2.1.

The signal to be amplified is first passed through a network (the lineariser), which has a transfer function that

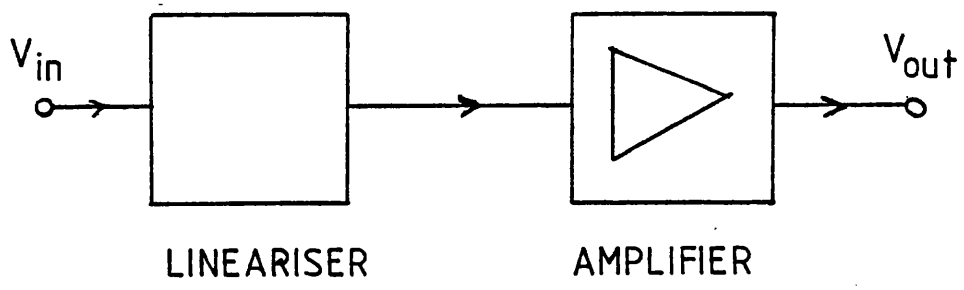

Figure 2.1 : Predistortion Linearisation

is non-linear by an amount exactly equal and opposite to that of the amplifier. The resulting predistorted signal forms the input to the amplifier. In the ideal case, the distortion introduced by the amplifier will then exactly compensate for the predistortion, giving a distortionless output. This is illustrated in Figure 2.2.

Such an approach has been used on an HF SSB transmitter by Rockwell (26). In this particular case, the amplifier to be linearised was a two-stage tuned valve amplifier operating at 7MHz with a peak envelope power of 35W. The lineariser consisted of a network of resistors and diodes, chosen largely by trial and error to give the maximum reduction in intermodulation distortion. The network finally used by Rockwell which gives a characteristic similar to that in Figure 2.2 is shown in Figure 2.3.

In operation, this circuit gave an improvement in intermodulation distortion of at least 15dB at either maximum power, or low power (-10dB), but not both. This is due presumably to changes in the amplifier characteristic with power level.

Another limitation of this technique is the fact that the amplifier will have a certain amplitude and phase response across the frequency band of interest. Since the lineariser is broadband, the accuracy of the distortion compensation is compromised. A possible solution to this, is to pass the signal through an equaliser in addition to the lineariser. This would ideally have an amplitude and phase response which is the complement of that of the amplifier,

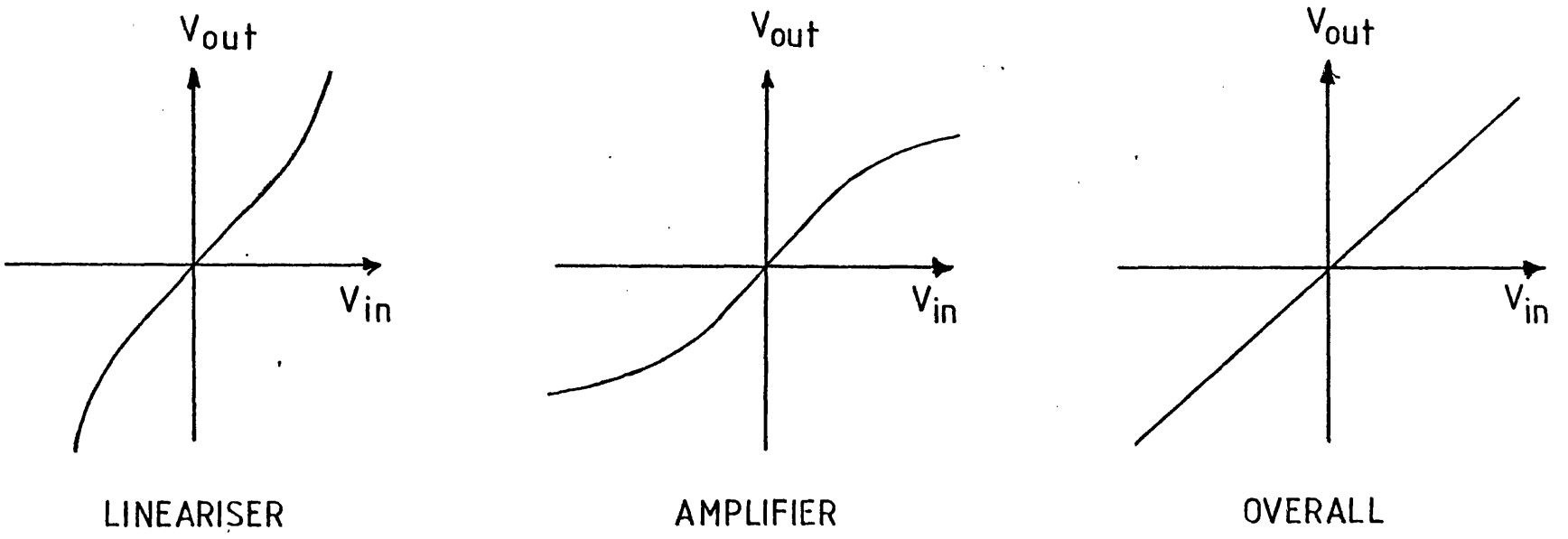

Figure 2.2 : Effect of the Predistortion Lineariser on the Transfer Characteristic

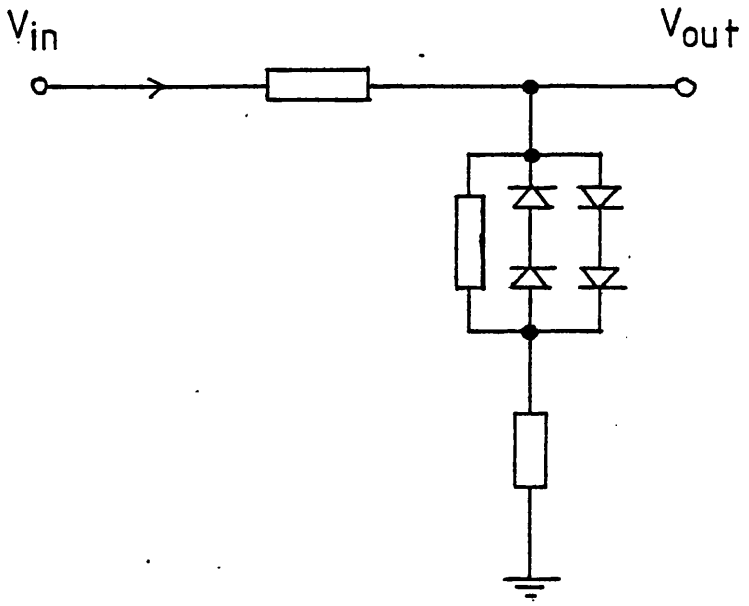

Figure 2.3 : Practical Predistortion Network

giving an overall flat response.

Kurokawa *et al* (27) has implemented the linearization/ equalisation technique at microwave frequencies. In this application, travelling wave tube and klystron amplifiers are used in high power (many hundreds of watts) satellite communications systems, carrying frequency division multiplex signals. Without linearisation, the only means of intermodulation interference reduction is to operate the amplifier with considerable back-off, typically 7dB. For 200W PEP output power, this requires an amplifier rated at 1Kw, which is hardly economic. Using a lineariser (in this case an FET amplifier), and an equaliser, the intermodulation distortion is reduced by 7-10dB across a 500MHz bandwidth at 6.2GHz. The amount of back-off can therefore be reduced, for the same, or slightly better intermodulation performance.

Many other authors have reported the successful use of predistortion (28, 29, 30, 31, 32, 33), but in each case the improvement obtained was similar to the above example.

These examples of predistortion show that the improvements obtained are quite small, and reduce with increasing frequency. The efficacy of the technique is critically dependent on the compensating networks exactly balancing the non-linear transfer function, and the frequency variant characteristics of the amplifier.

In an application such as mobile radio, where an equipment may be subjected to extremes in environmental conditions, such as temperature, humidity, vibration, etc., it seems logical to assume that the RF amplifiers' characteristics

will change considerably in use. If so, the usefulness of predistortion is reduced further.

2.3 PREDISTORTION COMPENSATION OF AM TO PM CONVERSION

It was mentioned in Section 1.3 that AM to PM conversion is one of the main causes of distortion in RF amplifiers used for amplitude modulated signals, such as SSB.

One method of reducing incidental phase modulation, which falls into the predistortion category, is pre-phase modulation. Such a technique, applied to radio transmitters, has been described by Behrend (34). In this case (of an AM transmitter), the audio signal is applied to a phase modulator in the RF carrier signal path, preceding the amplitude modulator, as shown in Figure 2.4.

The audio signal processing is necessary to compensate for the fact that the phase distortion generated by the amplitude modulator and power amplifier, is a non-linear function of signal amplitude.

Behrend reports that this phase correction is effective, although he gives no quantitative results.

In common with any form of predistortion, pre-phase modulation is a purely open-loop technique. It can therefore take no account of changes in amplifier characteristics.

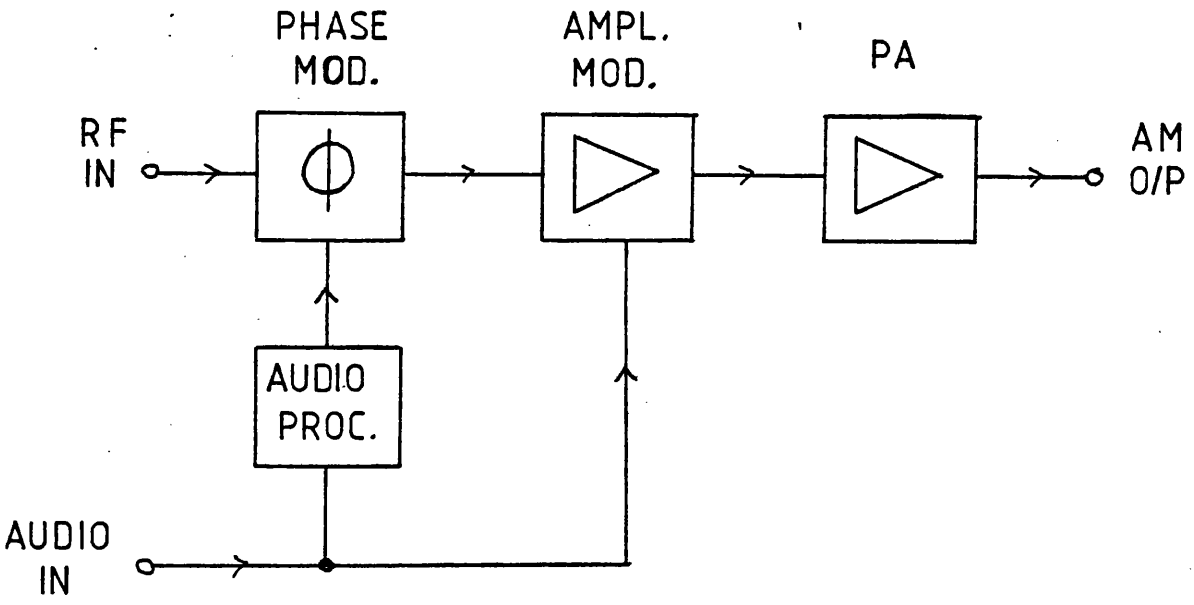

Figure 2.4 : Pre-phase Modulation

2.4 FEEDFORWARD

The principle of feedforward was invented in 1925 by H.S. Black of the Bell Telephone Laboratories, who was granted a patent for the technique in 1928 (35).

Black's specific aim was to increase the load carrying capacity of carrier telephone repeater amplifiers, by allowing them to operate closer to the saturation point, with reduced distortion. To accomplish this, the configuration of Figure 2.5 was used.

The input signal, as well as being applied to the main, distorting amplifier, is also passed through a phase shifting network. This ideally has the same phase response as the amplifier, and for a broadband amplifier, a simple time delay may suffice. A sample of the amplifier output is then subtracted from the delayed input, leaving the distortion or error signal. Feedforward correction can then be implemented by amplifying this error term in a separate amplifier and adding the result to the main amplifier output. If the second phase shifter in Figure 2.5 exactly compensates for the delay in the auxiliary amplifier, and the levels are suitably matched, the distortion will be perfectly cancelled at the overall output.

There has been little use made of the feedforward technique since 1925. The most significant revival of this system was made by Seidel and co-workers, in 1968 (36). Here, the main objectives were to improve the gain flatness, phase linearity and noise figures, of two broadband amplifiers operating in the bands 60-90MHz and 25-35MHz. However, in a

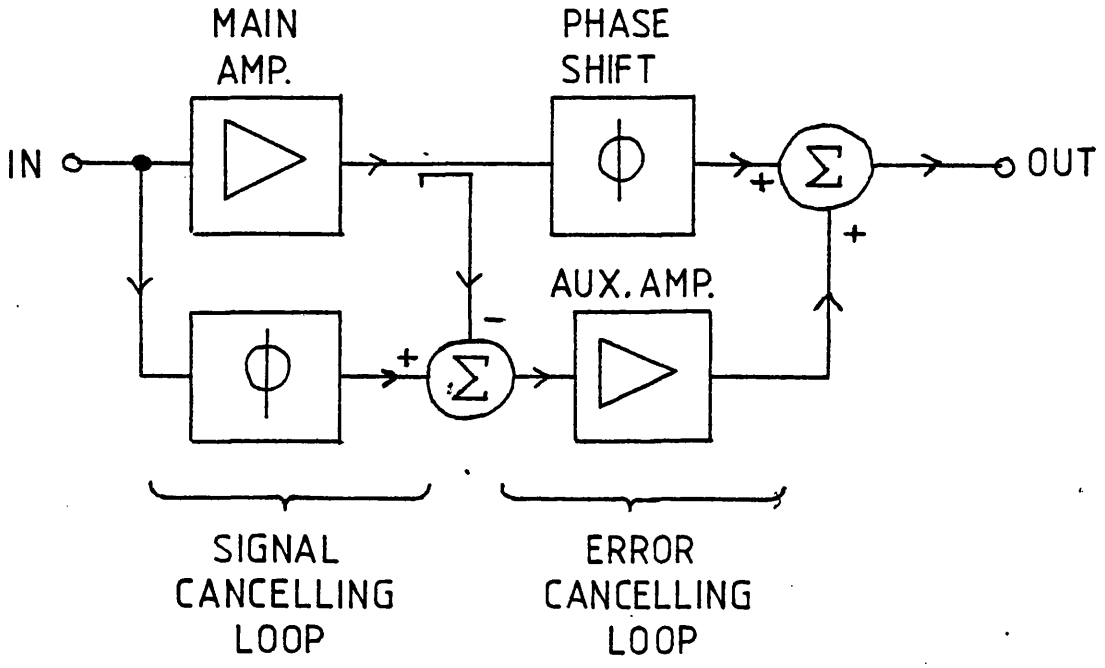

Figure 2.5 : Feedforward

later paper, also by Seidel (37), feedforward was applied to a coaxial repeater amplifier covering the range 0.5-20MHz. In this case the aim was to improve the intermodulation performance, and impressive results were obtained, with reduction of third order intermodulation by at least 35dB across the band. Such results should not be taken to be typical of the feedforward technique, however, since the particular amplifiers used were very low power (12.5dBm), and had excellent gain stability (to 0.001dB) versus time and frequency. Similar results have been obtained by Meyer *et al* (38), again on a repeater amplifier, but over a wider bandwidth (30-300MHz).

In a higher power application, perhaps more relevant to mobile radio, Bennet (20), has reported the results of applying feedforward to a commercial, 30W, HF amplifier. The improvements obtained here are less encouraging, with reduction of third order intermodulation distortion between 5 and 15dB across the band. It is interesting to note that when the main and auxiliary amplifiers were connected in parallel, with each operating at half power, (they were both of the same type), the improvement in intermodulation was little worse than when using the feedforward configuration.

The main reason for this poor performance, and indeed, the main limitation of the feedforward technique, is that the amplifiers must have a gain flatness of a fraction of a dB over the band. In addition, the phase shifting networks must closely match the amplifier phase shift to within a degree or so. Bennet has quantified these matching require-

ments for both the signal cancelling and error cancelling loops. For the signal cancelling loop, the balancing determines the relative power handled by the auxiliary amplifier. If, for example, the gain of the main amplifier varies by 2dB, and the phase by $\pm 10^{o}$, across the band, the auxiliary amplifier will have to handle a power level only 12dB below that of the main amplifier, not counting the fact that it must also handle the distortion components. In the case of the error cancelling loop, for a 1dB gain, and 10^{o} phase variation in the auxiliary amplifier, the distortion reduction would be 14dB. To improve this to 30dB requires the balancing to be accurate to within 0.3dB and 1 degree. However, even if such stringent requirements could be met, the overall distortion performance can never be better than that of the auxiliary amplifier, which as a result, would have to operate in class A to achieve acceptable linearity. The improvements gained by the use of feedforward, are therefore inevitably at the expense of efficiency.

To compound the already difficult problem of obtaining the required rigid amplifier specification, these parameters must be maintained as the system ages, and is subjected to varying environments. A means of alleviating this difficulty has been described by Lubell (22), which uses an adaptive error control system. No precise details are given, but the principle involved is to utilise feedback loops to automatically adjust the amplitude and phase of the signals at the two cancellation points in the feedforward system.

Applying this technique to a class C transistor amplifier operating at L-band (power level unspecified), Lubell reports an improvement in intermodulation distortion from -15dB to -30dB.

2.5 FEEDBACK

Following his work on feedforward, Black invented the principle of negative feedback in 1928, and was granted a patent in 1937 (39). In 1934, Black published his well known paper on 'Stabilised Feedback Amplifiers' (40), which gives a more useful summary of the technique, in comparison with the voluminous patent publication. Independently of Black, Posthumus of the Philips Company, was granted a UK patent on the feedback principle in 1930 (41).

A block diagram of the feedback technique applied to an amplifier is shown in Figure 2.6. By taking a sample, β, of the output signal and feeding this back to the input in antiphase, a reduction in gain is obtained:

$$A_c = \frac{A_o}{1 + \beta A_o} \qquad (2.1)$$

where: A_c = closed loop gain

A_o = open loop gain

β = feedback factor

Therefore:

$$A_c \rightarrow \frac{1}{\beta}, \text{ if } A_o \text{ is large} \qquad (2.2)$$

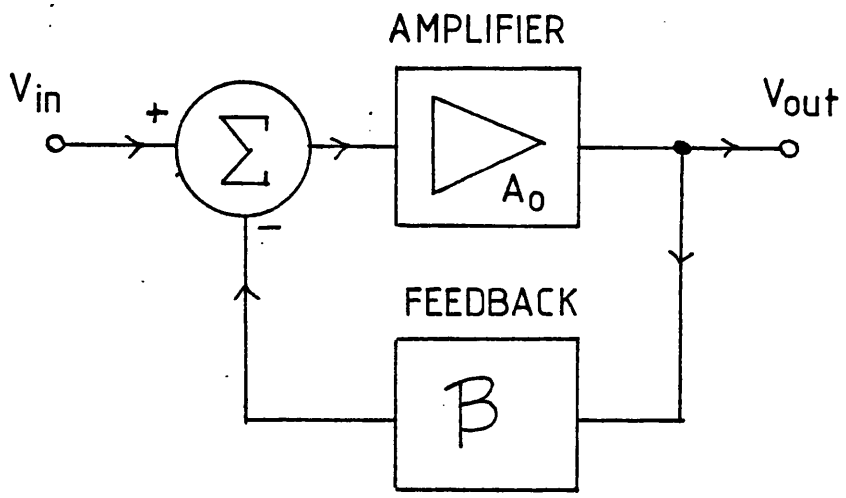

Figure 2.6 : Feedback

Providing the loop gain, $A_o\beta$, is large, the closed loop gain becomes virtually independent of the amplifier, and is defined by passive components (in the network β). It is well known that distortion generated by the amplifier is also reduced by the feedback factor, $(1 + \beta A_o)$.

The maximum distortion reduction which can be obtained is defined by the maximum amount of feedback which may be applied consistent with stable operation. To maintain stability, the criterion set out by Black and Nyquist (42) must be met. This states that for loop gains greater than unity, the total loop phase shift should not exceed 180^o. Although this criterion can easily be met for audio frequency amplifiers, where many tens of dB of feedback can be applied, the same cannot be said of RF amplifiers, particularly multi-stage ones. To illustrate this point, consider the example of overall feedback applied to a cascade of three identical amplifier stages, each having a single pole frequency response. Appendix B shows that for a phase margin of stability of 40^o, only 10dB of feedback may be applied.

A few reports have appeared in the literature of feedback applied to multistage amplifiers (43, 44, 45), and these confirm the low levels of feedback which are possible (10 to 15dB). To increase the amount of feedback permissible, requires that the overall amplifier has a dominant pole, that is, one stage has a bandwidth much less than the others. This approach has been used by Leypold *et al* (46), in a novel arrangement, where the feedback is applied at IF. Despite using this technique however, only 15 to 20dB of feedback was achievable.

At UHF, the problems of applying feedback to an RF amplifier would clearly become even more severe. Not only is there the phase shift in the tuned matching networks to contend with, but also the physical length of the feedback loop becomes significant. At 450MHz, for example, a 90^{o} phase shift corresponds to a distance of under 17cm.

2.6 MODULATION FEEDBACK

For any radio frequency signal, it is the modulation of that signal which conveys the useful information. When such a signal is amplified, so long as the modulation, whether it is amplitude or angle, or a combination of both, is faithfully preserved, then the amplification is linear. Although the amplifier may produce harmonic distortion, that is, introduce components at or near harmonics of the carrier frequency, this presents little problem, as the harmonics can easily be filtered out. Such a filter often forms a constituent part of the amplifier in the form of tuned circuits.

This fact is exploited in the modulation feedback approach to linearising RF amplifiers. Both the amplitude and phase modulation of an RF signal can be represented by baseband signals, which may comprise audio frequency signals only. It is therefore relatively easy to apply very large amounts of negative feedback to these signals, in the same way that feedback is used to linearise high quality audio amplifiers. In principle then, the modulation, and hence

RF amplification can be made extremely linear.

The principle of amplitude or envelope feedback was invented by J.C. Schelleng of the Western Electric Co. in 1923, and a patent was granted in 1925 (47), pre-dating the inventions of both Black and Posthumus. His invention was applied to an AM radio transmitter taking the form of Figure 2.7.

A high power oscillator was amplitude modulated using the well-known Heising technique (48) in which the DC supply to the final stage is modulated. Ingeniously, the modulating amplifier also functioned as a rectifier for the A.C. mains supply. Unfortunately, without using excessively large smoothing components at the rectifier output, there was an unacceptably large residual ripple, at twice the mains frequency, superimposed on the wanted audio signal. Schelleng's primary objective was to reduce this ripple. This he accomplished by envelope detecting the output signal, and feeding back the recovered audio in phase opposition to the audio input signal.

Although the patent does not use the term 'feedback', the above system is nevertheless a negative envelope feedback system, and as such reduces amplitude non-linearity in both the modulator and power oscillator.

The first commercial application of this technique was in 1936 by Poppele *et al* (49), who described a 50KW medium wave broadcast transmitter. In this case, the Heising (anode) modulator operated at a relatively low power level, and was followed by a high power RF amplifier. A diode

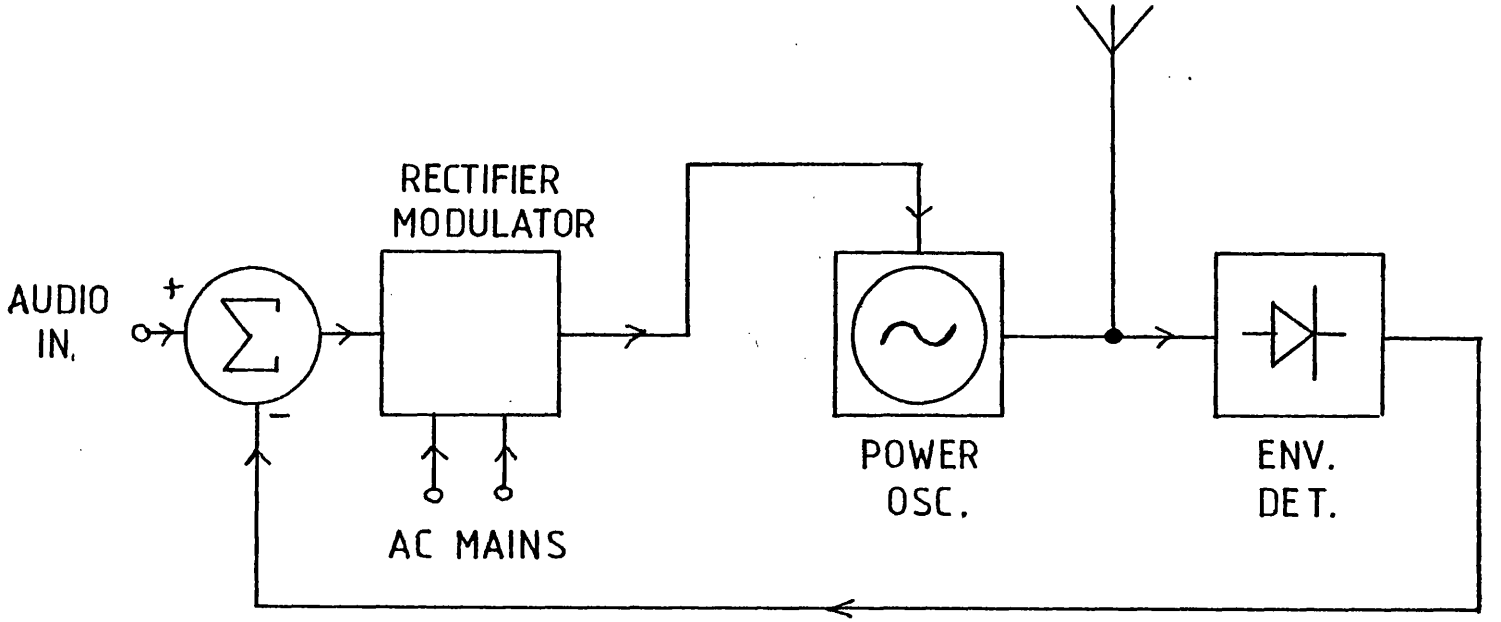

Figure 2.7 : Schellengs AM Transmitter Employing Envelope Feedback

detector was used to provide the audio feedback signal, as in the case of Schelleng's transmitter. Using this system, Poppele reported envelope distortion levels of typically 1% or -40dB.

The disadvantage of using envelope feedback in the configuration of Figure 2.7, is that it can only be applied to AM transmitters, since the input is an audio signal. For utilisation with linear amplifiers, a form of balanced feedback, first proposed by Terman (49) is necessary. This is shown in Figure 2.8.

Here, both input and output envelopes are detected and compared. The resulting error is amplified, and used to vary the amplifier gain, so as to correct any amplitude error between input and output. It is only this error which is reduced by the degenerative feedback action, the nominal amplifier gain is unchanged.

An important advantage of balanced envelope feedback, is that linearity of the envelope detectors is not important, so long as the two are identical. Distortion components appearing identically on each side of the comparator will obviously cancel out, and therefore have no effect on the system.

Bruene (43) has reported this form of feedback applied to HF, valve SSB transmitters. He obtained reduction of 3rd order intermodulation distortion from -15dB to -40dB on a two-tone test, but only for relatively narrow tone spacings of a few hundred Hz. The amplifiers used by Bruene contained many high-Q tuned circuits, and the delay thus introduced

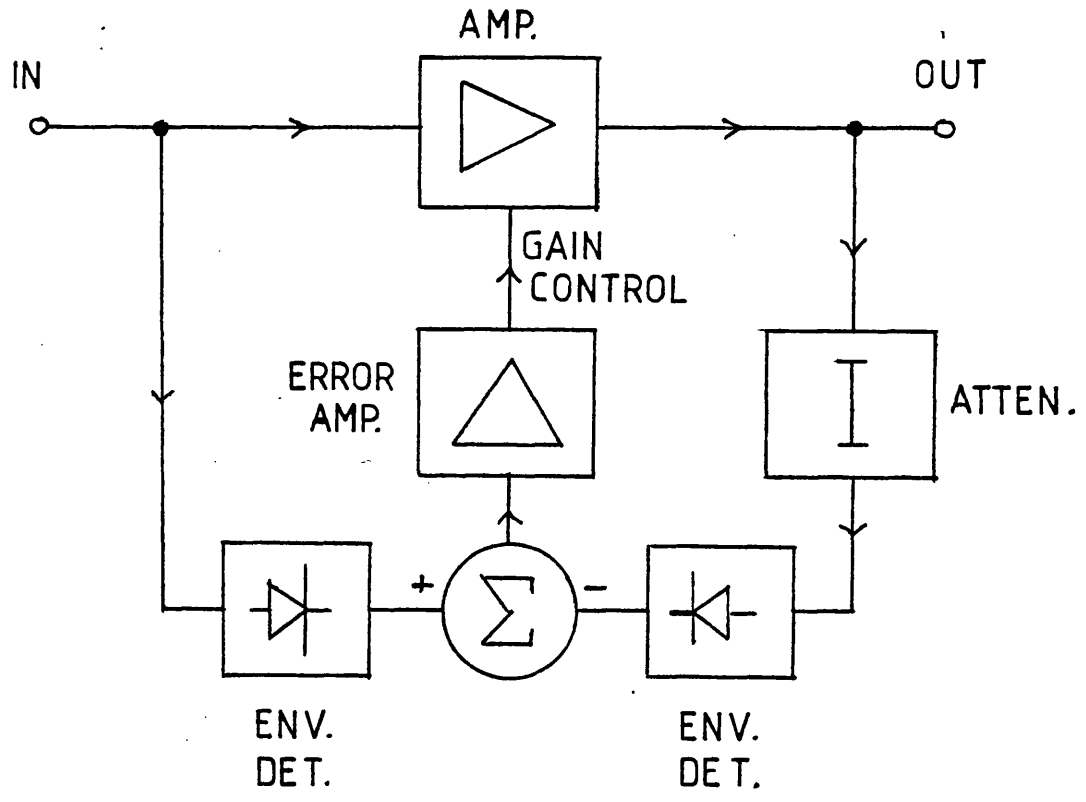

Figure 2.8 : Balanced Envelope Feedback

restricted the maximum stable loop bandwidth. This explains the poorer performance at wider tone spacing, or for higher order distortion products.

Solid-state RF amplifiers, by contrast, are usually either broadband, or, if tuned, have very low Q matching networks. An envelope feedback loop applied to such an amplifier, can therefore have a very much wider bandwidth. A wide band envelope feedback system has been described by Arthanayake and Wood (51). In this case, a class B transistor amplifier operating at 400MHz and 17W PEP was used. The authors report effective envelope linearisation for a two-tone test signal of 200KHz spacing. They also note that the main limitation of the technique is the linearity of the feedback circuit. With reference to the block diagram of Figure 2.8, it can be seen that the input envelope detector is outside the feedback loop. Therefore, to ensure feedback circuit linearity, the detectors must either be linear (in which case they are inherently matched), or, they can be non-linear, but identical, as mentioned previously.

It has been shown that with certain provisos, envelope feedback can provide a substantial reduction of amplitude non-linearity in RF amplifiers. In spite of this, such a feedback system is often insufficient to achieve adequate spectral purity at the amplifier output. This is due to AM to PM conversion. Solid-state amplifiers are particularly prone to this form of distortion. For example, Warren (52), has shown that for a typical HF solid-state amplifier, the output spectrum is little improved by the application of

envelope feedback. This does not imply that the amplitude distortion is negligible, but merely that the phase distortion is highly significant.

The use of phase modulation feedback applied to RF amplifiers, has received scant attention in the literature. To the author's knowledge, the first proposal of such a technique was made by Bradshaw of the Marconi Co., in his patent of 1971 (53). This system was applied to an HF linear amplifier simultaneously with balanced envelope feedback, and involved placing a voltage controlled phase shifter at the amplifier input. By comparing the phases of the input and output signals in a phase sensitive detector, the resultant voltage proportional to phase error, was amplified, and used to control the phase shifter. A block diagram (omitting the envelope feedback components) is shown in Figure 2.9.

Bradshaw does not give precise details as to the nature of the phase detector, but notes that it must contain whatever circuitry is necessary to compare the phases independently of signal amplitudes. The delay τ, is required to balance the time delay through the amplifier, so that the feedback loop always operates within its finite compensation range.

When applied to an HF (1-30MHz) amplifier, this technique presents the difficulty of designing a phase shifter to operate over many octaves of bandwidth. In addition, its phase shift coefficient, in terms of radians per volt, must remain approximately constant over the band, to avoid large changes in loop bandwidth. At higher frequencies, in the

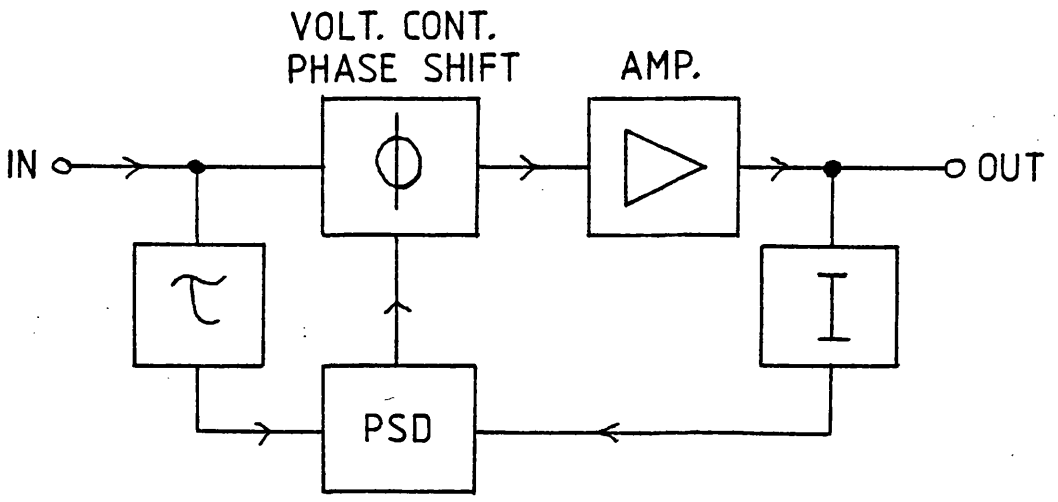

Figure 2.9 : Phase Modulation Feedback

VHF and UHF bands, the fractional bandwidths to be covered, are very much smaller (typically 1% or less), easing this problem. However, the static phase shift must still be balanced by a time delay. Any change in the electrical path length of the loop would require a readjustment of the delay. Although the balancing does not need to be exact, due to the negative feedback action which ensures the static phase error is always practically zero, a static offset in the phase shifter encroaches on its already limited range.

A novel solution to all of these problems is to use a phase-locked loop to provide the phase feedback. This was first proposed by Raab (54), although on a purely speculative basis. The first practical system to use a phase-locked loop in this way, is the Polar-loop technique, invented by Petrovic and Gosling (55). As well as providing reduction of phase distortion, this system goes one stage further, in that the phase-locked loop is utilised to provide frequency translation. A full description of the polar-loop technique is given in Chapter 3.

2.7 ENVELOPE ELIMINATION AND RESTORATION (EER)

The principle of envelope elimination and restoration (EER) was proposed in 1952 by L.R. Kahn (56), and is shown in the block diagram of Figure 2.10. Although an open-loop technique, it shares a degree of commonality with modulation feedback, in that it treats the amplitude and phase modulation of the input signal separately.

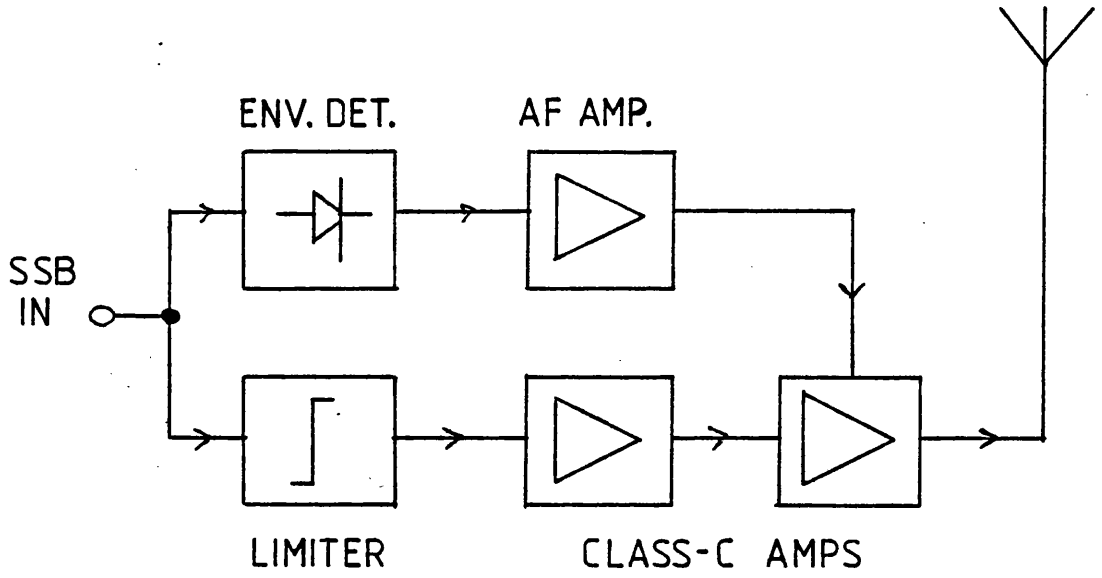

Figure 2.10 : Envelope Elimination and Restoration Transmitter

Referring to the diagram, the SSB input signal is resolved into polar coordinate form by being passed simultaneously through an envelope detector and a limiter. The envelope detector produces a baseband signal proportional to the instantaneous amplitude of the input, while the limiter produces a constant amplitude signal containing only the phase information. This limited, phase modulated signal is then amplified to any desired level in highly efficient class C amplifiers. To restore the envelope information, the final stage is high-level amplitude modulated by the amplified envelope signal. Ideally, the resulting output is a perfectly reconstructed SSB signal at high power level.

Since all the RF amplifiers operate in class C, and the audio amplifier/modulator operates in class B, the overall efficiency can be very high. In his later paper (57) Kahn shows that in a typical valve implementation of the system at HF, the overall efficiency is 69% compared with 47% for a linear amplifier. More recently, Petrovic (21) has applied the Kahn technique to a solid-state VHF transmitter, and has obtained an efficiency of 40%. This compares favourably with a conventional, VHF, solid-state linear amplifier, which has an efficiency of only 13% under the same conditions.

Unfortunately, the intermodulation performance of the Kahn transmitter is little, if any, better than that of a conventional exciter/linear amplifier arrangement. Petrovic reports 3rd order distortion products 20dB below the tone

level on a two-tone test. This is due almost entirely to imperfections in the high-level amplitude modulator.

Any practical modulator will be non-linear, and will therefore produce envelope distortion. In addition, variations in device capacitance with signal level will generate AM to PM conversion. Another problem associated with the Heising (anode/collector/drain) modulator is its inability to reduce the output envelope completely to zero. Even though the modulating voltage may be at zero, the RF signal at the final stage input will leak through the feedback capacitance of the device. In the case of a bipolar transistor, the collector-base junction becomes forward-biassed in this situation, providing an additional leakage path. The full implications of this defect only become apparent when the nature of the phase modulated signal at the modulator input is considered. If the SSB input signal is two equal tones (a standard test), the phase component is equivalent to a carrier, phase modulated by a square wave. This signal has a very broad spectrum, and so must not be allowed to leak through to the output, if unwanted spurii are to be avoided. Neutralisation can be used to counter the capacitive feedthrough effect, but not the collector-base junction problem.

Apart from the modulator being non-ideal, the polar resolving process will not be perfect. The envelope detector will be non-linear, and the limiter will possess AM to PM conversion, further degrading the reconstructed output.

2.8 CONCLUSION

The foregoing investigation into linearisation techniques has shown that both predistortion and feedforward are capable of relatively small improvements, of the order of 10dB, when applied to RF power amplifiers. They are both open loop techniques which therefore require careful setting up, and will be prone to drift with environmental changes. Feedforward also has the additional disadvantages of high complexity, and poor efficiency due to the requirement for a second amplifier.

Feedback overcomes the problems of open loop systems, but is of limited use in RF amplifiers due to stability aspects. However, when the feedback system is rearranged such that it is applied only to the signal modulation, a much larger amount of feedback is feasible.

To realise maximum benefit from the modulation feedback technique, both envelope and phase feedback must be applied, since practical RF amplifiers distort both these parameters. Since the polar loop technique is the most effective means of implementing simultaneous envelope and phase modulation feedback, this is the most appropriate technique for the linearisation of an SSB transmitter, whilst maintaining good efficiency.

CHAPTER THREE

THE POLAR LOOP TECHNIQUE

3.1 INTRODUCTION

The Polar Loop Technique was evolved from the Kahn principle of resolving the input signal into polar coordinate form, retaining the high efficiency of the EER system, but improving its linearity by the use of modulation feedback. A block diagram of the system is shown in Figure 3.1.

It can be seen that the RF stages of the transmitter are particularly simple, comprising a voltage controlled oscillator (VCO), buffer amplifier, amplitude modulator and class C power amplifier. In practice, the latter two blocks may be combined, resulting in a further simplification. By simultaneously manipulating the control voltages of the VCO and amplitude modulator, an SSB signal may be generated at the output. This is accomplished as follows:

The SSB input signal is generated at intermediate frequency (IF) and at low power level (typically 0dBm), by the conventional filter method:- the audio input signal amplitude modulates a carrier in a double balanced mixer to produce a double sideband, suppressed carrier signal. This is then passed through a crystal filter which suppresses one of the sidebands, leaving the required SSB signal at its output.

A sample of the transmitter output is attenuated, and

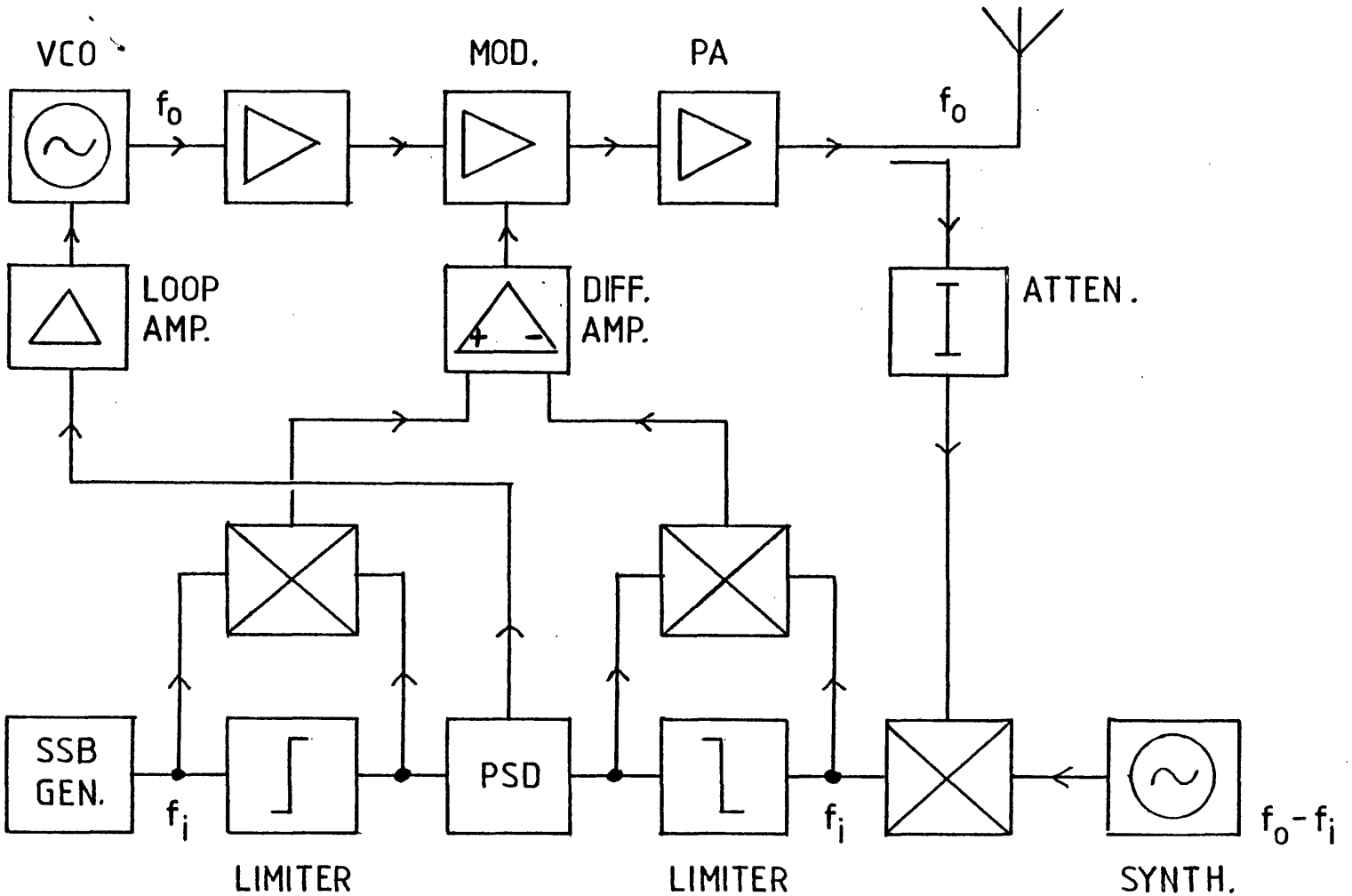

Figure 3.1 : The Polar-Loop Transmitter

translated (usually down) in frequency to the same IF.

The two IF signals are both hard limited, to remove any envelope modulation, and phase compared in a phase sensitive detector (PSD). The resulting output voltage, proportional to phase error, is filtered and amplified, and used to control the VCO. The whole transmitter is thus configured as a phase locked loop (PLL). By suitable choice of loop gain and bandwidth, the output phase can be made to closely approach that of the SSB input.

Envelope modulation at the output is obtained using a form of balanced envelope feedback. A differential amplifier compares the detected envelopes of the SSB input and frequency translated output, and generates the amplitude modulating voltage so as to minimise the error by negative feedback action. The two envelopes are conveniently detected, by utilising the two limited signals to synchronously demodulate their unlimited counterparts: a process equivalent to full-wave rectification.

It will be apparent that the two feedback loops in a polar loop transmitter differ from the balanced feedback configurations previously described. They are entirely responsible for generating the required modulation, as well as reducing any distortion. This factor must therefore feature in the feedback loop design. For VHF and UHF SSB applications, it will be shown that the loop bandwidth requirements for accurate modulation, can easily be met in practice. However, present day HF SSB transmitters are also required to transmit independent sideband (ISB) signals

where two independent SSB signals are transmitted simultaneously, above and below the suppressed carrier.

To implement an HF ISB polar loop transmitter would therefore require wider loop bandwidths. Unfortunately, the time delay inherent in practical HF power amplifiers (particularly at the low end of the band), means that the maximum stable loop bandwidths are inadequate for ISB operation. For this application, a different configuration, known as the polar loop transmitter - type 2, is more appropriate. Here, the polar loop feedback principle is applied to a conventional exciter/linear amplifier transmitter as shown in Figure 3.2. The polar loop circuits then only correct for distortion, allowing a relaxation of the bandwidth requirements. Further information on the type 2 transmitter, and problems associated with applying the polar loop to HF, are covered extensively by Warren (52). Unless the term 'type 2' is specifically mentioned, reference to the polar loop throughout this thesis will assume the EER (type 1) configuration of Figure 3.1.

Use of the polar loop technique at VHF and UHF results in a considerable reduction in the complexity of the transmitter, compared with conventional techniques. To convert low-level SSB at IF, to high-power SSB at channel frequency in the usual way, would require numerous mixing and filtering processes, followed by linear amplification. All of which reduces efficiency and linearity. Although the polar resolving and feedback circuits are complex, they operate at a fixed IF or baseband, and therefore readily

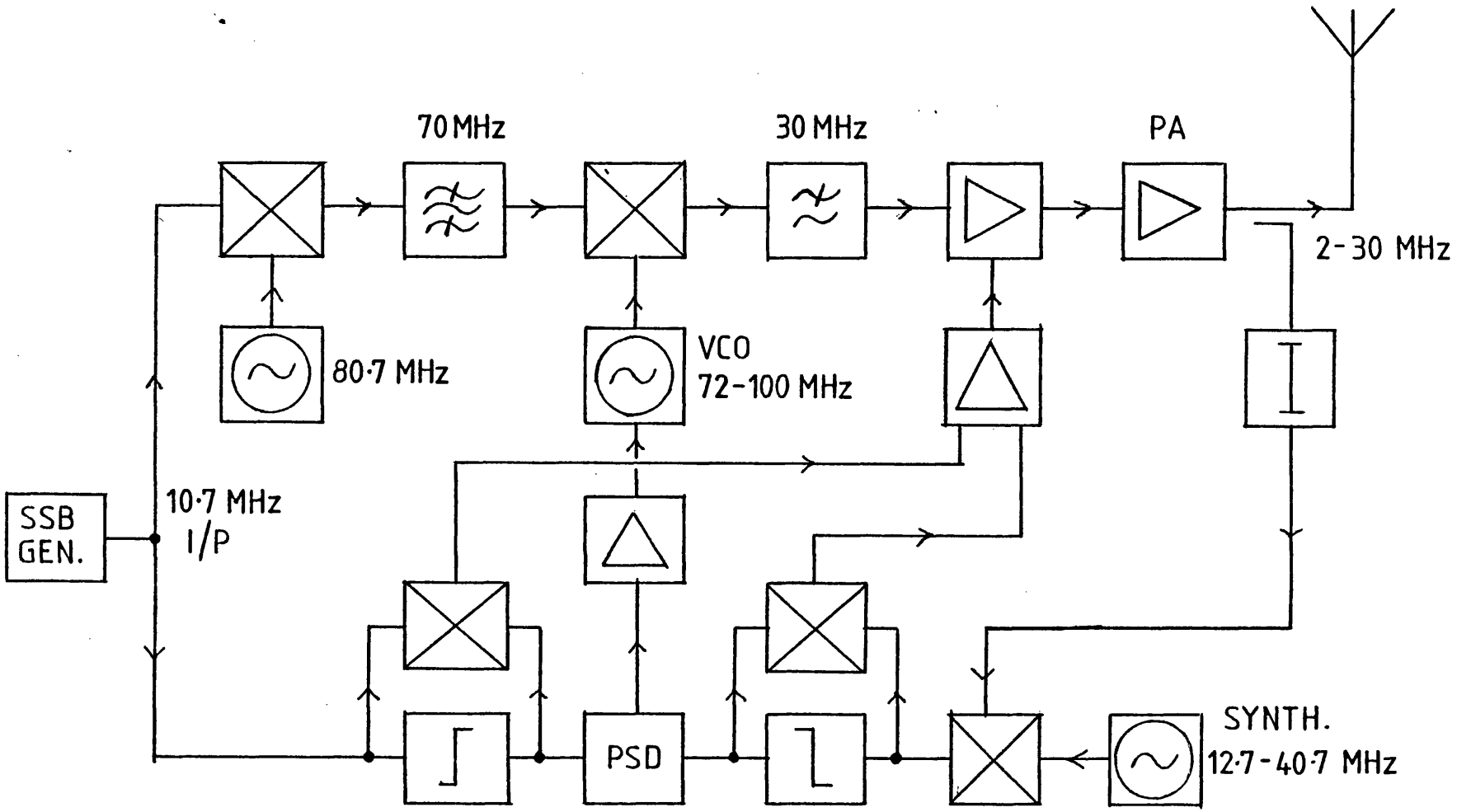

Figure 3.2 : Polar-Loop Transmitter Type-2

lend themselves to integrated circuit realisation. This is important since it would allow SSB transmitters to be physically compact, which is advantageous if SSB handportables are to be a reality.

There are a number of important differences between the Kahn EER system and the polar loop technique, apart from the inclusion of negative feedback by the latter.

The first is that a Heising modulator, and its associated high power audio amplifier, are no longer required. Modulation can be performed at low level on a grid, base or gate, since the non-linearity so introduced will be cancelled by feedback action. The losses in the audio amplifier are avoided, hence the overall efficiency must be improved. A second but related point, is that modulation need not be applied to the final stage, as in the Kahn transmitter, but can be made prior to additional (non-linear) amplification within the feedback loops. An advantage of this is that the limited isolation in the amplitude modulator (particularly at UHF), will be improved by the threshold action of the following Class C amplifier. The leakage of the phase component, associated with the Kahn transmitter, is thus reduced. Thirdly, the frequency translation process in the polar loop is performed by the phase-locked loop, unlike the Kahn system which requires up-conversion of the phase component. Finally, due to the balanced nature of the polar coordinate resolution, the two limiters and the two envelope demodulators do not have to be ideal, so long as each pair is accurately matched. Forming both resolvers on the same

integrated circuit will obviously help in this respect.

Until now, published results of applying the polar loop technique to practical systems, have been for HF (58), VHF low band (59) and VHF high band (60). These authors report third order intermodulation products typically in the range -50 to -60dB, on a two-tone test. They have also achieved efficiencies only slightly reduced from those using the same power amplifiers at saturation. Petrovic and Smith (60), for example, note an efficiency of 36% for a 170MHz polar loop transmitter producing two tones, compared with 41% in a CW mode. This represents a reduction of only 12%.

A Polar Loop Transmitter synthesises the RF spectrum at its output by means of two negative feedback loops to control the instantaneous amplitude and phase of the output signal. The accuracy to which the loops are able to replicate the amplitude and phase of the input is a function of their bandwidths. The following sections look at the theoretical requirements for the bandwidths in order to achieve good spectral purity, both in terms of spurious frequency components and noise levels.

Also covered are the effects on the output spectrum of deficiencies in the performance of critical components of the transmitter.

3.2 THE CONVOLUTION PROCESS OF EER

The following derivation obtains expressions for the polar coordinates of an SSB signal. Such a signal can be written in the form:-

$$e(t) = A(t) \cos[\omega_c t + \phi(t)] \qquad (3.1)$$

where ω_c = angular carrier frequency

$A(t)$ = instantaneous amplitude

$\phi(t)$ = instantaneous phase.

It can also be written as:-

$$e(t) = m(t) \cos \omega_c t - H[m(t)] \sin \omega_c t \qquad (3.2)$$

where $m(t)$ is the modulating signal

$H[m(t)]$ is its Hilbert transform.

Expressions for the polar coordinates of the SSB signal, $A(t)$ and $\phi(t)$ can thus be written:-

$$A(t) = \left\{ m^2(t) + H[m(t)]^2 \right\}^{\frac{1}{2}} \qquad (3.3)$$

and, $$\phi(t) = \tan^{-1} \frac{H[m(t)]}{m(t)} \qquad (3.4)$$

If the modulating signal consists of two sinusoidal components of amplitudes E_1 and E_2 and angular frequencies ω_1 and ω_2, as illustrated vectorially in Figure 3.3, then $m(t)$ can be written as:-

$$m(t) = E_1 \cos \omega_1 t + E_2 \cos \omega_2 t \qquad (3.5)$$

and,

$$H[m(t)] = E_1 \sin \omega_1 t + E_2 \sin \omega_2 t \qquad (3.6)$$

Thus, $A(t)$ and $\phi(t)$ become:-

$$A(t) = E_1 \left[1 + \frac{E_2^2}{E_1^2} + 2 \frac{E_2}{E_1} \cos (\omega_2 - \omega_1)t \right]^{\frac{1}{2}} \qquad (3.7)$$

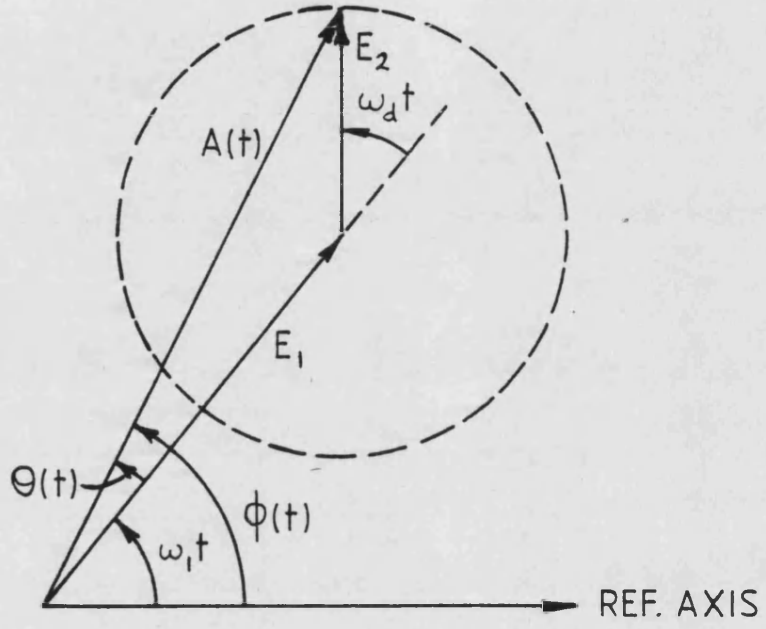

Figure 3.3 : Vectorial Representation of a Two-tone SSB Signal

$$\phi(t) = \tan^{-1} \frac{E_1 \sin \omega_1 t + E_2 \sin \omega_2 t}{E_1 \cos \omega_1 t + E_2 \cos \omega_2 t} \qquad (3.8)$$

If the ratio of the tone amplitudes E_2/E_1 is expressed as ρ, and the tone spacing $(\omega_2 - \omega_1)$ as ω_d, then:-

$$A(t) = E_1(1 + \rho^2 + 2\rho \cos \omega_d t)^{\frac{1}{2}} \qquad (3.9)$$

and

$$\phi(t) = \omega_1 t + \tan^{-1} \frac{\rho \sin \omega_d t}{1 + \rho \cos \omega_d t} \qquad (3.10)$$

If the phase component is referred to one of the tones such that:

$$\phi(t) = \theta(t) + \frac{\tan^{-1} \rho \sin \omega_d t}{1 + \rho \cos \omega_d t} \qquad (3.11)$$

where $\theta(t)$ is the phase of $A(t)$ relative to E_1

Hence: $$\theta(t) = \frac{\tan^{-1} \rho \sin \omega_d t}{1 + \rho \cos \omega_d t} \qquad (3.12)$$

The functions $A(t)$ and $\theta(t)$ are plotted against the phase angle, $\omega_d t$, for several values of ρ, in Figures 3.4 and 3.5.

To obtain the spectra of $A(t)$ and $\theta(t)$, each must be expanded as a Fourier series (117) to give:-

$$A(t) = E_1 \sum_{n=0}^{\infty} A_n(\rho) \cos n \omega_d t \qquad (3.13)$$

where $$A_n(\rho) = 2(-1)^n \left[\frac{1.3....(2n-1)}{n!}\right]\left(\frac{\rho}{n}\right)^n \times$$

$$\left[\frac{-1}{2n-1} + \frac{1}{n+1}\left(\frac{\rho}{2}\right)^2 \sum_{k=2}^{\infty} \frac{1(3)....(2k-1)}{k!\ 2^{2k}} \cdot \right.$$

$$\left. \frac{(2n+1)(2n+3)....(2n+2k-3)}{(n+1)(n+2)....(n+k)} \rho^{2k}\right] \qquad (3.14)$$

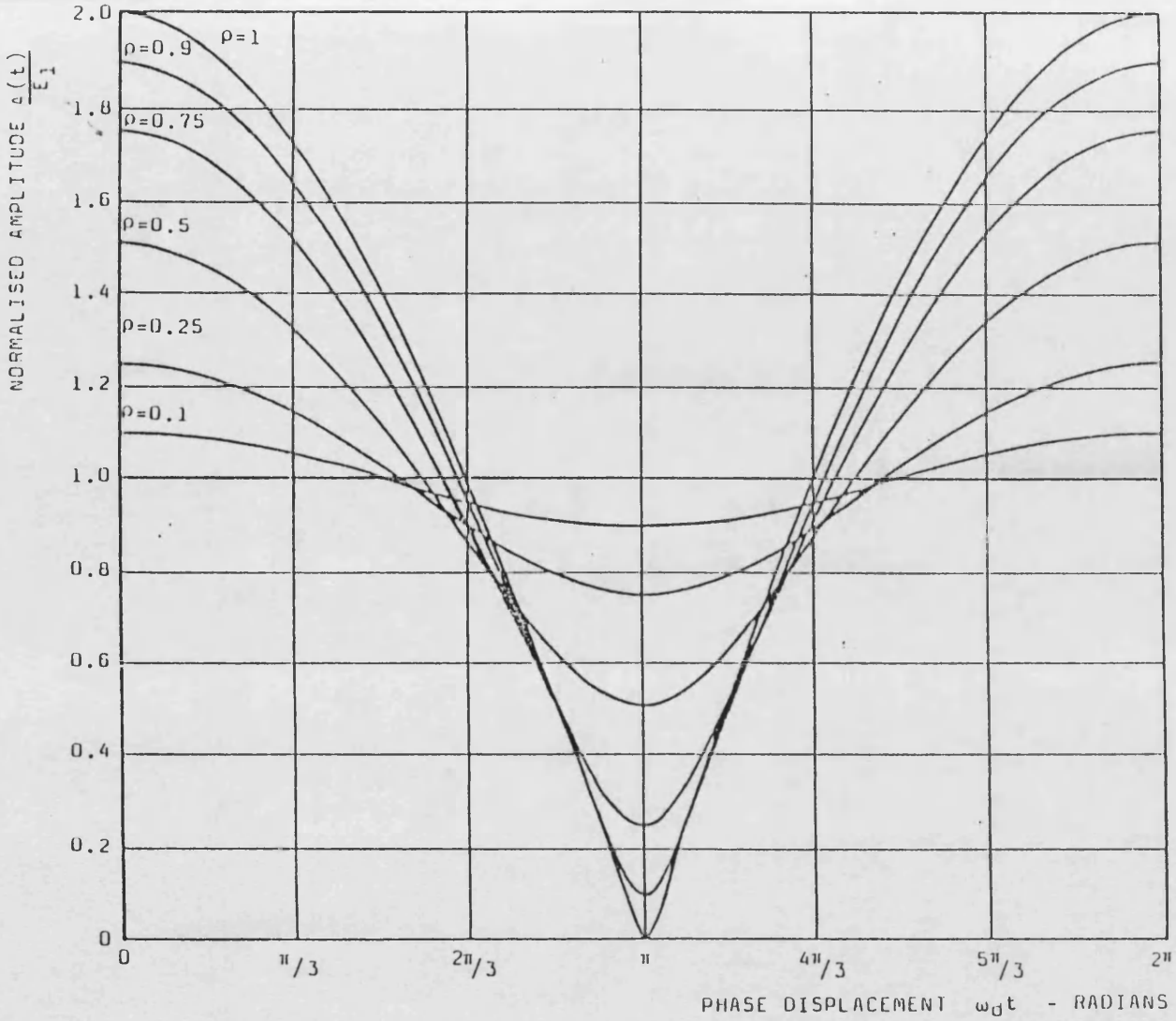

Figure 3.4 : Amplitude Function A(t) plotted versus Phase Angle $\omega_d t$

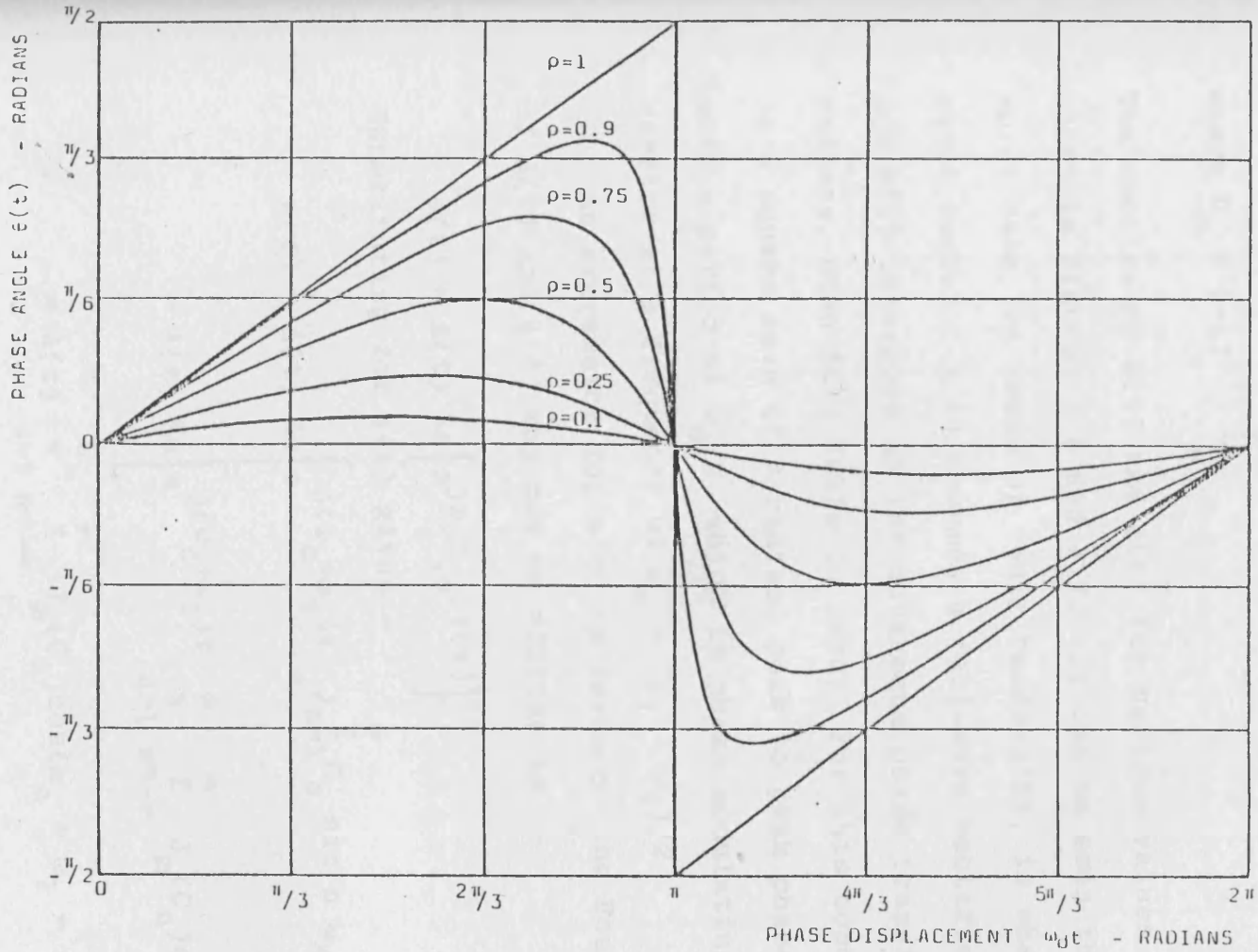

Figure 3.5 : Phase Function θ(t) plotted versus Phase Angle $\omega_d t$

and

$$\theta(t) = \sum_{n=1}^{\infty} C_n \sin n\,\omega_d t \qquad (3.15)$$

$$\text{where } C_n = (-1)^{n+1}\,\frac{\rho^n}{n} \qquad (3.16)$$

The spectra of A(t) and θ(t) for various values of ρ are shown in Figures 3.6 and 3.7. It can be seen that the worst case, in terms of their bandwidths, is when ρ=1 (two equal tones). A(t) becomes a full-wave rectified sinusoid, and θ(t) undergoes an instantaneous phase transition of π radians, when A(t) falls to zero. For this condition, φ(t) is a square wave of π radians peak to peak phase excursion, with a period of $\omega_d/2$, which is phase modulating an imaginary carrier at a frequency of $\omega_c + (\omega_1 + \omega_2)/2$

An expression for e(t) in terms of the Fourier series of A(t) and φ(t) may now be written as :-

$$e(t) = A(t)\ \mathrm{Re}\left[e^{j\omega_c t}.e^{j\phi(t)}\right] \qquad (3.17)$$

Substituting for φ(t) gives:-

$$e(t) = A(t)\ \mathrm{Re}\left[e^{j(\omega_c+\omega_1)t}\ .e^{j\sum_{n=1}^{\infty} C_n \sin n\,\omega_d t}\right]$$

$$= A(t)\ \mathrm{Re}\left[e^{j(\omega_c+\omega_1)t}\ .\ \prod_{n=1}^{\infty}\ \sum_{m=-\infty}^{\infty} J_m(C_n)e^{jnm\omega_d t}\right]$$

$$= A(t)\ \prod_{n=1}^{\infty}\ \sum_{m=-\infty}^{\infty} J_m(C_n)\cos(\omega_c + \omega_1 + nm\omega_d)t \qquad (3.18)$$

where J_m are Bessel functions of the first kind and mth order.

Substituting for A(t) gives:-

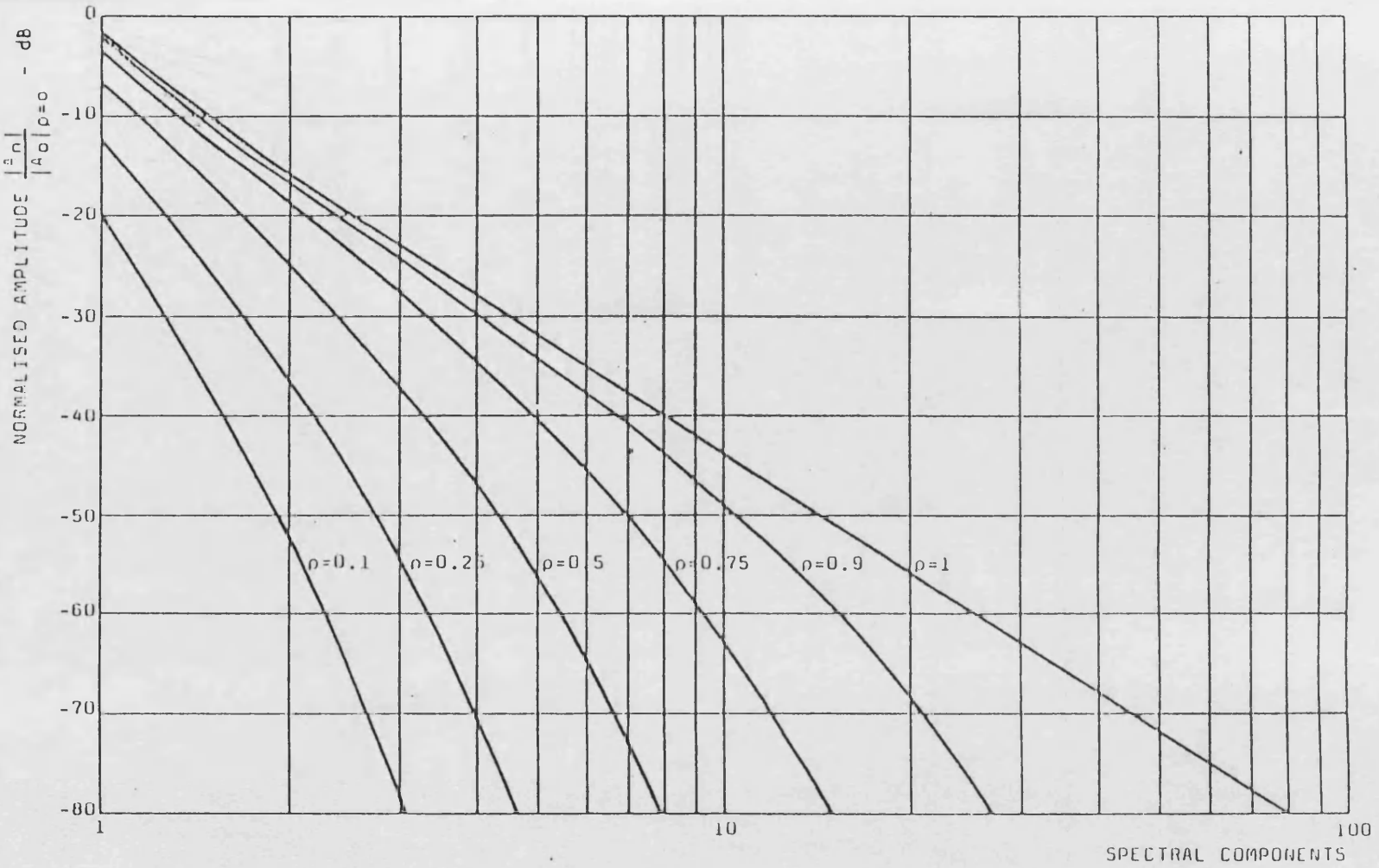

Figure 3.6 : Spectrum of the Amplitude Component A(t)

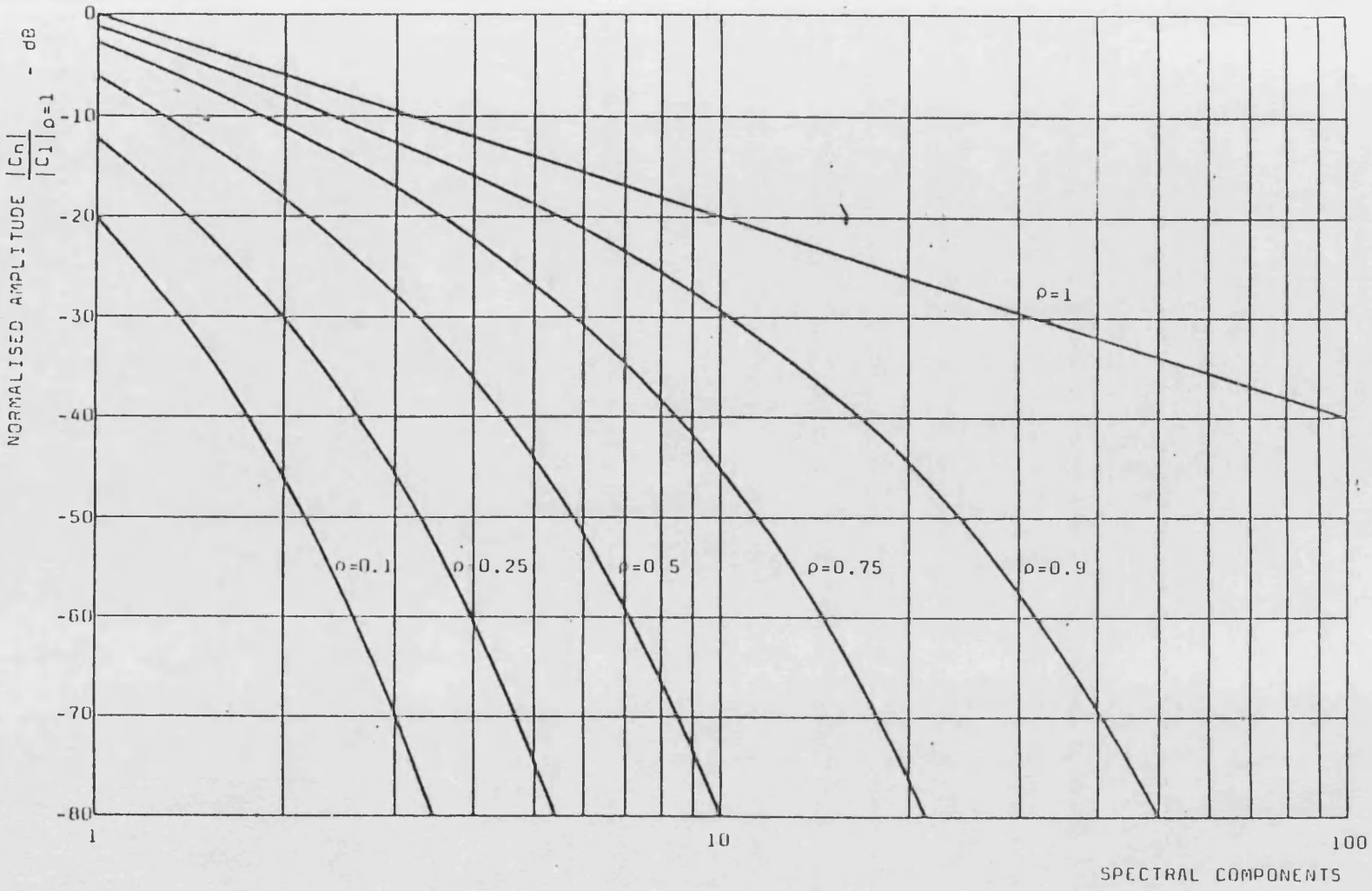

Figure 3.7 : Spectrum of the Phase Component θ(t)

$$e(t) = E_1 \sum_{n=0}^{\infty} A_n(\rho) \cos n\,\omega_d t \times$$

$$\prod_{n-1}^{\infty} \sum_{m=-\infty}^{\infty} J_m(C_n) \cos (\omega_c + \omega_1 + nm\omega_d)t \qquad (3.19)$$

The functions A(t) and $\phi(t)$ have infinitely many components. To determine the effect of bandlimiting them (as a practical system must do), Kaya (61), has carried out extensive computer simulations of the convolution process. In his simulation work, the amplitude and phase components were bandlimited by first order lowpass filters (representing the feedback loops), and the convolution evaluated for several values of filter cutoff frequency. In each case the input signal comprised two equal tones (since this is the worst case condition), with a tone spacing of 500Hz. The resulting output spectra have shown that bandwidths of 25KHz for both A(t) and $\phi(t)$, are sufficient to reduce all spurious components to less than -87dB relative to the wanted output. Examples of the computed output spectra are shown in Figure 3.8 for equal amplitude and phase bandwidths of 400, 200, 100, 50 and 25KHz. Figure 3.9 shows the effect of maintaining the amplitude loop bandwidth at 400KHz while reducing the phase bandwidth as in Figure 3.8. Finally, Figure 3.10 keeps the phase bandwidth at 400KHz for several values of amplitude bandwidth. It may be seen that if the amplitude and phase bandwidths are maintained equal, each doubling of bandwidth produces a corresponding 12dB reduction in the spurious level. At 400KHz bandwidth, the third order products are 136dB below the tone level. Figures 3.9 and 3.10 show that

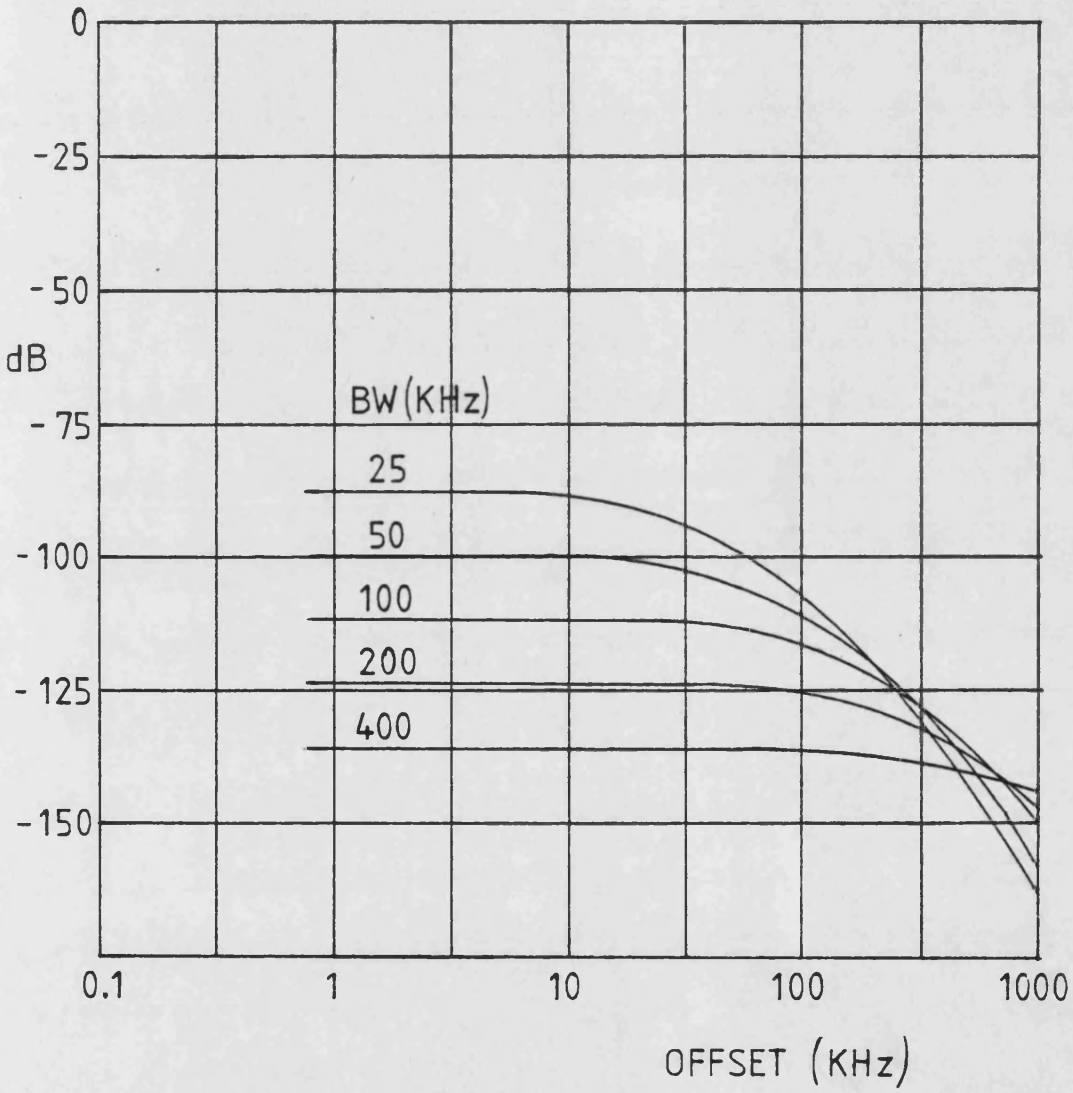

Figure 3.8 : Intermodulation Distortion Spectra obtained by Computer Simulation. (For Several Values of Loop Bandwidth.)

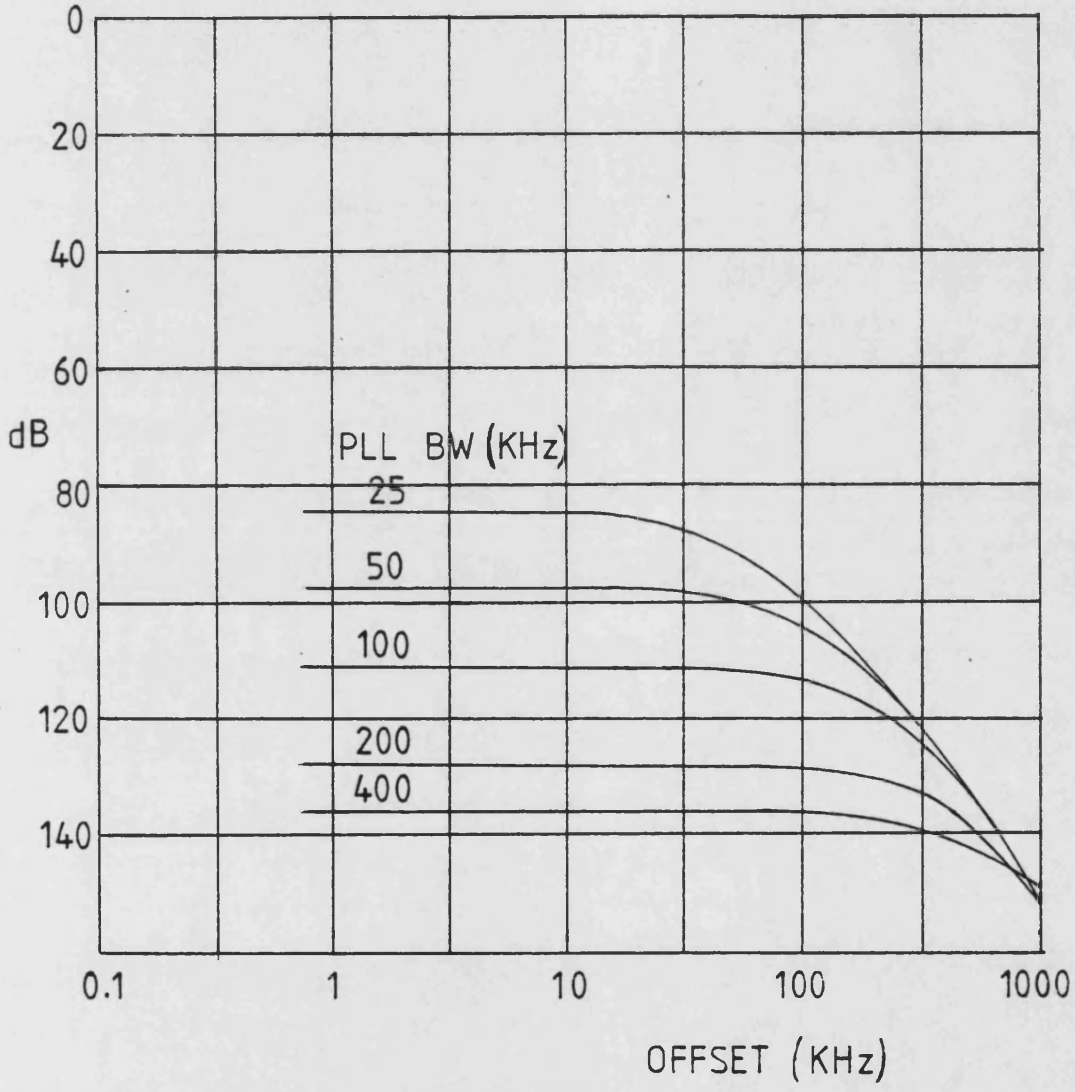

Figure 3.9 : Intermodulation Distortion Spectra obtained by Computer Simulation (Ampl. BW Fixed at 400KHz)

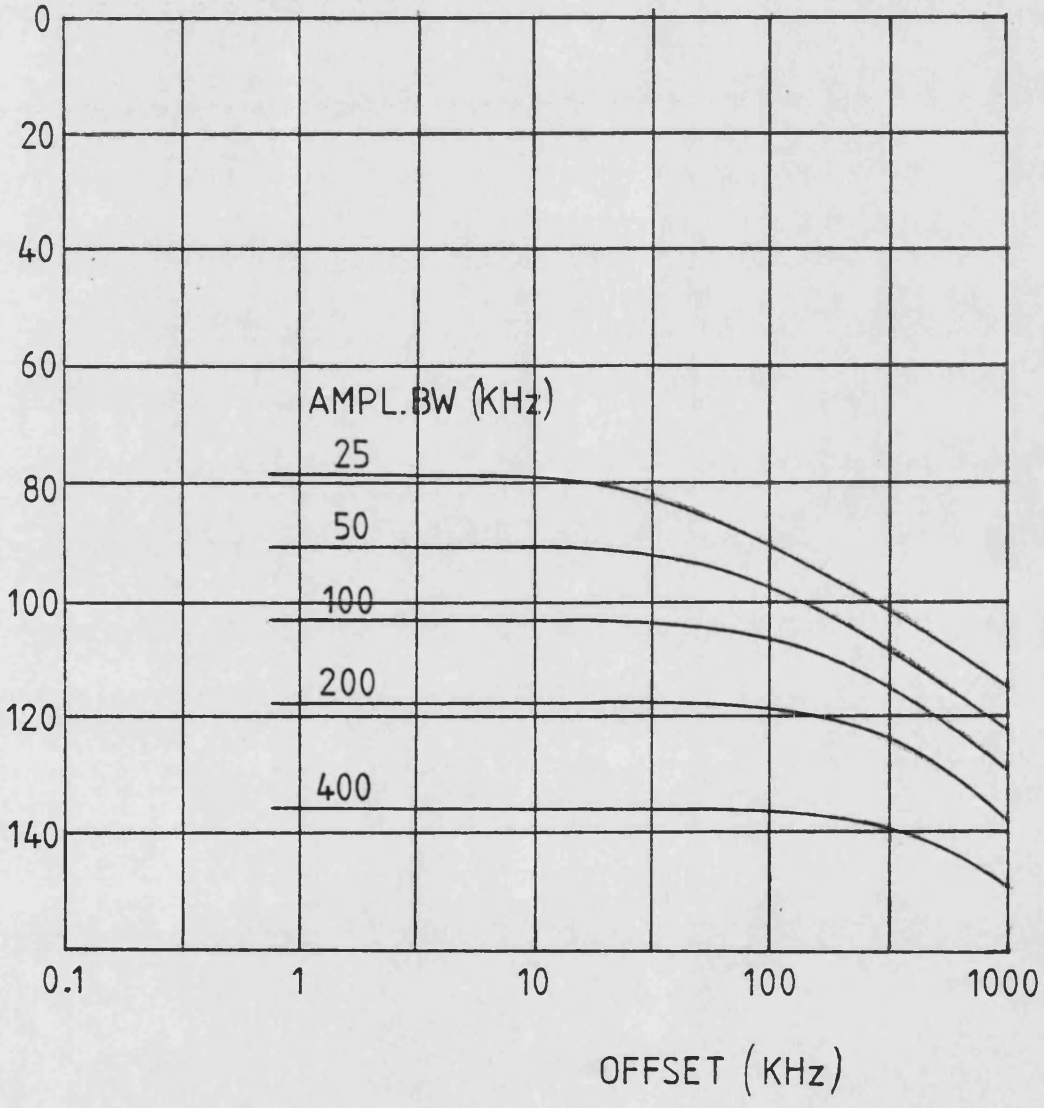

Figure 3.10 : Intermodulation Distortion Spectra obtained by Computer Simulation (PLL BW Fixed at 400KHz)

reducing just one of the bandwidths produces larger spurii than reducing both of them. In this situation, however, there is a time delay between the amplitude and phase components which causes an additional degradation (see Section 3.3.3).

3.3 LINEARITY CONSIDERATIONS

3.3.1 Loop Bandwidths Required for Distortion Reduction

It was seen in Chapter 1 that the level of intermodulation distortion generated by conventional RF amplifiers is high, between -15 and -30dB, typically. To determine the feedback loop bandwidths required to reduce this to acceptable levels, a specific example of an input signal must be chosen. A test signal widely used for evaluating communications systems is the two equal tone signal, where the tone spacing is a few hundred Hz. This signal has its energy concentrated over a bandwidth similar to that of a typical speech signal (13), but unlike speech, the levels of intermodulation distortion may be accurately quantified. Thus a two-tone signal of 500Hz spacing was used for most of the transmitter testing. For such a signal, third order intermodulation products will occur at an offset of 750Hz from the centre frequency. To reduce these products from -15dB (assuming a Class C amplifier) to say -70dB, will require 55dB of negative feedback. If a first order loop gain versus offset frequency characteristic is assumed, then this corres-

ponds to a loop bandwidth of:-

$$B = 0.75 \text{ alog } \left[\frac{55}{20}\right] = 420\text{KHz}.$$

This figure can serve only as a guide since a polar loop transmitter applies its feedback separately to amplitude and phase distortion, whereas the distortion seen at the output is a combination of both. However, practical results obtained during previous work have tended to confirm this prediction. Petrovic (59) has found that loop bandwidths of the order of 200KHz were required to achieve the best linearity from a VHF polar loop transmitter. Similarly, Warren (51) used the polar loop technique to linearise a solid state class AB HF amplifier. In this case bandwidths of 50KHz were sufficient, due to the reduced distortion in conventional mode, in comparison with a class C amplifier. It was also found by Warren that amplitude and phase distortion were of similar magnitudes. Using either loop in isolation gave little improvement.

3.3.2 Effect of Leakage in the Amplitude Modulator

The analysis of Section 3.2 has shown that the phase component of the output signal, which is generated by the VCO, can have a very wide spectrum. If this signal is allowed to leak through the amplitude modulator, even when the modulator is nominally at zero gain, there will clearly be a large number of spurious components at the output. The magnitude of the unwanted components relative to the wanted sideband can be calculated in the following way.

Let the wanted output, and the phase component leakage be as shown in Figure 3.11, (assuming two equal tones).

The isolation of the modulator, a, is given by:-

$$a = \frac{2A}{V_s}, \text{ where } A = \text{tone amplitude}$$

$$V_s = \text{leakage amplitude}$$

or, as a decibel relationship:-

$$\alpha = 20 \log a = 20 \log \left[\frac{2A}{V_s}\right] \qquad (3.20)$$

The amplitude of the leakage components, V_n, is a scaled version of the phase component:-

$$V_n = \frac{4V_s}{2\pi} \cdot \frac{1}{(2n-1)} \qquad (3.21)$$

Thus, the amplitude of the leakage components, L_n, relative to the wanted sidebands is given by:-

$$L_n = \frac{V_n}{A} = \frac{4V_s}{2\pi(2n-1)A} \qquad (3.22)$$

But, $\frac{V_s}{2A} = \frac{1}{10^{\alpha/20}}$

Hence, $L_n = \frac{4}{\pi(2n-1)10^{\alpha/20}}$ (3.23)

So, for example, a modulator isolation of 70dB, would give rise to unwanted third order products (when n=2) of -77dB relative to the wanted output. Such an isolation level can easily be achieved in practice, particularly when a class C amplifier follows the modulator to increase the effective isolation by its threshold action.

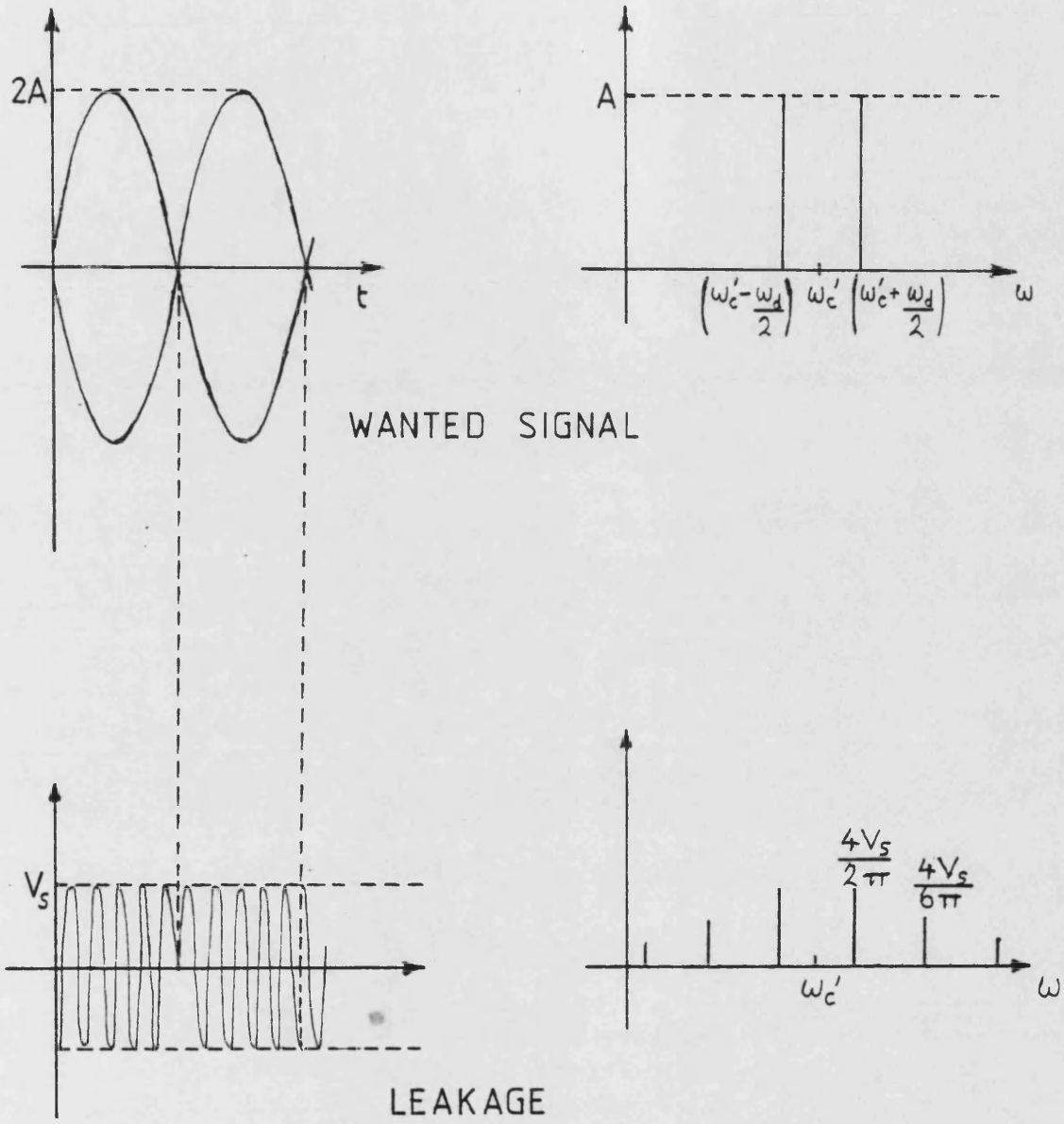

Figure 3.11 : Wanted and Leakage Signals appearing at the Transmitter Output when the Amplitude Modulator has a Finite Leakage

3.3.3 Effect of Timing Error between Amplitude and Phase Components

If there is a timing error between the phase modulated signal applied to the amplitude modulator input and the amplitude control voltage, spurious components will appear at the output. The level of these spurii relative to the wanted output can be calculated as follows:-

Consider the worst case condition of a two equal tone signal. The square wave phase component will appear displaced in time relative to the amplitude component, as shown in Figure 3.12. Thus, for the duration of the timing error between each envelope zero-crossing and the corresponding delayed phase reversal, the overall output will have a phase error of 180°. These phase inverted regions are equivalent to the wanted signal plus an inverted version of the wanted signal of twice the wanted amplitude. The wanted signal may be written as:-

$$e(t) = 2A \cos \frac{\omega_d t}{2} \cos \omega_c' t \qquad (3.24)$$

where A = tone amplitude

ω_d = tone spacing

ω_c' = imaginary carrier midway between two tones

and the unwanted output due to timing error as:-

$$g(t) = \Delta(t) \cos(\omega_c' t + \pi) \qquad (3.25)$$

where $\Delta(t)$ is a gated version of $A(t)$ as shown in Figure 3.12(c).

For small timing errors (corresponding to phase errors less

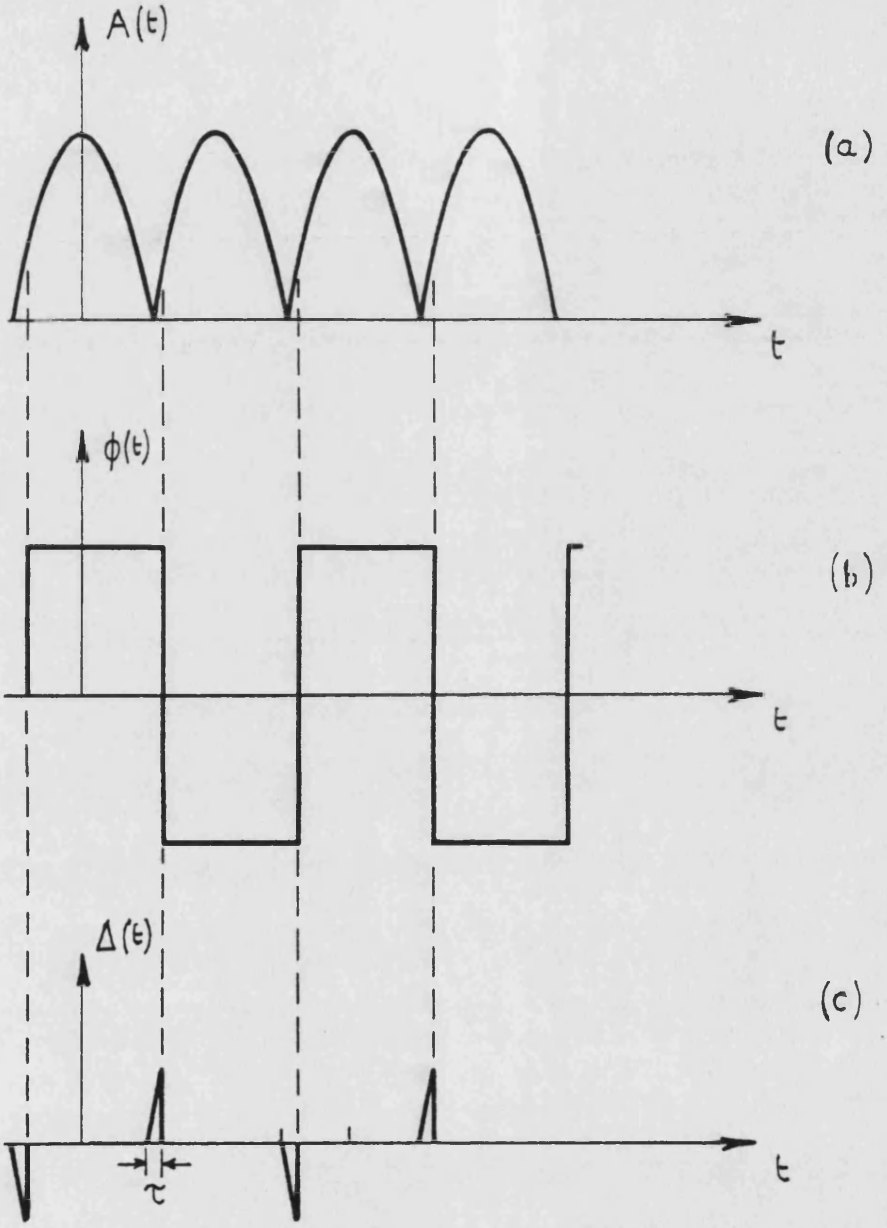

Figure 3.12 : Timing Error between Amplitude and Phase Components

than 5^{o}), an expression for $\Delta(t)$ as a Fourier series is shown in Appendix E to be:-

$$\Delta(t) = \frac{8A \sin\theta}{\pi\theta} \sum_{n=1}^{\infty} \frac{\sin\frac{n\pi}{2}}{n^2} \left[X \cos n\frac{\omega_d t}{2} + Y \sin n\frac{\omega_d t}{2} \right] \tag{3.26}$$

where θ = phase error corresponding to timing error τ of $2\theta/\omega_d$

$X = n\theta \cos n\theta - \sin n\theta$

$Y = n\theta \sin n\theta + \cos n\theta - 1.$

Substituting for $\Delta(t)$ into equation 3.26 gives an expression for the unwanted components as:-

$$g(t) = \frac{8A \sin\theta}{\pi\theta} \sum_{n=1}^{\infty} \frac{\sin\frac{n\pi}{2}}{n^2} \left[X \cos n\frac{\omega_d t}{2} + Y \sin n\frac{\omega_d t}{2} \right] \cos(\omega_c' t + \pi) \tag{3.27}$$

Or, rearranging $\Delta(t)$ in polar form:-

$$g(t) = \frac{8A \sin\theta}{\pi\theta} \sum_{n=1}^{\infty} \frac{\sin\frac{n\pi}{2}}{n^2} \left[X^2 + Y^2 \right]^{\frac{1}{2}} \cos\left[n\frac{\omega_d t}{2} + \beta \right] \cos(\omega_c' t + \pi) \tag{3.28}$$

where $\beta = \tan^{-1}\left[\frac{Y}{X}\right]$.

Hence:-

$$g(t) = \frac{-4A \sin\theta}{\pi\theta} \sum_{n=1}^{\infty} \frac{\sin\frac{n\pi}{2}}{n^2} \left[X^2 + Y^2 \right]^{\frac{1}{2}} \left\{ \cos\left[\left(\omega_c' - n\frac{\omega_d}{2} \right) t - \beta \right] + \cos\left[\left(\omega_c' + n\frac{\omega_d}{2} \right) t - \beta \right] \right\} \tag{3.29}$$

The amplitude of these unwanted components relative to the tone level, A, is therefore:-

$$G_n = \frac{4 \sin\theta \sin\frac{n\pi}{2}}{\pi\theta\, n^2} \left[X^2 + Y^2\right]^{\frac{1}{2}} \qquad (3.30)$$

The value of G_n has been computed for several values of n and θ, and these are tabulated in Table 3.1. It can be seen that except for very large phase errors, the spurii form a wide, flat spectrum at the output.

Order (n)	Relative amplitude (-dB)				
	$\theta = 0.25^o$	$\theta = 0.5^o$	$\theta = 1^o$	$\theta = 2^o$	$\theta = 5^o$
1	98.3	86.3	74.2	62.2	46.3
3	98.3	86.3	74.2	62.2	46.3
5	98.3	86.3	74.2	62.2	46.3
7	98.3	86.3	74.3	62.2	46.4
9	98.3	86.3	74.3	62.2	46.4
15	98.3	86.3	74.3	62.3	46.7
21	98.3	86.3	74.3	62.3	47.1
31	98.3	86.3	74.3	62.5	48.1
51	98.3	86.3	74.4	63.0	51.3

Table 3.1 Amplitude of Spurious Components due to Phase Error

In practice, the main source of phase error would be due to differences between the two loop bandwidths. To quantify this, let the feedback loops be represented by first order lowpass filters, with transfer functions given by:-

$$\frac{V_{out}}{V_{in}}(\omega) = \frac{1}{1 + j\omega\tau} \qquad (3.31)$$

where $1/2\pi\tau$ = the loop bandwidth (Hz).

The time delay, T, due to each feedback loop will be:

$$T = \frac{d\phi}{d\omega} = \frac{d}{d\omega}\left[\tan^{-1}(\omega\tau)\right] \qquad (3.32)$$

$$= \frac{\tau}{1 + \omega^2\tau^2}$$

For $\omega \ll 1/\tau$, $T \rightarrow \tau$.

Thus, taking an extreme combination of bandwidths of 400KHz and 25KHz, the timing error would be:-

$$\frac{1}{2\pi.25.10^3} - \frac{1}{2\pi.400.10^3} = 6\mu s$$

If the tone spacing is 500Hz, this corresponds to a phase error of approximately 0.5 degrees, which from Table 3.1, gives a spurious level of -86dB. However, since the amplitude and phase feedback loops would normally have similar bandwidths (because the amplitude and phase distortion are usually similar in magnitude), the phase error, and its associated spurii can be expected to be much less.

3.3.4 Effect of Limiter Threshold

The limiters used for extracting the phase component from the SSB input and feedback signals will have a finite gain. The result of this will be to produce a threshold effect. Below a certain threshold of input signal amplitude, the limiter output would be insufficient to synchronously demodulate the input, and the corresponding envelope output

would fall to zero. Thus, the transmitter output would be zero whenever its amplitude falls below the limiter threshold.

To determine the effect of this on the output spectrum, consider the two equal tone signal, since in this case the envelope crosses the limiter threshold. As in the analysis of the effect of timing error, the wanted signal may be modelled as a sine wave of frequency $\omega_d/2$ multiplying an imaginary carrier, ω_c', mid-way between the two tones. When there is a finite limiter threshold, the output would appear as shown in Figure 3.13(a). Thus the unwanted components are due to a gated version of the sine wave, shown in Figure 3.13(b), multiplying an inverted version of the imaginary carrier.

The Fourier series expansion of this gated sine wave, designated $\ell(t)$, is shown in Appendix F to be:-

$$\ell(t) = \frac{8A \sin\theta}{\pi\theta\, n^2} \sum_{n=1}^{\infty} (\sin n\theta - n\theta \cos n\theta) \sin \frac{n\,\omega_d t}{2}$$

for n odd (3.33)

$= 0$, for n even.

where A = tone amplitude

2θ = portion of 'missing' signal expressed as an angle.

Thus the unwanted components at the transmitter output can be expressed as:-

$$L(t) = \frac{8A \sin\theta}{\pi\theta\, n^2} \sum_{n=1}^{\infty} (\sin n\theta - n\theta \cos n\theta) \sin \frac{n\,\omega_d t}{2} \cdot \cos(\omega_c' t + \pi) \qquad (3.34)$$

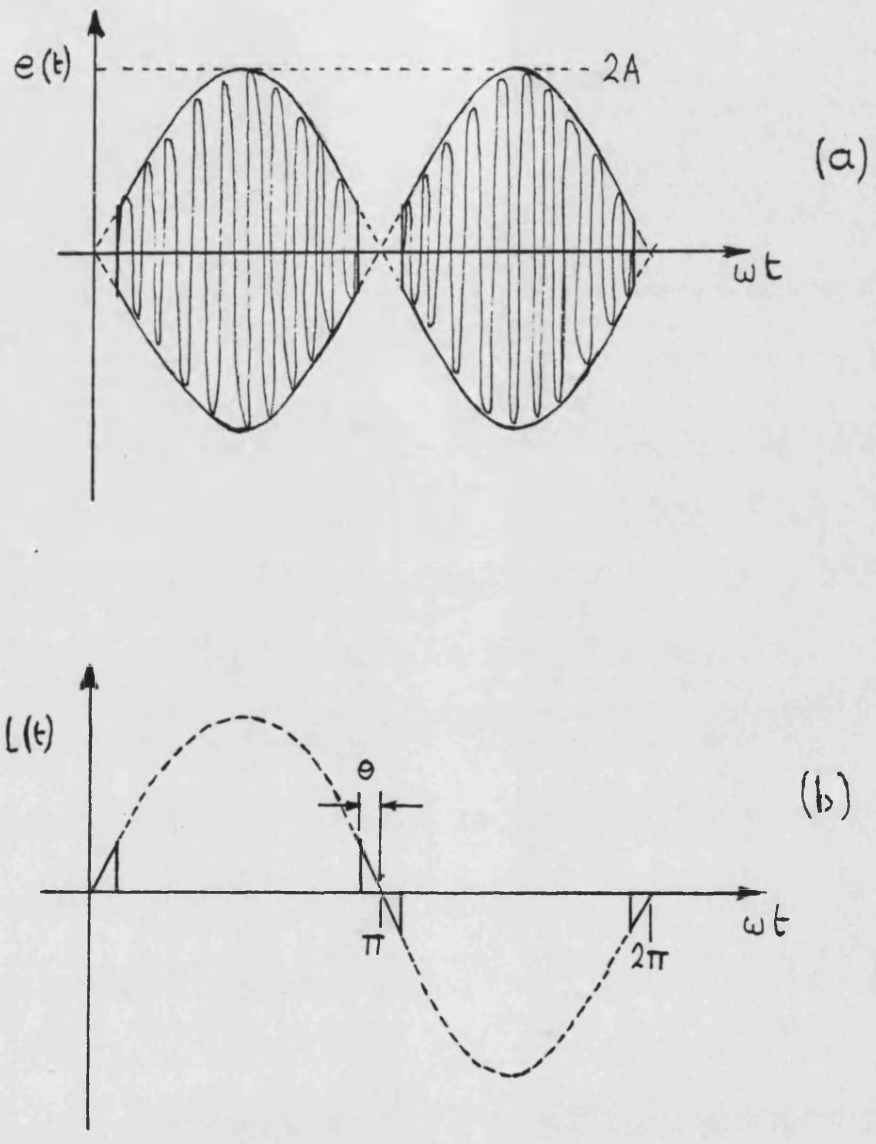

Figure 3.13 : Effect of Limiter Threshold

$$= \frac{4A \sin}{n^2} \sum_{n=1}^{\infty} (\sin n\theta - n\theta \cos n\theta)$$

$$\left[\cos\left(\omega_c't - \frac{n\,\omega_d t}{2} + \pi\right) + \cos\left(\omega_c't + \frac{n\,\omega_d t}{2} + \pi\right)\right]$$

where n is odd. (3.35)

The amplitude of these components relative to the tone level is therefore:-

$$L(n) = \frac{4 \sin \theta}{\pi\theta\, n^2} (\sin n\theta - n\theta \cos n\theta) \quad (3.36)$$

By inspection of Figure 3.13, it may be seen that θ is related to the limiter threshold voltage V_t, by:-

$$V_t = 2A \sin \theta \quad (3.37)$$

If the limiter input is assumed to be 0dBm PEP, and the threshold voltage is assumed to be equal to the limiting sensitivity (that level at which the output has fallen by 3dB), then the typical magnitude of the unwanted components may be calculated:-

For $V_t = 100\mu V_{rms}$, $\theta = 4.5.10^{-4}$ rad

$= 0.026^{o}$

which results in the spurii tabulated in Table 3.2.

Order (n)	Relative Amplitude of Spurious Components (dB)
3	-199
5	-194
7	-191
51	-174
101	-168
1001	-148
5001	-139
10001	-188

Table 3.2 Spurious components due to a 100μV limiter threshold

It is apparent that for a 100μV limiter threshold (which represents a relatively low sensitivity limiter), the spurious components produced are negligibly small.

3.3.5 Effect of Non-linearity in the Polar Resolver

The effectiveness of the feedback loops in reducing distortion is defined by feedback theory, providing the two polar resolving circuits are identical. Phase distortion introduced by the limiters due to AM to PM conversion, and amplitude non-linearity in the demodulators, will have no effect on the output spectrum, if it occurs equally for both the input and feedback signals. Any imbalance between the two sides cannot be corrected by feedback action, and therefore will result in distortion at the output. The mag-

nitude of this effect will depend on how well matched the two resolving circuits can be made in practice.

3.4 NOISE CONSIDERATIONS

3.4.1 Phase Noise

The level of phase noise appearing at the output of a polar loop transmitter may be readily predicted using phase locked loop theory.

A phase locked loop has three sources of phase noise:-

(i) The free-running VCO.

(ii) The reference oscillator (or oscillators).

(iii) The loop components such as the PSD and loop amplifier.

These are shown in the block diagram of Figure 3.14.

The negative feedback action of the PLL is such that within its bandwidth, the loop will tend to track the noise due to the reference signal and loop components, while suppressing the noise due to the VCO. Outside the loop bandwidth, the output noise will tend towards that of the free-running VCO. These effects are well known, and have been quantified by many authors (63, 64, 65, 66, 67). They can be summarised as follows:-

The suppression of the VCO noise is given by:-

$$\frac{\theta_o(s)}{\theta_v(s)} = \frac{s}{s + k_o\, k_d\, F(s)} \qquad (3.38)$$

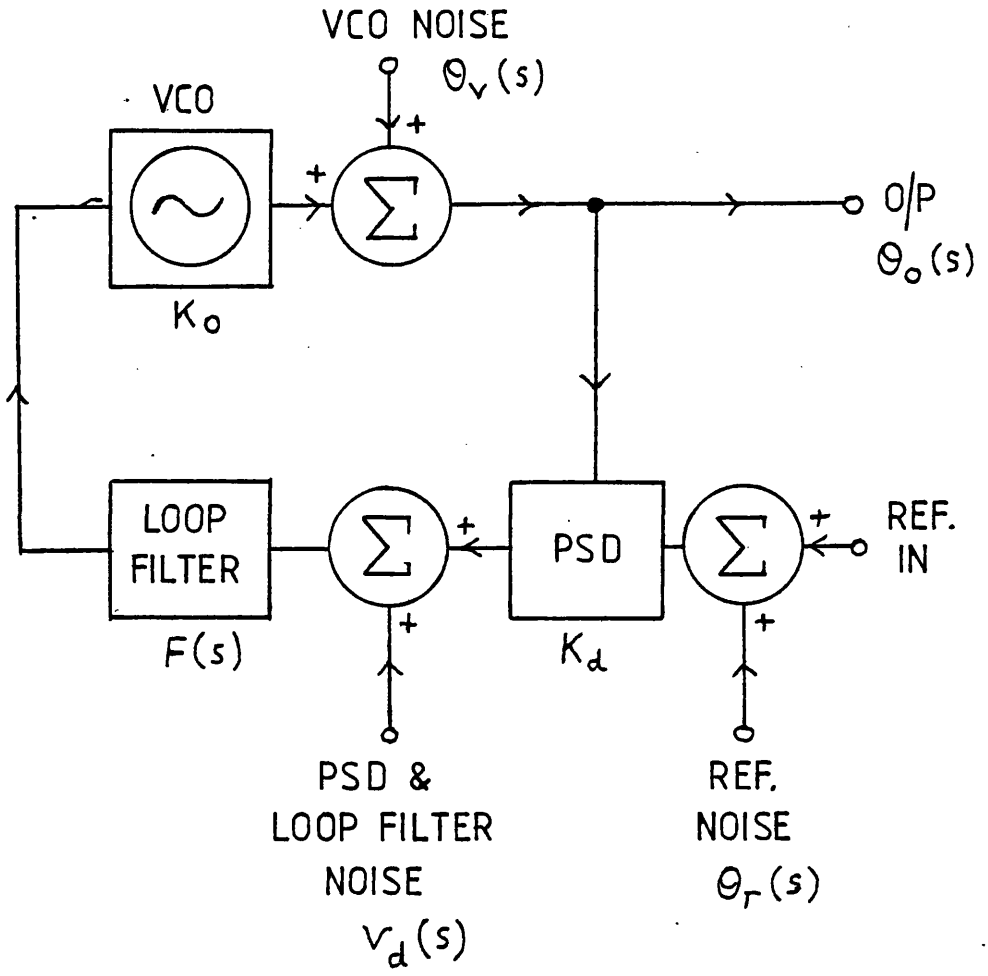

Figure 3.14 : Noise Contributions in a Phase-locked Loop

where $\theta_o(s)$ = output phase noise (rad)

$\theta_v(s)$ = phase noise of free-running VCO

k_o = VCO constant (r/s/V)

k_d = PSD constant (V/r)

F(s) = loop filter transfer function.

If a conventional active loop filter is used, with a transfer function:

$$F(s) = \frac{1 + s\,\tau_2}{s\,\tau_1}$$

Then:

$$\frac{\theta_o(s)}{\theta_v(s)} = \frac{s^2}{s^2 + \frac{k_o\,k_d\,\tau_2}{\tau_1}\,2 + \frac{k_o\,k_d}{\tau_1}} \qquad (3.39)$$

Which, if $1/\tau_2 \ll k_o\,k_d\,\tau_2/\tau_1$, can be approximated by:-

$$\frac{\theta_o(s)}{\theta_v(s)} = \frac{s^2}{\left[s + \frac{1}{\tau_2}\right]\left[s + \frac{k_o\,k_d\,\tau_2}{\tau_1}\right]} \qquad (3.40)$$

This is the equation of a highpass filter which suppresses the VCO noise by 6dB/oct in the region $1/\tau_2 \leqslant \omega \leqslant k_o\,k_d\,\tau_2/\tau_1$, and by 12dB/oct for $\omega < 1/\tau_2$. A typical VCO phase noise spectrum, falling by 6dB/oct away from the centre frequency would therefore be suppressed as shown in Figure 3.15.

Similarly the effects of the PLL on the PSD and loop filter noise, and on the reference noise, may be written:-

$$\frac{\theta_o(s)}{V_d(s)} = \frac{k_o\,F(s)}{s + k_o\,k_d\,F(s)} \qquad (3.41)$$

where $V_d(s)$ = noise voltage due to PSD and loop filter, and:

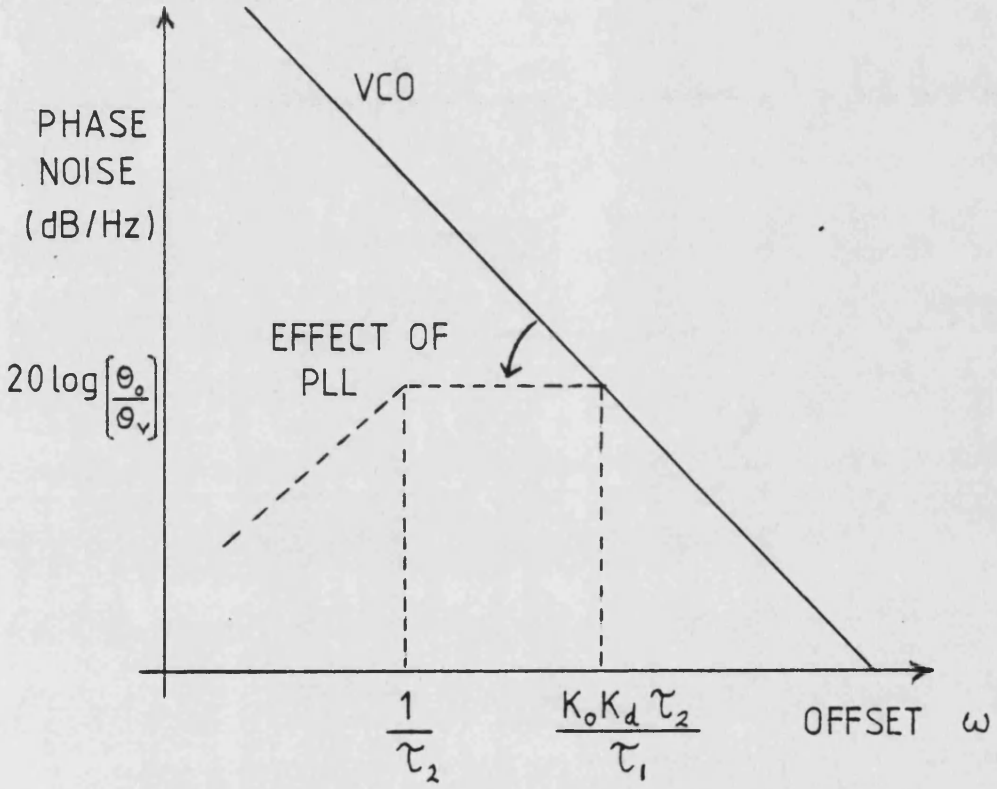

Figure 3.15 : Suppression of VCO Noise in a PLL

$$\frac{\theta_o(s)}{\theta_R(s)} = \frac{k_o\, k_d\, F(s)}{s + k_o\, k_d\, F(s)} \qquad (3.42)$$

where $\theta_R(s)$ = phase noise of reference osc.

The noise voltage $V_d(s)$ may be represented as an equivalent phase noise at the PSD input, $\theta_d(s)$. Thus:-

$$\frac{\theta_o(s)}{\theta_d(s)} = \frac{k_o\, k_d\, F(s)}{s + k_o\, k_d\, F(s)} \qquad (3.43)$$

Equations (3.42) and (3.43) show that the noise contributions from all of the loop components apart from the VCO, undergo a first order lowpass filtering action by the PLL, with a cutoff frequency of $k_o\, k_d\, F(s)$. An example of this is shown in Figure 3.16. The overall output phase noise level is given by the summation of the noise levels due to each element of the loop:-

$$\theta_o(s) = \theta_v(s)\, \frac{s^2}{\left[s + \frac{1}{\tau_2}\right]\left[s + k_o\, k_d\, \frac{\tau_2}{\tau_1}\right]} + [\theta_R(s) + \theta_d(s)]\, \frac{k_o\, k_d\, F(s)}{s + k_o\, k_d\, F(s)} \qquad (3.44)$$

The minimum value of $\theta_o(s)$ is defined by those regions of $\theta_v(s)$ and $[\theta_R(s) + \theta_d(s)]$ which are unaffected by the loop, these being outside the loop bandwidth, and within the loop bandwidth, respectively. This implies that the optimum bandwidth (for minimum noise) occurs at the intersection of $\theta_v(s)$ and $[\theta_R(s) + \theta_d(s)]$, as shown in the example of Figure 3.17.

Prediction of the optimum bandwidth for a polar loop transmitter therefore requires the noise levels produced by

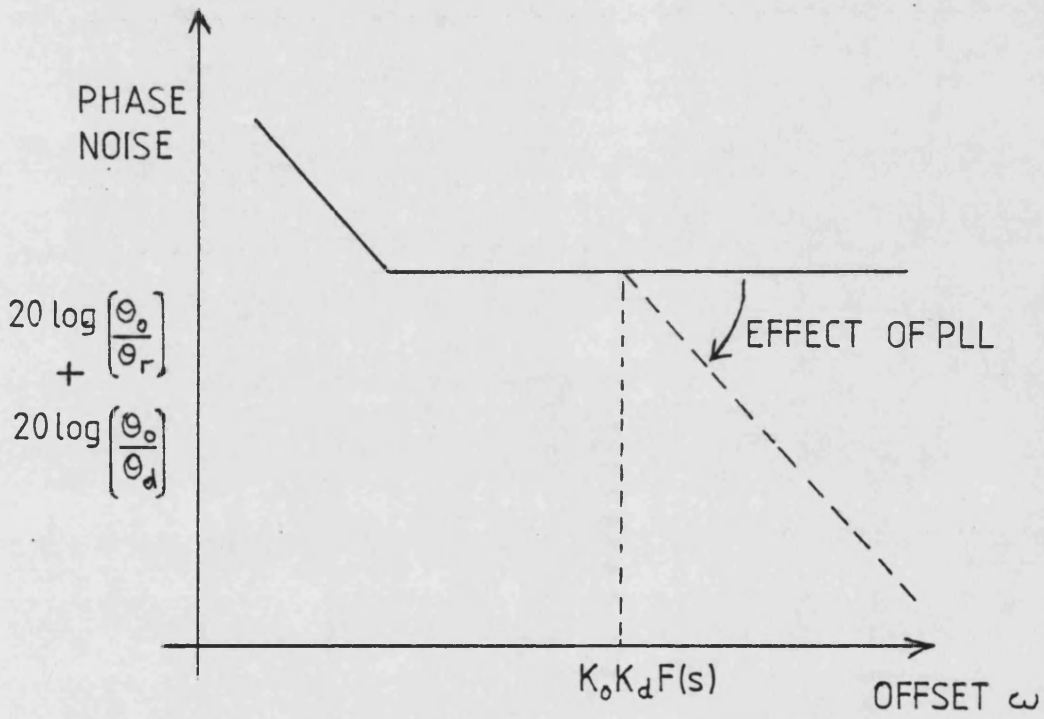

Figure 3.16 : Suppression of Reference and Loop Component Noise by a PLL

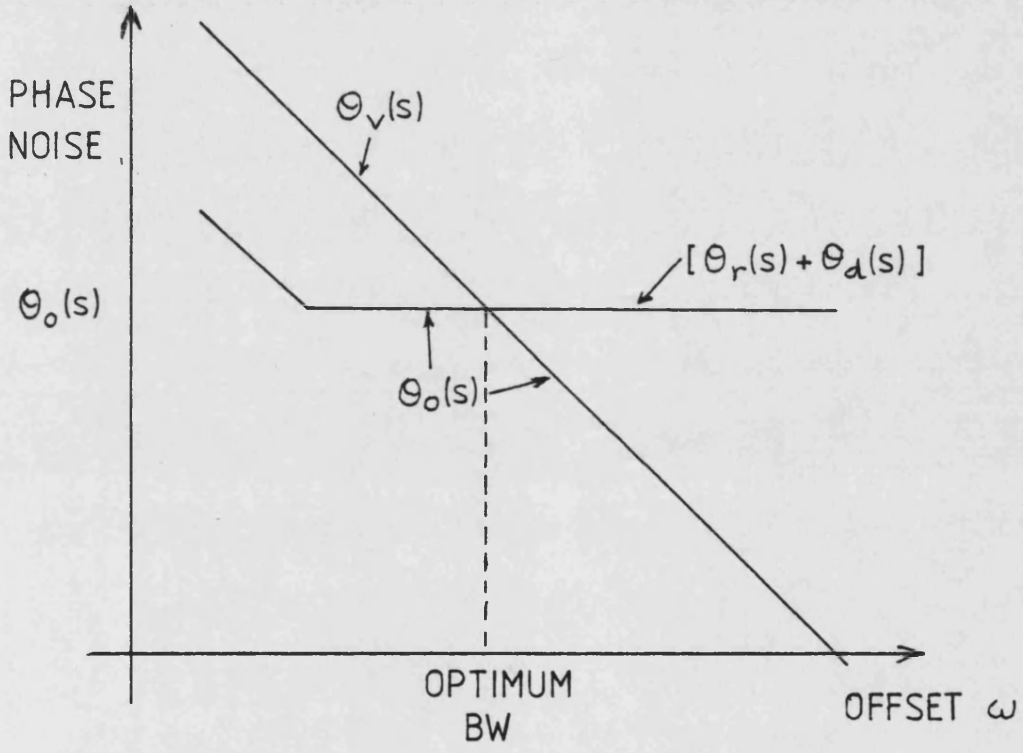

Figure 3.17 : Optimum (Minimum Noise) Bandwidth for a PLL

its constituent parts to be known (see Section 5.5.3).

3.4.2 Amplitude Noise

Baseband noise in the constituent parts of the amplitude feedback loop will produce AM noise sidebands at the transmitter output. The main sources of this noise are shown in Figure 3.18, where the symbols are defined as follows:-

v_{ni} = AM content of input noise (from the SSB generator)

v_{nba} = equivalent input noise of buffer amplifier

v_{nm} = equivalent input noise of the mixer

v_{nda} = equivalent input noise of the differential amplifier

A_{ba} = voltage gain of buffer amplifier

A_m = voltage conversion gain of the mixer (d.c. output/rms input)

V_{dc} = d.c. level out of mixer corresponding to transmitter producing full power (CW).

The noise level out of the buffer amplifier would therefore be:-

$$V_{nba(out)} = A_{ba}\sqrt{\left(V_{nba}^2 + V_{ni}^2\right)} \quad V/\sqrt{Hz} \qquad (3.45)$$

Hence the noise appearing at the demodulator output would be:

$$V_{nm(out)} = A_m\sqrt{\left[V_{nm}^2 + A_{ba}^2\left(V_{nba}^2 + V_{ni}^2\right)\right]} \quad V/\sqrt{Hz} \qquad (3.46)$$

Since the resolver circuit for the feedback signal will also contribute an equal amount of noise to that above, the total noise appearing at the differential amplifier input can be written:-

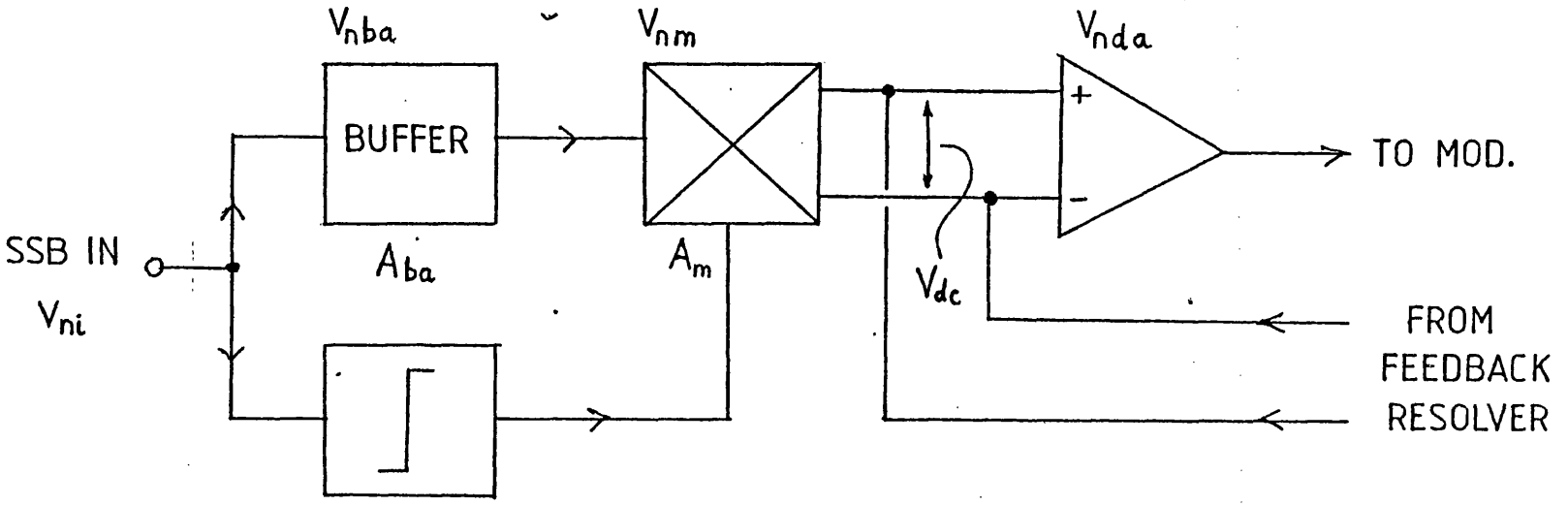

Figure 3.18 : AM Noise Sideband Contributions

$$V_{nda(tot)} = \sqrt{\left\{ V_{nda}^2 + 2A_m^2 \left[V_{nm}^2 + A_{ba}^2 \left[V_{nba}^2 + V_{ni}^2 \right] \right] \right\}} \quad (3.47)$$

Thus, the signal to noise ratio, in terms of peak envelope power relative to the total AM noise sideband power is given by:-

$$SNR_{AM} = 10 \log \left\{ \frac{V_{DC}^2}{V_{nda}^2 + 2A_m^2 \left[V_{nm}^2 + A_{ba}^2 \left[V_{nba}^2 + V_{ni}^2 \right] \right]} \right\} \text{dB/Hz} \quad (3.48)$$

for offsets less than the loop bandwidth.

Outside the loop bandwidth, the noise sidebands can be expected to fall by 6dB/octave (assuming a first order loop).

3.5 CONCLUSION

Analysis of the EER technique of generating an SSB signal, has shown that a polar loop transmitter need have loop bandwidth of only 25KHz in order to produce an output spectrum with very low spurious levels. With both feedback loops set to this value, computer simulation has shown that the level of third order intermodulation products on a two-tone test would be -87dB relative to the tone level. However, the necessity to reduce the distortion generated by the RF amplifier increases this requirement to several hundred KHz.

Other imperfections in the transmitter which may also degrade the spectrum, notably leakage in the amplitude modulator, timing error between the amplitude and phase

components, and loss of signal at low level due to limiter threshold, have also been examined. In each case, the effects can be reduced to negligible proportions.

Minimisation of the output phase noise level gives rise to an optimum bandwidth, although this cannot be quantified without knowledge of the practical system.

CHAPTER FOUR

APPLICATION OF THE POLAR LOOP TECHNIQUE TO UHF

4.1 INTRODUCTION

Factors affecting the performance of a polar loop transmitter were discussed in Chapter 3. Some of the potential degradations will increase in severity as the technique is applied at frequencies higher than have been used previously. This Chapter looks at these aspects in more detail, with a view to applying the technique at frequencies of 450 and 950MHz.

Other possible problem areas which may arise out of operation at UHF, are also examined.

4.2 EFFECT OF UHF OPERATION ON LINEARITY

4.2.1 Power Amplifier Distortion

Intermodulation distortion generated by an RF power amplifier is a result of two properties of the active devices used. The first is amplitude non-linearity, the second is AM to PM conversion. Assuming that attention is restricted to solid-state, and in particular, bipolar transistor amplifiers, the former effect is due to the non-linear relationship between collector current and base-emitter voltage. Although one would not expect this to be a frequency dependent effect, practical experience has shown (10) that UHF devices do have transfer characteristics less linear than

their lower frequency counterparts. A possible explanation for this is that device capacitances form a more significant part of the tuned matching networks than at lower frequencies. Thus, if the capacitances change with power level, the networks are seriously detuned, resulting in an unwanted amplitude variation. Additionally, UHF power transistors usually have low gains, 6dB typically, compared with 10-16dB for most HF and VHF devices. This means that localised negative feedback is not feasible for UHF transistors whereas it can be applied to HF and VHF transistors, giving a small improvement in the distortion levels.

In recent years, a new family of RF power devices has appeared known as Power-FETS. These have characteristics closer to square law rather than exponential, and hence produce lower levels of intermodulation distortion than equivalent bipolar transistors (68). However, as yet there are no devices suitable for UHF operation.

The second distortion mechanism to be considered is AM to PM conversion. This is caused by the variation in transistor output capacitance, as noted in Chapter 1. It was seen that the phase shift versus capacitance change is inversely proportional to the total effective tuned circuit capacitance. Since the capacitance of the amplifier tuned circuits (or equivalent matching networks) must reduce with increasing frequency, the AM to PM conversion can be expected to worsen also.

One further aspect of UHF operation concerning the power amplifier is the performance of the amplitude modulator.

Since the isolation of the modulator will inevitably worsen as the frequency is increased, this will preclude the use of a class AB or class B power amplifier. Rather, a class C amplifier would be essential by virtue of its input threshold, which could be used to advantage to effectively increase the overall isolation, and hence reduce the leakage of the phase component to the output. The use of the power amplifier in its least linear mode is therefore mandatory.

In summary then, a UHF power amplifier is likely to have poorer linearity than an amplifier designed for operation at lower frequencies.

4.2.2 The VCO Buffer Amplifier and Amplitude Modulator

In a polar loop transmitter, the output from the VCO must be brought up to a sufficient power level to drive the amplitude modulator, which in turn drives the power amplifier. Since the power amplifier operates in class C in the interests of good efficiency, its input impedance will vary widely with signal level. At low level, below the point of conduction, the input will appear almost entirely reactive, whereas at high level, it will be mostly resistive as the input dissipates power. If the reverse isolation of the VCO buffer amplifier and amplitude modulator is poor, then this impedance variation will cause a variation in the effective impedance presented to the VCO. This in turn will cause an unwanted frequency modulation of the VCO in sympathy with the envelope function.

Provided the phase locked loop bandwidth is greater than the deviation due to the impedance fluctuation, the loop will be able to track the modulation and remain in lock (69). However, due to the finite amount of negative feedback which the PLL is able to apply, there will be residual FM sidebands at the transmitter output, which may be significant. To predict the magnitude of this effect, the expressions derived in Appendix G may be used. These show that for a typical UHF Colpitts oscillator operating at 450MHz, the change in frequency of oscillation with change in load capacitance and load resistance is:-

$$\frac{df_o}{dC_L} = -3.8\text{MHz/pF}$$

and

$$\frac{df_o}{dR_L} = 8.8\text{KHz}/\Omega$$

where: f_o = frequency of oscillation

C_L = load capacitance

R_L = load resistance (parallel).

Clearly, capacitance change has the largest effect, as might be expected intuitively. To minimise the unwanted FM, it is important therefore that the modulator has minimal change in input capacitance with power level, and that the buffer amplifier has very good isolation.

The reverse isolation of an amplifier stage is governed mainly by its input to output capacitance. Referring to the diagram in Figure 4.1, the feedback capacitance C_{fb}, in conjunction with Z_{in} and Z_{out}, form a π-section attenuator to signals or impedance changes at the output. Of these, only the feedback capacitance is not under the control of the designer. Minimising this is thus a matter of selecting a device with the lowest possible capacitance. A study of manufacturers' data sheets for numerous UHF devices reveals the results summarised in Table 4.1.

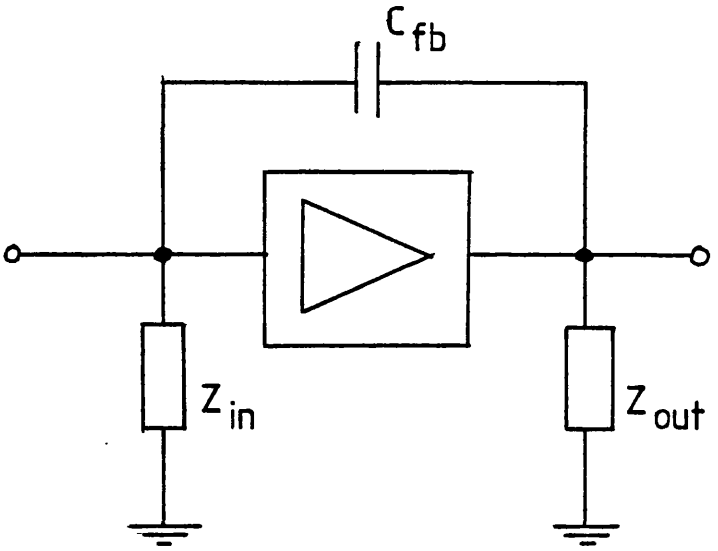

Figure 4.1 : Amplifier Feedback Capacitance

Device type	Range of typical feedback capacitance (pF)
Bipolar transistor	0.8-5
Junction FET	0.8-5
Single, insulated gate MOSFET	0.5-2
Single, insulated gate Power FET	5-40
Dual, insulated gate MOSFET	0.02-0.05

Table 4.1 Comparison of the feedback capacitances of various devices

Clearly, the dual-gate MOSFET has by far the lowest capacitance and is therefore the best device to use as the VCO buffer amplifier.

For the amplitude modulator, there are other requirements which must be met as well as good isolation. These are:-

(i) Stable operation at all gain settings.

(ii) Minimal change in input impedance with control voltage variation (to minimise 'VCO pulling').

(iii) Wide modulation bandwidth (should be much greater than amplitude feedback loop bandwidth to avoid compromising loop stability).

(iv) Minimal baseband power required to drive control input.

To establish the best type of modulator which would satisfy all these criteria, a survey of amplitude modulators was carried out. The results are presented as follows:-

(a) JFETs and Bipolar transistors

There are two ways in which JFETs or bipolar transistors may be used as modulators. The first is to modulate the drain (or collector) supply voltage, known as the Heising modulator after its inventor. The second is to superimpose the modulation on the RF carrier at the input (gate or base). Heising modulation is unsuitable for this application due to the large baseband power required, since the full drain (or collector) current must be supplied by the audio driving amplifier. Gate (or base) modulation does not suffer from this difficulty, and reports have appeared in the literature of successful applications of gate modulated JFETs (70, 71, 72, 73), and base modulated bipolar transistors (74, 75, 76). Unfortunately, none of these authors address the main problem of UHF operation - achieving adequate isolation. For example, a feedback capacitance of typically 2pF in conjunction with a source impedance of 200Ω, implies a maximum attenuation of only 6dB at 450MHz, which is totally inadequate. An additional problem is the variation in input impedance. A JFET will vary its gate to source capacitance, while a transistor will vary its base-emitter resistance with control voltage.

(b) Power FETs

The Power FET is a relatively recent RF device, which has an insulated gate structure, and is capable of operating at many tens of watts of output power. These devices have been very successfully utilised as amplitude modulators, using gate modulation (77), but only at HF and VHF. At the time of writing, no suitable devices were available for UHF operation, due mainly to the relatively large feedback capacitances which they possess.

(c) PIN diodes

The PIN diode has many applications, of which amplitude modulation is one (78). This device functions by varying its RF resistance with the d.c. current flowing through it, and can be varied from a few ohms to several Kilohms. Due to its intrinsic (I) layer between the 'P' and 'N' layers, the feedthrough capacitance in the 'off-state' is very low, 0.2pF typically. Thus it is possible to achieve over 30dB of attenuation at 450MHz in a 50Ω system. Associated with a PIN diode is a charge storage time, τ, which defines the switching time. This is usually in the range 0.1-3μs. Initial experimentation with a 0.1μs diode, showed that in an analogue modulation mode, the modulation bandwidth was much less than that implied by the 0.1μs specification. RF envelope risetimes of several μs were noted, which is too slow for this application. Other drawbacks of the PIN diode are: impedance variation and the relatively large control current needed (tens of mA).

(d) Schottky diode balanced mixers

Although the diode ring balanced mixer could be used as a modulator, it shares some of the disadvantages of the PIN diode, namely, the input impedance variation, and the large control power required. It is also a completely passive device and so must be associated with additional amplification, particularly as its output power level is likely to be very low (< 1mW).

(e) Dual-gate MOSFETS

As noted previously, the dual-gate MOSFET has very low feedback capacitance, giving it excellent isolation. A value of 0.03pF with a load impedance of 200Ω corresponds to 35dB of attenuation at 450MHz. Since the gates are of the insulated type, there is little change in input impedance with gate voltage. Negligible gate power is required from the modulating amplifier and due to the low gate to source capacitance (< 2pF typically), modulation bandwidth can be made very wide (several MHz).

(f) Selection of Amplitude Modulator

From this review of modulator types, it can be seen that the dual-gate MOSFET meets all the requirements of the UHF modulator, and is therefore the obvious choice for use in the practical system.

4.3 EFFECT OF UHF OPERATION ON PHASE NOISE

Of the constituent parts which make up a polar loop transmitter, and which make a significant contribution to its output phase noise level, only the VCO and the downconversion oscillator operate at, or near channel frequency. Since the practical downconversion oscillator would be synthesised, it would require a VCO virtually identical to that used in the main transmitter circuit. The effect of UHF operation on the output phase noise is therefore defined by the phase noise performance which can be achieved in a UHF VCO.

The following sections look at the criteria affecting oscillator noise level, and review the possible oscillator designs to establish the type most applicable to a UHF polar loop transmitter.

4.3.1 Oscillator Phase Noise

Oscillators for use at radio-frequencies all utilise some form of resonator to provide selectivity, ensuring that oscillation takes place at a particular frequency. If the resonator is single port, then the oscillator active device acts as a negative resistance to cancel the positive load resistance. If it is two-port, then the resonator is configured as a positive feedback path around an amplifier.

The negative resistance or amplifier gain will, in practice, be a non-linear function of signal amplitude, defining the maximum output power level for which oscillation can be sustained.

Many researchers have made mathematical analyses of such oscillators (for example, 79, 80, 81, 82, 83, 84), but a particularly simple treatment has been made by Leeson (85) for the feedback oscillator. All of these works derive the output spectrum of the oscillator to be as shown in Figure 4.2. Malling (84) has shown that the negative resistance type oscillator can be transformed into the feedback oscillator configuration, and therefore has the same form of spectrum. This has been verified experimentally by Leeson (86), who compares the spectra of several different types of microwave sources, all of which conform to Figure 4.2.

Referring to the diagram, it can be seen that for offset frequencies outside the resonator bandwidth, the spectrum is simply the thermal noise level degraded by the device noise figure. This is random fluctuation in both amplitude and phase. Moving in from the oscillator bandwidth, the noise level rises with a second order dependence on offset frequency. This is random phase modulation of the oscillator, or phase noise. Note that the slope in this region is -6dB/octave, since the power, as opposed to voltage spectrum, is being considered. At closer offsets, the phase noise displays a third order response. This is due to '1/f' (or flicker or excess) noise in the active device, at baseband, increasing the unwanted phase modulation. The offset below which this becomes significant is typically 100KHz (86).

To minimise the oscillator phase noise, it is clear that the device noise figure should be as low as possible,

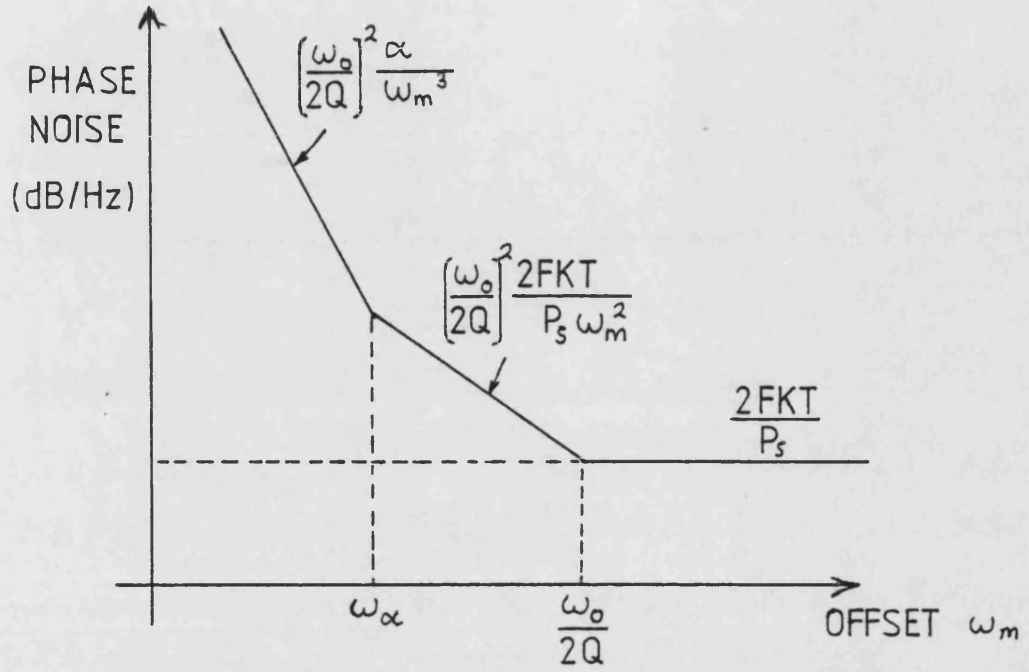

Figure 4.2 : Oscillator Phase Noise Spectrum

where:-

ω_o = Frequency of Oscillation

Q = Loaded Quality Factor

ω_m = Offset Frequency

F = Device Noise Figure

K = Boltzmanns Constant

T = Absolute Temp.

P_s = Signal Power

ω_α = 1/f Noise Break Frequency

and the carrier power level as large as possible. The only other factor over which the designer has some control, is the resonator Q, and since the spectrum is inversely dependent on Q^2, this is the single most important aspect of the oscillator design. Also notable is the fact that the phase noise level is proportional to $(\omega_0)^2$. Thus, for a given Q-factor, a noise degradation of at least 13dB can be expected at 450MHz, in comparison with a VHF oscillator at 100MHz, for example. At 950MHz, this becomes 19dB.

4.3.2 Review of Oscillator Designs

This review surveys oscillator configurations with particular emphasis placed on their Q-factors. Also considered are: tuning range, since a practical transmitter would be required to tune over several MHz, suitability for voltage control, and modulation bandwidth. Since phase locked loop bandwidths of up to a few hundred KHz are required, the modulation bandwidth of the VCO should be much greater than this in order to avoid reducing the loop stability margin.

(a) Crystal oscillators

Quartz crystal resonators utilise the piezoelectric properties of quartz. If an alternating voltage is applied to electrodes on opposite faces of a quartz crystal, the crystal will vibrate. At a certain frequency, dependent on the dimensions of the crystal, it will exhibit a mechanical resonance, at which the vibrational amplitude is a maximum. This resonance produces a corresponding peak in the energy

absorbed from the source of excitation, and hence a minimum in the electrical impedance presented by the electrodes. The resonator can therefore be represented by an equivalent series resonant circuit in parallel with the inter-electrode and holder capacitance, as shown in Figure 4.3.

Crystals will also resonate at overtones, that is to say, frequencies which are approximately odd-number multiples of the fundamental mode.

The Q-factors of crystal resonators are very high, typically in the range 10^4 to 10^5, but can be in excess of 10^6 for precision crystals (87). For this reason a properly designed crystal oscillator can have very low phase noise.

To facilitate voltage tuning of such an oscillator, a varactor diode can be associated with the capacitance C_0. The motional (series resonant) arm then acts as the inductor in an equivalent parallel resonant circuit. Characterisation of voltage-controlled crystal oscillators (VCXOs) has received little attention in the literature, the most notable papers being due to Stanesby (88), and more recently, Garner (89). These authors note that the tuning range of a VCXO is limited by the parallel to motional capacitance ratio, and is given approximately by the expression:-

$$\frac{\Delta_\omega}{\omega_s} \approx \frac{C_1}{2C_0} = \frac{1}{2p} \qquad (4.1)$$

where Δ_ω = max. freq. deviation (r/s)

ω_s = series resonant freq. (r/s)

C_1 = motional arm capacitance (F)

C_0 = parallel capacitance (F)

p = capacitance ratio.

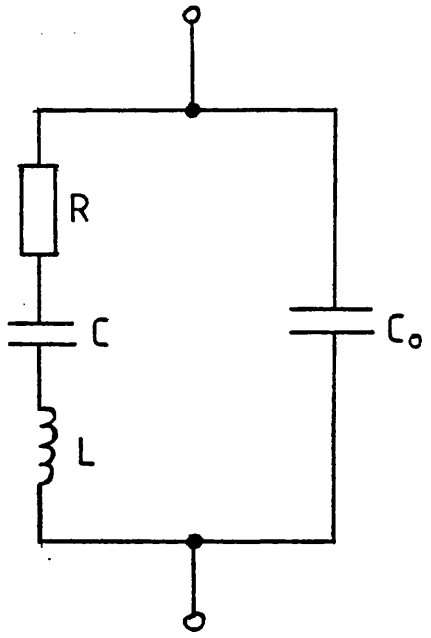

Figure 4.3 : Equivalent Circuit of a Quartz Crystal Resonator

In practice, for a fundamental mode crystal, this tuning range will be between 10^{-5} and 10^{-3}, corresponding to 4.5 and 450KHz for a 450MHz oscillator. By connecting an inductor in parallel with the crystal, C_0 can be partially tuned out, reducing ρ. Garner has shown that a tuning range of up to 10^{-2} (4.5MHz) is achievable in this way, but at the expense of lowering the Q-factor to 10^3. However, since fundamental mode crystals cannot be fabricated for use significantly above 10MHz (87), this implies frequency multiplications of 45 (or 95) times are required for this application. Thus, the effective Q-factor is then only $10^3/45$ (or $10^3/95$) which is 21 (or 11). The use of an overtone mode oscillator does not help in this respect, since the tuning range reduces by the overtone number squared (89).

(b) Surface acoustic wave oscillators

In common with bulk quartz crystals, surface acoustic wave devices rely on the piezoelectric excitation of a mechanical vibration in an elastic solid. As their name implies though, the displacement is confined to one surface of the material only. This phenomenon was first investigated by Rayleigh (90), but it was not until the advent of the interdigital transducer in 1965 (91), that practical devices appeared.

A surface acoustic wave (SAW) device consists of a piezoelectric substrate, usually either quartz, or more commonly, lithium niobate, upon which is deposited one or more interdigital transducers (IDT). The two devices rele-

vant to oscillator applications are: the delay-line and the resonator, as shown in Figure 4.4.

Consider first the delay line. If this is configured as the feedback element around an amplifier, and the loop gain is greater than unity, then oscillation can occur at any frequency where the total loop delay corresponds to an integer number of wavelengths. This condition is satisfied by a comb of frequencies spaced by $1/T_d$, where T_d is the total delay time (92). To ensure single mode operation, the delay line amplitude response must be tailored, such that the loop gain condition is satisfied at only one frequency. This is accomplished by making the inter-finger spacing of the IDTs equal to half a wavelength at the desired frequency, and by making the number of finger pairs equal to the number of wavelengths of delay (93). The effective Q of the delay line depends on its phase slope (rate of change of phase with frequency) which is equal to the time delay. The relationship is given by Underhill (94) as:-

$$Q = \pi M \qquad (4.2)$$

where M = number of wavelengths delay.

Since the propagation velocity of surface acoustic waves is typically of the order of 3000m/s (96), high M-value lines can be fabricated which are physically quite small. For example, if M = 300, giving a Q of approximately 1000, the line length at 450MHz would be only 2mm, allowing the packaged device to be very rugged, ideally suited to the mobile radio environment.

Equation 4.2 implies that the Q-factor can be increased

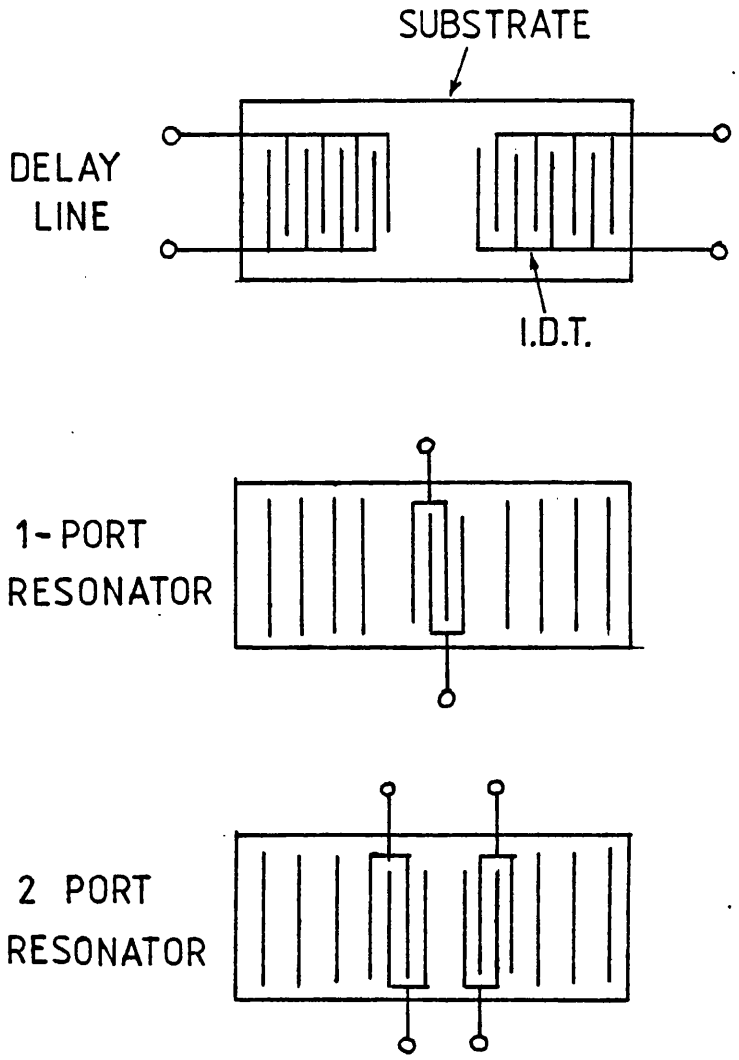

Figure 4.4 : Surface Acoustic Wave (SAW) Delay Line and Resonators

virtually without limit - allowing any phase noise specification to be met. However, when voltage tuning is required, Q and tuning range are inversely related. By inserting an additional (voltage variable), phase shift within the loop, frequency modulation can be effected. Gratze (93) shows that the tuning range is given by:-

$$\frac{\Delta f}{f_o} = \frac{\Delta \phi}{2\pi M} = \frac{\Delta \phi}{2Q} \qquad (4.3)$$

where Δf = frequency deviation (Hz)

f_o = centre frequency (Hz)

$\Delta \phi$ = voltage controlled phase shift (rad).

If the phase shifter has a range of 90^o, and a tuning range of 1MHz at 450MHz is required, the Q will therefore be 350.

Clearly, in practice, a compromise between Q and tuning range must be reached, but the examples show that Qs of several hundred are entirely feasible, in conjunction with adequate tuning ranges.

The other SAW device useful for oscillator stabilisation is the SAW resonator, which can either be in one or two-port configurations. Unlike the delay-line, where the wavefronts propagate from one IDT to the other, in the resonators, the waves travel back and forth between reflectors, setting up a standing-wave pattern. This acoustic resonance causes a corresponding resonance in the electrical impedance at the port(s) almost identical to that of a bulk crystal resonator. The equivalent circuits which model SAW resonators near resonance, are likewise very similar to

those of their volume wave counterparts, and according to (97) are shown in Figure 4.5.

The series resonant circuit represents the acoustic cavity resonance, C_0 is the interelectrode and stray capacitance, and R_0 is a radiation resistance representing loss due to the imperfect reflectors.

Bell and Li (97) have made a comprehensive study of the loss mechanisms in SAW resonators, and have shown that the theoretical maximum Q factor is limited by substrate and diffraction losses. Values in excess of 10^4 at 1GHz are reported, depending on the material used. In practice, other losses limit the Qs obtainable but they are nevertheless usually very much higher than delay line Q factors. Joseph (92) reports a 394MHz two-port resonator with a Q of 8600.

To voltage control a two-port resonator oscillator, it is necessary to use an electronic phase shifter in the loop, as in the case of the delay-line. This results in a tuning range little greater than the device bandwidth, 46KHz in the example above. The same author reports a frequency drift of 140KHz over a 100°C temperature range for this oscillator, implying that some form of temperature stabilisation would be required if the PLL is to remain locked. Other researchers have confirmed this difficulty. Ragan (97) notes a drift with temperature, three times greater than the tuning range, for a 200MHz oscillator. Even if the stability problem can be eliminated, the tuning range is still an order of magnitude too low for a polar-loop application.

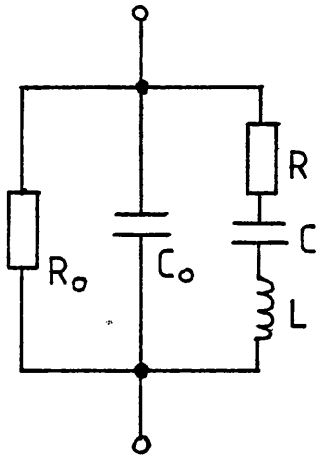

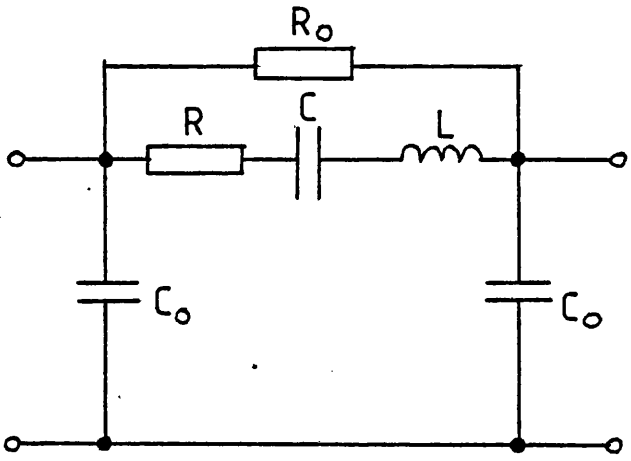

Figure 4.5 : Equivalent Circuits of
One and Two-Port SAW Resonators

From the similarity of their equivalent circuits, it is apparent that the one-port resonator can be used in conventional crystal oscillator circuits. This means it may be used as a high-Q reactance rather than a bandpass filter, as formed by the two-port device. Joseph shows that there are regions of shallower phase slope above and below resonance, where the device is reactive. In this mode, tuning ranges of 400-500KHz are possible, but the higher insertion loss and lower effective Q, means that the advantage over the delay line is lost. It has been shown (98), that a one-port SAW resonator can be made with a distributed structure, where the transducer is interdigitated with the reflectors, resulting in a wider bandwidth. Such devices may prove useful for oscillator frequency control.

In a novel development, Cross *et al* (99) have added a third IDT to a two-port resonator, to produce a three-port device. By connecting an impedance across the central port, the resonant frequency is found to vary in accordance with its magnitude. Although the work is at an early stage, tuning ranges up to 0.5% (2.25MHz at 450MHz) are predicted, with Q-factors no worse than those of conventional two-port resonators.

(c) Ferromagnetic resonance oscillators

Certain substances, said to be gyromagnetic, change their character of propagation of electromagnetic energy when a steady magnetic field is applied to them.

In gyromagnetic compounds, spinning electrons give rise

to a magnetic dipole and an angular momentum for their associated ions. If an external magnetic field is applied, these dipoles will tend to align themselves with the field. Any displacement from the alignment will cause them to precess about the field axis by gyroscopic action, with a frequency of rotation proportional to the applied field, H_o (100). When a radio frequency field is applied in addition but perpendicular to the d.c. field, a resonant condition will exist if its frequency is near or equal to the natural precession frequency of the spin system.

The gyromagnetic materials commonly used at microwave frequencies, are the ferromagnetic oxides known as ferrites. A ferrite which has been used extensively for microwave filters and resonators, is yttrium iron garnet (YIG), due to its particularly sharp resonance. The Q-factor of a YIG resonator varies according to its geometry and the degree of surface polishing, but is usually several hundred (101). Practical devices use a sample of YIG (usually a sphere or disc) to couple two electromagnetic ports such as loops, waveguides or striplines (101). The coupling is a maximum at the resonant frequency of the ferrite.

Oscillators using ferromagnetic resonators can have both low phase noise and wide tuning ranges. Unfortunately, relatively large and slow acting electromagnets are required to vary the resonant frequency, giving an inadequate modulation bandwidth.

(d) Cavity resonator oscillators

A cavity resonator comprises electrically conducting walls, enclosing a dielectric region, of such dimensions that a resonance of electromagnetic energy can exist for certain frequencies.

Many geometric forms of cavity are possible among the commonest types being: rectangular, cylindrical, spherical, coaxial or helical. In all cases, at least one of the internal dimensions must be an exact multiple of half-wavelengths at the resonant frequency. When RF energy is coupled into the cavity at this frequency, standing-waves of electric and magnetic fields will be set up. Once excited, the oscillating fields will decay only due to power dissipated in the walls and in the dielectric (usually air), and since both these losses can be made low, the available Q-factors can be very high. Many authors have made theoretical analyses of the Q-factors of various cavities, for example, (100, 102, 103). In (104) practical Q-factors are given, which at 1GHz lie between 10^4 and 10^5 depending on the geometry. These are unloaded values. When connections are made to an external circuit either via a probe (electric field coupling), or a loop (magnetic field coupling), to form an oscillator, the loading so caused will reduce these figures.

To voltage control a cavity oscillator it is necessary to use a varactor diode connected to the circuit. The additional capacitance introduced, is balanced by a shift downwards in resonant frequency, where the cavity behaves

as a high-Q inductor. In practice, this can be conveniently implemented by using a coaxial cavity with one end short-circuited. The open-end will then appear inductive if the cavity is less than one quarter wavelength long, in accordance with simple transmission line theory. A varactor diode connected at this point completes the resonant circuit. Since the varactor will inevitably be lossy, a further Q degradation will result, depending on the tuning range required, and hence on how significant a part of the equivalent tuned circuit the varactor is. In laboratory cavity signal generators, phase noise levels of -140dB/Hz at 20KHz offset are possible, over an octave tuning range of 250 to 500MHz.

An obvious disadvantage of using a cavity at UHF, is the relatively large physical dimensions required: a quarter wavelength at 450MHz for example, is 17cm. Although of no consequence electrically, this factor may be important in a mobile radio situation where space is at a premium. For hand-held portables, there is no doubt that a cavity would be totally impractical. The use of a dielectric other than air will help in this respect, since the wavelength in a medium reduces by a factor of $\sqrt{\varepsilon_r}$, where ε_r is the relative dielectric constant (100).

A further development is to eliminate the metal cavity walls, and use the piece of dielectric as a resonator in its own right. Although there will be loss in the dielectric, the absence of conductor loss means that the Q-factors of dielectric resonators can be as high as those of cavities (105).

The physical forms usually used are either cylindrical (106) or rectangular (107).

Unlike the cavity, which is not readily interfaced with printed circuitry, the dielectric resonator may be simply coupled to an oscillator circuit by mounting on the same board, near to a microstrip transmission line, such that the electric and magnetic fields from the line impinge on the resonator (108). The tuned circuit formed by the resonator and the other elements of the oscillator, may be voltage tuned using a varactor as in the case of a cavity oscillator. Alley (67), has constructed such a VCO, using a dielectric resonator of barium titanate, with a Q of 14000. The phase noise level was -140dB/Hz ag 2KHz offset from 1GHz, although in this case the tuning range required was quite small at 40ppm. Larger ranges would mean an increased noise contribution from the varactor.

(e) LC Oscillators

The final category of oscillator to be considered in this review is the LC or inductor/capacitor oscillator. This is without doubt the most widely used form of oscillator to be found in radio communication equipments. It utilises the resonant circuit formed by the parallel connection of an inductor and capacitor as the frequency selective element in the feedback path of an amplifier. Voltage tuning is accomplished by associating a varactor diode with the capacitance. The two main forms of LC oscillator are the Colpitts and Hartley, named after their inventors, and shown in Figure 4.6.

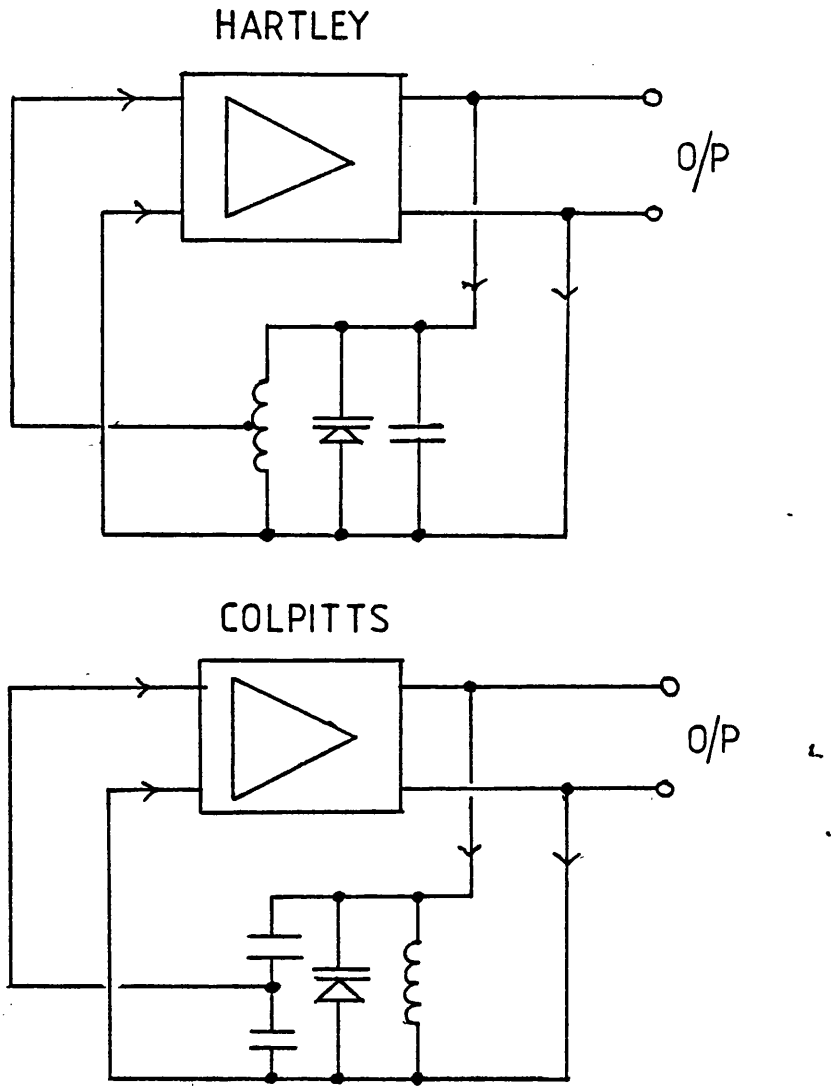

Figure 4.6 : LC Oscillator Configurations

Although there are many variations possible on the two configurations shown, these serve to illustrate the two forms of feedback arrangement, namely, either a capacitive or inductive potential divider.

The Q-factor of an LC-resonator (or 'tank'-circuit) will be governed almost entirely by that of the inductor if this is implemented as a simple coil. The author has made measurements of the Q-factor at UHF of several coils with inductances of up to 20nH. Values of between 20 and 50 were found to be typical. In contrast, low-loss ceramic capacitors can have Q-factors of several hundreds at frequencies below 1GHz. Clearly, a UHF oscillator employing such an inductor would have a very poor performance.

An alternative means of implementing an inductance is to use a transmission line short-circuited at one end. The open end will have an inductive reactance given by:-

$$X_L = Z_o \tan\left(\frac{2\pi\ell}{\lambda}\right) \Omega \qquad (4.4)$$

where Z_o = characteristic impedance of line

ℓ = length of line (m)

λ = wavelength (m)

Using: $X_L = 2\pi fL$ and $c = f\lambda$ gives:-

$$L = \frac{Z_o}{2\pi f} \tan\left(\frac{2\pi f\ell}{C}\right) H \qquad (4.5)$$

where f = frequency (Hz)

C = velocity of propagation (m/s)

A particularly practical form of transmission line, which has found widespread use in microwave circuits, is the

microstrip. This takes the form of a thin conducting strip separated from a groundplane by a dielectric, as shown in Figure 4.7.

The characteristic impedance of microstrip is determined by the width to height ratio (W/h), and the relative dielectric constant, ε_r, assuming that the strip thickness, t, is negligible compared to W. There have been many derivations of the characteristic impedance, but most only apply over a narrow range of W/h ratios. The most accurate is due to Wheeler (109) and Sobol (110). Sobol's formula for characteristic impedance is reproduced here:-

$$Z_o = \frac{377}{\left(\frac{W}{h}\right)\sqrt{\varepsilon_r}\left[1 + 1.735\ \varepsilon_r^{-0.074}\left(\frac{W}{h}\right)^{-0.836}\right]} \qquad (4.6)$$

Losses in microstrip arise in both the conductors and the dielectric. A comprehensive study (with experimental verification) of these losses has been made by Pucel (111). Approximate formulae, derived from Pucel's work are given by Liao (102):-

Q-factor due to conductor loss (copper):-

$$Q_c = 478{,}000h\ \sqrt{f_{GHz}} \qquad (4.7)$$

Q-factor due to dielectric loss:-

$$Q_d = \frac{1}{\tan\theta} \qquad (4.8)$$

where $\tan\theta$ is the dielectric loss tangent.

Substituting typical values based upon the widely used $\frac{1}{16}$" thick Teflon material gives:-

$Q_c = 510$, at 450MHz

and $Q_d = 560$.

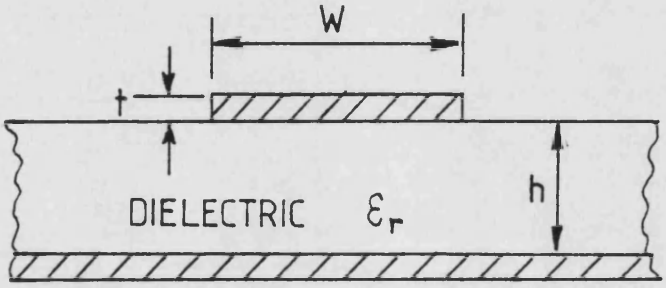

Figure 4.7 : Section through Microstrip Transmission Line

Hence, the overall Q-factor would be 270, an order of magnitude better than the coil inductor.

Since tuning is accomplished with a varactor, the tuning range and modulation bandwidth requirements are easily met.

(f) Selection of Oscillator type

This review has shown that three of the oscillators considered are potentially suited to a UHF polar loop application:- the 3-port SAW resonator, the cavity oscillator and the microstrip-LC oscillator. The first is a new development, and not yet commercially produced. The remaining two each require a varactor for tuning, which at UHF would have a Q-factor of typically 200. Hence, both types would have similar overall Q-factors. In view of its smaller size and ease of physical implementation, the microstrip oscillator is therefore the most appropriate.

4.4 CONCLUSION

It has been shown that in general, the open-loop linearity performance of a polar loop transmitter will be worse at UHF than at lower frequencies. The large amount of distortion generated by the power amplifier must be accepted, if the efficiency advantage of Class C operation is to be obtained. The reduction of this distortion must therefore rely entirely on the polar feedback. Degradation of the output spectrum due to imperfect isolation in the VCO buffer amplifier and amplitude modulator, will inevitably worsen as

the frequency is increased. However, this effect can be minimised through the use of high isolation devices, in particular the dual-gate MOSFET.

The phase noise performance will depend to a large part upon the phase noise of the VCO, which must inherently degrade as the frequency of oscillation is increased. To counter this property, the oscillator Q-factor must be increased. A review of oscillator designs has shown that the most appropriate and practical means of achieving this is to use an LC oscillator with the inductor implemented in microstrip form.

CHAPTER FIVE

DESIGN OF THE UHF POLAR LOOP TRANSMITTER

5.1 INTRODUCTION

Theoretical aspects of the Polar Loop Transmitter have been covered in the previous chapters, both in general, and for the particular case of UHF operation.

Practical designs for the transmitter circuits will now be presented. Desirable features of the designs which have emerged from the theoretical work, have been included wherever this is possible.

Chronologically, the 450MHz transmitter was constructed and evaluated before the 950MHz transmitter. As a result of this, aspects in need of further investigation which became apparent in the first transmitter, were concentrated on in the second design.

5.2 DESIGN OF THE RF CIRCUITS

5.2.1 The Voltage Controlled Oscillator

It has been established in Chapter 4 that an LC Voltage Controlled Oscillator employing a microstrip inductor is most appropriate to the UHF Polar Loop Transmitter. On this basis, practical designs for the 450MHz and 950MHz VCOs are now presented.

5.2.1.1 450MHz VCO

The VCO may use either a bipolar transistor or a field effect transistor (FET) as its active device. Examination of manufacturers' data for devices of comparable output power, revealed that both types had similar gains and noise figures (10 and 3dB being typical values, respectively). However, the FET has the advantage of simpler biassing requirements. Referring to the schematic of Figure 5.1, the base bias for the bipolar transistor must be extremely well decoupled. If it is not, low frequency noise could modulate the transistor working point, and so degrade the oscillator phase noise. In contrast, the corresponding gate bias for the FET is simply a connection to ground.

The device selected for the practical circuit was the J309 FET. This is specifically designed for VHF and UHF amplifier and oscillator applications. It gives its maximum gain of 10dB in common gate configuration at 450MHz, and has a noise figure of 3dB. It also has very low '1/f'-noise, the break frequency is only 3KHz. The Colpitts configuration is the most convenient for the common-gate format, and results in the oscillator circuit shown in Figure 5.2.

The choice of component values is a compromise. The capacitor values should be as large as possible to minimise the dependence of the oscillator on the non-linear, temperature dependent device capacitances. Similarly, the microstrip inductance should predominate over the device lead inductance. On this basis 10nH and 12pF were chosen for

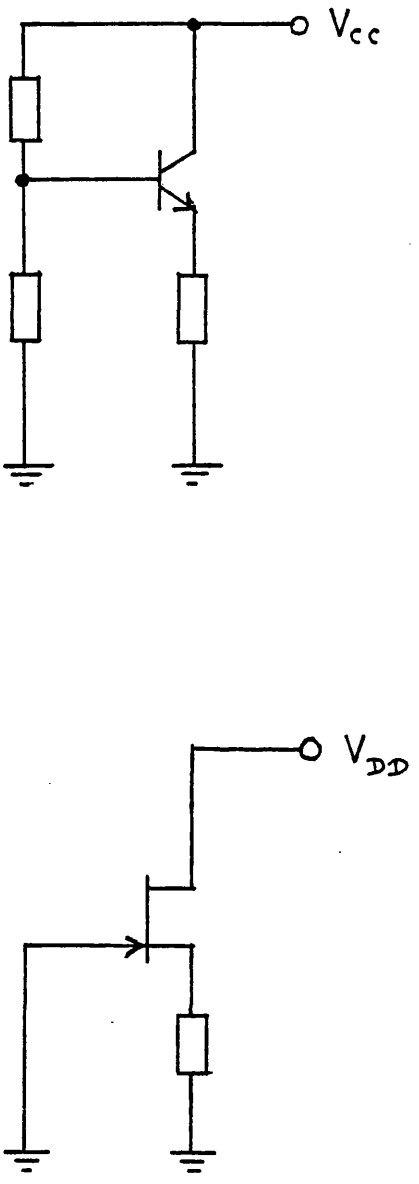

Figure 5.1 : Bipolar and JFET Biassing Arrangements

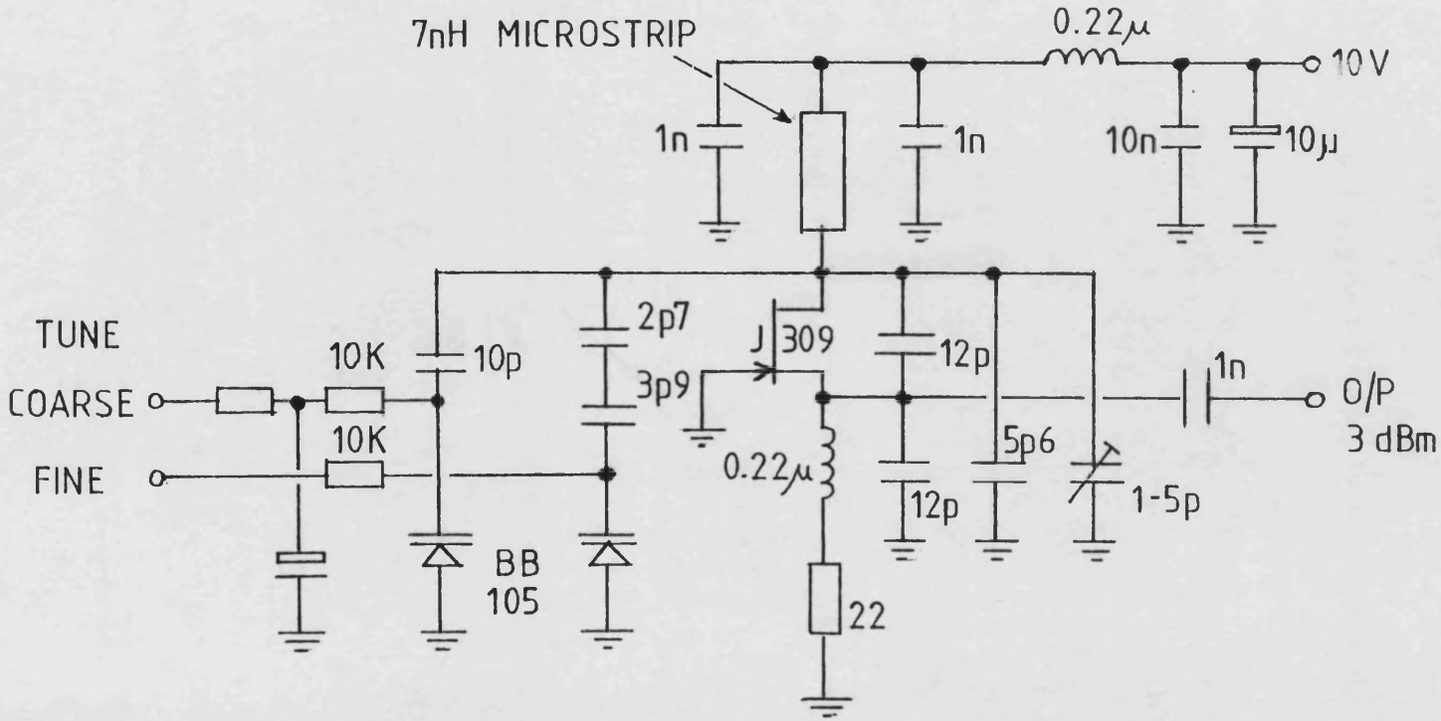

Figure 5.2 : 450MHz VCO Circuit

the overall tuned circuit element values. The microstrip dimensions were calculated from the equations 4.5 and 4.6. Two varactor diodes were used, one for the main phase locked loop error voltage and the other for coarse tuning. These give VCO constants of 240KHz/V and 1.8MHz/V, respectively, and have the characteristics shown in Figures 5.3 and 5.4. As explained in Section 3.4, this approach minimises the effect of baseband noise on the VCO control input, but still allows temperature compensation by voltage control. The temperature characteristic of the oscillator is shown in Figure 5.5.

5.2.1.2 950MHz VCO

The Colpitts configuration used for the 450MHz oscillator is impractical for use at 950MHz. Component values would have to be extremely small, to the extent of being comparable with the capacitances and lead inductances of the device itself. To overcome this difficulty, a circuit was evolved based upon an oscillator design originally proposed by Lampkin in 1939 (112). A simplified diagram of this oscillator is shown in Figure 5.6.

It can be seen that the circuit is essentially that of the Hartley oscillator, but with an additional 'tap' on the inductor. This arrangement allows the device capacitances to be shunted by a very low reactance due to the inductor, and also minimises the loading on the tuned circuit.

Applying this technique to the 950MHz oscillator results in the circuit of Figure 5.7. The device used is the BF960

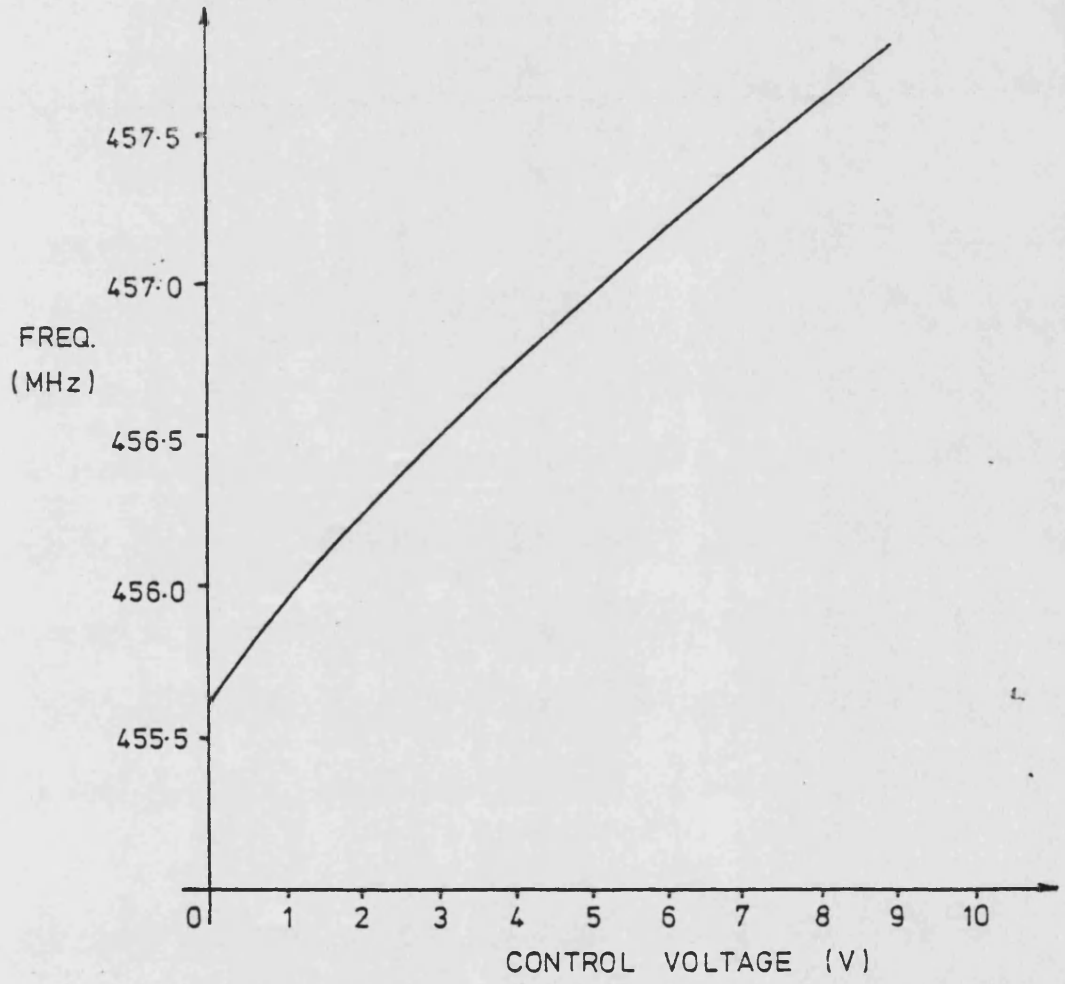

Figure 5.3 : 450MHz VCO Fine Tuning Characteristic

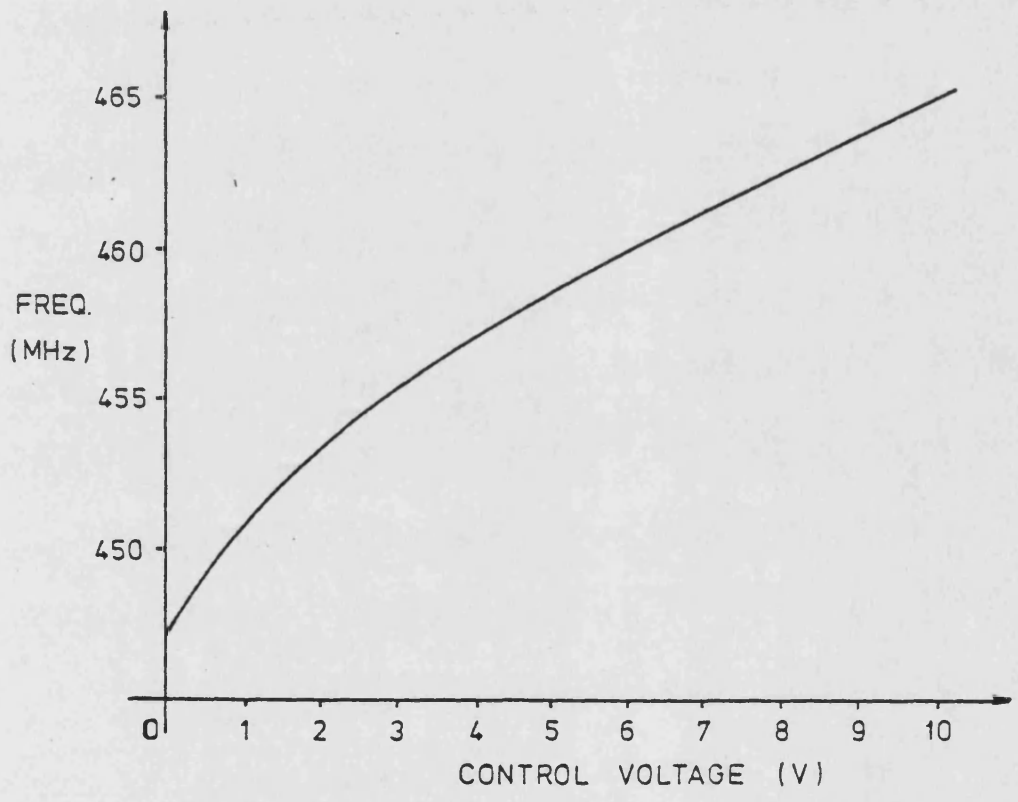

Figure 5.4 : 450MHz VCO Coarse Tuning Characteristic

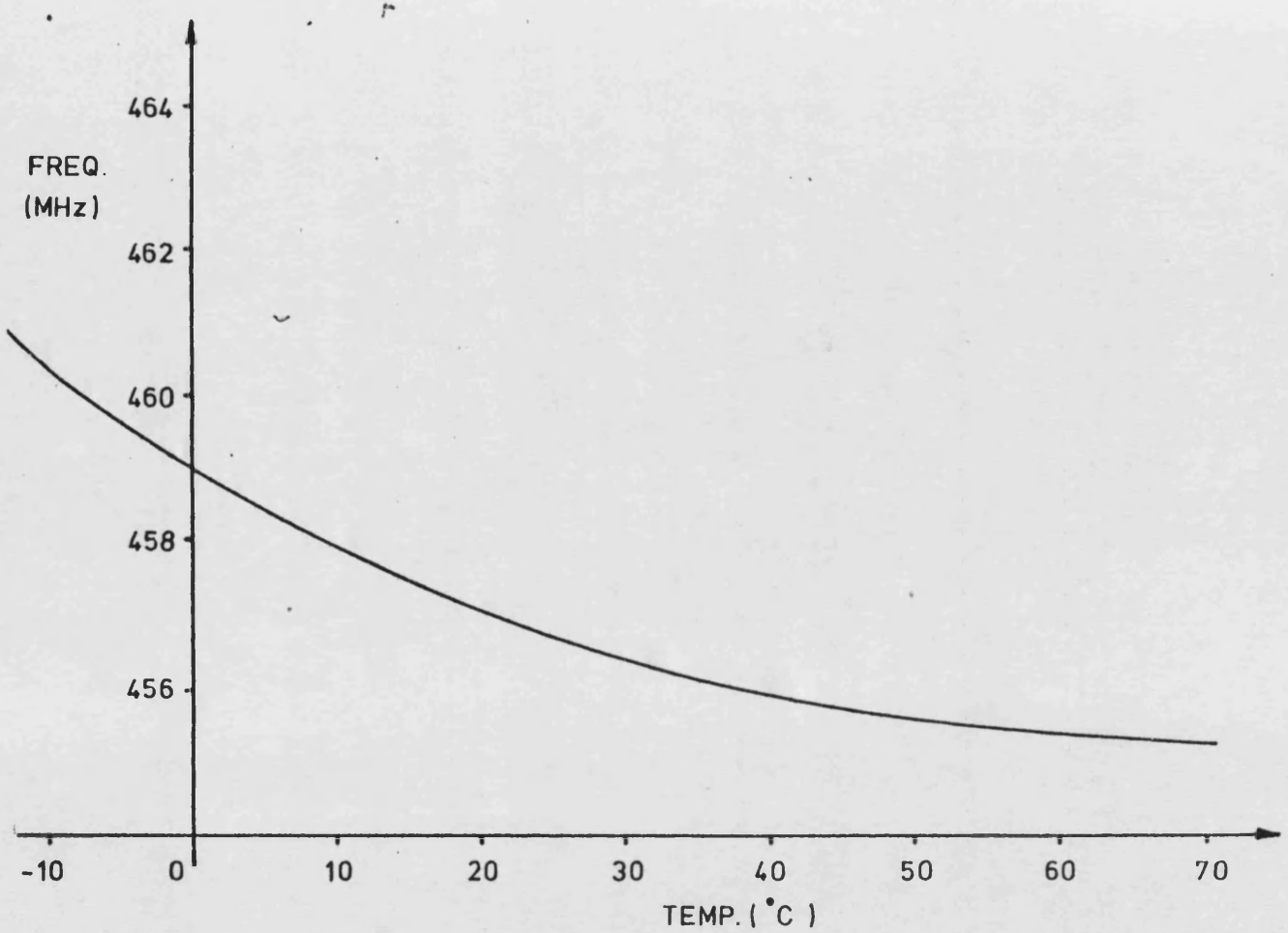

Figure 5.5 : 450MHz VCO Temperature Characteristic

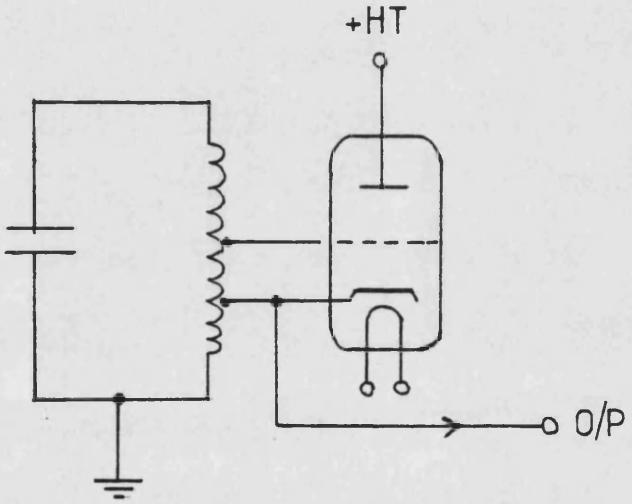

Figure 5.6 : Lampkins Oscillator

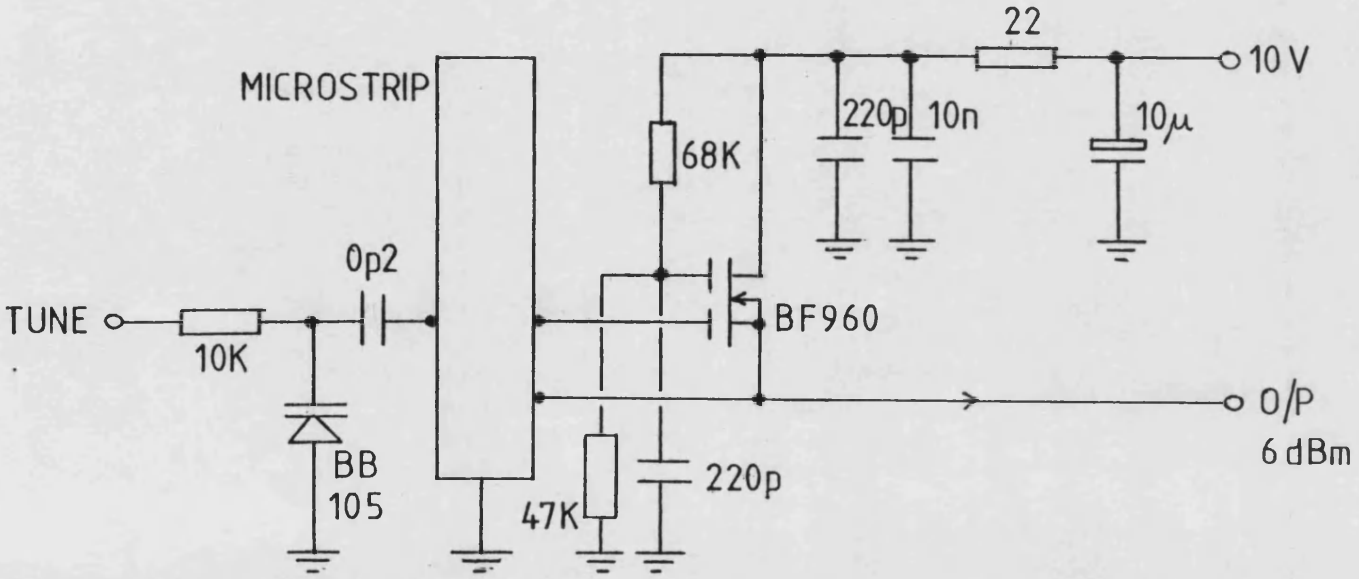

Figure 5.7 : 950MHz VCO Circuit

rather than the J309, since the latter has insufficient gain for 950MHz operation.

In this design, the capacitive element of the tuned circuit is due almost entirely to the varactor and its coupling capacitor, which is very small. This results in the microstrip being almost a quarter wavelength long.

To ensure oscillation, the gate to source and source to ground dimensions were made equal. This gives a voltage gain of 6dB between source and gate due to the transformer action of the microstrip line, which more than compensates for the loss between gate and source due to the device. A line impedance of 23Ω was used, which results in the device being shunted by an inductive reactance of approximately 10Ω. This is an order of magnitude lower than the gate to source capacitive reactance.

The characteristic of this VCO is shown in Figure 5.8. The constant of 670MHz/V is larger than that of the 450MHz oscillator, because a different form of PSD was used in the 950MHz transmitter (see Section 5.3.4). Another consequence of this, is that a second coarse tuning varactor is not required, since the oscillator's drift with temperature (shown in Figure 5.9) may be corrected with the first varactor alone.

5.2.2 The VCO Buffer Amplifier

It has been shown that the most important function of the VCO Buffer Amplifier is to isolate the VCO from load impedance changes. Furthermore, the most critical parameter

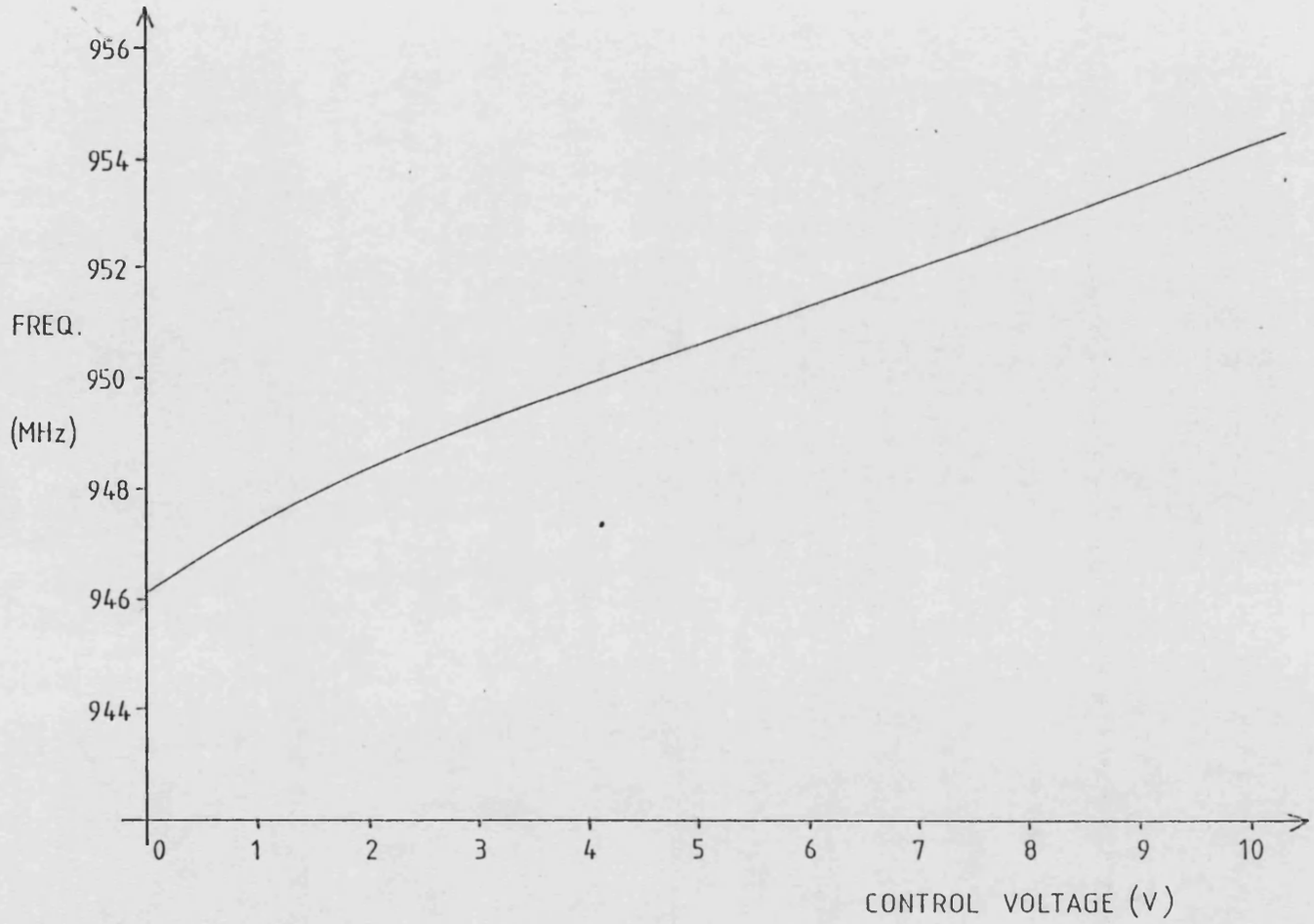

Figure 5.8 : 950 MHz VCO Tuning Characteristic

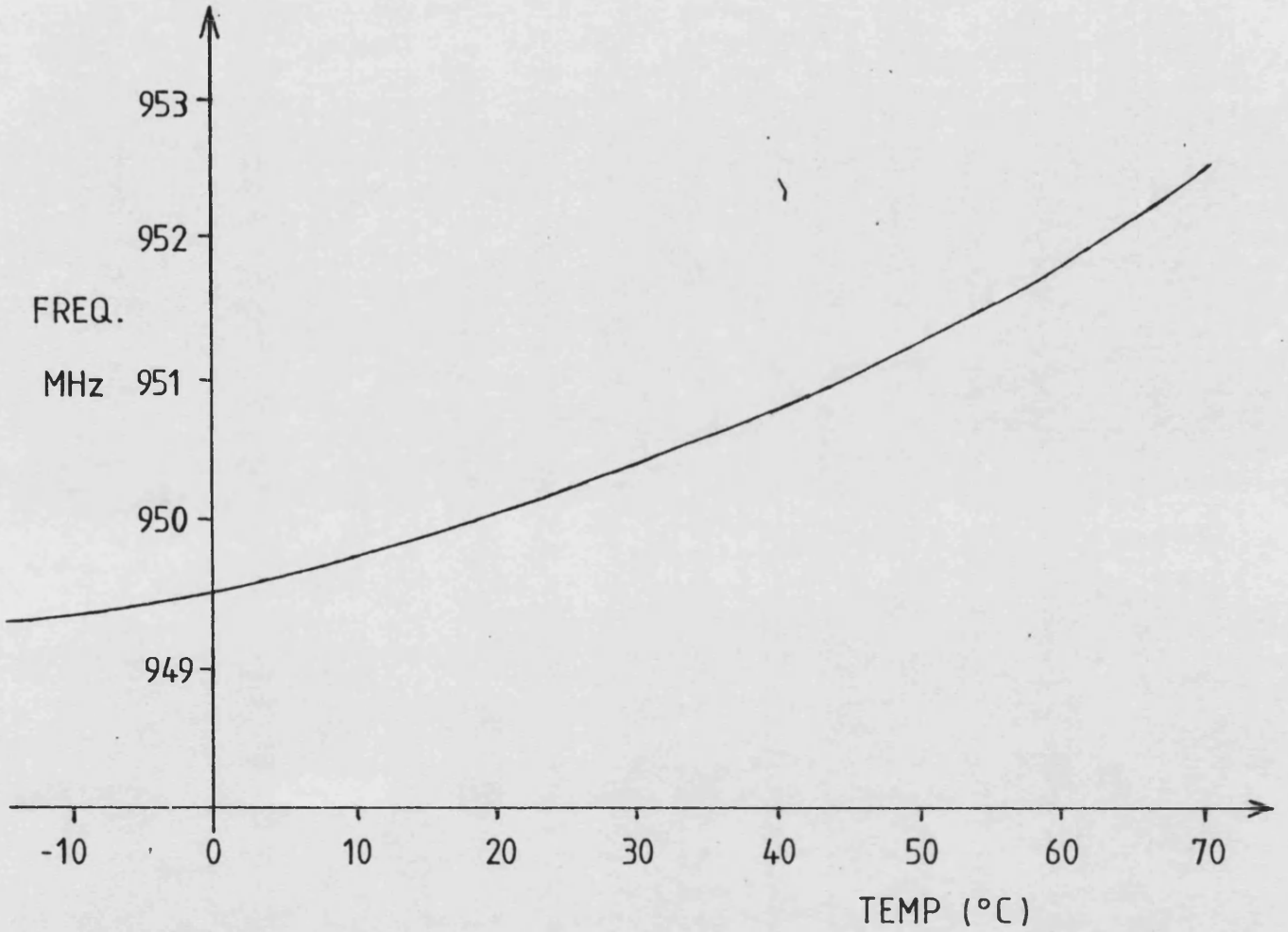

Figure 5.9 : 950MHz VCO Temperature Characteristic

of each buffer stage is its feedback capacitance, which should be as low as possible.

Both bipolar and junction field effect transistors have feedback capacitances of the order of a few picofarads, which makes them unsuitable for this application. A device which does meet the requirement is the dual-gate FET. This has a second screening gate positioned between the first gate and drain, consequently the input to output isolation is excellent. The BF960, as used in the 950MHz VCO, is one of the best devices of its kind, possessing a feedback capacitance of typically 0.02pF. Two such buffer stages proved to be extremely effective in isolating the VCO. In the case of the 450MHz transmitter, the maximum frequency pulling of the VCO due to subsequent amplitude modulation of the signal was less than 1KHz. This compares with several hundred KHz, when a JFET buffer amplifier was used. The circuit diagram of the two stage dual gate FET buffer amplifier is shown in Figure 5.10.

The 450MHz and 950MHz circuits for the buffer amplifier are very similar. The main difference, apart from the obvious scaling down of component values at 950MHz, is the way in which the tuned circuits are implemented. For the 950MHz version, the inductance and capacitance are formed using a short and open circuited microstrip transmission line respectively.

5.2.3 The Amplitude Modulator

The review of the many forms of amplitude modulator in

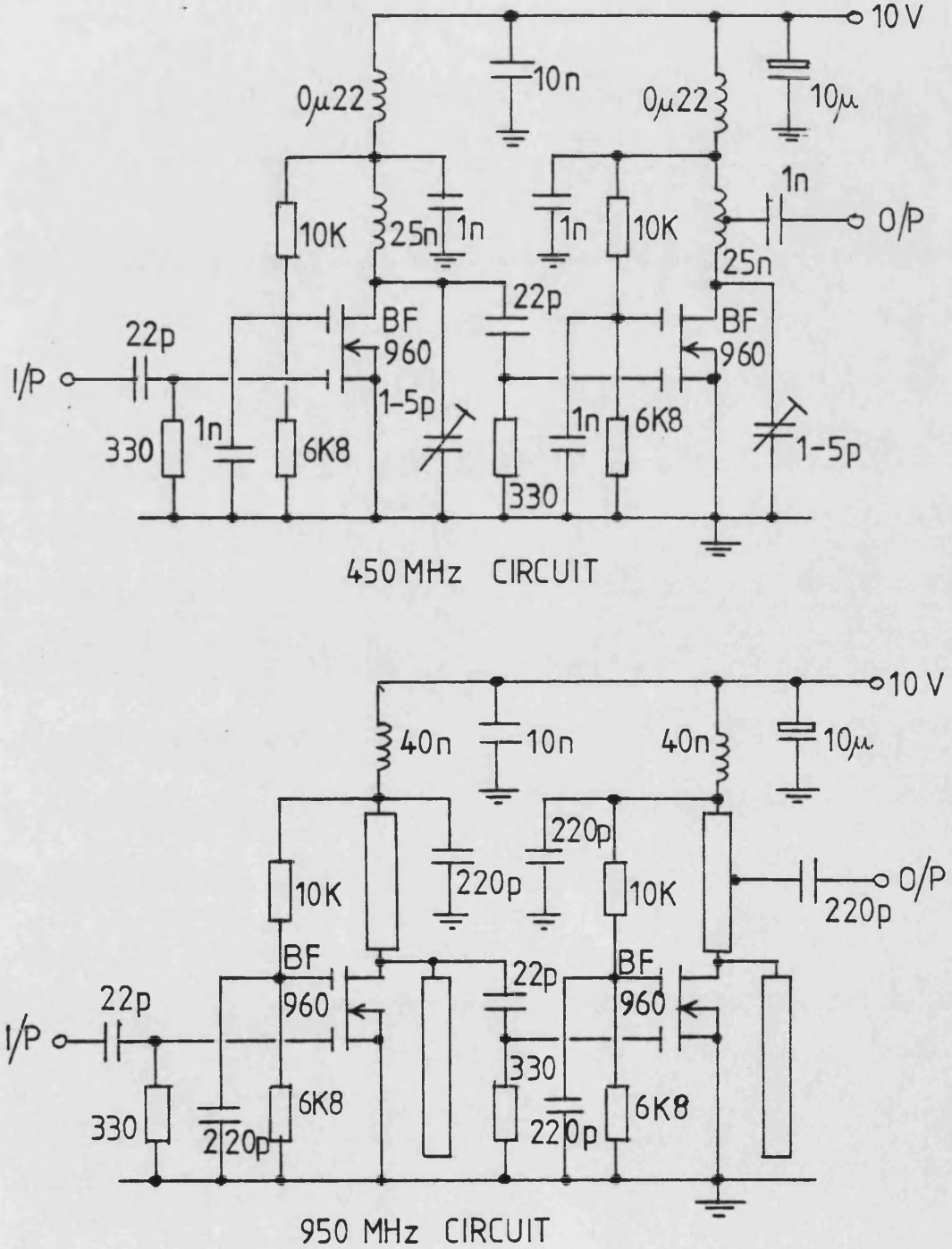

Figure 5.10 : VCO Buffer Amplifier Circuits

Chapter 4, established that the dual-gate FET is the most suitable device. It possesses the required features of large gain control range, minimal change in input impedance with gain variation, wide modulation bandwidth, stable operation at all gain settings, and draws negligible power from the modulating voltage source. The practical circuit of the amplitude modulator is shown in Figure 5.11, and again this employs the BF960 device. As in the case of the VCO buffer amplifier, the 450MHz and 950MHz circuits are distinguished by the use of microstrip lines in the latter. It can be seen that both circuits use two devices connected in parallel. This permits a maximum output power of 22dBm to be obtained, which is sufficient to directly drive the following power amplifier. The direct paralleling is only feasible by virtue of the fact that FETs have negative temperature coefficients of drain current, and so inherently current share.

The only unusual feature of the circuits shown, is the application of the gain control voltage to gate 1. The conventional arrangement is to apply the RF input to gate 1, and the control voltage to gate 2. However, in order to provide the maximum isolation between input and output, gate 2 (the screening gate) should be well decoupled. Unfortunately this would also limit the modulation bandwidth, which may degrade the amplitude feedback loop stability. A second factor is the voltage swing which must be applied to gate 2 in order to obtain the full amplitude variation from cut-off to saturation. This is typically -3V to +5V, which

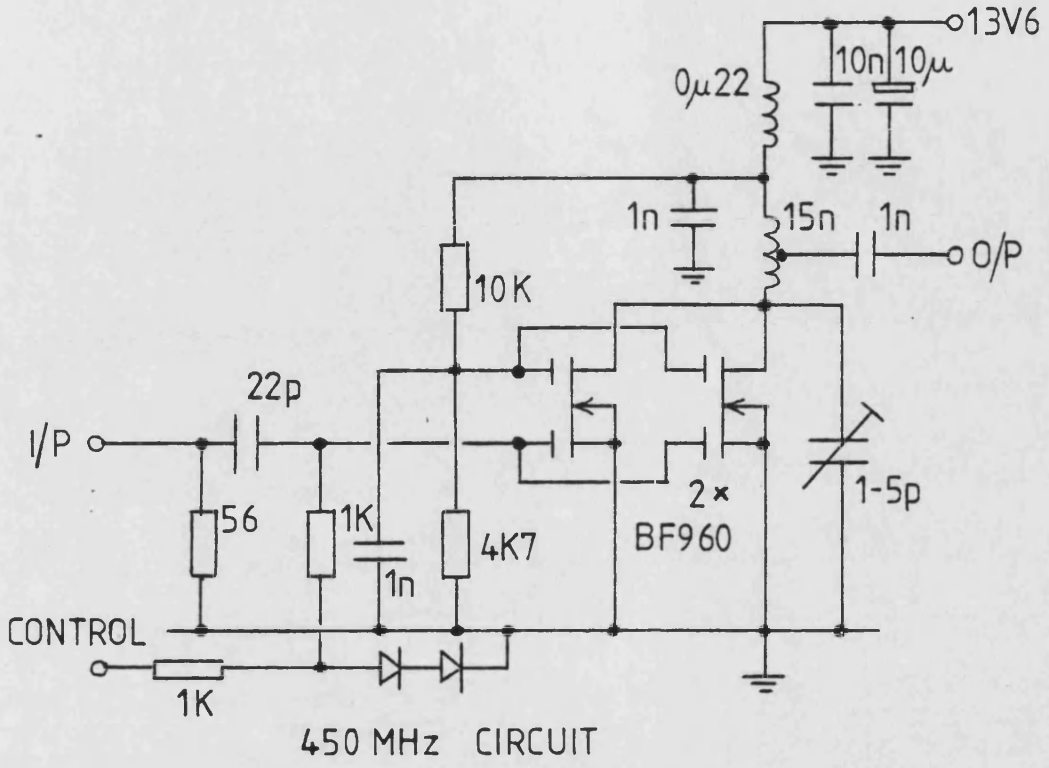

450 MHz CIRCUIT

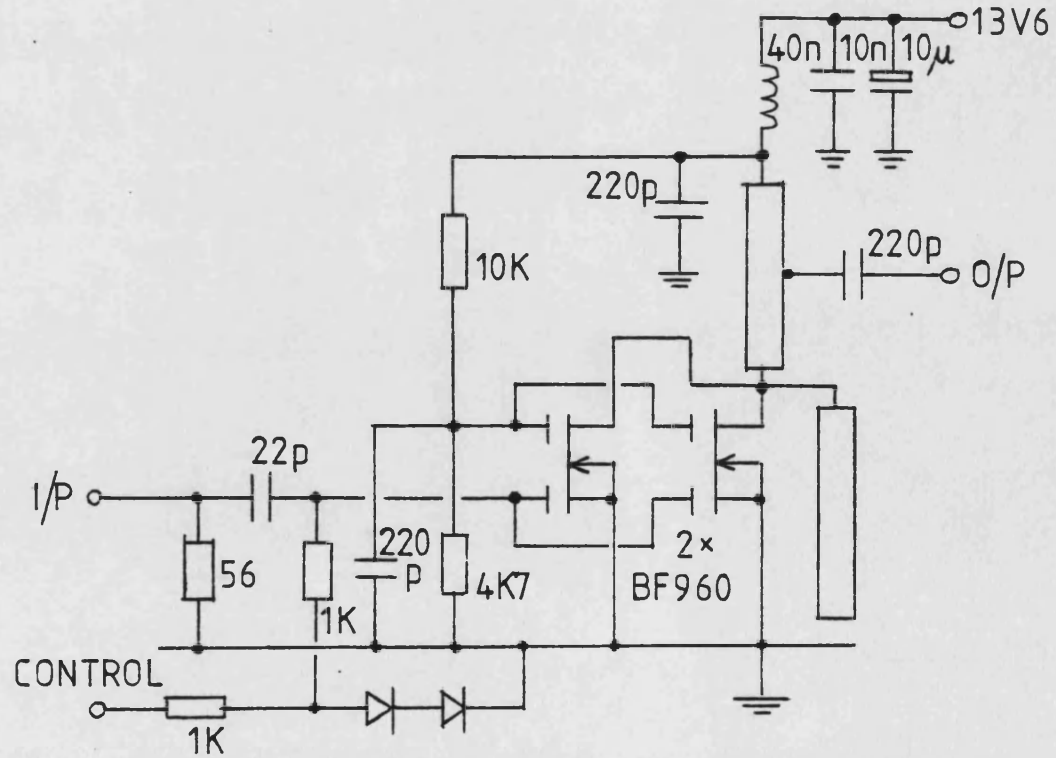

950 MHz CIRCUIT

Figure 5.11 : Amplitude Modulator Circuits

could result in the modulating amplifier slew rate limiting. In view of these potential problems, gate 1 was used both as the RF and the modulation input. This resulted in a modulation bandwidth of 3.5MHz and a total control voltage excursion of -3V to +1V. The amplitude control characteristics of the 450MHz and 950MHz modulators are shown in Figures 5.12 and 5.13. Also shown are the characteristics of the modulators and their associated power amplifiers when combined. It can be seen that the threshold action of the class C amplifiers considerably increases the control range to in excess of 80dB.

5.2.4 The Power Amplifier

5.2.4.1 The 450MHz Power Amplifier

For the 450MHz transmitter, advantage was taken of one of the many commercially available power amplifier modules manufactured for this band. Such modules are invariably class C biassed since they are intended primarily for inclusion in FM equipments. The module used is a 3-stage amplifier, which has a saturated output power of 10W minimum, and a gain of 20dB. Its efficiency in CW mode is 35%. The circuit diagram for this amplifier is shown in Figure 5.14.

A simple resistive potential divider provides a sample of the output signal for the feedback circuits.

5.2.4.2 The 950MHz Power Amplifier

When the 950MHz transmitter was constructed, there were no power amplifier modules available for this frequency.

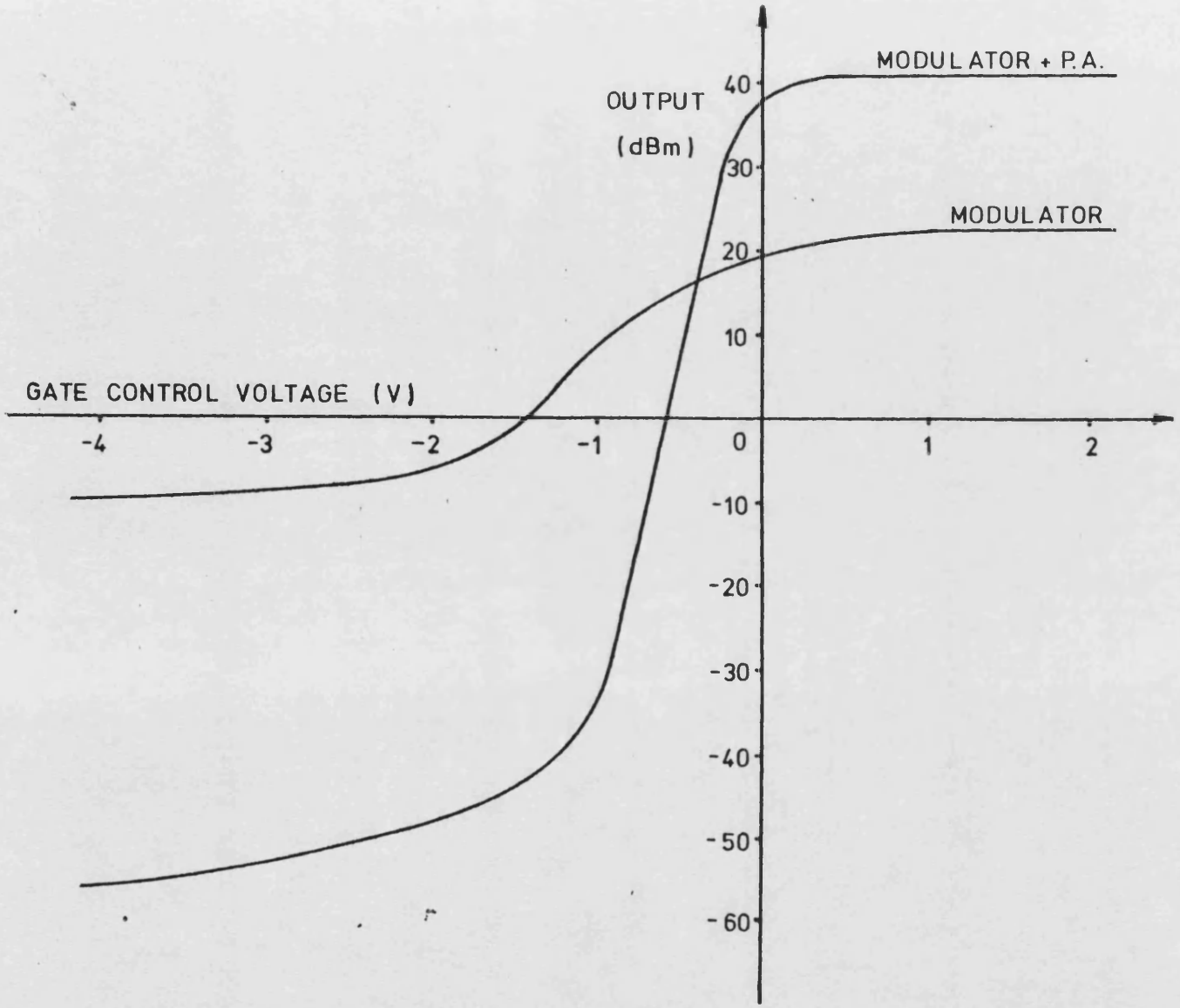

Figure 5.12 : Amplitude Control Characteristic of the 450MHz Amplitude Modulator

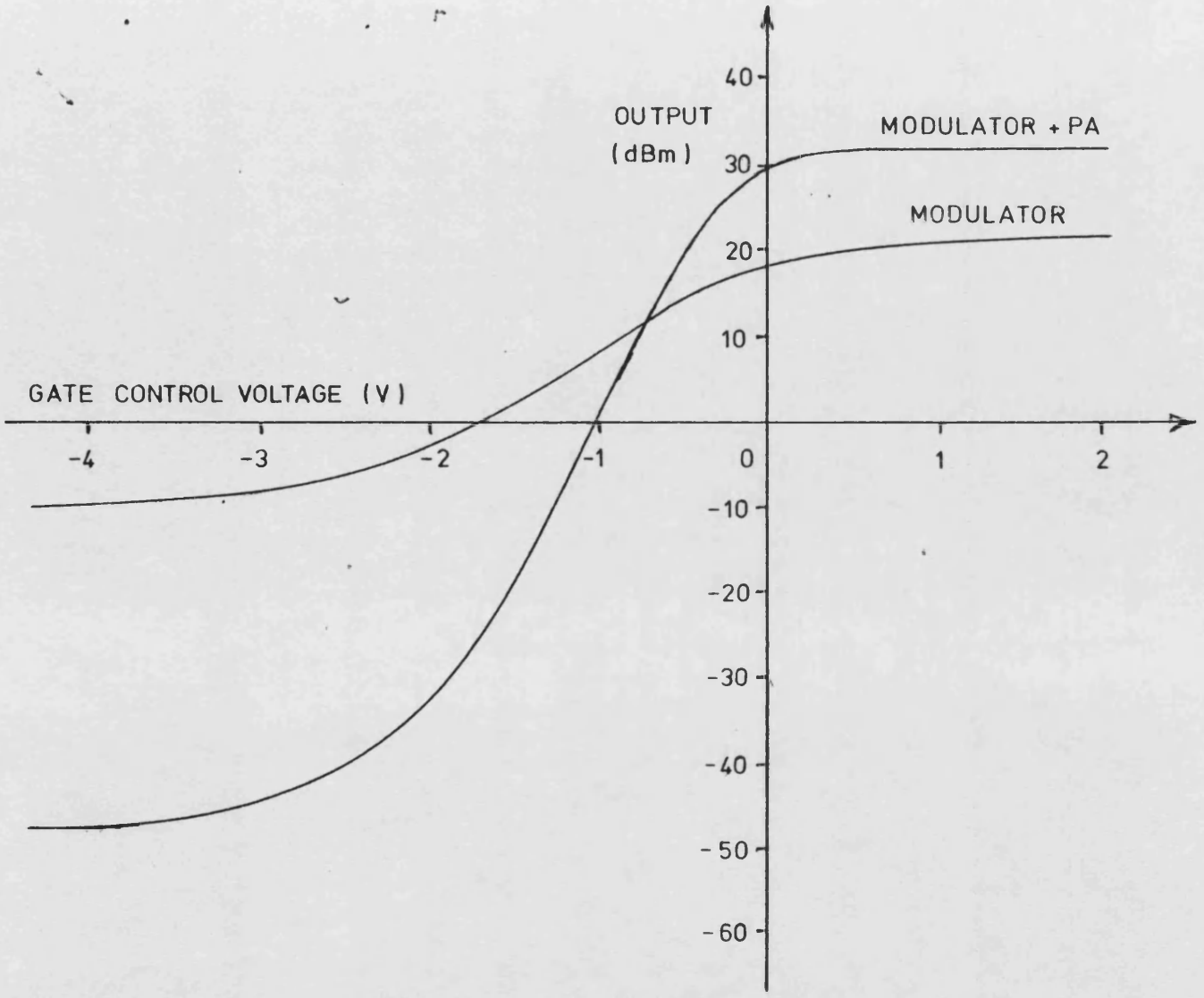

Figure 5.13 : Amplitude Control Characteristic of the 950MHz Amplitude Modulator

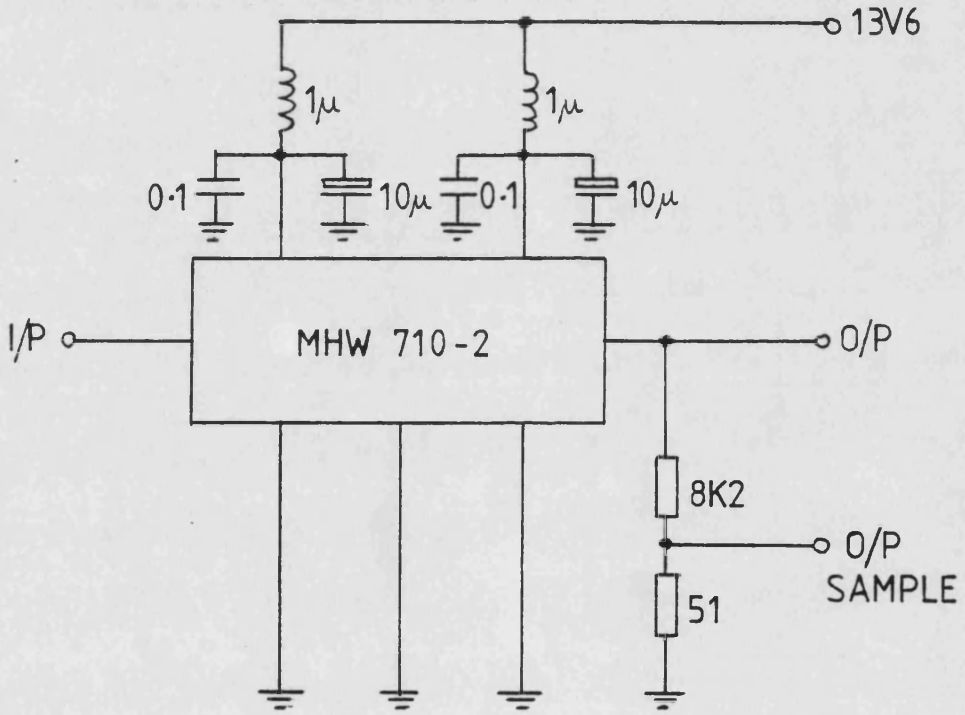

Figure 5.14 : The 450MHz Power Amplifier

Consequently a discrete component version was designed. Suitable transistors were selected from the wide range available. These were the BFR96 and BFQ34, which are 0,5 and 2W devices, respectively. Both of these transistors can be used in broadband applications, which makes them uncritical with regard to impedance matching. Simple, single section networks of microstrip transmission lines can be used as shown in the circuit diagram of Figure 5.15.

A loose capacitive coupling to the output line provides a sample of the output signal.

5.2.5 The Downconversion Oscillator

For the downconversion oscillator, two approaches were evaluated. Firstly, in the 450MHz transmitter, a very simple arrangement of a crystal oscillator followed by a frequency multiplier was used. This would be the likely technique adopted in a single channel transmitter. Secondly, in the 950MHz transmitter a conventional phase locked loop synthesiser was constructed, this being more representative of a multi-channel transmitter.

5.2.5.1 The 450MHz Downconversion Oscillator

Referring to the circuit diagram of Figure 5.16, a 7th overtone crystal oscillator operates at 73MHz and is used to drive a transistor frequency multiplier stage. The second harmonic at 146MHz is selected by a double tuned circuit. This feeds a second stage of frequency multiplication which is tuned to the third harmonic at 438MHz. The UHF output

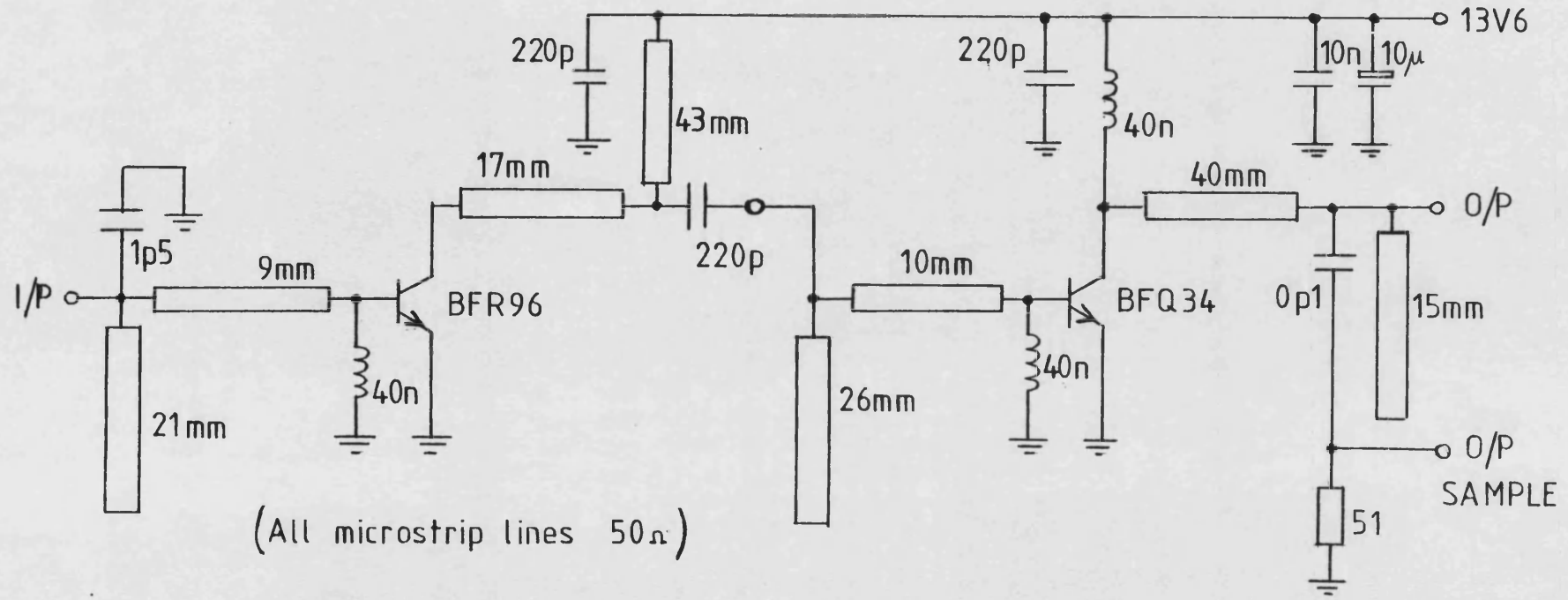

Figure 5.15 : The 950MHz Power Amplifier

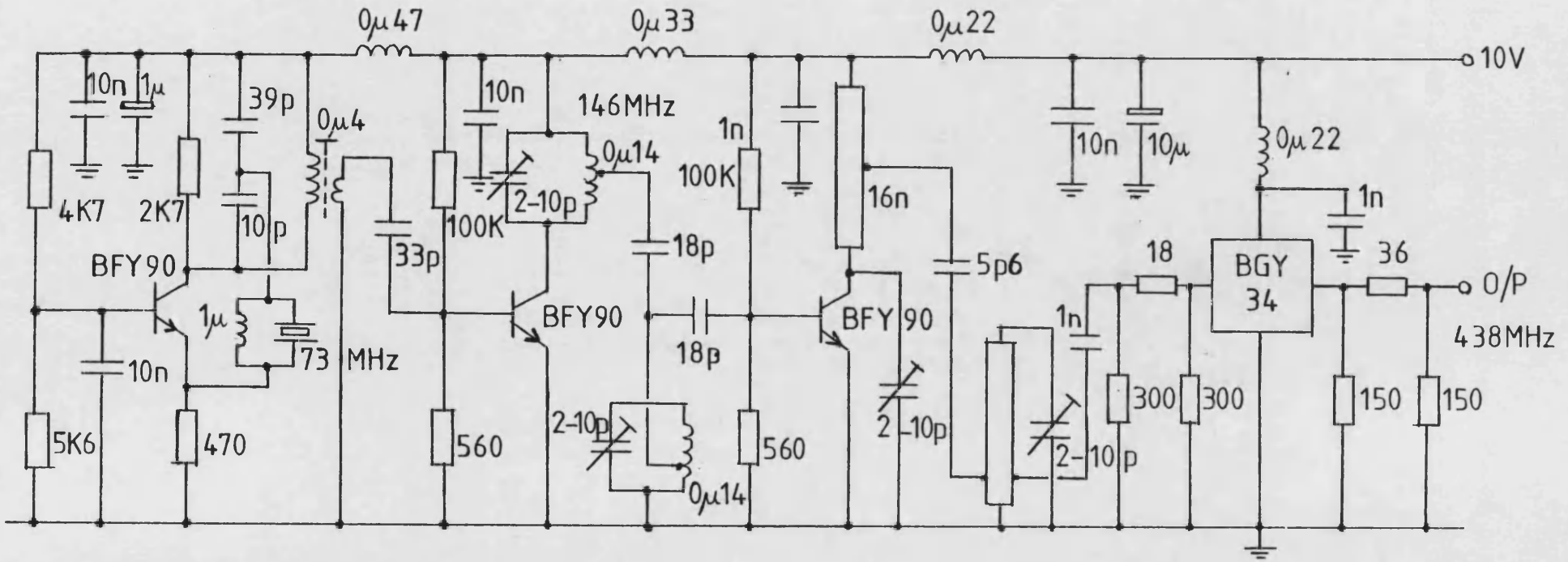

Figure 5.16 : 450MHz Downconversion Oscillator

feeds an amplifier module which increases the power level to in excess of the 13dBm required by the downconversion mixer. The selectivity of the multiplier stages is sufficient to suppress all unwanted subharmonic outputs to over 70dB below the wanted signal. The phase noise of this circuit was found to be excellent. Its measurements involved mixing the output down to IF using a laboratory cavity oscillator (HP8640B). The resulting noise spectrum (shown in Figure 5.17) was identical to that of the cavity generator alone, hence the actual phase noise spectrum must be significantly better than this.

5.2.5.2 The 950MHz Downconversion Oscillator

The downconversion signal for the 950MHz transmitter was generated using the circuit of Figure 5.18. A VCO operating at 960MHz feeds a buffer amplifier to give an output power of 16dBm as required by the downconversion mixer. Both the VCO and its buffer follow the designs described in Sections 5.2.1 and 5.2.2. A sample of the output at approximately 3dBm is fed to an ECL digital divider which provides a fixed division ratio of 10. A second divider further divides the frequency by a factor of 8 to give a final output at 12MHz. This signal, and the output of a 12MHz crystal oscillator are phase compared in an ECL phase sensitive detector. The phase detector output, in balanced form, is low pass filtered by a low noise amplifier which in turn, feeds the VCO control input. The VCO is therefore phase locked to the 12MHz reference frequency.

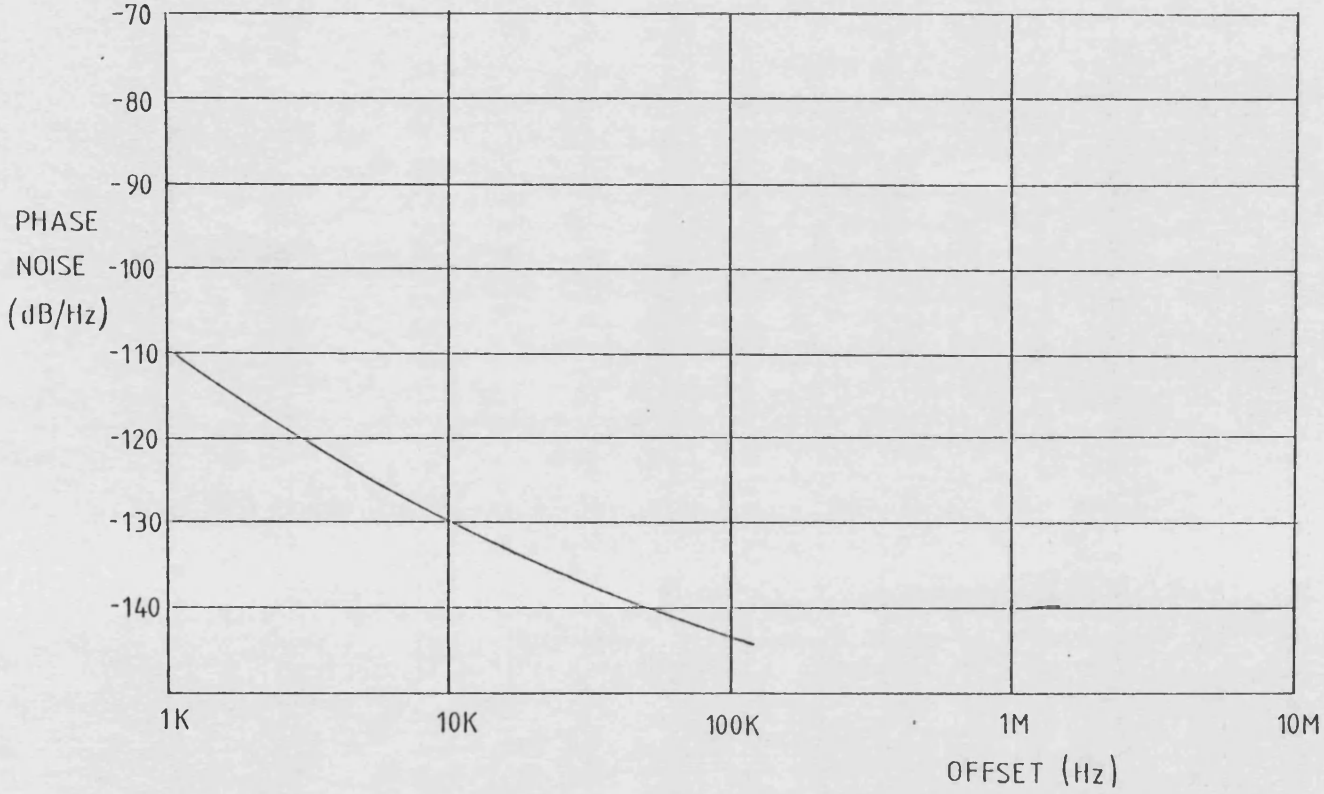

Figure 5.17 : Phase Noise Spectrum of the 450MHz Downconversion Oscillator

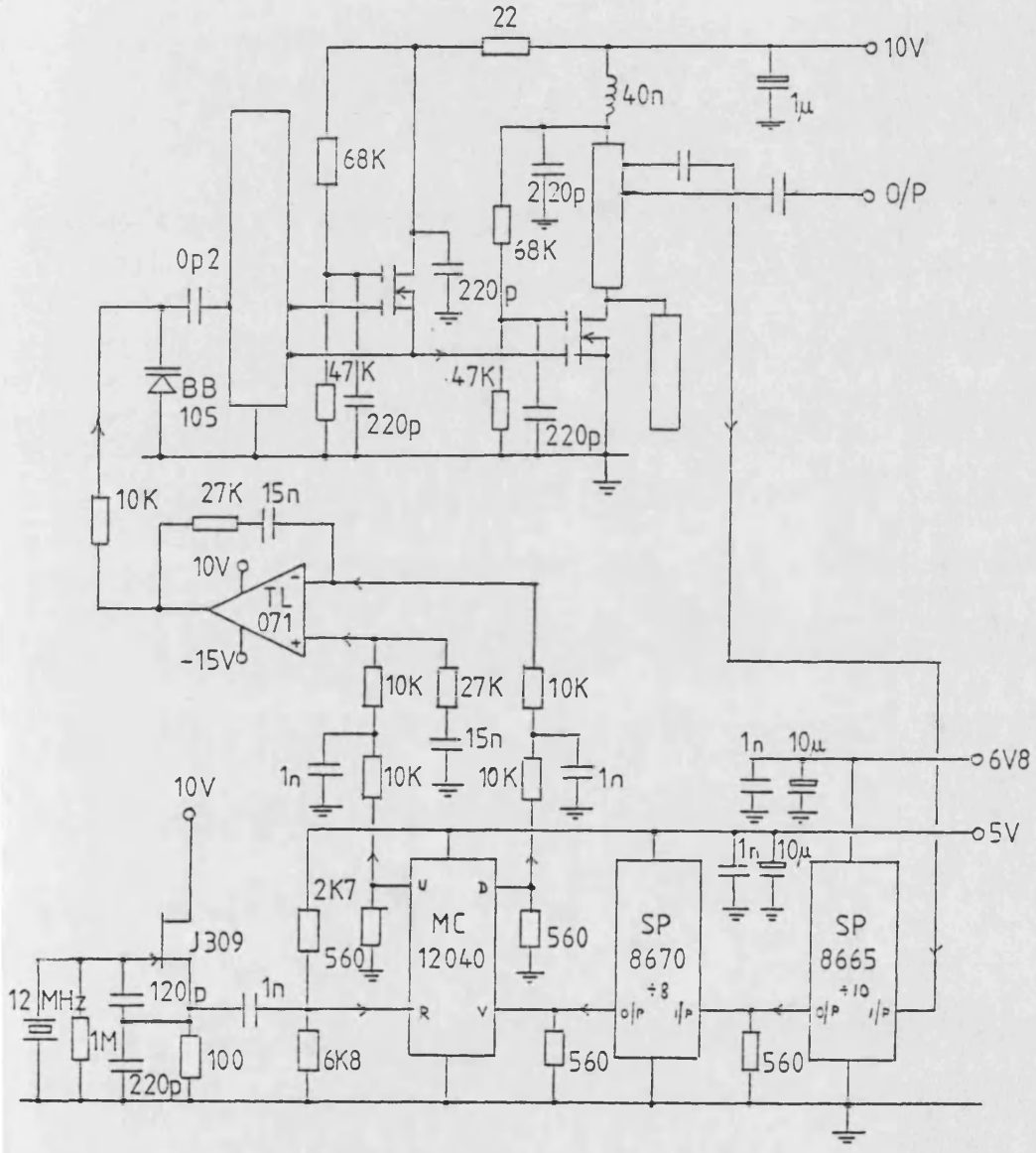

Figure 5.18 : 950MHz Downconversion Oscillator

Loop filter values were chosen to give a loop bandwidth of 2KHz. The measured phase noise spectra of Figure 5.19 show that this bandwidth gives a phase noise level only slightly worse than the unlocked VCO. As the loop bandwidth is widened, the close-in (< 10KHz offset) noise improves but at the expense of a degradation at large offsets. When the bandwidth was made 90KHz for example, a wide plateau of noise was produced due to the effective frequency multiplication of the reference oscillator and divider noise floor.

5.3 DESIGN OF THE IF AND CONTROL CIRCUITS

5.3.1 The Downconverter

The downconverter consists of a double balanced mixer to frequency translate a sample of the output signal down to the IF. This is followed by an IF amplifier to restore the signal to a level suitable for driving the polar resolving circuits. The circuit used in the 450MHz transmitter is shown in Figure 5.20.

It can be seen that the sample of the transmitter output is attenuated 16dB before being applied to the mixer. This is to ensure adequate linearity. Since the downconverter is outside the feedback loop of the transmitter, non-linearity in this stage would go uncorrected. At the level shown, the downconverter generates third order intermodulation products 70dB below the wanted output.

However, the low signal level results in a less than

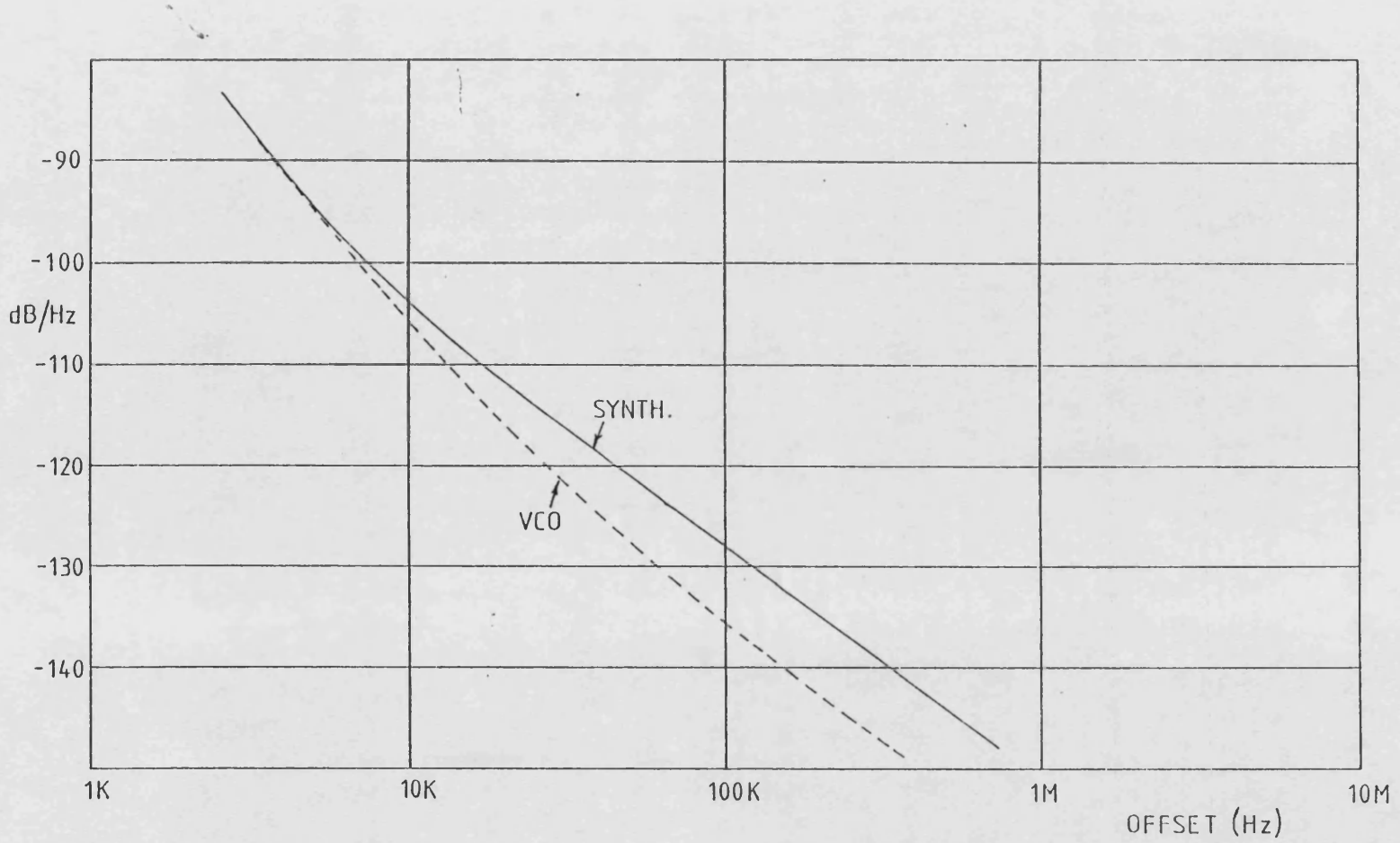

Figure 5.19 : Phase Noise Spectrum of the 950MHz Downconversion Oscillator

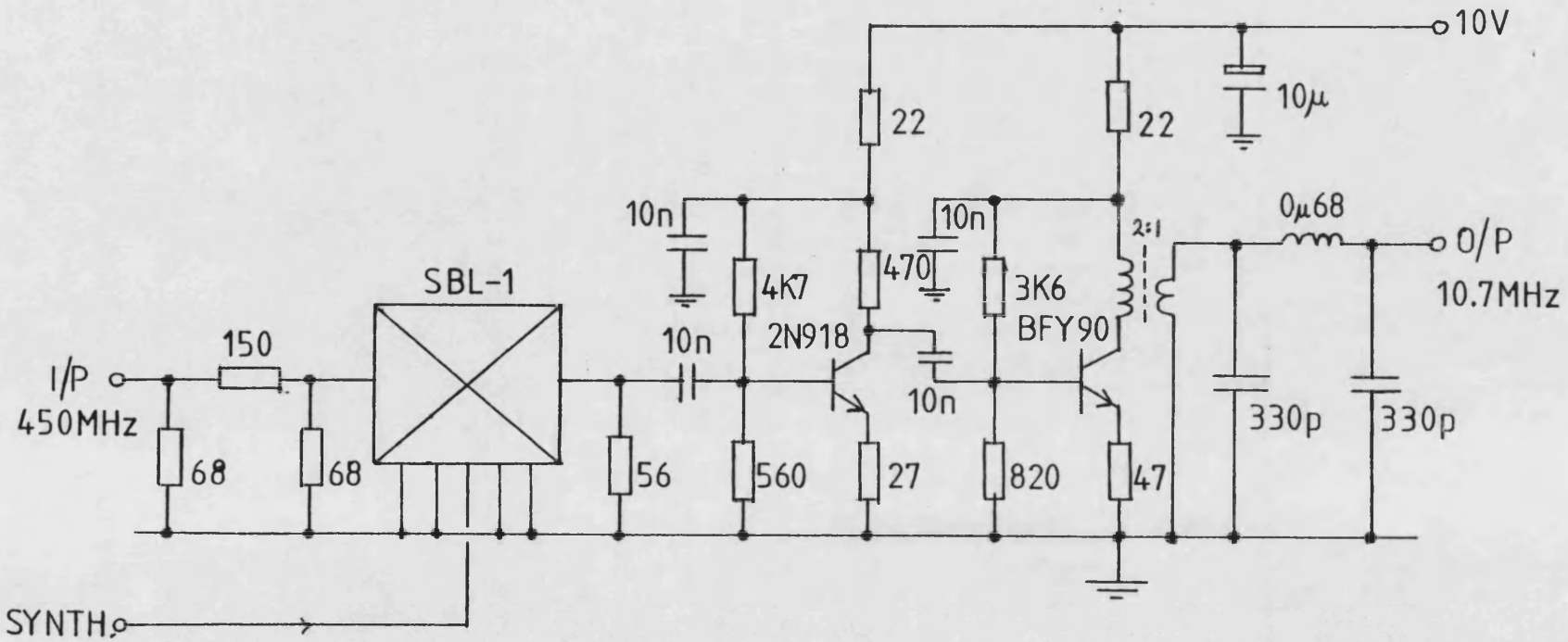

Figure 5.20 : 450MHz Downconverter

ideal signal to noise ratio. The broadband output noise level was found to be -130dB/Hz. In the 950MHz transmitter, this aspect was improved upon by using a high level mixer and a low noise FET for the first stage of the IF amplifier, as shown in the circuit of Figure 5.21. An improvement in the noise level to -140dB/Hz was obtained.

Both downconverter designs feature lowpass filters at their outputs. These serve to suppress the UHF products appearing at the mixer outputs and to reduce harmonics of the 10.7MHz IF signal.

5.3.2 The SSB Generator

The function of the SSB generator is to frequency translate the baseband input (which may be speech, data, or test-tones, for example) up to the intermediate frequency for input to the polar resolver.

For this application the filter method was used since it provides a very simple means of achieving excellent unwanted sideband suppression (>60dB). The circuit diagram of the SSB generator used in the 450MHz transmitter is shown in Figure 5.22. The audio and local oscillator signals are applied to a double balanced mixer, type MD113 to produce a double sideband suppressed carrier signal at the mixer output. Carrier suppression is adjusted by means of a d.c. bias applied to the audio input, and is typically -30dB relative to the sidebands. An IF of 10.7MHz was chosen, firstly, because this is one of the standard frequencies used for crystal filters, and secondly because it

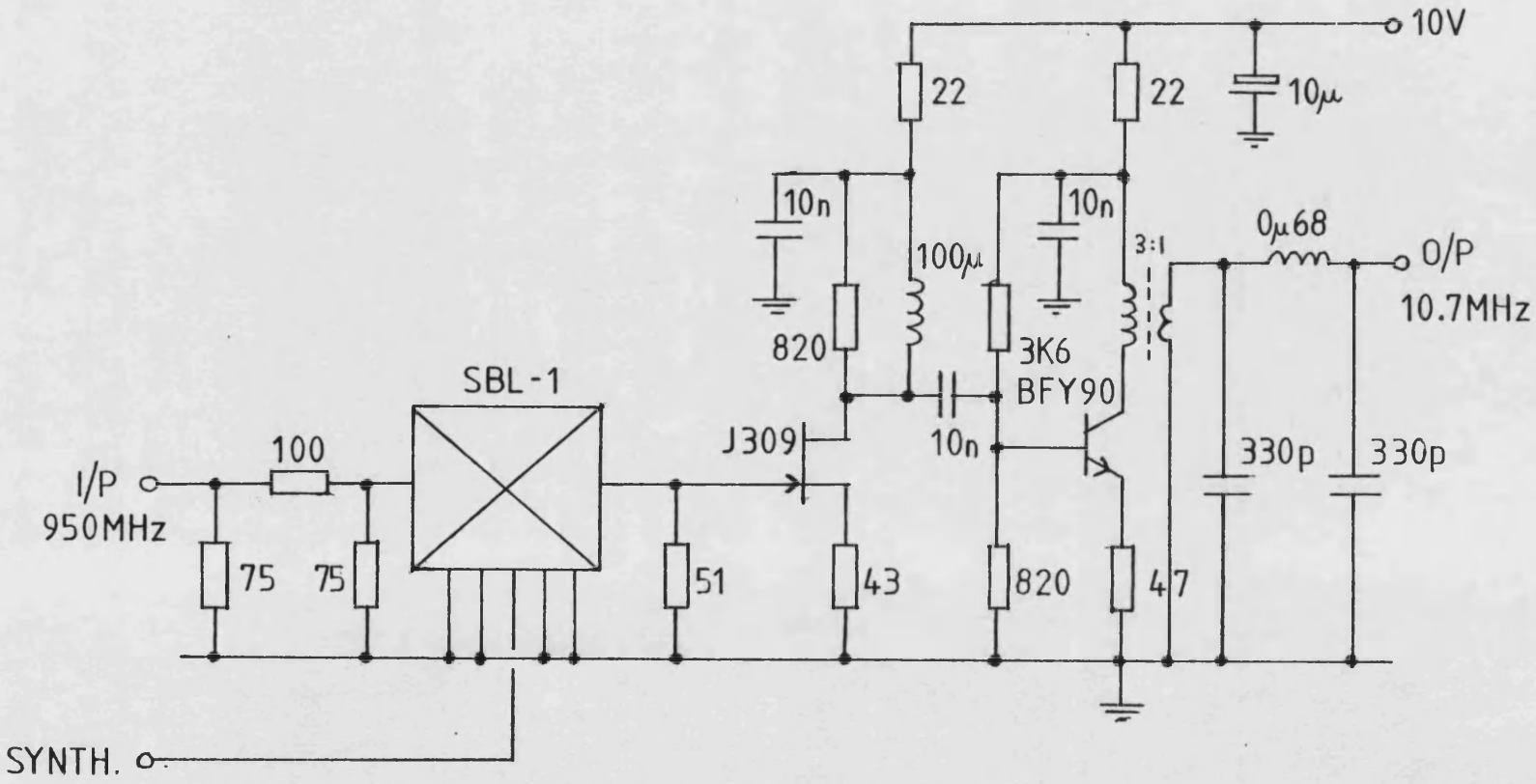

Figure 5.21 : 950MHz Downconverter

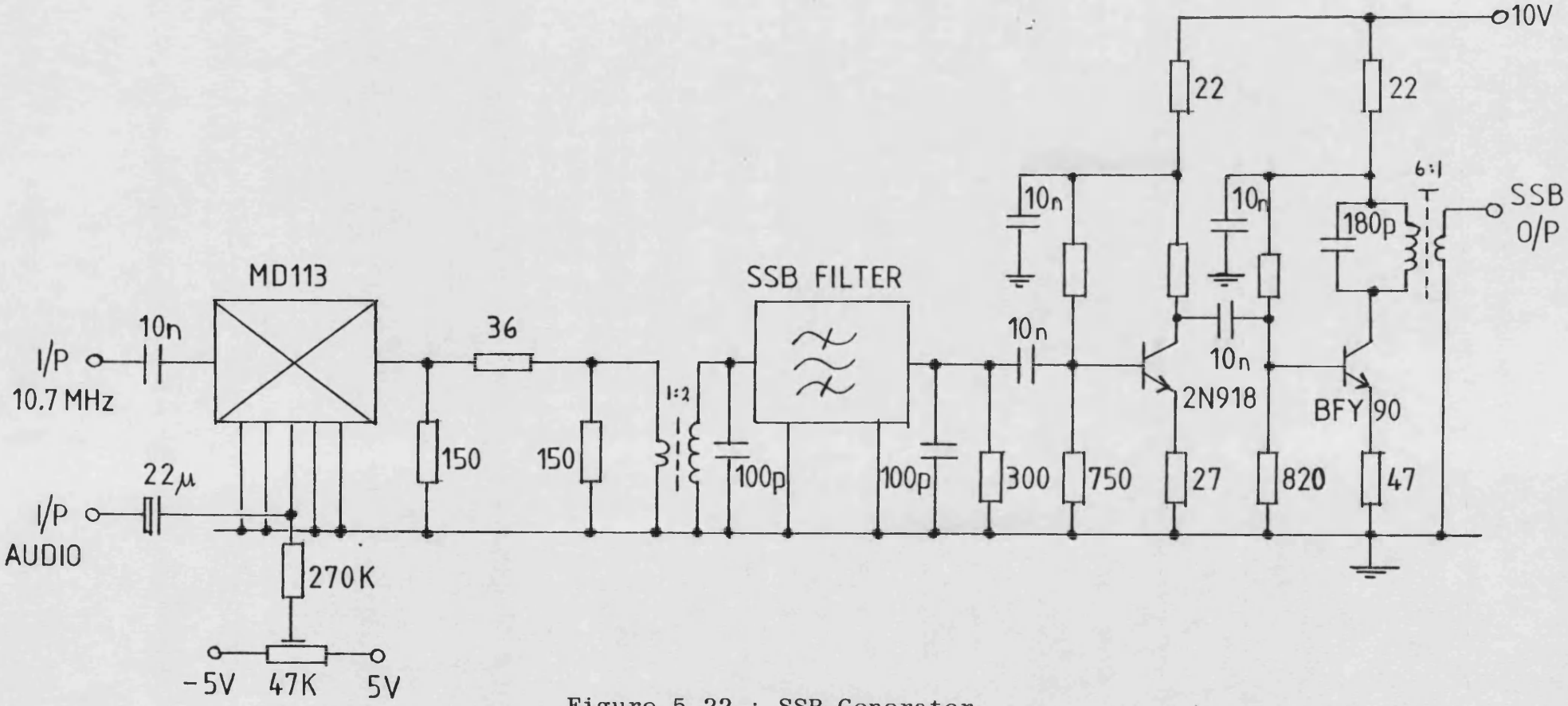

Figure 5.22 : SSB Generator

is a good compromise between filtering requirements and limiter performance in the polar resolver. (See Section 5.3.3.) The mixer output is matched to the following 8-pole crystal filter via a 6dB attenuator and a transformer. Figure 5.23 shows the frequency response of this filter. The passband width is approximately 2.4KHz, the carrier is suppressed a further 20dB, and the unwanted sideband rejection is >76dB. Following the filter, a 2 stage IF amplifier similar to that used in the downconverter increases the signal level to 0dBm.

It can be seen that a very low audio level was used (-23dBm). This was necessary in order to achieve acceptable linearity. However, as in the case of the downconverter circuit, the low signal level resulted in a poor signal to noise ratio (-120dB/Hz).

For the 950MHz transmitter, an improved SSB generator was designed. This is shown in Figure 5.24. In this circuit, a high level mixer is used which permits a much higher audio input level without degrading the linearity. A further improvement is obtained by the use of FET buffer amplifiers before and after the crystal filter. This arrangement provides an excellent impedance match for both the mixer and filter, whilst avoiding the signal to noise ratio degradation introduced by the 6dB attenuator in the original design. The measured noise floor of the improved SSB generator was found to be less than -140dB/Hz. Both SSB generators had identical linearity performance. With an audio input of two equal tones the resulting SSB output spectrum was as

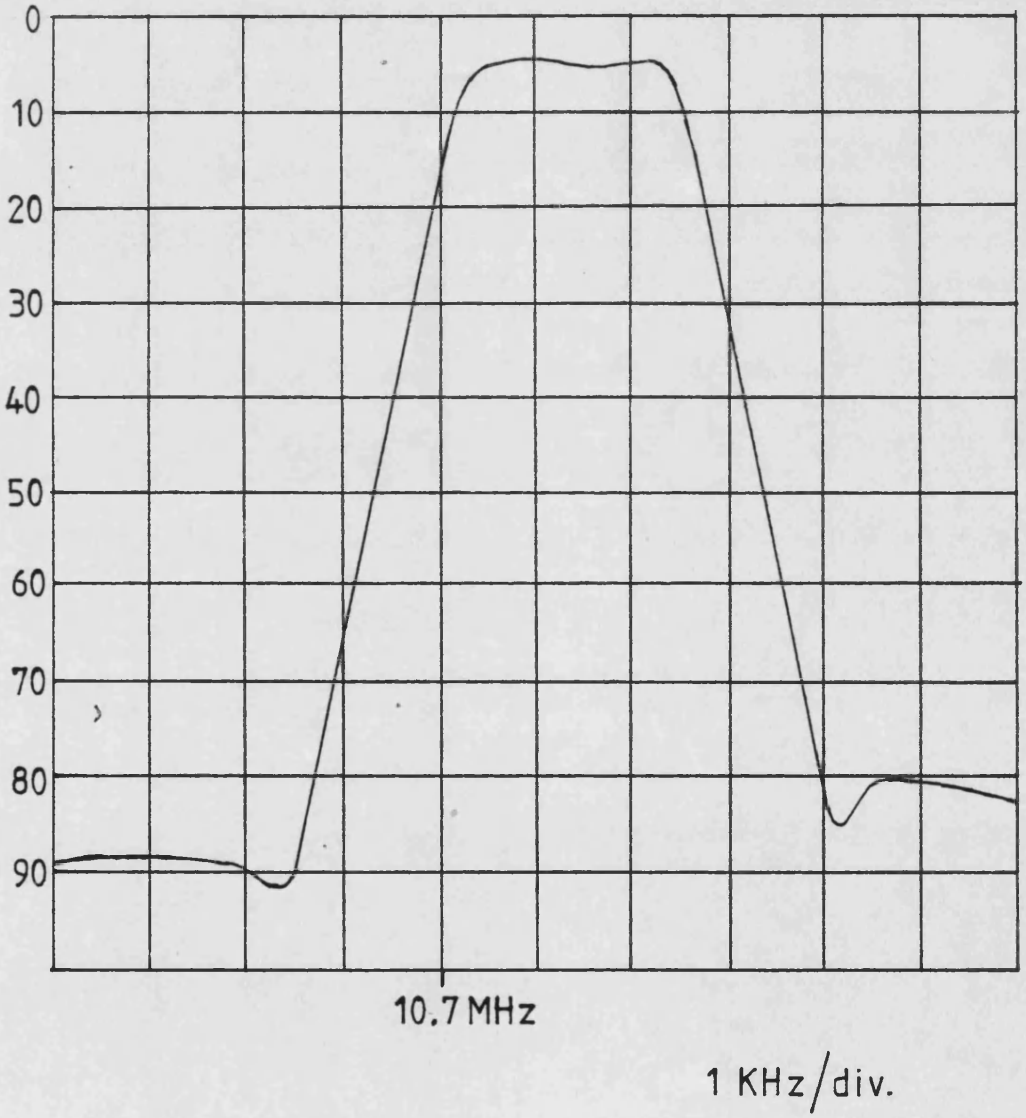

Figure 5.23 : SSB Crystal Filter Frequency Response

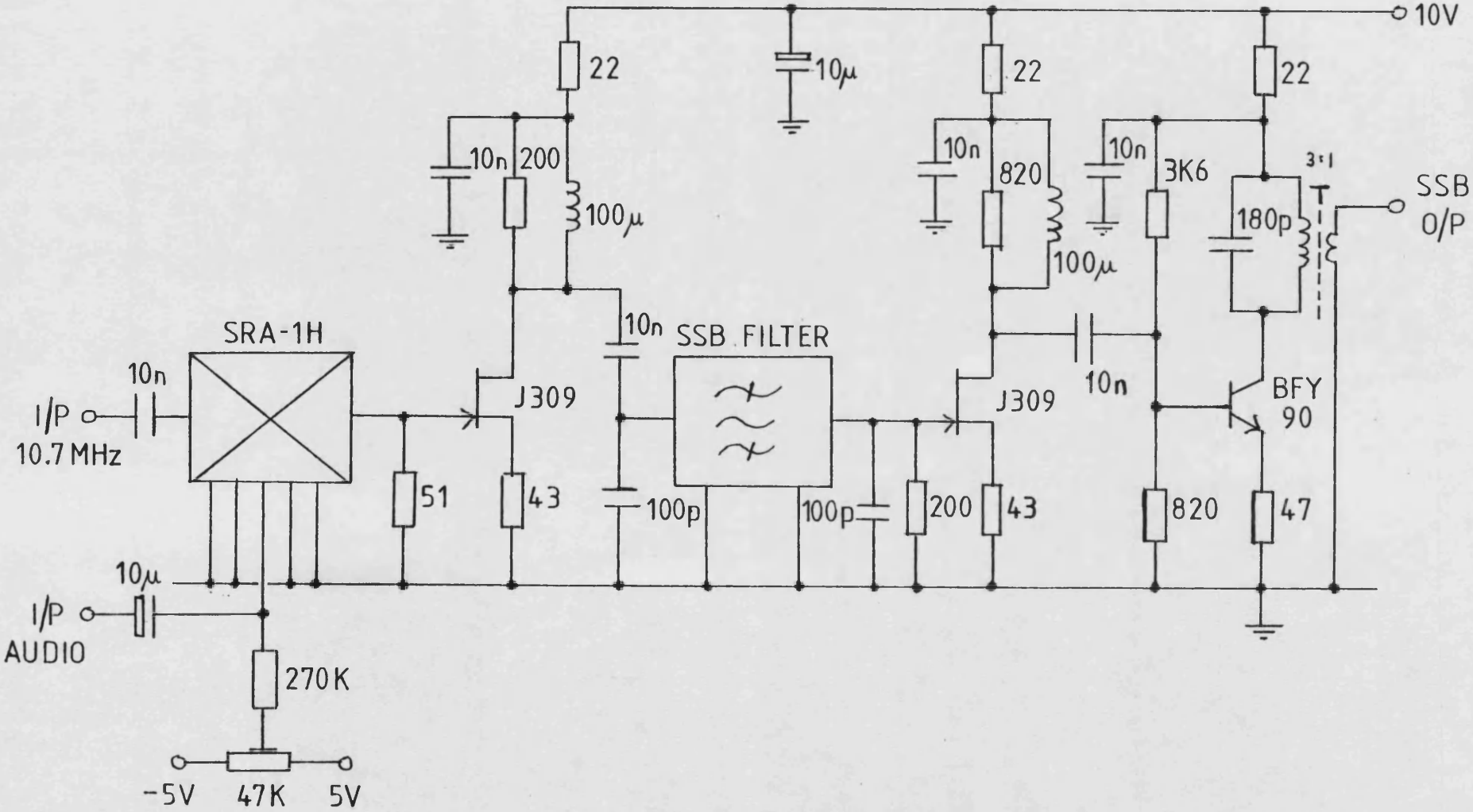

Figure 5.24 : Improved SSB Generator

shown in Figure 5.25. Third order intermodulation products were -74dB relative to the tone level.

5.3.3 The Polar Resolver

The polar resolver converts into polar coordinate form the outputs of the SSB generator and the downconverter.

The phase component of each signal is obtained by hard limiting to remove the amplitude modulation, whilst the envelope component is produced by rectification and lowpass filtering. Diode detectors are unsuitable for use an envelope demodulators in this application due to their inadequate dynamic range. In an unbiassed mode, a silicon diode would cease to rectify below 0.6V peak, or, if biassed into conduction, would be grossly non-linear. This would aggravate the matching of the two detectors and would make the feedback loop gain amplitude dependent. For these reasons, and the fact that limiters are required to obtain the phase component, the envelope demodulation was accomplished by multiplying each input signal by the limited version of itself. This process is equivalent to full-wave rectification.

The choice of IF was made on the basis of the following factors:-

(i) Both the envelope component and the phase detector output must be lowpass filtered to suppress the IF content and leave only the baseband information. Since such filtering restricts the maximum stable loop bandwidth, it is therefore desirable that the IF be as high as possible.

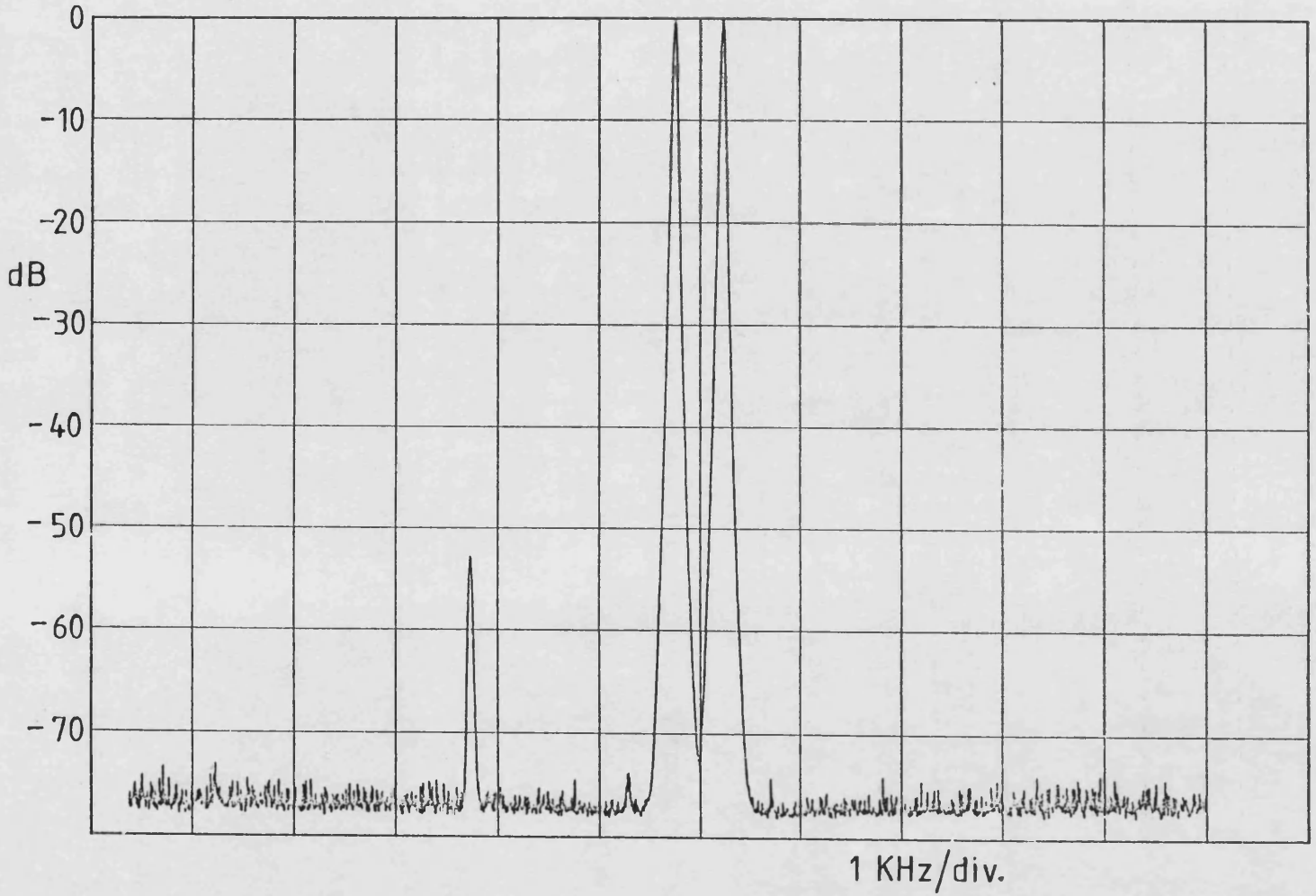

Figure 5.25 : SSB Generator Output Spectrum with Two-tone Input

(ii) Very few limiters will operate at frequencies significantly above 10MHz. Also, AM to PM conversion worsens as the frequency is increased.

(iii) SSB crystal filters tend to be manufactured at what have become standard frequencies, e.g.:- 1.4, 10.7, 21.4MHz.

In view of these restrictions, 10.7MHz was selected as the best compromise

The combination of limiter and double balanced mixer, which together comprise the polar resolver, is conveniently available as a single integrated circuit. Such devices are widely used in the IF sections of FM receivers. In this case the balanced mixer is used as part of the quadrature detector. Manufacturers data for several limiter/demodulator ICs were examined, and on the basis of frequency response, sensitivity, and the provision of balanced outputs (to minimise d.c. drift), the SL624 device was selected. This is specified as operating at up to 30MHz, and requires 100μV rms for full limiting. The latter figure corresponds to -66dB relative to the peak envelope input level of 0dBm, although the limiter output is sufficient to drive the phase detector interface circuit at -70dBm into the limiter.

It was mentioned in Chapter 3 that it is very important for the two polar resolvers to be closely matched, so that any distortion introduced by one side is cancelled out by that in the other. To satisfy this requirement, a special device was obtained from the manufacturer, comprising two SL624 chips taken from the same silicon wafer, mounted on a

common substrate.

The overall circuit diagram of the dual polar resolver is shown in Figure 5.26. It can be seen that whilst the input signals drive the limiters directly, the signals to the demodulators are attenuated by 12dB. This is to ensure that the demodulators operate in their linear regions. Provision for fine adjustment of one of the attenuators allows the input levels to each resolver to be matched.

The envelope signals are taken from the demodulator outputs in balanced form to minimise d.c. drift, which is predominantly a common mode signal. The outputs are cross-coupled such that cancellation takes place. Any error is amplified by a high slew rate, high gain differential amplifier, which in turn controls the amplitude modulator. A d.c. offset adjustment allows any d.c. imbalance in the demodulators or the amplifier to be nulled. Finally, the compensation capacitor, C_c, can be used to vary the amplitude loop bandwidth.

After the 450MHz transmitter had been constructed and evaluated, a number of shortcomings in its performance became apparent, which were due largely to deficiencies in the polar resolvers. It was found that in general the matching between the two resolvers in the dual version of the SL624 was poor. This was due mainly to the fact that the limiter sections were prone to oscillation. An input level of typically -50dBm was insufficient to completely suppress this instability, and resulted in gross mismatch of the input and feedback signals at low level. A particu-

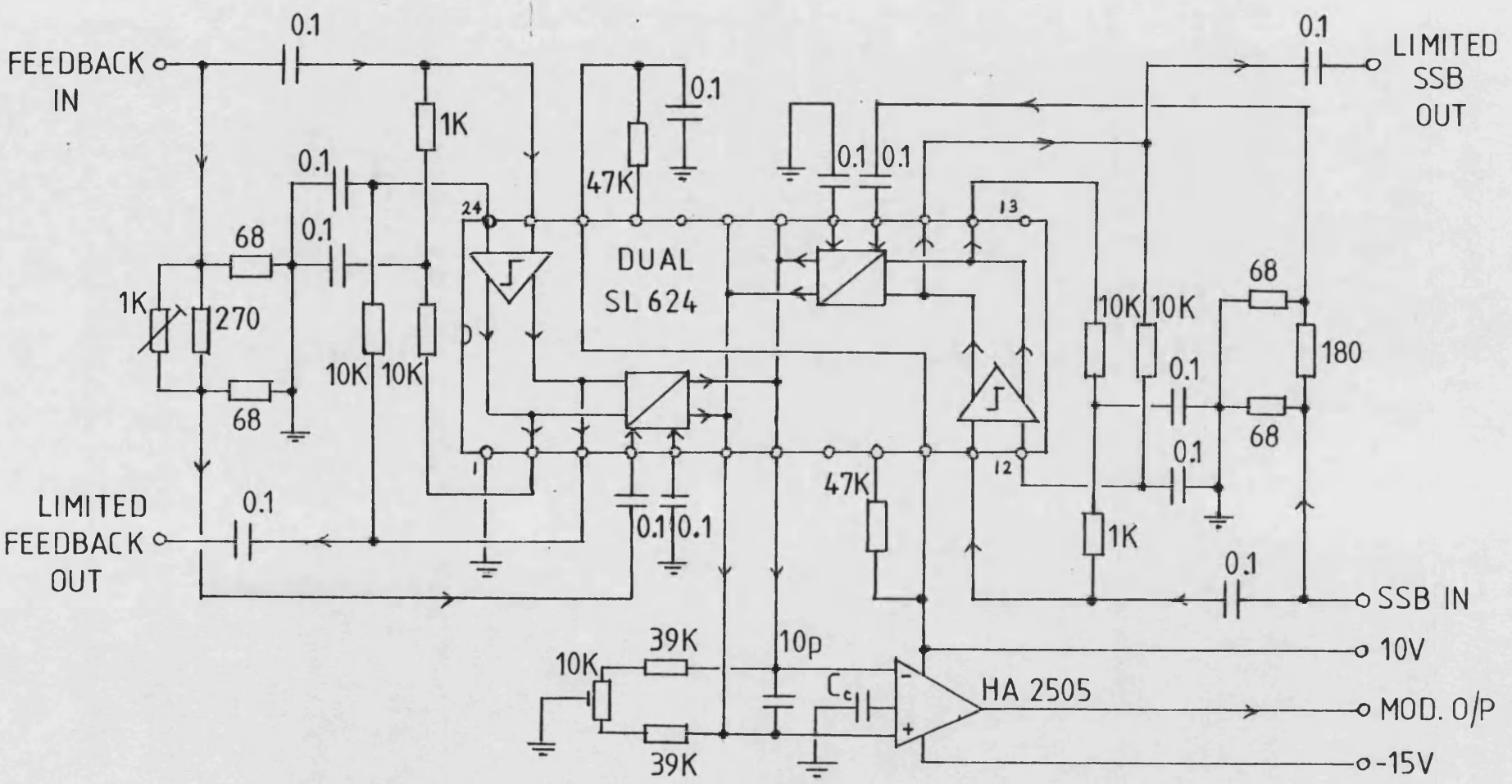

Figure 5.26 : Polar Resolver

larly revealing test is to examine the system behaviour when the input is a two equal tone signal, since in this case the envelope falls to zero. The effect of the mismatch at the crossover region was as shown in Figure 5.27. As the envelope reduces, the limiter instability increases, until the feedback system loses control of the output which abruptly collapses to zero. The output only reappears when the SSB input envelope exceeds that due to the limiter oscillation.

In order to overcome this difficulty, the potential alternative devices were reappraised. Whilst several of them had limiter sections which did not have the instability problem of the SL624, none of them also had suitable demodulator sections. In view of this it was decided to use separate limiters and demodulators. This approach allowed a much wider choice of limiters. It also permitted a thorough investigation to be made into the sources of mismatch in the polar resolver, since limiters and demodulators could be evaluated independently.

During a survey of limiter circuits, it was found that the HA12412 device had the highest sensitivity of all those examined (12μV for full limiting). Further investigation showed that this sensitivity was achieved without instability occurring in the absence of an input signal. This was confirmed by measurement of the broadband noise level appearing at the output. With a CW input signal of 0dBm, the measured noise level was -137dB/Hz compared with -125dB/Hz for the SL624.

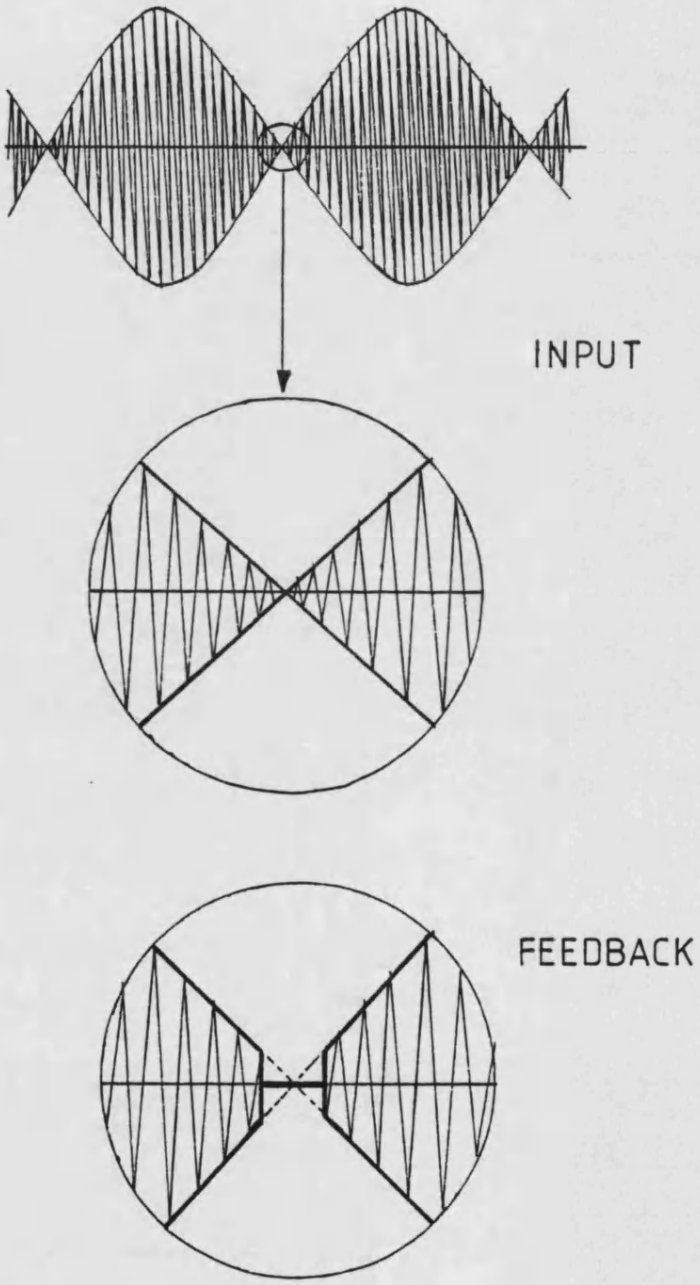

Figure 5.27 : Effect of Limiter Instability on the Zero-Crossing Region of a Two-tone SSB Signal

For the demodulator section, the SL6640 high level active mixer was chosen. This device has the best linearity performance of all the integrated circuit mixers. Third order intermodulation levels are -70dB for a two-tone input of 0dBm PEP. It also has the advantage of a balanced output configuration.

The overall circuit diagram of the revised dual polar resolver, incorporating the HA12412 and SL6640, is shown in Figure 5.28.

It can be seen that dual-gate FET buffer amplifiers are interposed between each input and its associated demodulator. This is to prevent unwanted feedback around the limiters via the leakage through the demodulators. The reverse isolation of the buffer stages is in excess of 70dB at 10.7MHz, which, combined with the 30dB of isolation in the demodulators, eliminates the possibility of limiter oscillation. The remainder of the circuit design closely resembles that of the initial polar resolver design.

5.3.4 The Phase Sensitive Detector

The phase sensitive detector compares the phase of the limited SSB input signal with that of the limited frequency translated output signal, and generates a voltage proportional to the instantaneous phase difference.

One of the requirements of the phase locked loop is that it must be able to track large and rapid phase excursions of the input signal. The most severe case in this respect is the two equal tone signal, since the phase reverses

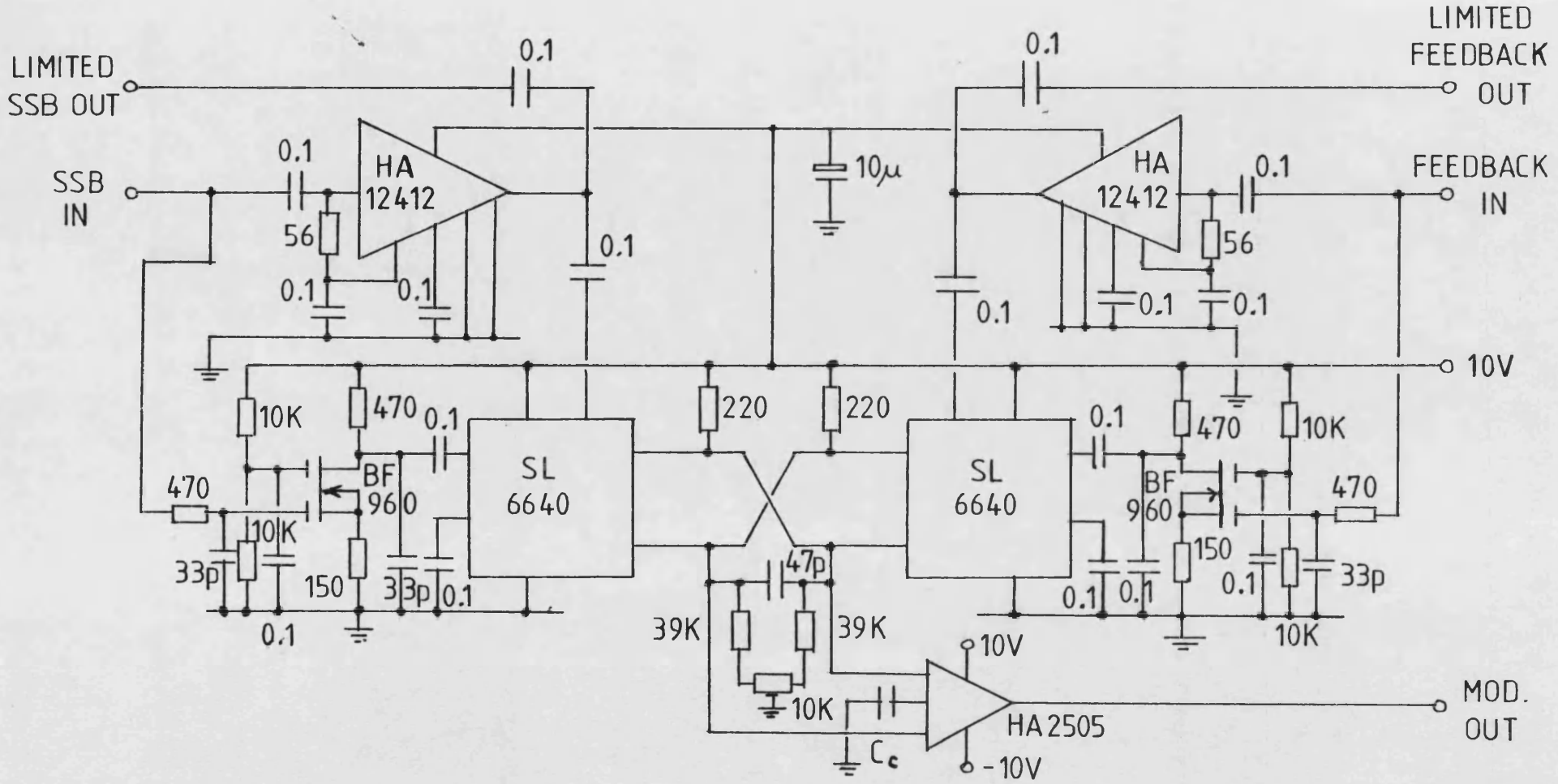

Figure 5.28 : Improved Polar Resolver

at each envelope zero-crossing. The PSD must therefore be able to sense phase differences of up to $\pm 180^{o}$ ($\pm\pi$ radians). Some phase detectors, such as the analogue multiplier, or its digital equivalent, the Exclusive-OR gate, can only operate over a range of $\pm 90^{o}$, and so are unsuitable. The EX-OR gate for example, has a triangular characteristic as shown in Figure 5.29. If the loop has a stable operating point on the positive slope of the characteristic, a phase transition of π rad would move the loop to the opposite polarity (unstable) detector slope. Assuming that the operating point is close to the null output phase of $\pi/2$, then the error signal after the phase reversal has occurred will still be small, making the loop slow to recover equilibrium. If the error voltage is exactly zero, then the loop may hesitate for many loop time constants before responding. This latter phenomenon is termed 'hang-up' (116), and is clearly undesirable.

An alternative form of PSD which does not suffer from this problem, is the frequency and phase detector based on D-type flip-flop circuits. This arrangement, shown in Figure 5.30, can detect phase errors of up to $\pm 2\pi$ rad, and has the characteristic shown in Figure 5.31. A phase shift of $\pm\pi$ would produce a large output voltage thus there is no possibility of hang-up effects. Another advantage of this type of PSD is that it also detects frequency error. If there is a frequency difference between the two input signals, the corresponding phase error will be continually ramping between 0 and $+2\pi$ or 0 and -2π for positive or

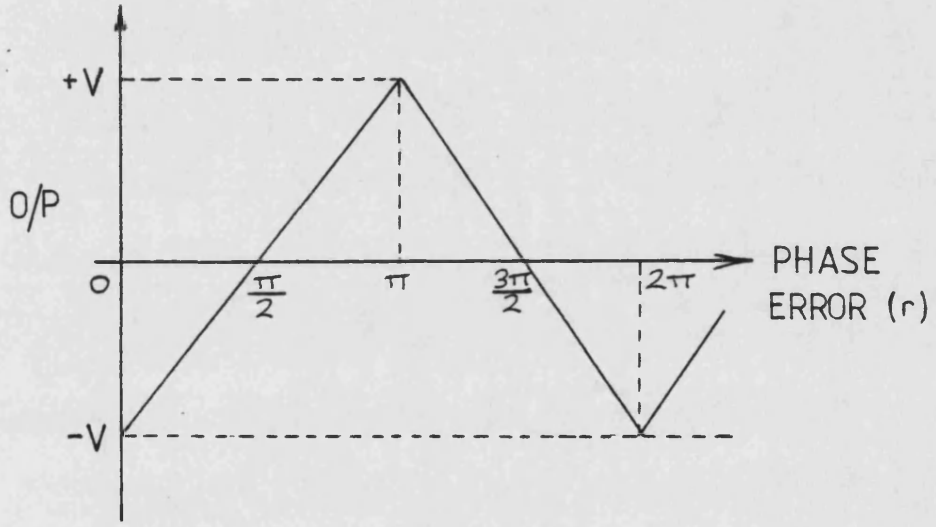

Figure 5.29 : Exclusive -OR Gate Phase Sensitive Detector Characteristic

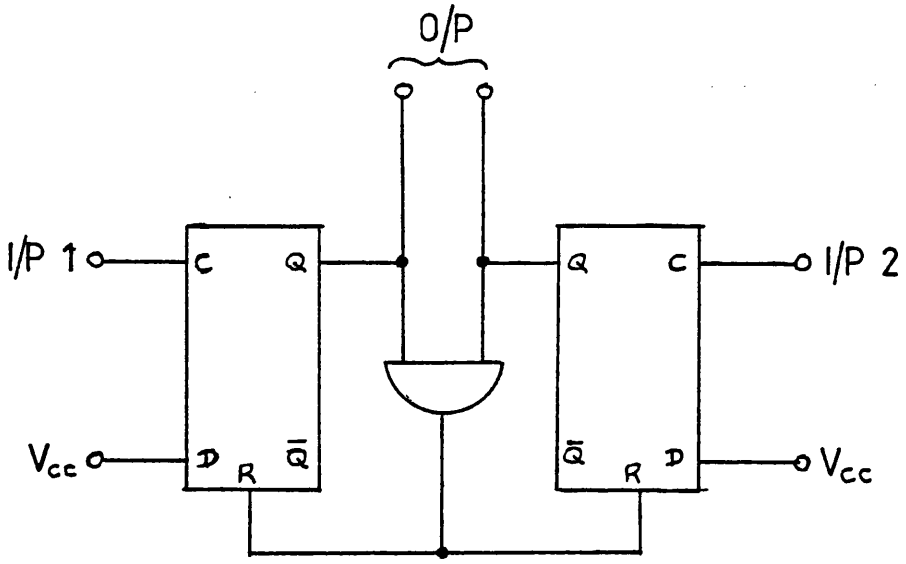

Figure 5.30 : D-Type Flip-Flop Phase Sensitive Detector

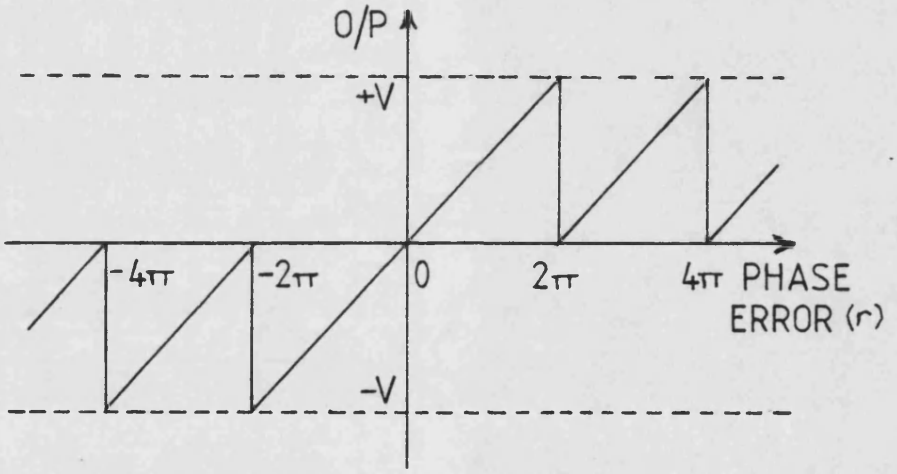

Figure 5.31 : D-Type Flip-Flop Phase Sensitive Detector Characteristic

negative frequency offsets respectively. By virtue of the characteristic, the output voltage will therefore have a d.c. level of the same polarity as the frequency offset. The implication of this property is that a loop using such a PSD can acquire lock even though it may be initially outside the capture range predicted by phase-locked loop theory. For a UHF polar-loop transmitter application, this ability is highly desirable: at switch-on, the VCO may be several MHz from the required frequency, but the loop bandwidth would typically be only a few hundred KHz. In view of this, and the capability of sensing phase reversals, the D-type PSD was selected.

To implement the circuit of Figure 5.30, Schottky TTL D-type flip-flops and NAND gates were used as shown in Figure 5.32. Since the limiter outputs are typically 400mVpp, interface circuits are necessary to bring the signals up to TTL levels. This was accomplished as shown in the diagram using 'Schmidt trigger' NAND gates connected as inverters. By applying resistive negative feedback around the gates, the effective hysteresis voltage is reduced, allowing triggering from the limiter signals.

The outputs from the two D-type flip-flops consist of pulses at a 10.7MHz rate with a duration proportional to phase error. A low-noise operational amplifier, type TL071, was used to low pass filter these outputs in order to extract the d.c. component for application to the VCO control input. The TL071 has a unity gain bandwidth of 3MHz, above which its response falls sharply, giving sufficient

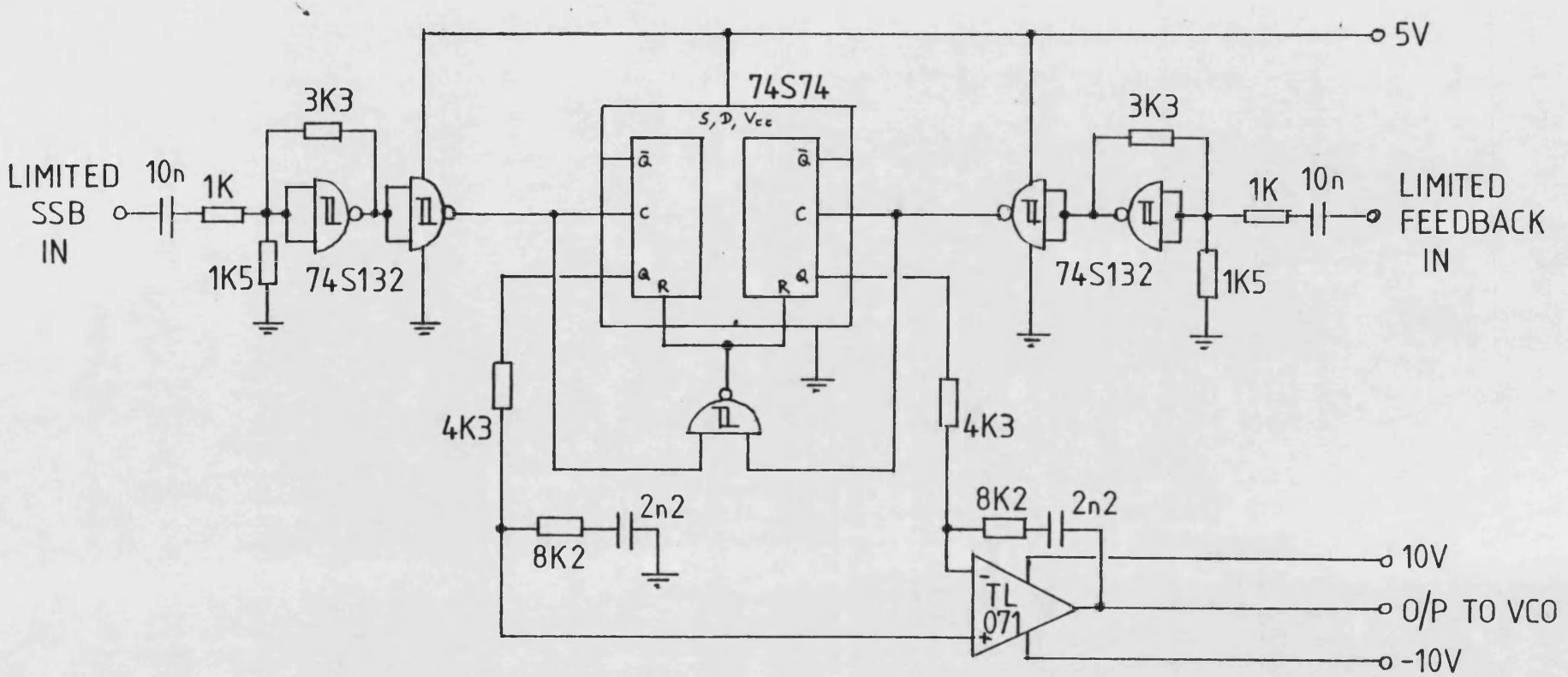

Figure 5.32 : Schottky TTL D-Type Flip-Flop PSD Circuit

attenuation at 10.7MHz to suppress reference sidebands at the transmitter output to 70dB below the wanted signal. The type of loop filter used and its design are covered in Section 5.4.

When phase noise measurements were made on the 450MHz transmitter, the Schmidt triggers and the PSD were found to be significant contributors to the total noise level. A noise floor of -125dB/Hz was measured for the overall PSD circuit, which is equal to the level produced by the SL624 limiters. It was postulated that this relatively high noise level may be due to fluctuations in the switching levels of the logic gates causing a corresponding timing jitter of the transitions in the digital waveforms. If true, this implies that a faster logic family would possess lower phase noise, since the absolute value of the timing jitter would be reduced. Figure 5.33 clarifies this. To confirm this belief, an ECL version of the D-type flip-flop PSD (type MC12040), was constructed, and evaluated in the 950MHz transmitter. As expected, a considerable improvement in phase noise was obtained, to a level of -137dB/Hz. A circuit diagram of the ECL PSD is shown in Figure 5.34. By virtue of the reduced voltage swing required by ECL gates in comparison with TTL, simple JFET amplifiers could be used for the limiter interface.

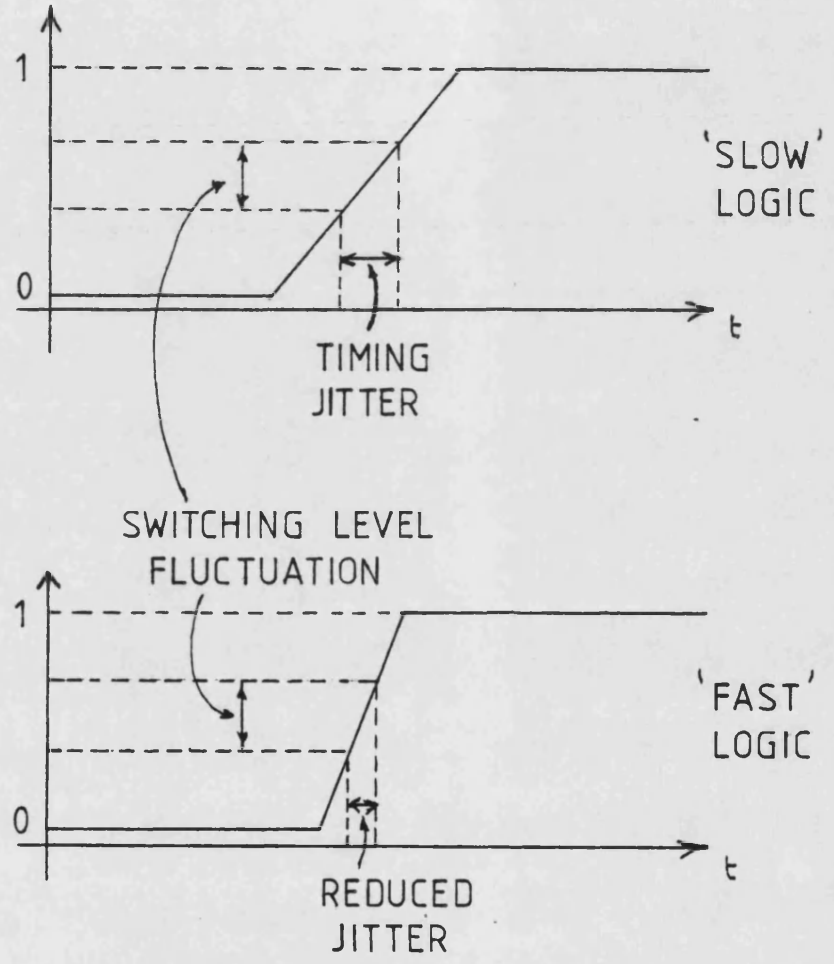

Figure 5.33 : Effect of Logic Speed on Timing Jitter

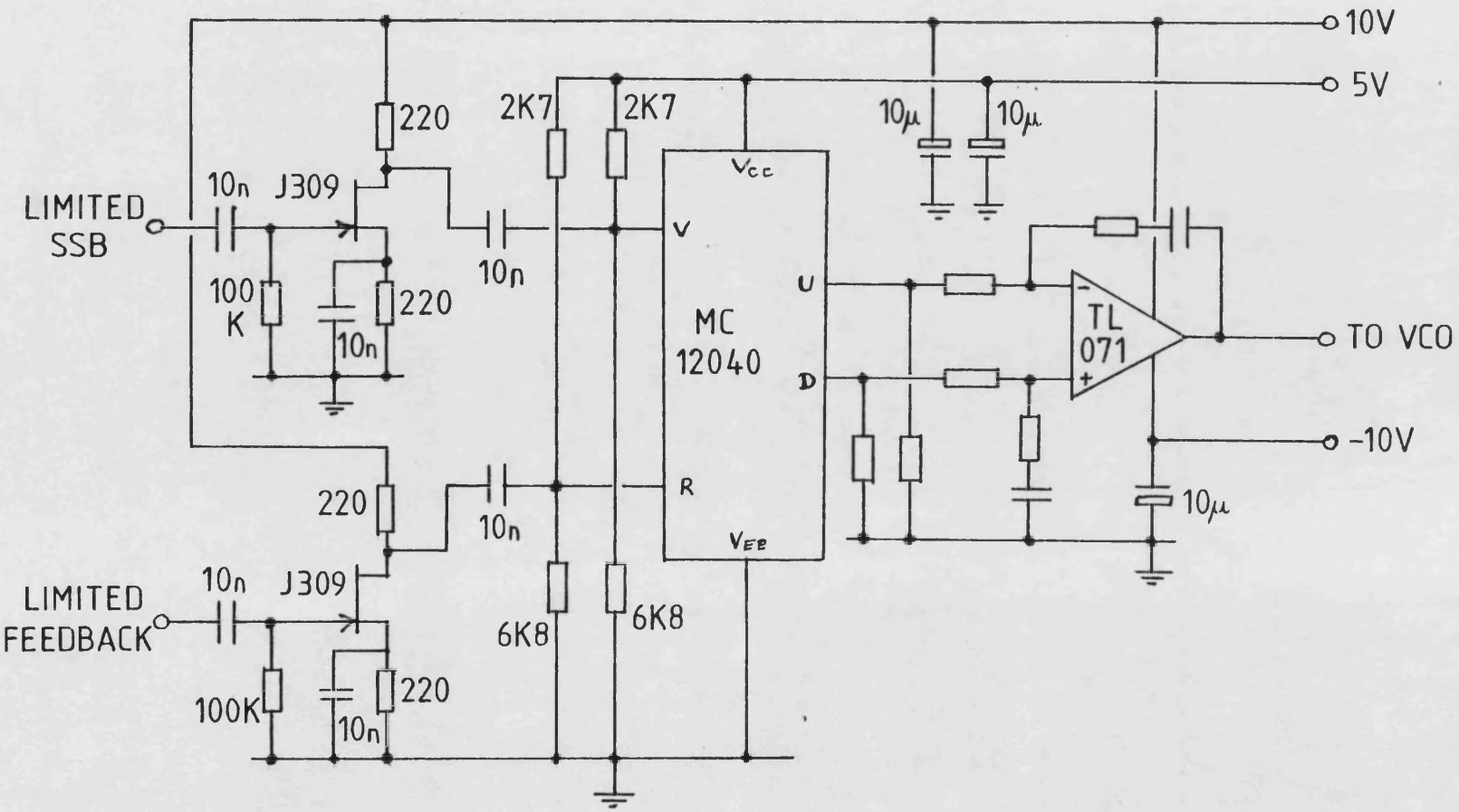

Figure 5.34 : ECL D-Type Flip-Flop PSD Circuit

5.4 PHYSICAL CONSTRUCTION OF THE TRANSMITTERS

The transmitter circuits were constructed on double sided printed circuit board with ground plane, in accordance with good RF practice. Those parts of the transmitters particularly sensitive to spurious signal pick-up, such as the VCOs, were mounted in separately screened enclosures as shown in Figure 5.35. The individual circuits were mounted in a screened chassis, with all RF interconnections made with coaxial cable, as shown in Figure 5.36.

5.5 DESIGN OF THE FEEDBACK LOOPS

5.5.1 Basis of the Design

The theoretical aspects covered in Chapter 3 have shown that there are several conflicting requirements placed on the feedback loops. The analysis of the convolution process, the need to reduce the distortion generated in the RF circuits, and the need to minimise the noise level at the transmitter output, each suggest different values for the loop bandwidths. For this reason, it was decided at the outset not to design the transmitters with fixed bandwidths, but to examine the effect of varying the bandwidths on the practical system. In this way, it could be established whether suitable compromise values exist.

The design of the feedback loops is therefore reduced to the following three aspects:-

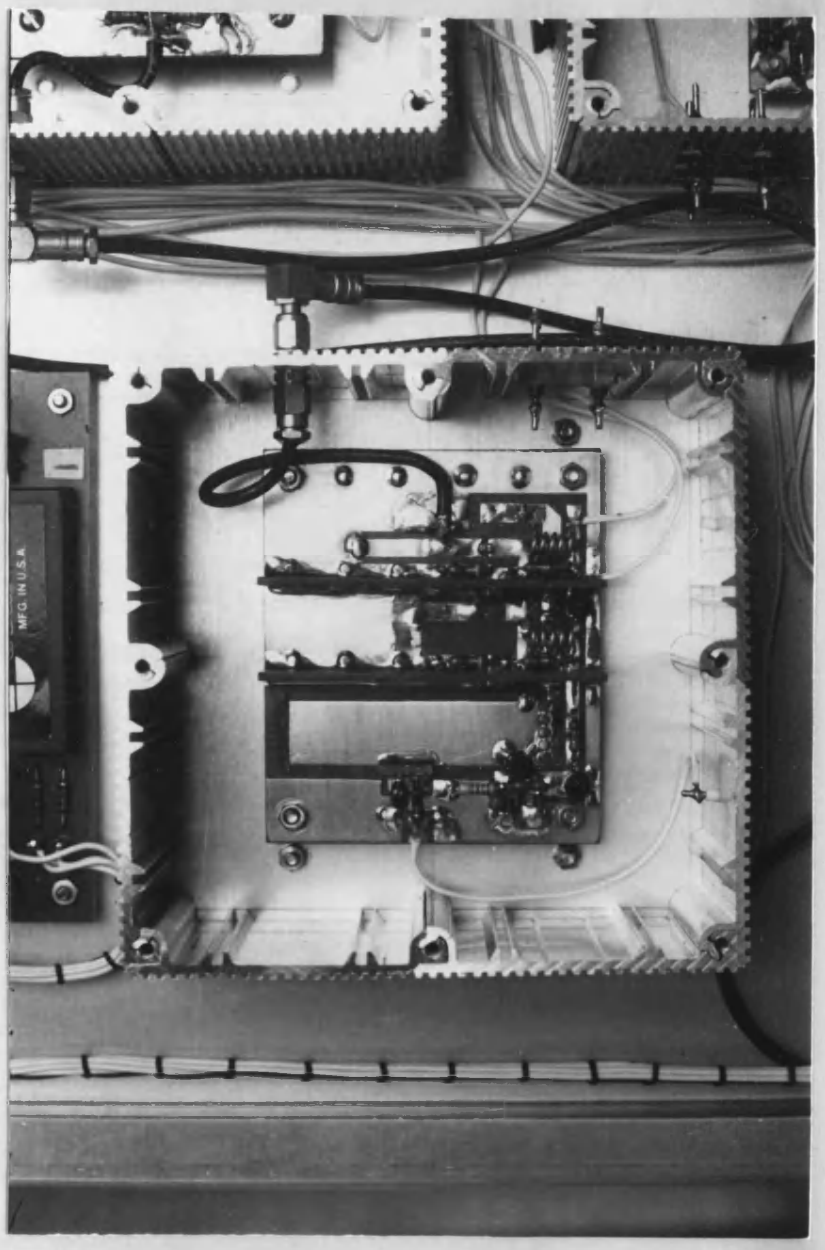

Figure 5.35 : Physical Implementation of the VCO

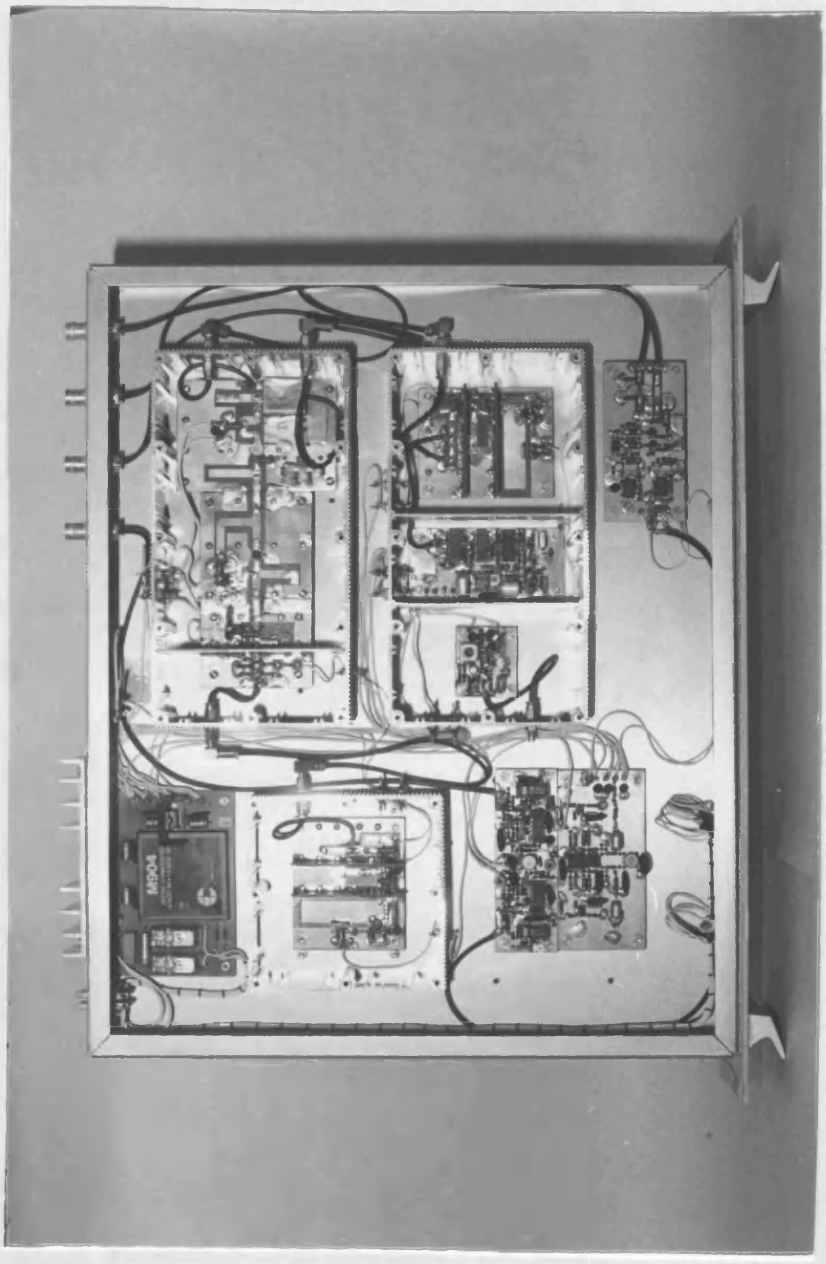

Figure 5.36 : The Complete 950MHz Transmitter

(i) The maximum bandwidth which may be achieved - determined by stability considerations.

(ii) Provision for varying the bandwidths.

(iii) Practical considerations such as: tracking frequency drift, slew-rate limitations, etc.

5.5.2 The Amplitude Loop

5.5.2.1 Loop Stability

The amplitude feedback is applied by comparing the demodulated envelope signals produced by the two polar resolvers, and amplifying the error in a differential amplifier to produce the modulator control voltage. Referring to the diagram in Figure 5.37, the entire transmitter circuitry from amplitude modulator control input, to envelope demodulator output, can be represented by an equivalent baseband network. The amplitude and phase response of this 'network', in conjunction with the open-loop response of the differential amplifier will therefore define the closed loop response, and the stability margin.

The magnitude of the modulator control voltage is fixed by the RF circuits. Its maximum value is that which drives the RF power amplifier into saturation, while the minimum value reduces the output to zero. Similarly, the demodulated envelope signal level is set by the IF signal level into the demodulators, which is the maximum level consistent with good linearity. To measure the frequency response of the equivalent baseband network, a sinusoidal voltage was applied to the modulator control input and the

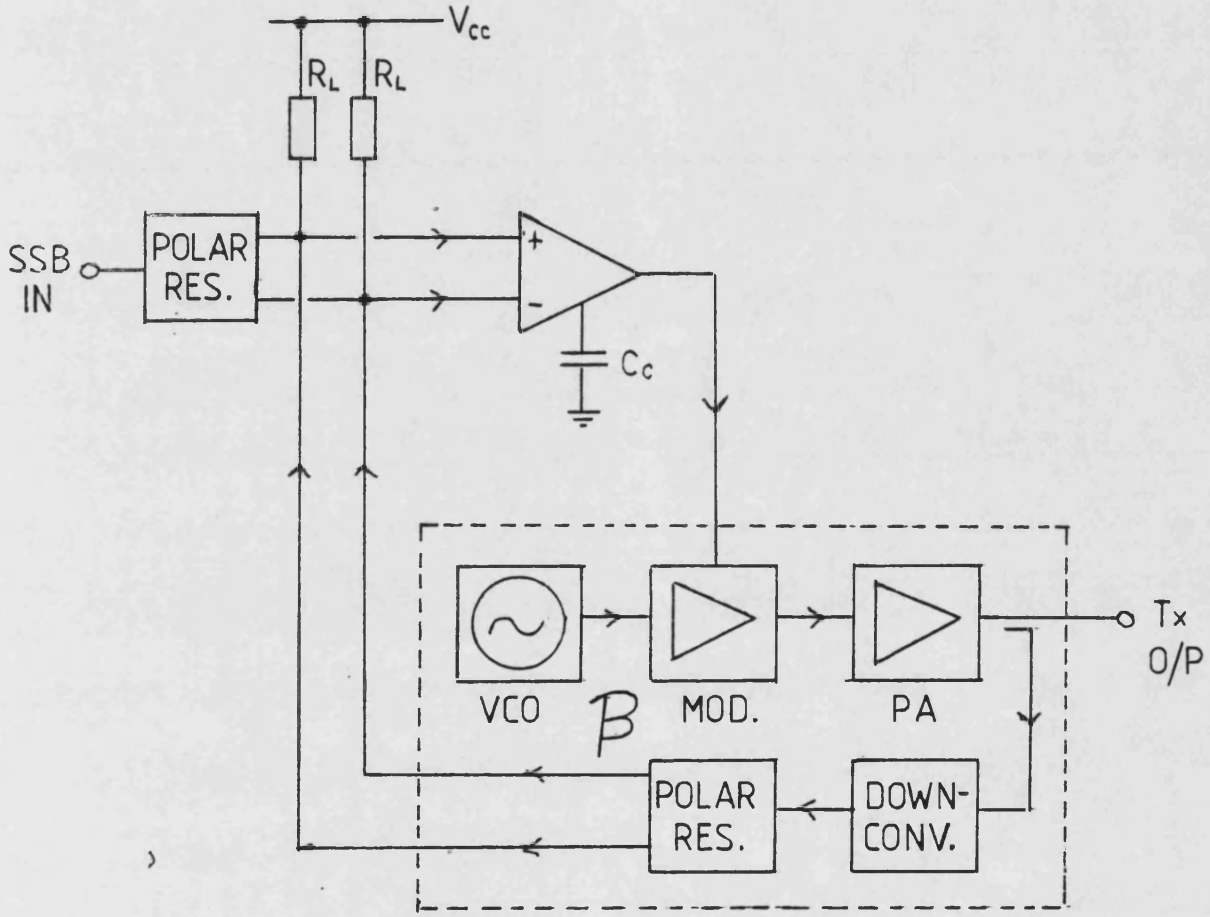

Figure 5.37 : Equivalent Circuit of the Amplitude Feedback Loop

demodulated output was measured. The level was chosen to give a 30% modulated AM output at a peak level 1dB below saturation, in order to avoid a grossly distorted output which could have led to misleading results. The measured response for the 950MHz transmitter is shown in Figure 5.38. Also shown is the differential amplifier open-loop response for several values of compensation, capacitance, reproduced from the manufacturer s data.

According to simple feedback theory, the closed loop response of the amplifier will be given by:-

$$A_{CL} = \frac{A_{OL}}{1 + \beta.A_{OL}} \qquad (5.1)$$

where A_{CL} = Closed loop voltage gain

A_{OL} = Open loop voltage gain

β = Feedback factor.

$\therefore$ When A_{OL} is large (at low frequencies):-

$$A_{CL} \rightarrow \frac{1}{\beta}$$

And, when A_{OL} is small (at high frequencies):-

$$A_{CL} \rightarrow A_{OL}$$

If the product $\beta.A_{OL}$ (the loop gain) has a first order dominated frequency response, then the closed loop bandwidth will be that frequency at which:-

$$A_{CL} = \frac{A_{OL}}{1 + j1}$$

which is when: $\beta.A_{OL} = 1$, or $\frac{1}{\beta} = A_{OL}$.

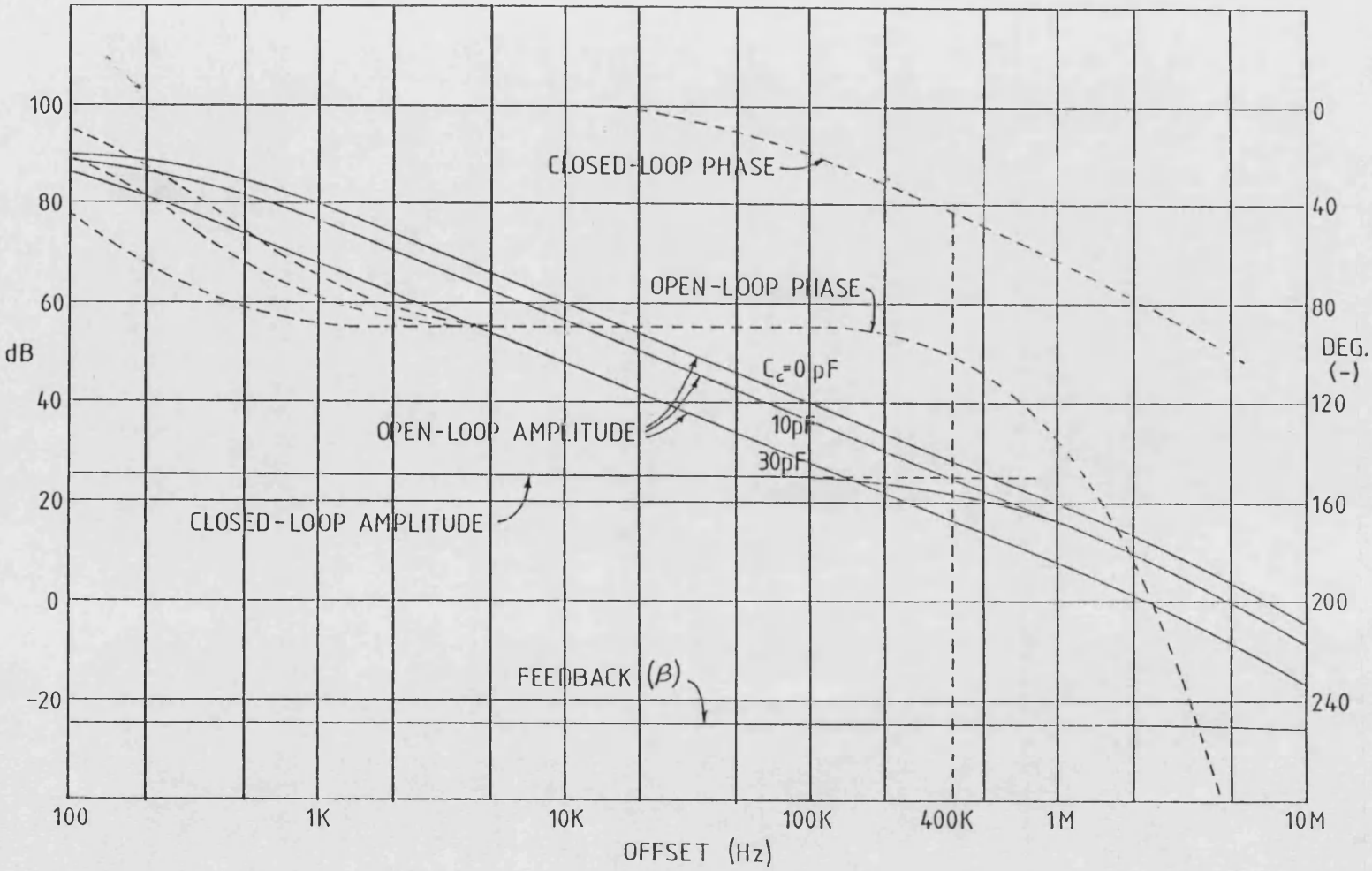

Figure 5.38 : Frequency Responses for the 950MHz Transmitter Amplitude Loop

Taking the example of 10pF compensation capacitance applied to the amplifier, it can be seen from Figure 5.38 that the $1/\beta$ response intersects A_{OL} at a frequency of 400KHz. Since the total loop phase shift at this frequency is 100^{o} (i.e. 80^{o} phase margin of stability), the closed loop response can be expected to have a virtually first order characteristic. To confirm this, the closed loop response was measured by applying an AM signal to the input resolver, and observing both the demodulator output and the modulator control voltage. The result of this measurement is also shown in Figure 5.38, and clearly verifies the prediction.

An identical procedure was carried for the 450MHz transmitter amplitude loop, and the results are shown in Figure 5.39. In this case, the demodulator output voltage is larger, giving a lower closed loop gain. Also, the phase shift within the demodulators is greater than that in the 950MHz transmitter, which results in a reduced phase margin of 40^{o}. This is confirmed by the closed loop response, which displays a peak of 1dB at the loop bandwidth of 500KHz.

5.5.2.2 Loop Bandwidth Variation

Variation of the loop bandwidth may be accomplished in one of three ways:-

(i) By varying the amplifier compensation capacitance.

(ii) By inserting an attenuator between the amplifier output and the modulator control input.

(iii) By attenuating the input signal to each polar resolver.

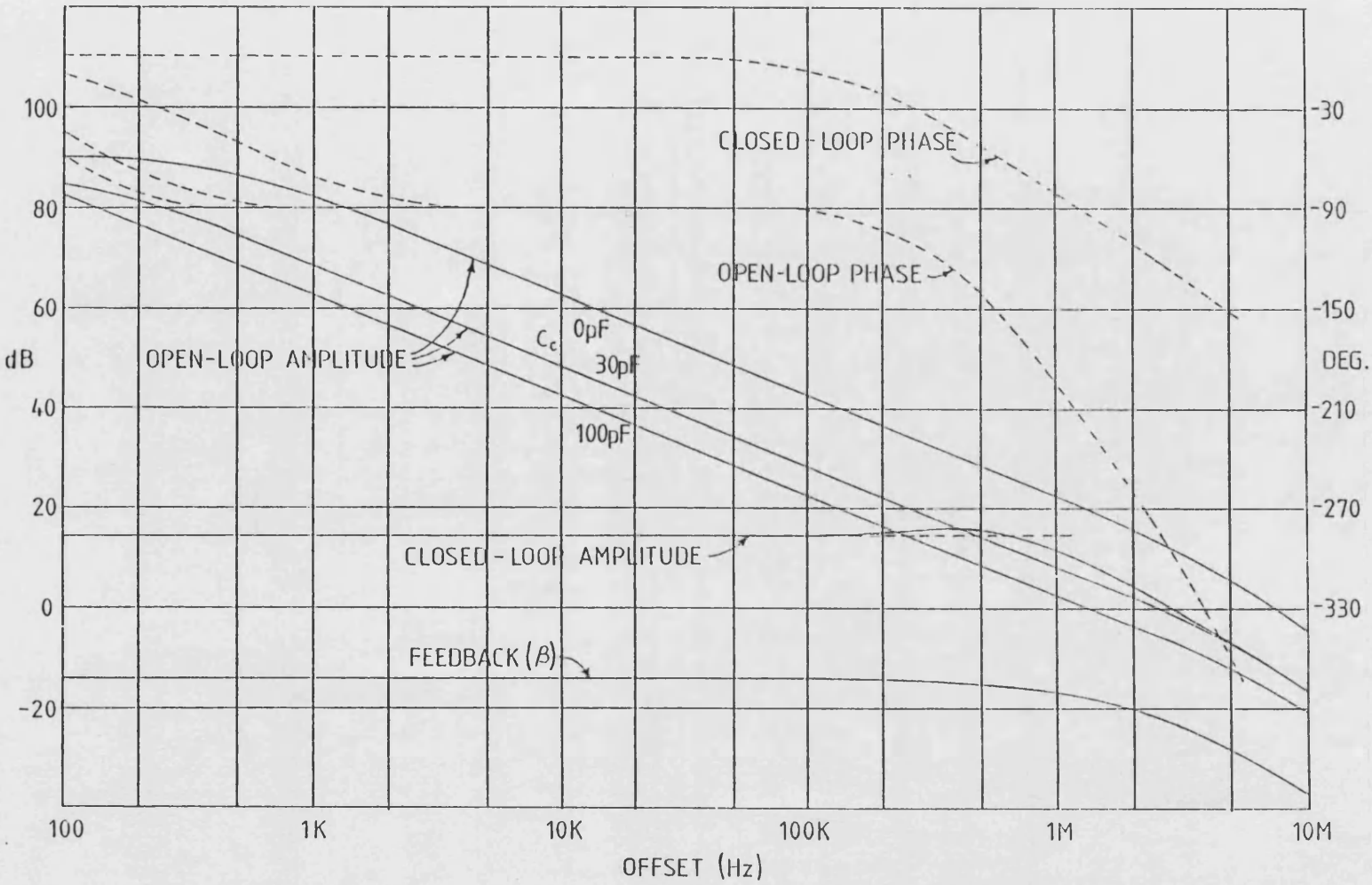

Figure 5.39 : Frequency Responses for the 450MHz Transmitter Amplitude Loop

The first technique results in a variation in slew-rate capability, although since this is in direct proportion to the bandwidth variation, the stability margin is not compromised. The second method has the disadvantage that since the modulator control voltage must be maintained, the amplifier could be driven into clipping. Finally, the third method is aggravated by the problem of d.c. offset or drift at the demodulator outputs. Since the first method does not have any disadvantages, and is simple to implement, this was used in the tests on bandwidth variation reported in Chapter 6.

5.5.2.3 Prediction of Amplitude Loop Noise Level

With the practical circuit designs and the closed loop response of the amplitude feedback loop both known, the contribution to the transmitter output noise level made by the amplitude loop can now be predicted.

The block diagram of Figure 5.40 shows the relevant constituent parts of the 950MHz transmitter amplitude loop, and gives the signal and noise levels assuming a CW input of 0dBm (corresponding to the maximum transmitter output power).

Buffer amplifier equivalent = $6nV/\sqrt{Hz}$

input noise $\equiv$ -151dBm/Hz

SSB generator noise level = -140dBm/Hz, which is assumed to comprise equal components of amplitude and phase noise (-143dBm/Hz, each).

Hence total effective input noise = -142dBm/Hz.

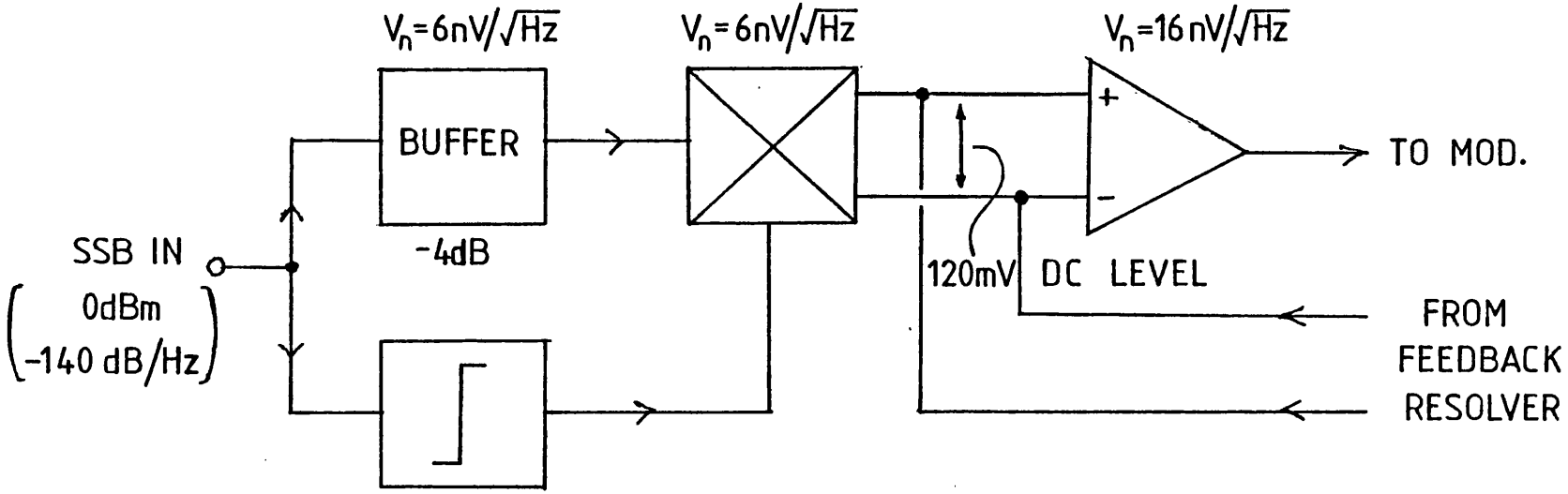

Figure 5.40 : AM Noise Sideband Contributions

Although the buffer stage gives 4dB loss, there is no significant SNR degradation since the input noise level is over 20dB above thermal noise.

Demodulator equivalent input noise = $6nV/\sqrt{Hz}$

$\equiv$ -147dB/Hz

(rel. to -4dBm).

Which gives a total effective noise level at the demodulator input of -140dB/Hz (rel. to -4dBm).

Differential amplifier equivalent input noise = $16nV/\sqrt{Hz}$

$\equiv$ -136dB/Hz

(rel. to 120mV).

Hence total effective noise level at amplifier input is given by the summation on a power level basis of:

-136dB/Hz due to the amplifier

and, -140dB/Hz due to each of the two resolvers.

Which is: <u>-134dB/Hz</u>.

Thus, the transmitter can be expected to have AM noise sidebands with a total power level of -134dB/Hz below PEP, at frequency offsets up to the loop bandwidth. Beyond the loop bandwidth, the lowpass filtering action of the loop will cause a 6dB/octave roll-off. This is shown in Figure 5.41.

Although the signal from the VCO is nominally at a constant amplitude, there may also be an AM noise content which would degrade the above figure.

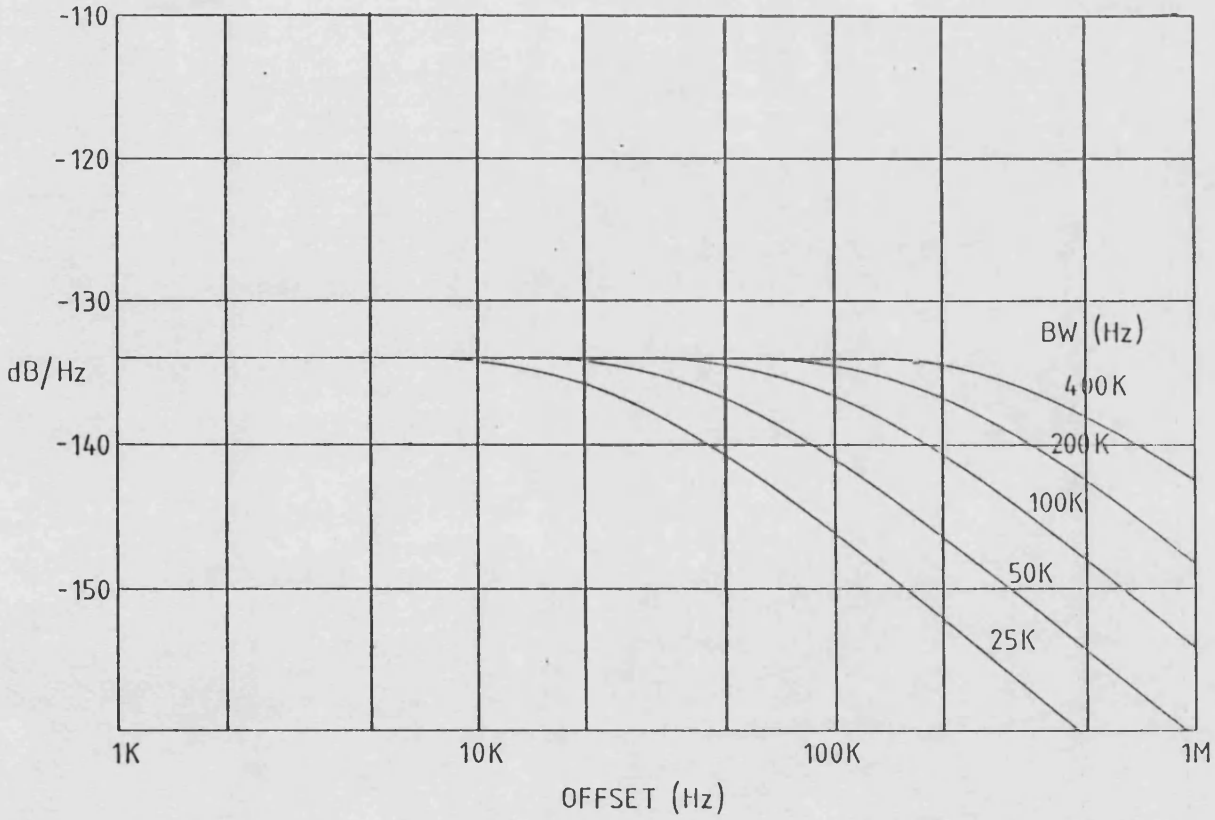

Figure 5.41 : Predicted AM Noise Sideband Level for the 950MHz Transmitter

5.5.3 The Phase Locked Loop

5.5.3.1 Choice of Loop Constants

In a Polar Loop Transmitter, the phase locked loop has three main functions:-

(i) To generate the phase component of the output signal.

(ii) To reduce phase distortion generated by the RF circuits.

(iii) To correct for any drift in the VCO centre frequency.

Previous work on HF and VHF Polar Loop transmitters (58 and 59), has shown that the first requirement is met most successfully if the loop is of first order. In particular, when the loop was made to track sudden phase changes (as in the case of a two equal tone signal), the intermodulation products were found to worsen if the loop was allowed to overshoot or ring (indicative of a second order loop). A first order loop is also desirable for good stability, since changes in loop gain (due to temperature variation for example), would not compromise the stability margin.

An unfortunate disadvantage of the first order loop is that its tracking, or hold-in range, is equal to twice the loop bandwidth, which in this case is no more than a few hundred KHz. However, the frequency drift with temperature of the practical VCOs greatly exceeds this. Over the commercial temperature range of -10 to +70^{o}C, the 450MHz and 950MHz oscillators drift by 5MHz and 3MHz, respectively.

To overcome these two conflicting requirements, a novel loop filter was devised. If the 'integrate/lead' form of active filter as shown in Figure 5.42 is used, the tracking range becomes equal to the product of the VCO constant and the maximum output voltage from the filter. Such a filter would normally give a second order loop, since the integrating action of the VCO combined with the integrator in the filter produces a second order open-loop characteristic. If, however, the phase lead break point, given by $1/R_2C_2$, is made much less than the loop bandwidth B then the open-loop response will be essentially first order in the critical region near the loop bandwidth. The closed-loop response will therefore also have a first order characteristic. A full derivation of this is given in Appendix C since the author has not encountered this technique in the literature.

For a first order loop, PLL theory predicts that the loop bandwidth, B, is given by (113):-

$$B = K_o K_d A \quad \text{KHz} \qquad (5.2)$$

where K_o = VCO constant in KHz/V

K_d = PSD constant in V/rad

A = Any additional gain in the loop.

Using the active loop filter described, the additional gain, A, is due to the 'high frequency' gain: R_2/R_1.

The PSD constant, K_d, is determined by the physical circuit, hence only K_o and A can be varied to define the bandwidth. Stewart (114) has shown that K_o should not be made higher than necessary in order to avoid a phase noise degradation caused by baseband noise appearing on the VCO

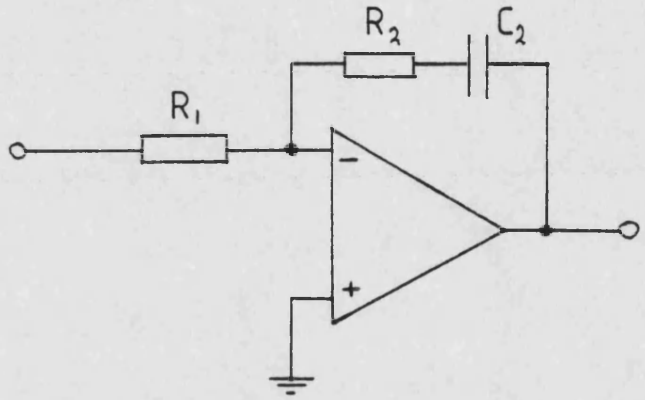

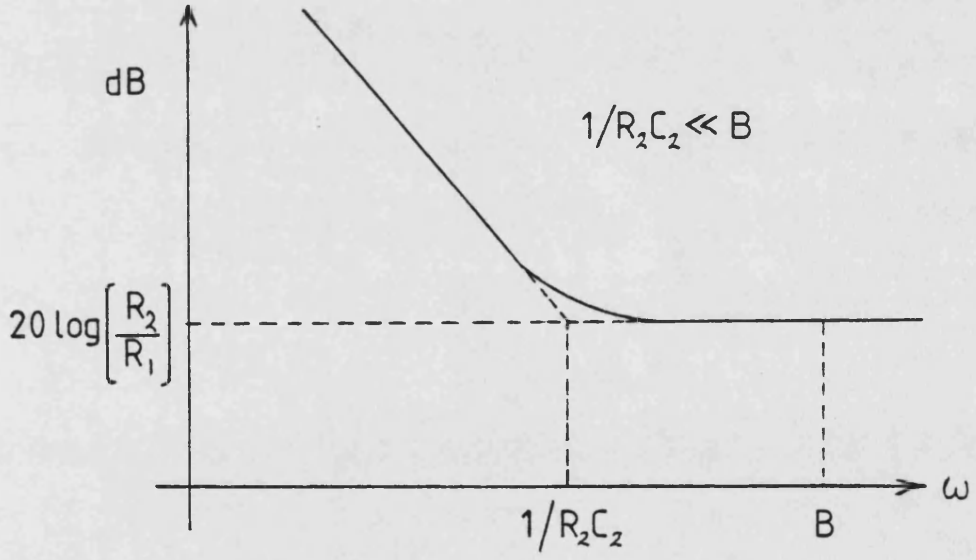

Figure 5.42 : Active Loop Filter

control input. One source of such noise quoted by Stewart, is that due to the varactor itself. This can produce an rms frequency deviation of the VCO of:-

$$\Delta f_{rms} = K_o.V_n \qquad (5.3)$$

where V_n = rms baseband noise voltage due to varactor. Which can be related to the single sideband signal to phase noise ratio by:-

$$SNR = -20 \log \left[\frac{\Delta f_{rms}}{\sqrt{2}.f_m}\right] \text{ dB/Hz} \qquad (5.4)$$

where f_m = Offset from carrier freq. (Hz).

In practice, it was found that neither the 450MHz or 950MHz oscillators showed any change in phase noise level with the varactor in or out of circuit. Thus it can be assumed that this noise contribution is well below that of the basic oscillator. It is clear, however, that a noise voltage or spurious signal on the VCO input from another source could be significant. To quantify this, consider the example of a K_o value of 2MHz/V. To achieve a phase noise level of -95dB/Hz at a 5KHz offset (the level measured for the practical VCOs), implies from equations 5.3 and 5.4 an equivalent noise voltage of 60nV/$\sqrt{Hz}$. This is less than an order of magnitude above the noise level produced by typical low noise operational amplifiers. It also implies that very good screening of the VCO would be needed in order to avoid spurious signals at this level.

In view of these figures, it was decided to keep the VCO constants well below the example given.

For the 450MHz transmitter, which used a TTL PSD with a K_d value of 0.5V/rad, a K_o of 240KHz/V was used, in conjunction with a filter gain of 2, which gives a bandwidth of 240KHz. This bandwidth gave the best linearity at the transmitter output, no further improvement being noted by making the bandwidth wider (see Section 6.2). The maximum loop filter output voltage is approximately 8V, giving a tracking range of 1.9MHz with the above K_o value. This is still inadequate to compensate for drift with temperature. Increasing K_o to give sufficient correction range would increase the susceptibility to spurious signals, and so is not desirable. To overcome this difficulty, a second, coarse tuning varactor was used on the VCO, fed from the control voltage via a lowpass filter of a few Hz cutoff frequency (see Figure 5.43). With a coarse tuning constant of 1.8MHz/V, this gives a tracking range of 14MHz, but does not affect the dynamic operation of the loop. Since this second varactor is heavily decoupled by the lowpass filter at baseband, the problem of spurious pick-up is avoided.

The 950MHz VCO has better temperature stability than the 450MHz oscillator and consequently did not require the use of a second varactor. A single VCO constant of 670KHz/V provides a tracking range of 5.4MHz, which is more than adequate. Due to the reduced PSD constant of 0.13V/rad, resulting from the use of the ECL device, a larger loop filter gain is needed. A factor of 4.6 produces a loop bandwidth of 400KHz, which was the widest bandwidth used during the measurements on the transmitter.

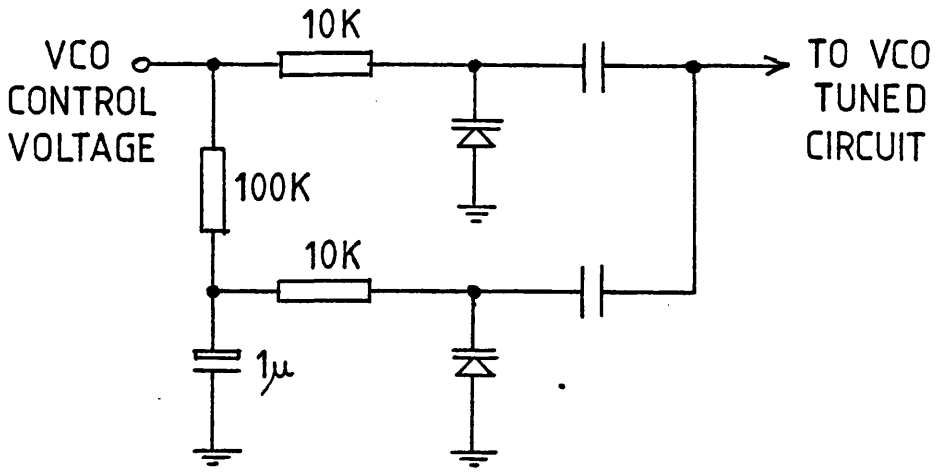

Figure 5.43 : Modification to VCO Control Input for Increased Tracking Range

For both transmitters, the value of C_2 in the loop filter was chosen to set the break frequency, $1/R_2C_2$, at least an order of magnitude below the loop bandwidth. This ensured a first order response.

5.5.3.2 Variation of PLL Bandwidth

As previously mentioned, only K_o and A can be altered to vary the loop bandwidth. However, varying K_o is physically inconvenient because it involves changing the VCO varactor coupling capacitor. Since the VCO is mounted in a completely screened enclosure, such a change is not a trivial procedure. Far more convenient is to change the values of R_2 and C_2. Reducing R_2 scales the bandwidth in direct proportion, provided C_2 is increased to maintain the relative position of the $1/R_2C_2$ break frequency. This was the method adopted.

5.5.3.3 Loop Stability

Steps taken to ensure that the PLL has a first order (and therefore unconditionally stable) response, have already been described. However, in practice there will inevitably be additional sources of roll-off and phase shift within the loop, which reduce the stability margin. Measurements made on the transmitters showed that the two main contributors to the excess phase shift were:-

(i) The loop filter.

(ii) The VCO control input (the varactor and its series resistor form a lowpass filter).

Figures 5.44 and 5.45 show the frequency responses of the 450MHz and 950MHz PLLs, respectively. The wider bandwidth and higher gain loop filter in the 950MHz case increases the excess phase, and hence reduces the stability margin in comparison with the 450MHz loop. The margin is still sufficient though, to give a closed-loop response free from peaking, and a corresponding transient response free from overshoot.

Measurement of the closed-loop response would ideally be made by applying a sinusoidally frequency modulated signal to the transmitter input, and observing the VCO control voltage (proportional to output frequency). Unfortunately, no signal generator was available at the time of the measurements capable of FM rates up to 1MHz. Consequently, the method adopted was to apply an unmodulated carrier to the transmitter input, and to insert a summing amplifier between the loop filter output and the VCO input, as shown in Figure 5.46. When a sinusoidal test signal is applied to the other summing input, the loop response can be seen by observing the filter output. Appendix D shows analytically that the ratio of filter output to test signal input is identically equivalent to the required closed-loop response.

5.5.3.4 Prediction of PLL Noise Level

As in the case of the amplitude loop of the 950MHz transmitter, knowledge of the practical circuit elements and of the PLL design, permits the expected transmitter

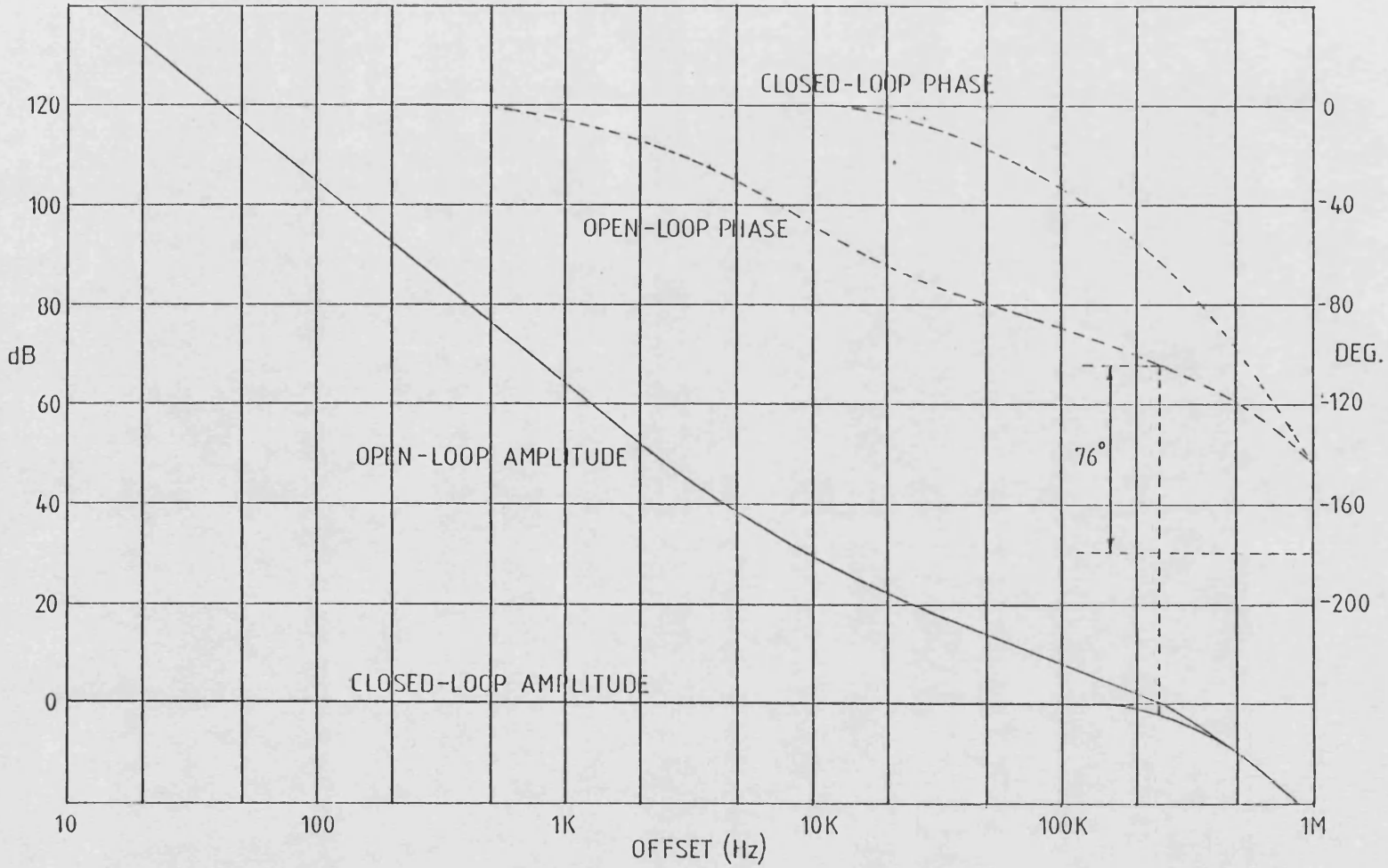

Figure 5.44 : Frequency Responses of the 450MHz Transmitter PLL

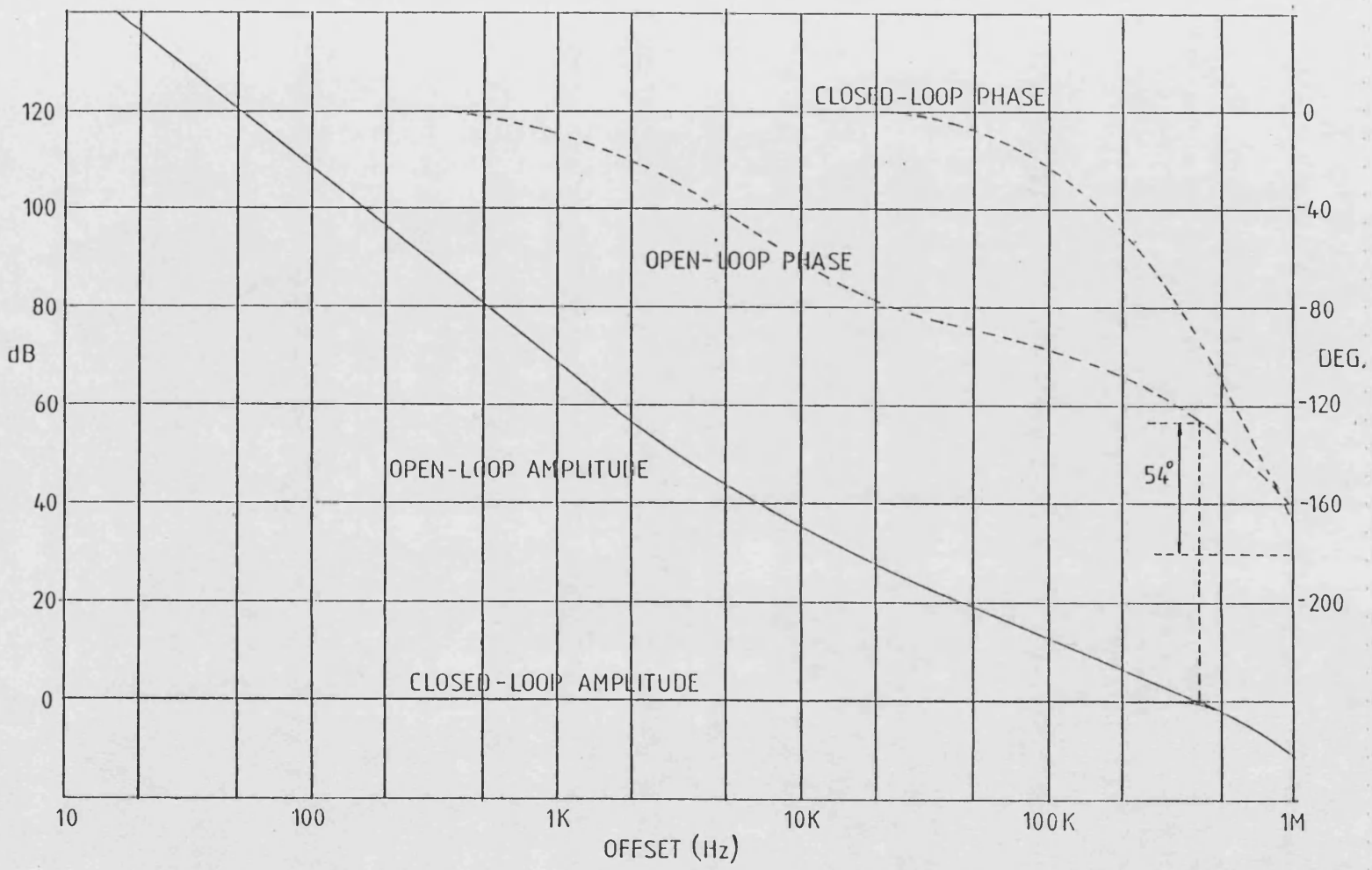

Figure 5.45 : Frequency Responses of the 950MHz Transmitter PLL

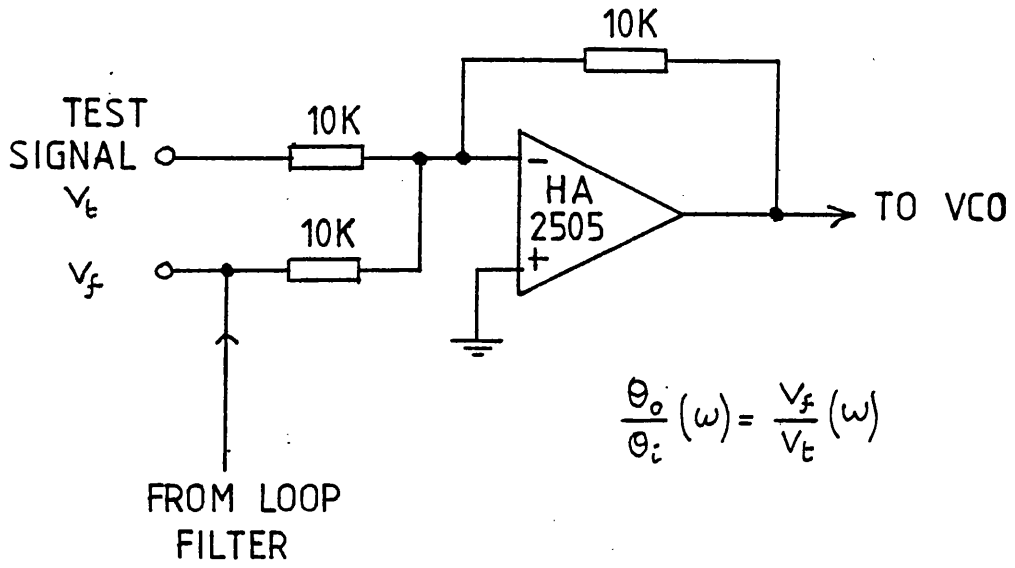

Figure 5.46 : Measurement of the Closed-Loop Response of the PLL

output phase noise level to be calculated. Figure 5.47 shows a simplified block diagram of the PLL, and gives the measured noise contributions for each component. The noise produced by the loop filter is given as an equivalent input noise voltage. To relate this to a phase noise level, it must be divided by the PSD constant, K_d:-

$$\therefore \text{ Equivalent phase noise due to loop filter} = \frac{V_n}{K_d}$$

$$= \frac{16.10^{-9}}{0{\cdot}13}$$

$$= 1{\cdot}2.10^{-7} \text{ rad}$$

$$\equiv -138\text{dB/Hz}.$$

It was seen in Chapter 3 that the action of the PLL is to highpass filter the VCO noise spectrum, with a cutoff frequency equal to the loop bandwidth, whilst the summation of the noise contributions due to the reference signals and the other loop components, is lowpass filtered. The latter spectrum is made up as follows:-

Synthesiser (see Figure 5.19)

SSB generator:	-143dB/Hz
Input limiter:	-137dB/Hz
PSD:	-137dB/Hz
Feedback limiter:	-137dB/Hz
Loop filter:	-138dB/Hz
Downconverter:	-143dB/Hz

The summation on a power level basis of these six frequency offset independent levels is:- -130dB/Hz. Figure 5.48 shows the combination of the synthesiser noise spectrum and the broadband level of -130dB/Hz lowpass filtered for various

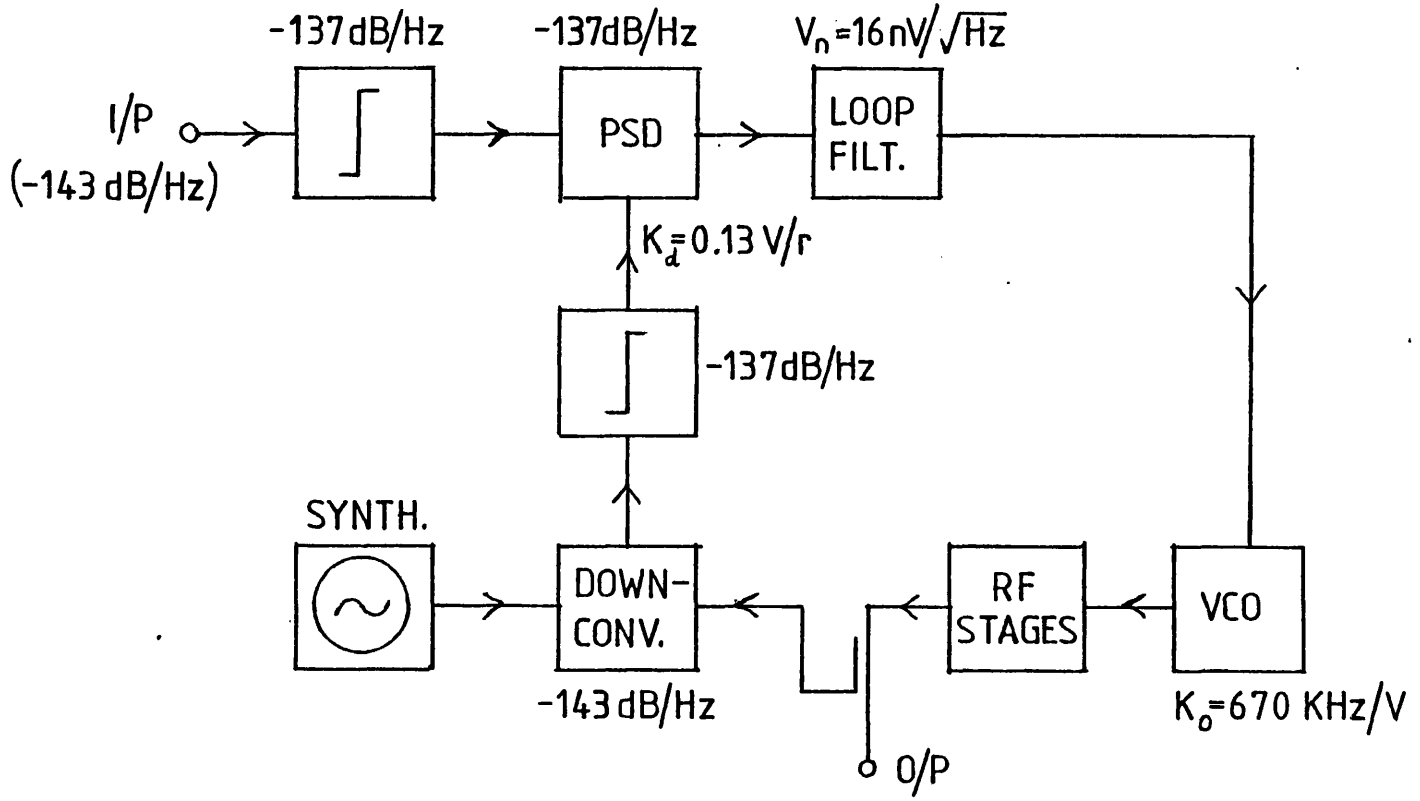

Figure 5.47 : Simplified Block Diagram of the PLL

values of loop bandwidth. Figure 5.49 shows the VCO noise spectrum highpass filtered at the same bandwidths. Note that the VCO noise is suppressed by 12dB/octave below the $1/R_2C_2$ break frequency of the loop filter, since the open-loop response is second order in this region. Finally, the expected spectra for the transmitter output phase noise are obtained by combining Figures 5.48 and 5.49, and are shown in Figure 5.50.

From the analysis of Chapter 3, the optimum bandwidth is given by the intersection of the VCO noise spectrum, and that due to the remainder of the loop components. Figure 5.51 shows that there is no clear intersection as such, since at low offsets, the two spectra are coincident, whereas at high offsets, the synthesiser and loop component noise dominates. This implies that the minimum achievable output phase noise is that of the free-running VCO, and consequently, that the loop bandwidth should be kept below approximately 15KHz (the point at which the two spectra diverge).

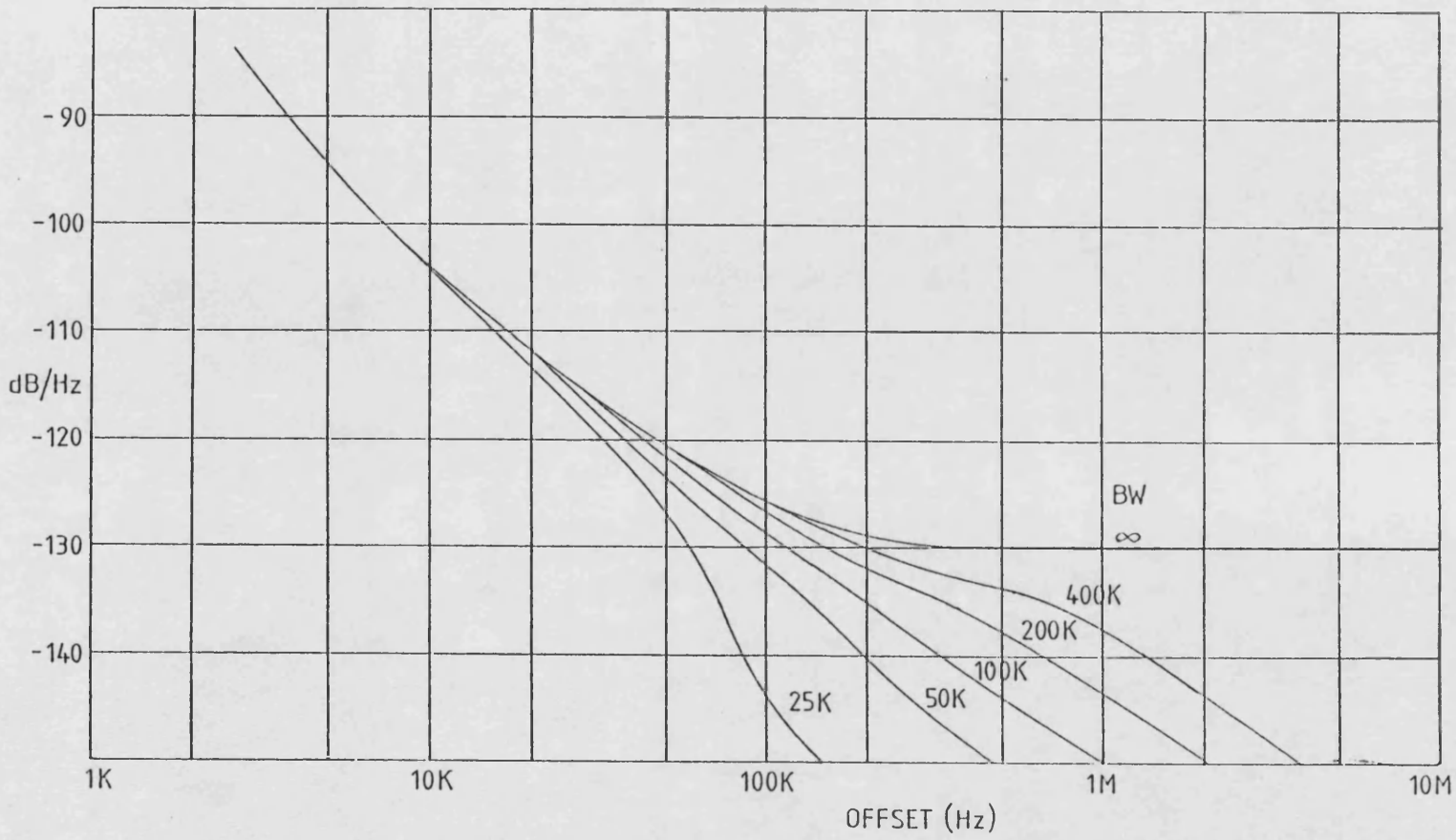

Figure 5.48 : Effect of the PLL on the Loop Noise Contributions (excluding VCO) for Various Bandwidths

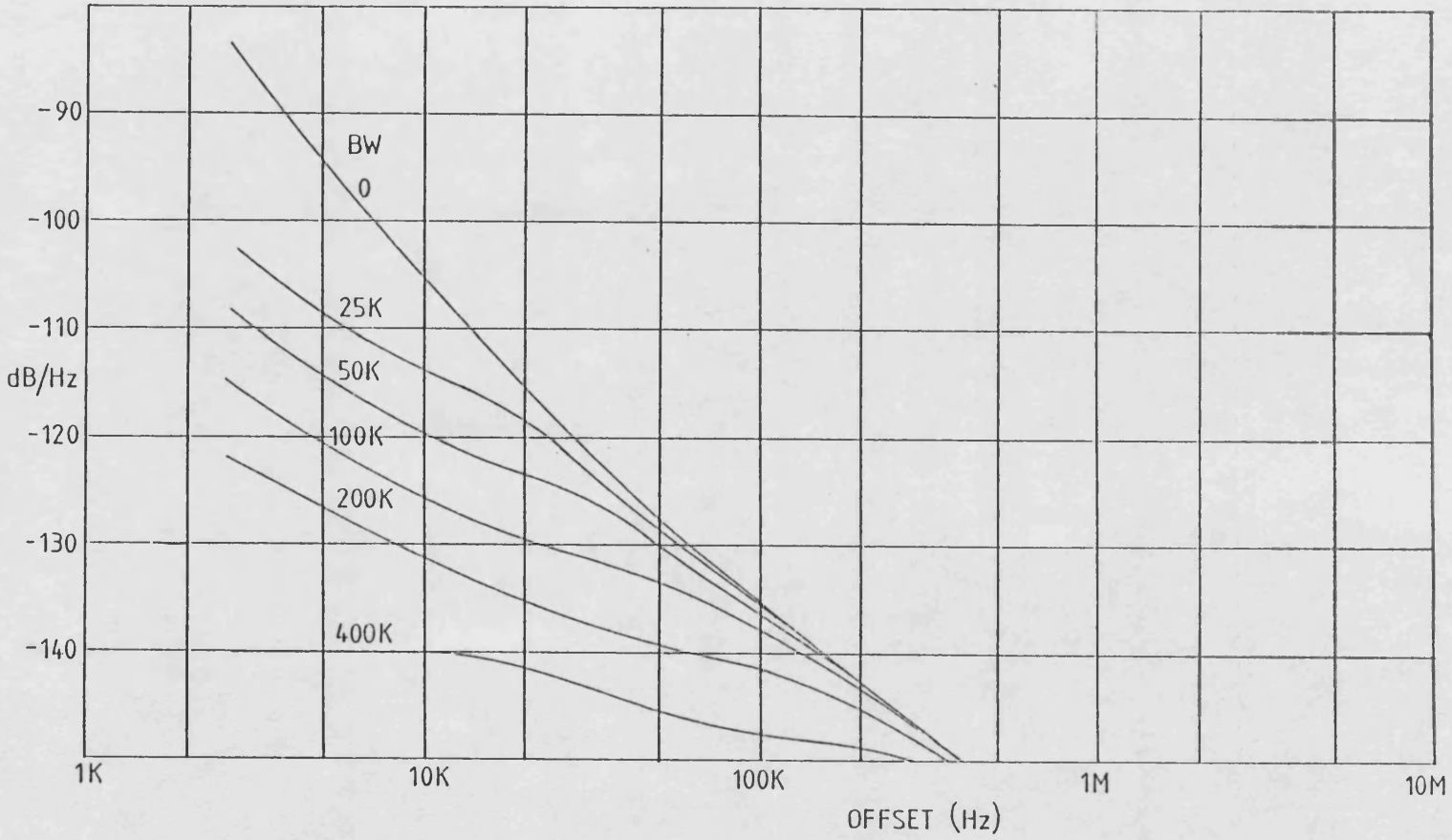

Figure 5.49 : Effect of the PLL on the VCO Noise for Various Bandwidths

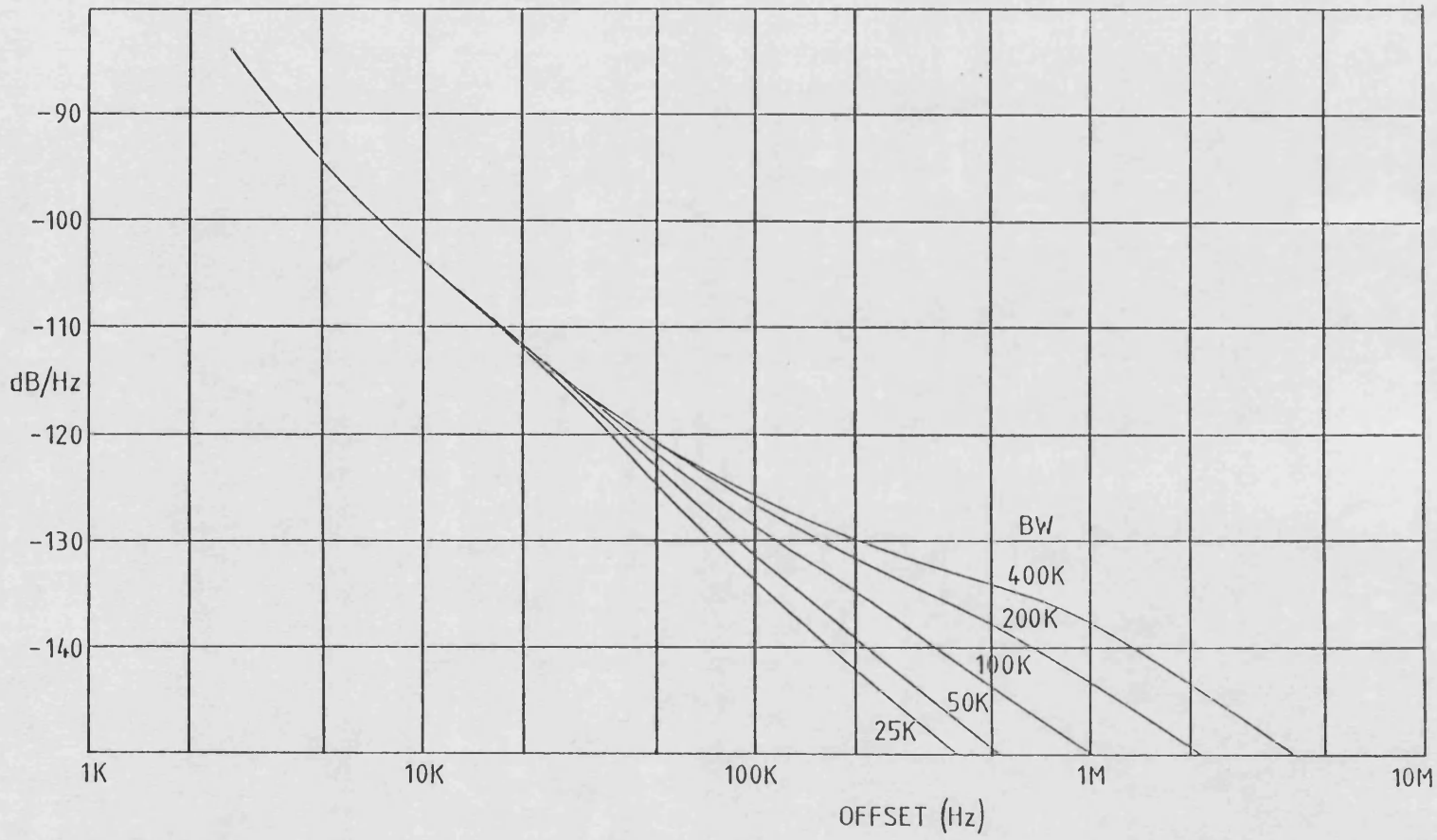

Figure 5.50 : Predicted Transmitter Phase Noise Spectra for Various Loop Bandwidths

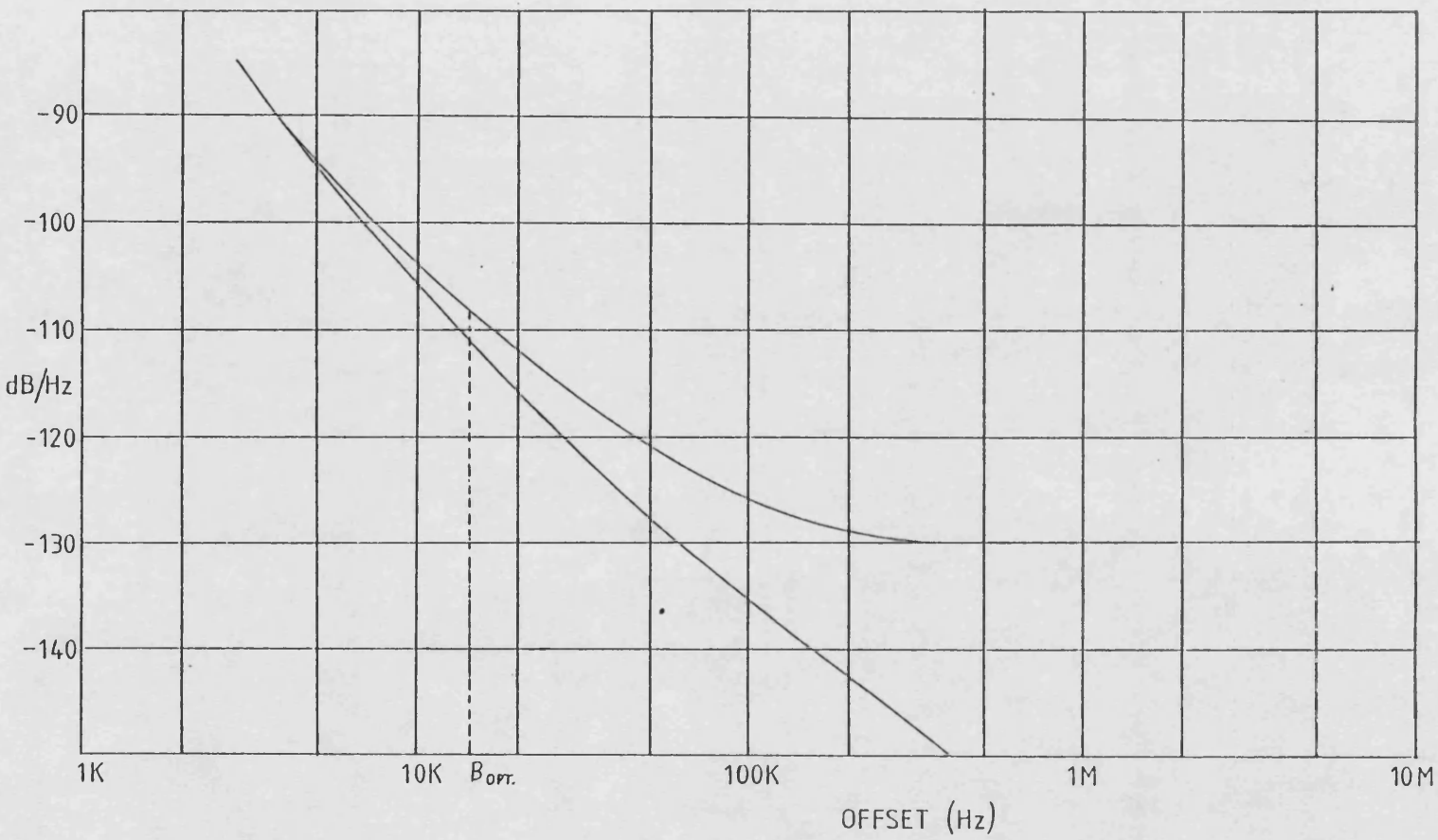

Figure 5.51 : Optimum PLL Bandwidth for Minimum Phase Noise

CHAPTER SIX

MEASURED RESULTS ON THE UHF TRANSMITTERS

6.1 INTRODUCTION

This Chapter documents the results of measurements made on the practical UHF polar loop transmitters, in terms of their linearity and noise level spectra.

As was mentioned in Chapter 5, early evaluation of the 450MHz transmitter showed up several limitations in its circuitry, which gave an unnecessarily poor performance, particularly with respect to phase noise. As a result of this, improved circuits were developed for the 950MHz transmitter. For this reason therefore, the most extensive measurements carried out, and presented here, were made on the 950MHz transmitter.

6.2 LINEARITY OF THE TRANSMITTERS

6.2.1 Output Spectra

The output spectra of the transmitters are shown in Figures 6.1 to 6.28, where the input is either two equal tones with a spacing of 500Hz, or is a band of white noise with a bandwidth defined by the SSB filter response. The latter signal gives a good indication of the performance with a speech input, since the signal occupies the whole of the available bandwidth. The output power level was set at 10W PEP and 1.7W PEP for the 450MHz and 950MHz transmitters,

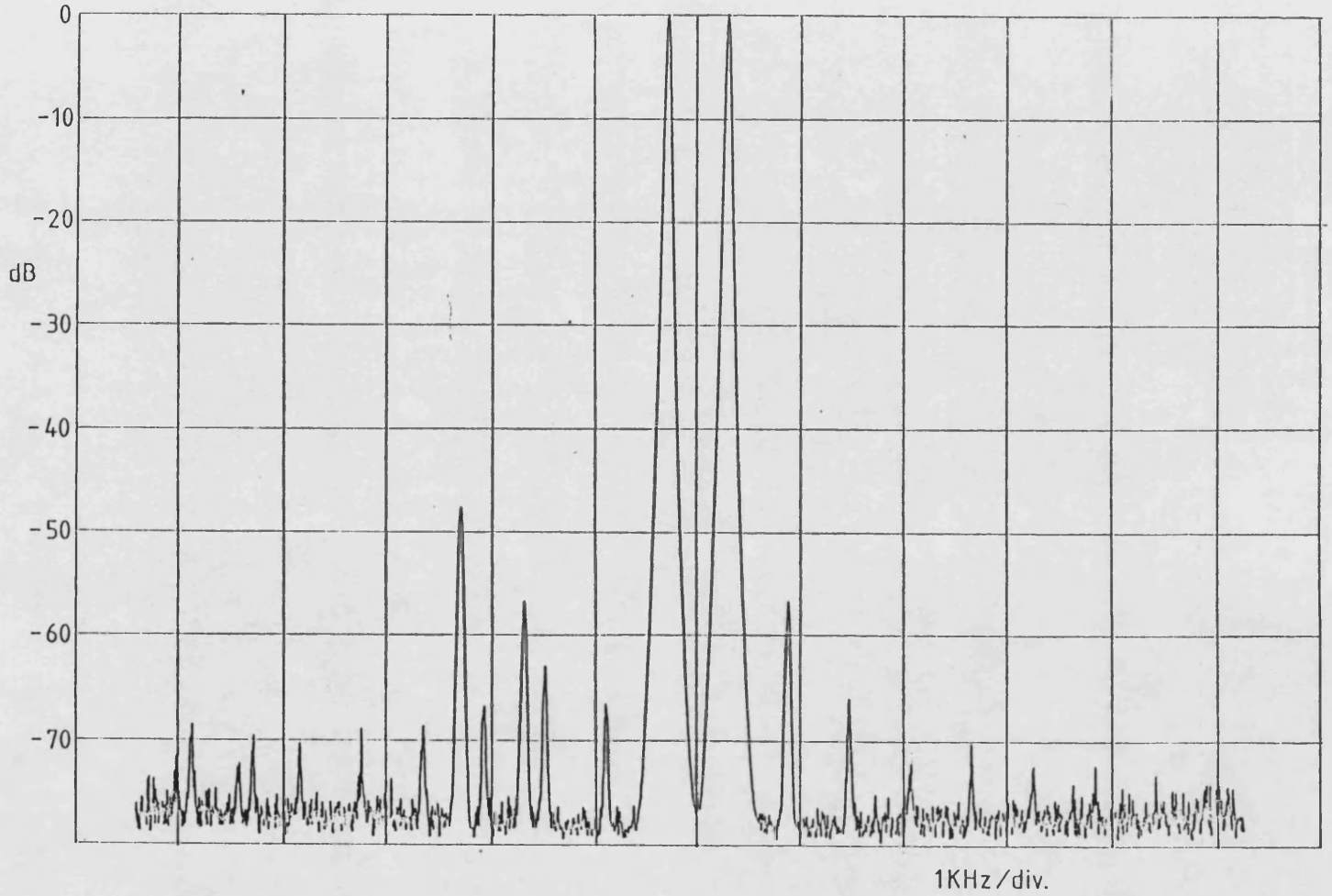

Figure 6.1 : 450MHz Transmitter Output Spectrum with Two-tone Input

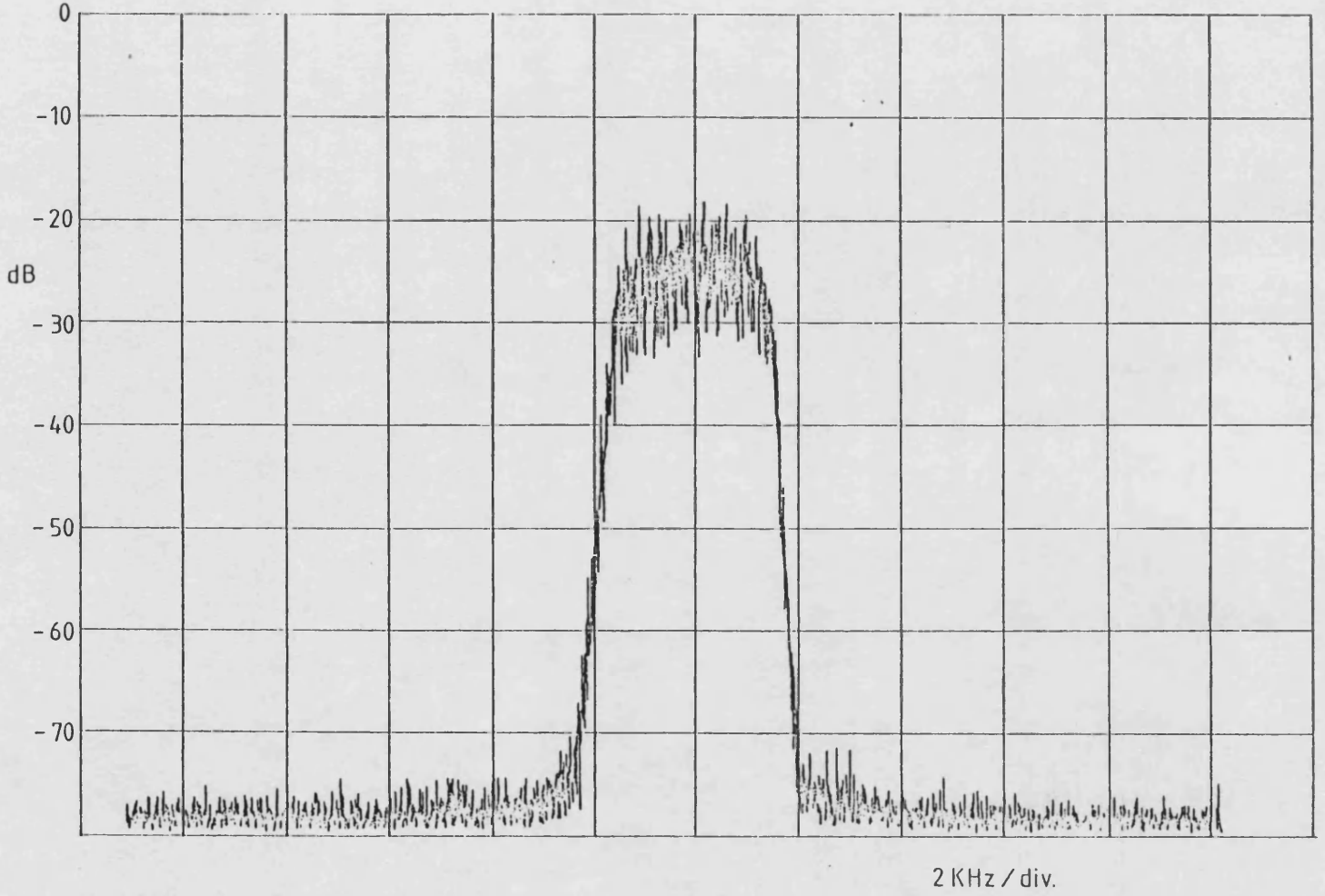

Figure 6.2 : 450MHz Transmitter Output Spectrum with White-Noise Input

respectively. These levels are within 1dB of the clipping point in each case. For the 950MHz transmitter, the effect of varying the feedback loop bandwidths was investigated. Figures 6.3 to 6.12 show the effect of reducing both bandwidths from their maximum values of 400KHz, in octave steps (6dB steps of loop gain), down to 25KHz. Figures 6.13 to 6.20 show the results of the same bandwidth reduction procedure, but with the PLL bandwidth fixed at 400KHz. Finally, Figures 6.21 to 6.28 keep the amplitude loop bandwidth fixed at 400KHz, while reducing the PLL bandwidth.

To show the effect of the bandwidth variation more clearly, the levels of 3rd, 5th and 7th order intermodulation products are plotted versus loop bandwidth in Figures 6.29, 6.30 and 6.31. It can be seen that there is no further improvement in 3rd order distortion for bandwidths greater than 100KHz, whereas the higher order products reach a minimum between 200 and 400KHz. Also notable is the fact that reducing the PLL bandwidth alone, introduces between 3 and 7dB more degradation in the distortion levels, than reducing only the amplitude loop bandwidth. If both loops are narrowed, the degradation is 1-2dB worse than that obtained by reducing just the PLL bandwidth. This implies that although the amplitude and phase distortion are of the same order of magnitude the phase distortion predominates.

It was noted during the course of the measurements that the distortion products drifted in amplitude over a period of tens of minutes, and that the drift seemed to correlate with ambient temperature variation. This effect was most

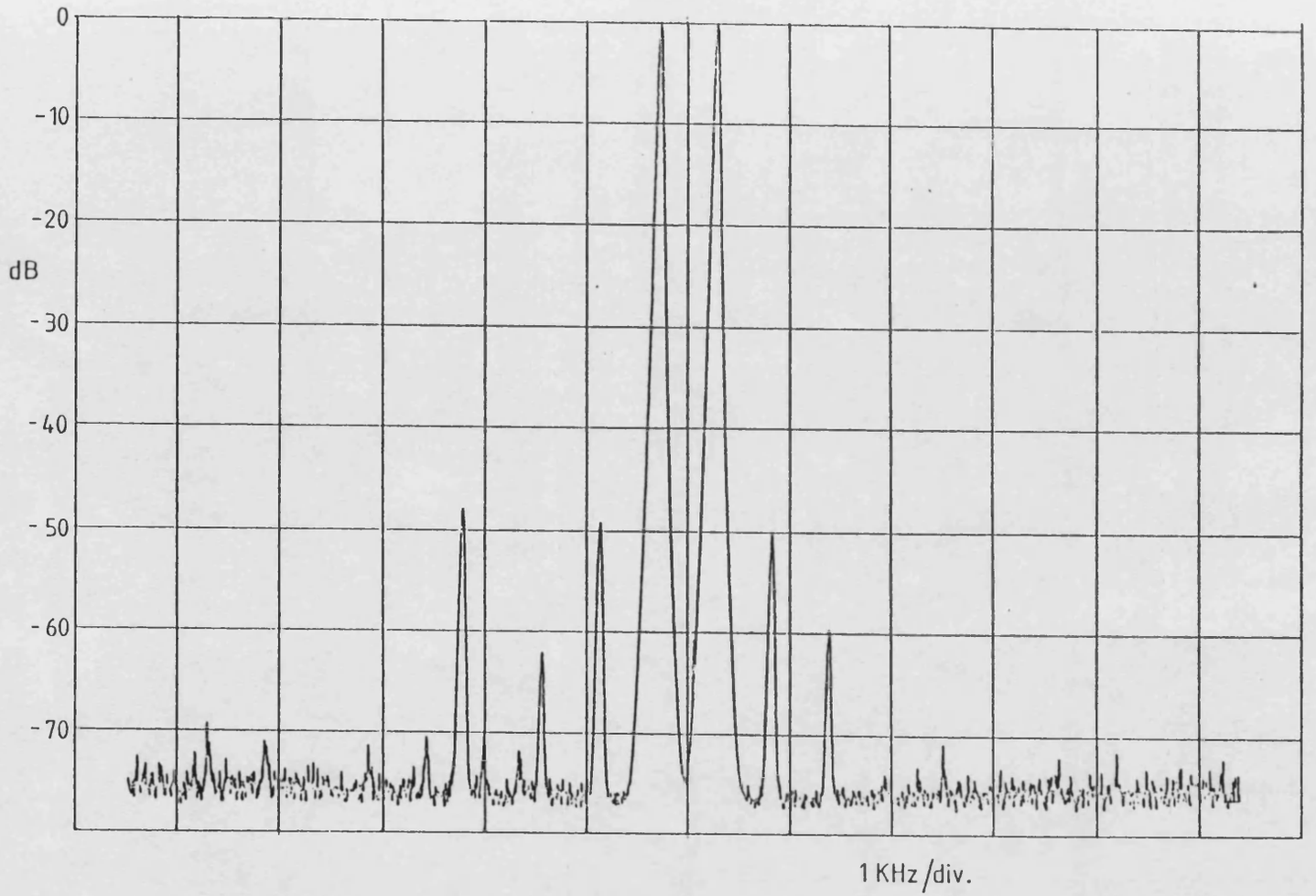

Figure 6.3 : 950MHz Transmitter Output with Two-tone Input (Both Loops 400KHz)

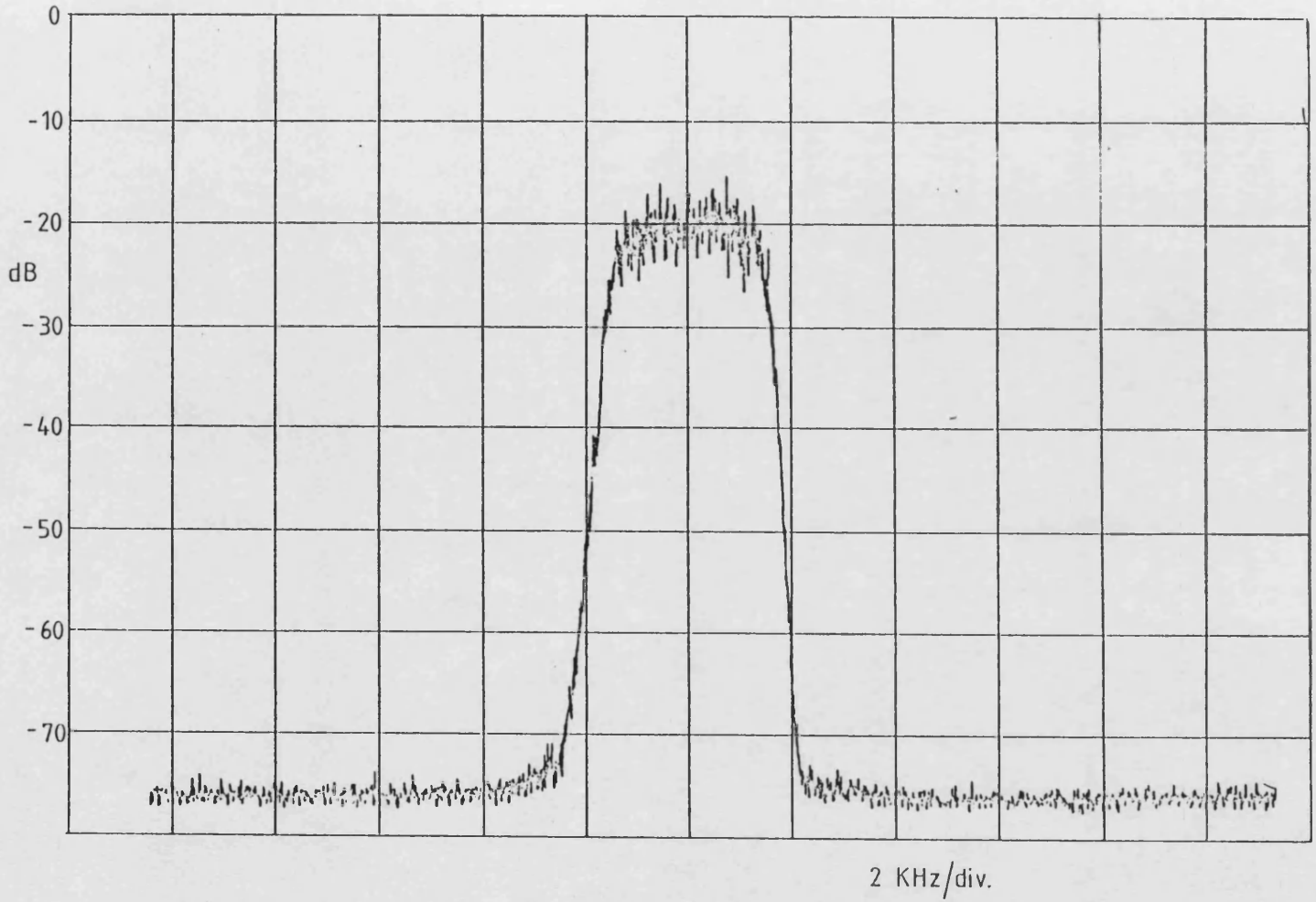

Figure 6.4 : 950MHz Transmitter Output with White Noise Input (Both Loops 400KHz)

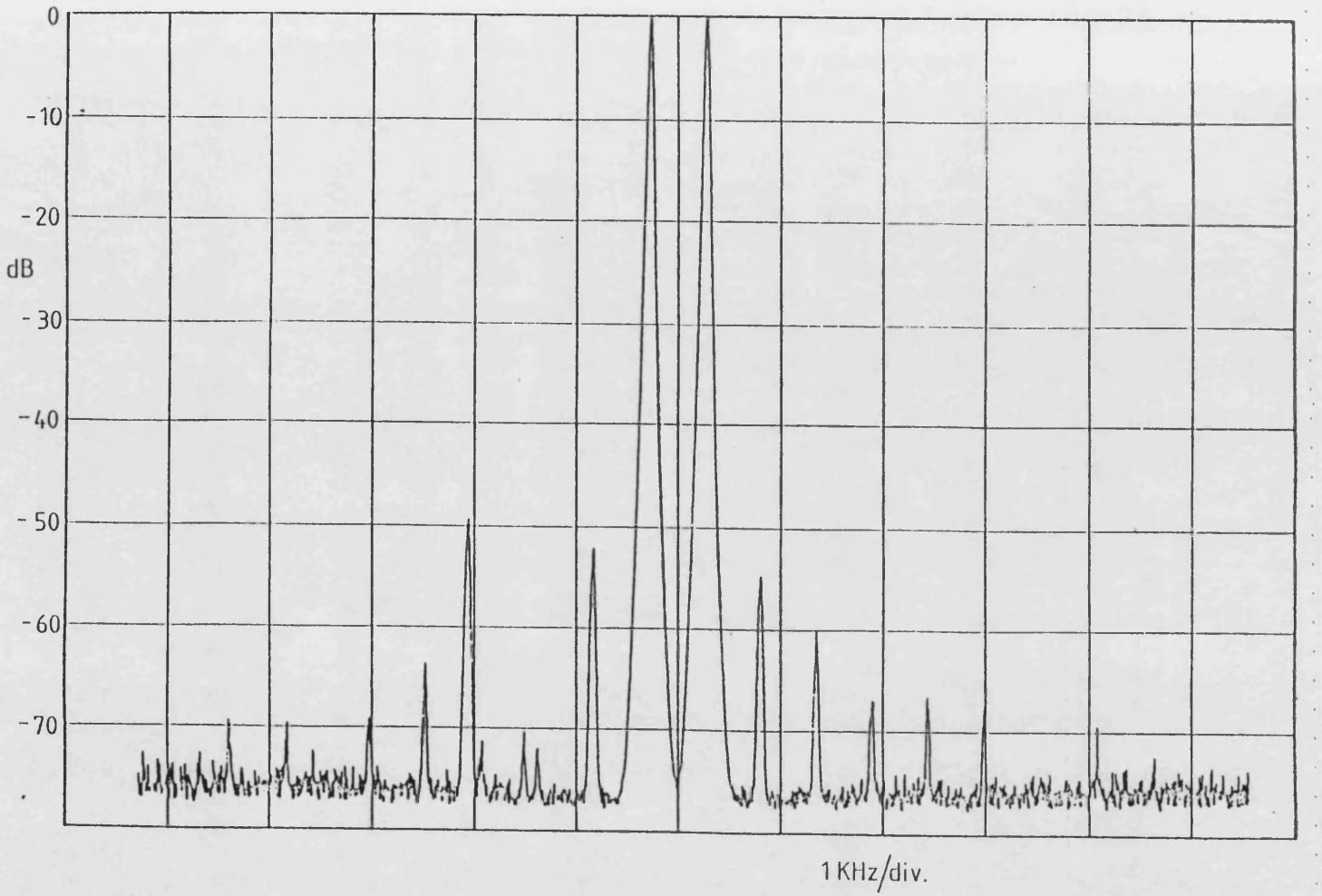

Figure 6.5 : 950MHz Transmitter Output with Two-tone Input (Both Loops 200KHz)

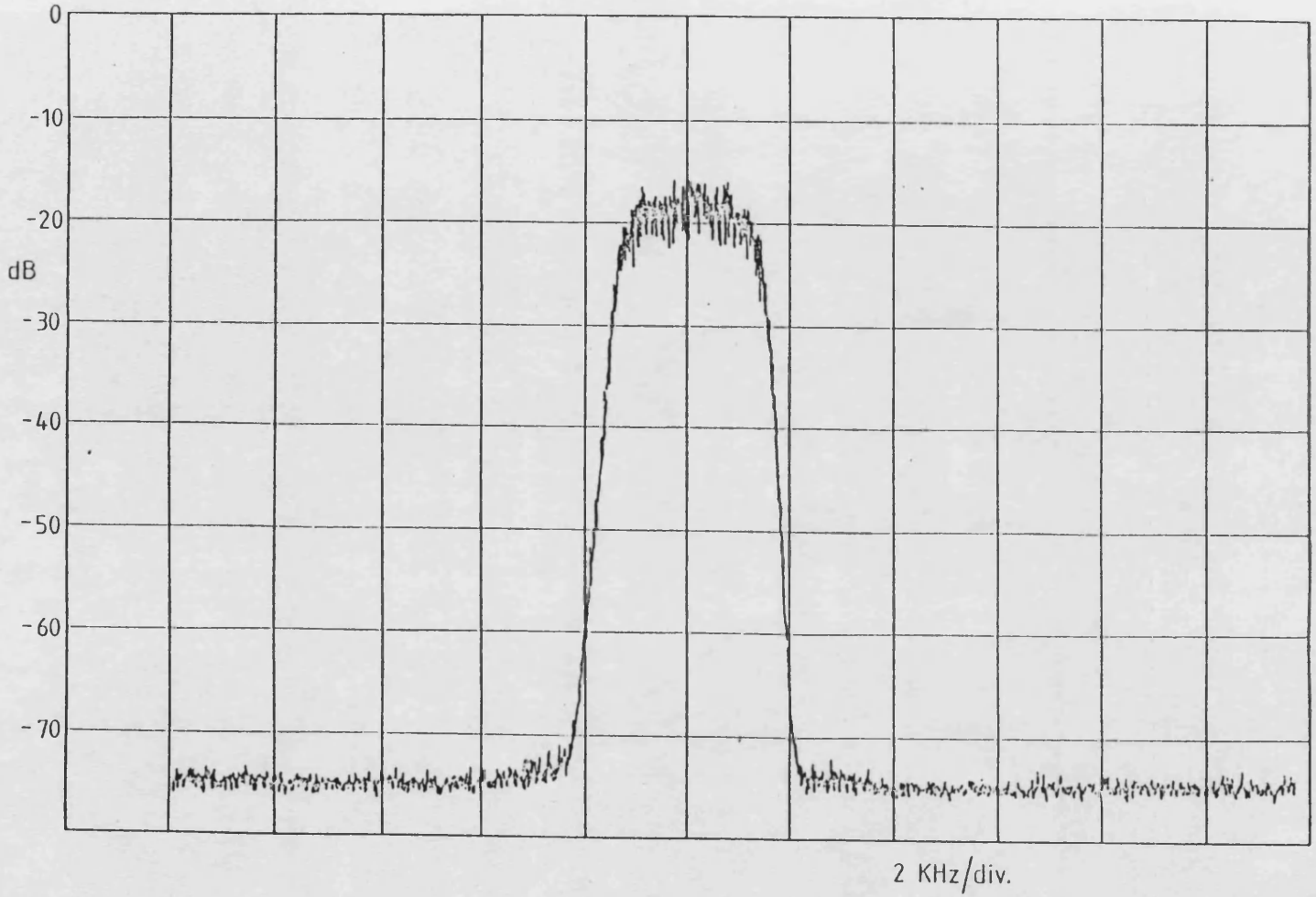

Figure 6.6 : 950MHz Transmitter Output with White Noise Input (Both Loops 200KHz)

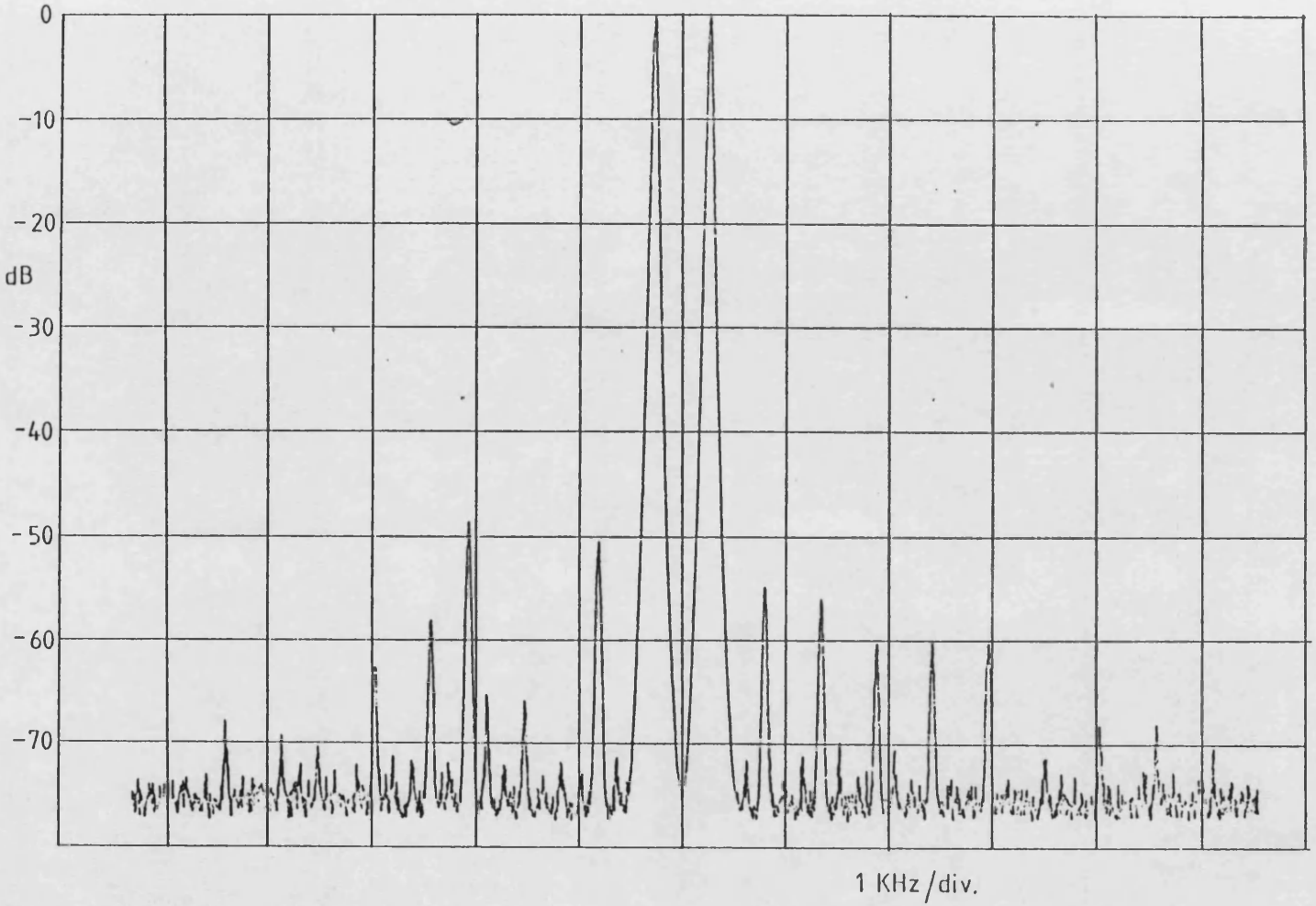

Figure 6.7 : 950MHz Transmitter Output with Two-tone Input (Both Loops 100KHz)

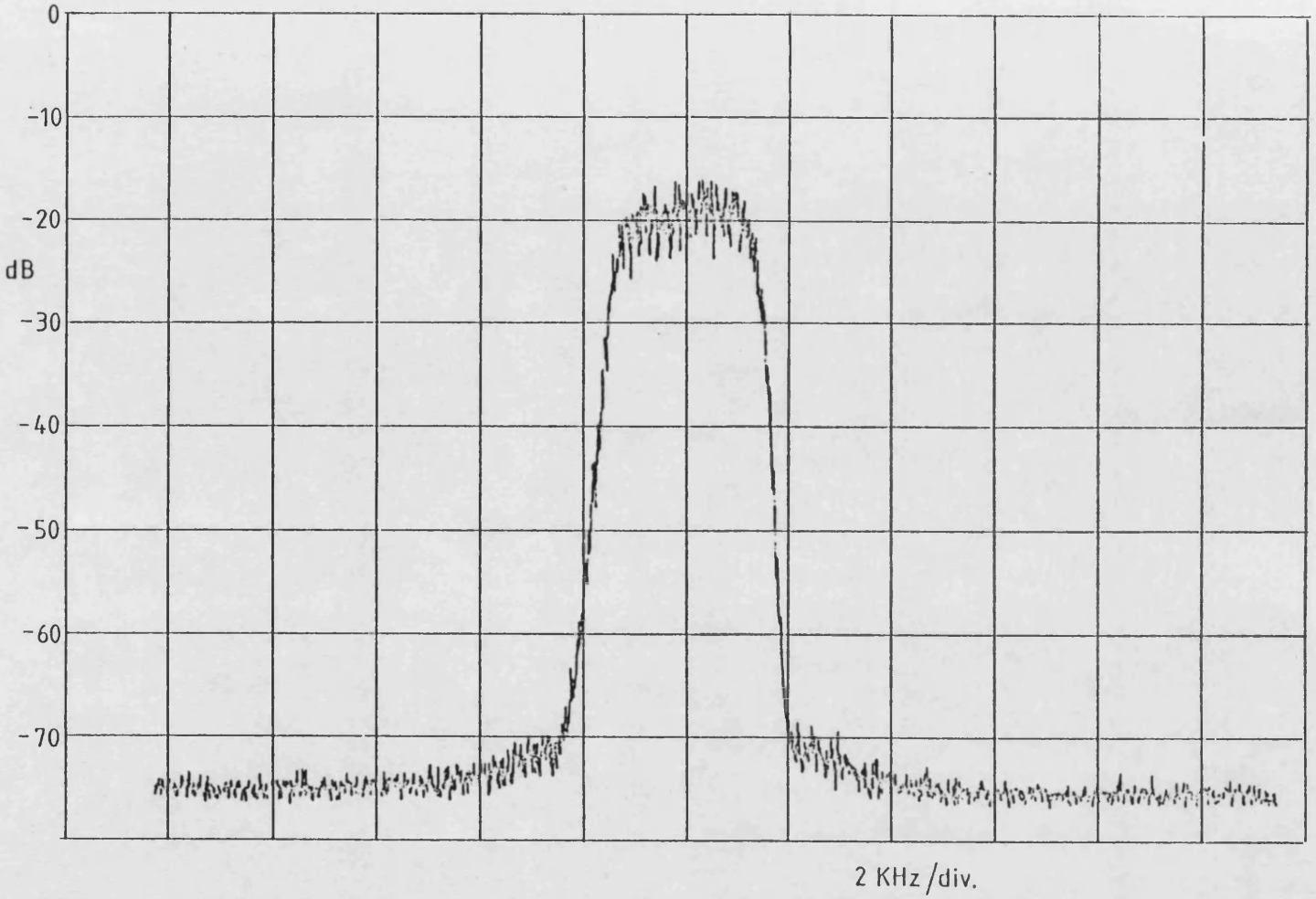

Figure 6.8 : 950MHz Transmitter Output with White Noise Input (Both Loops 100KHz)

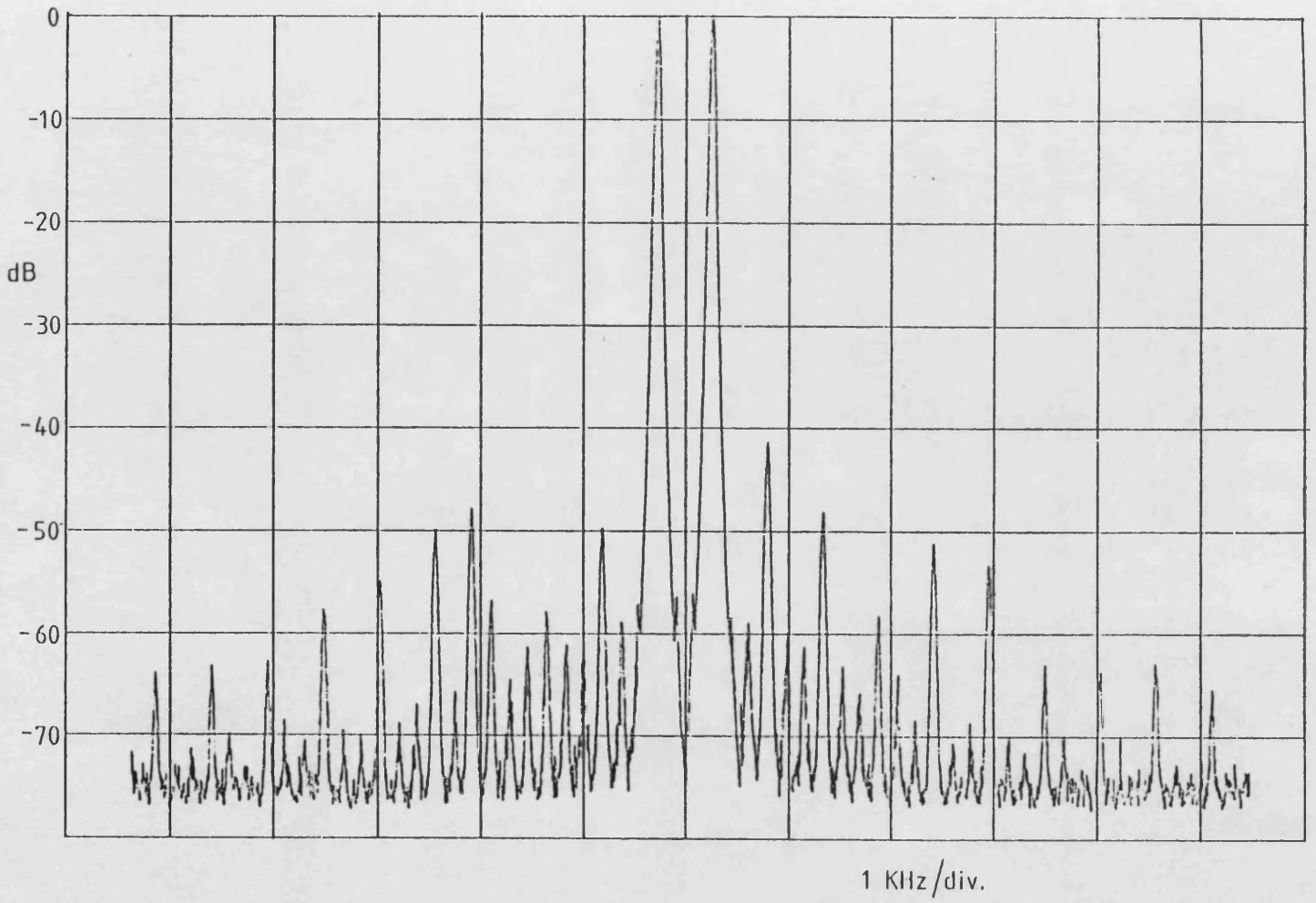

Figure 6.9 : 950MHz Transmitter Output with Two-tone Input (Both Loops 50KHz)

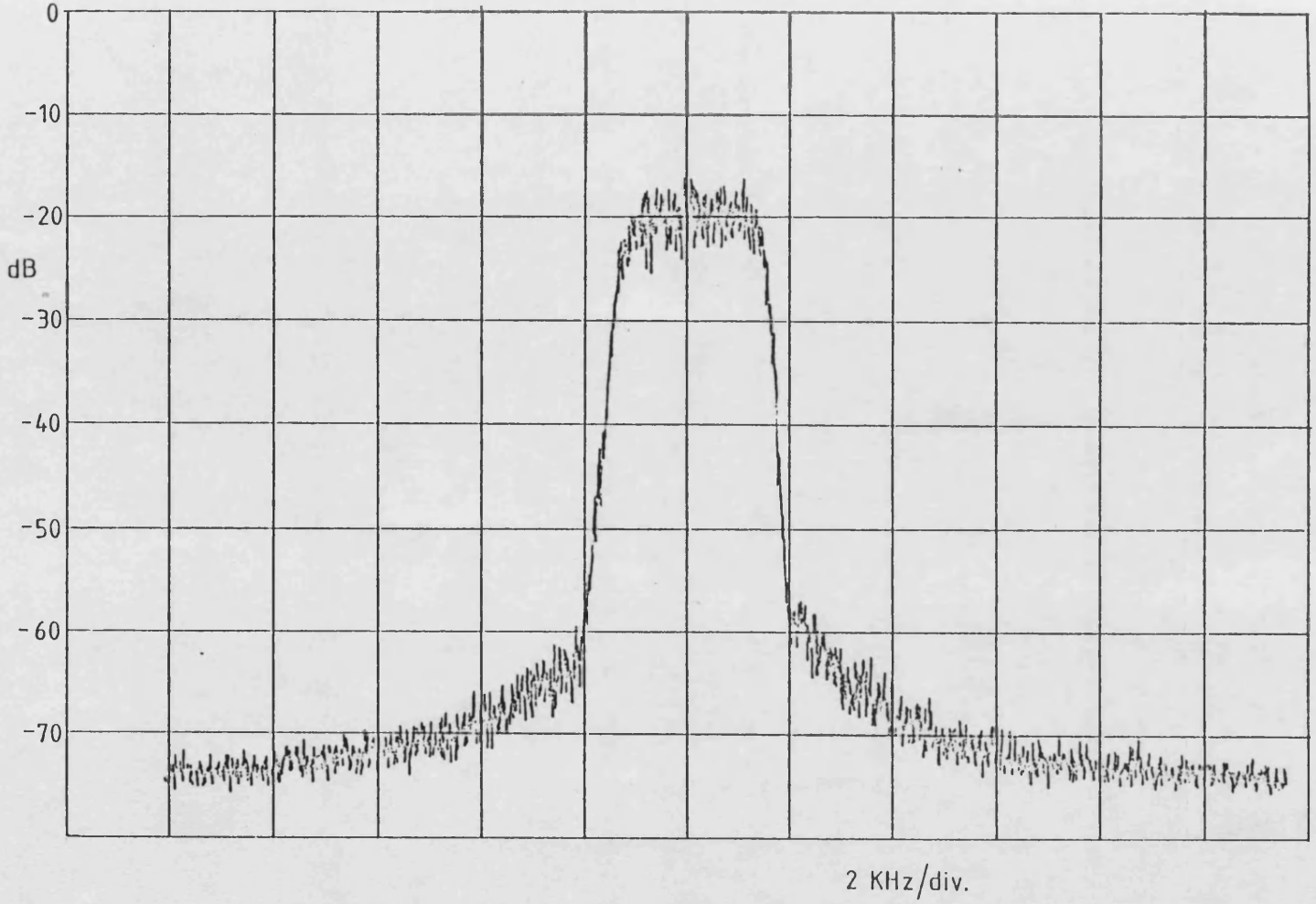

Figure 6.10 : 950MHz Transmitter Output with White Noise Input (Both Loops 50KHz)

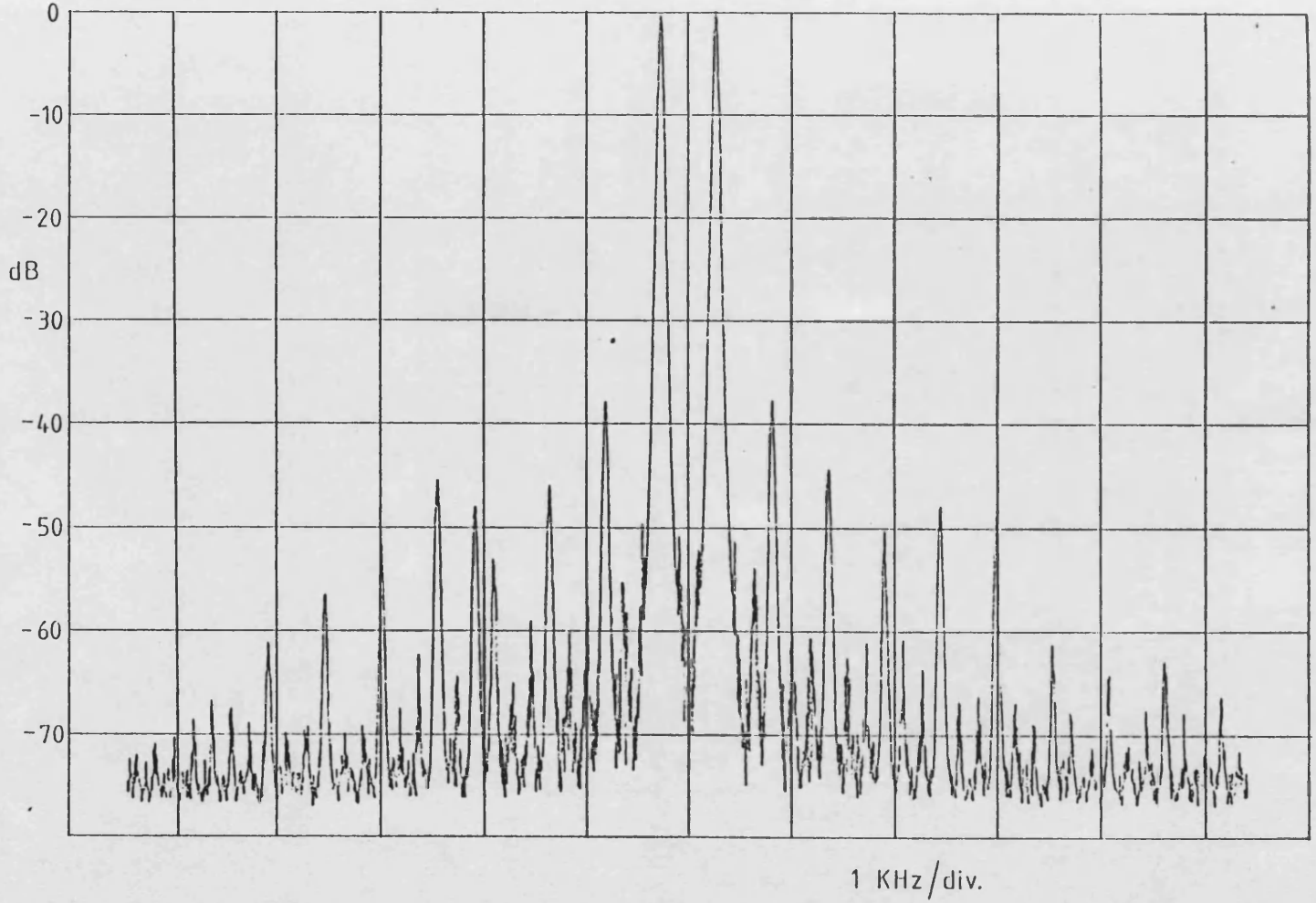

Figure 6.11 : 950MHz Transmitter Output with Two-tone Input (Both Loops 25KHz)

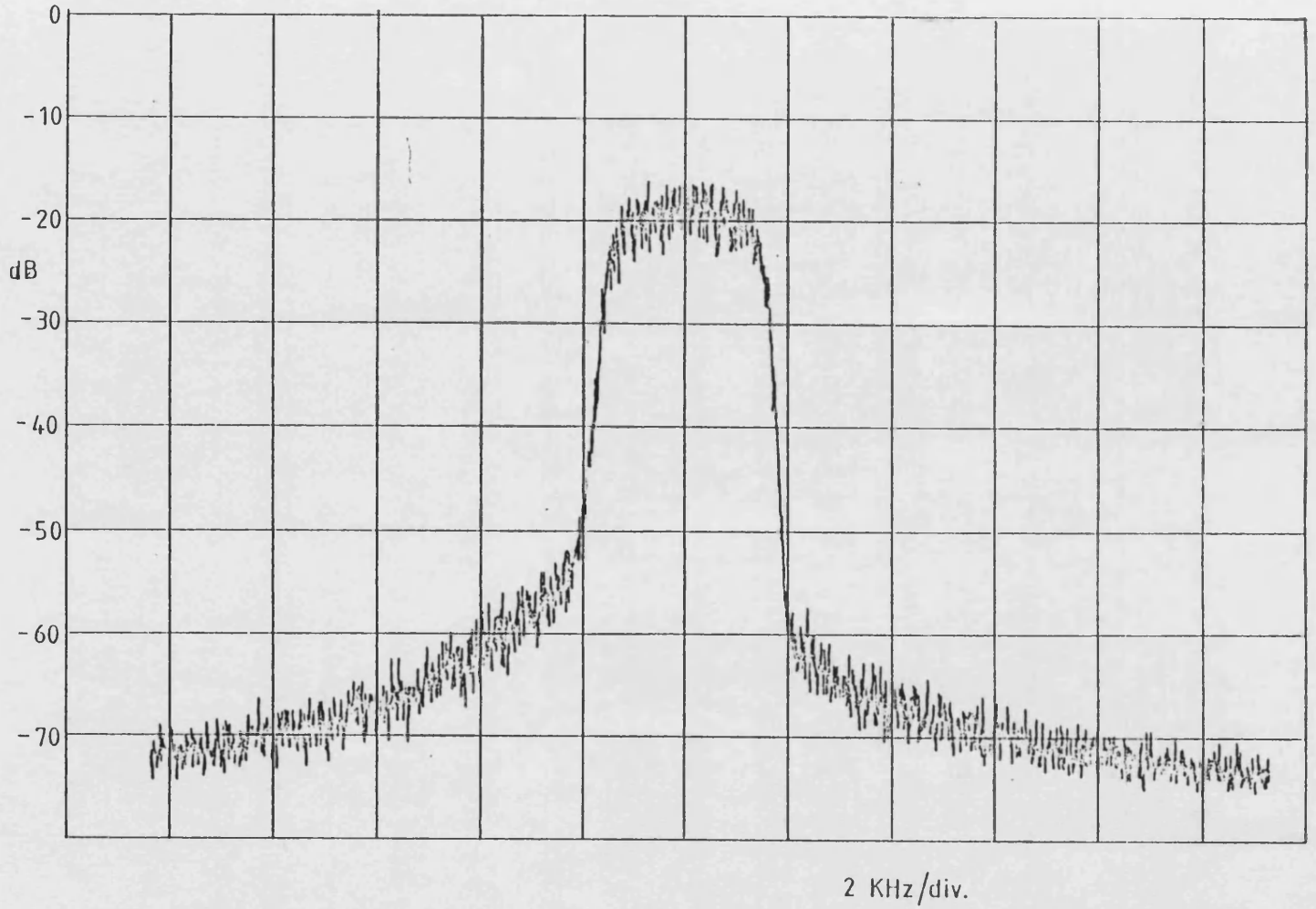

Figure 6.12 : 950MHz Transmitter Output with White Noise Input (Both Loops 25KHz)

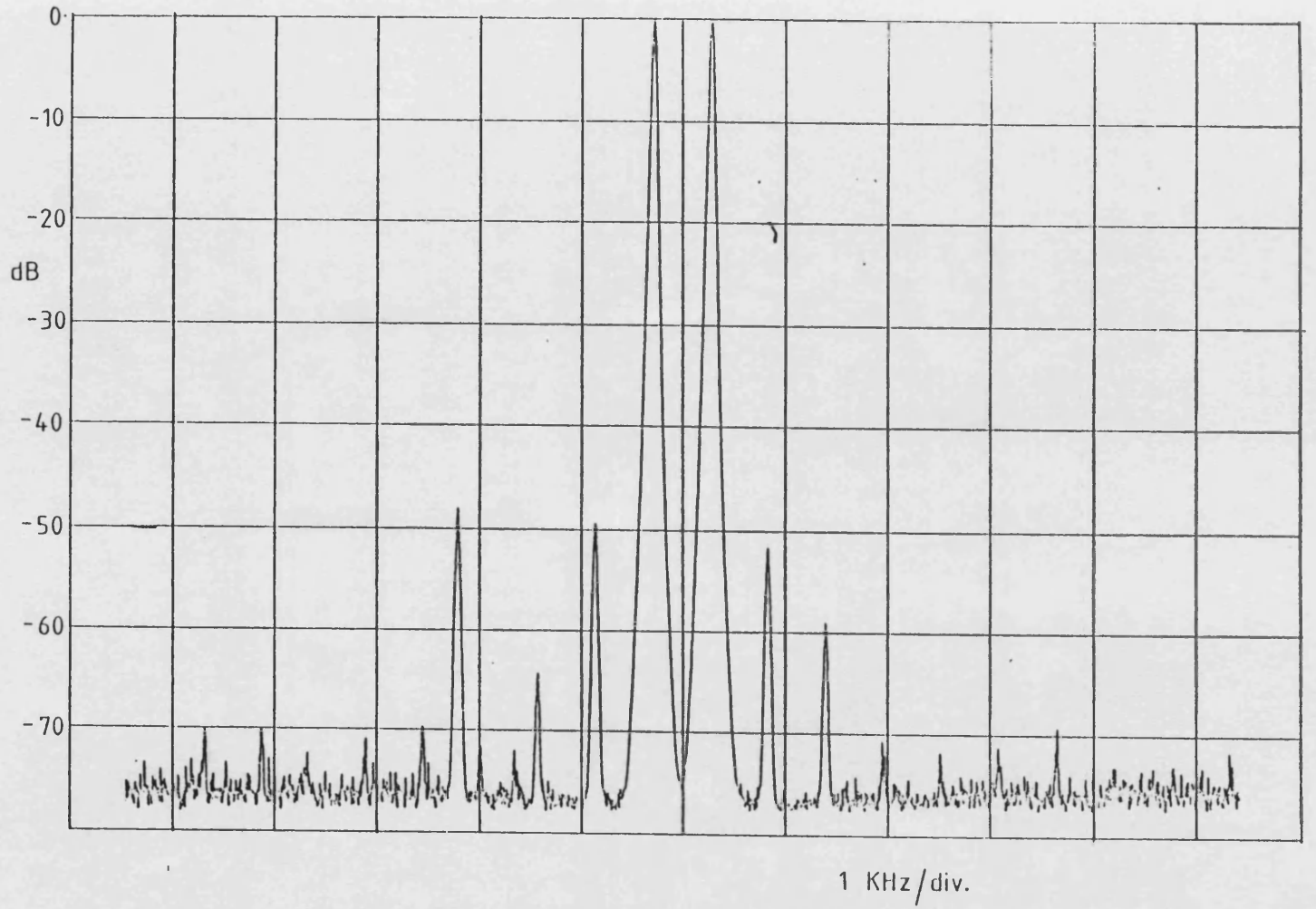

Figure 6.13 : 950MHz Transmitter Output with Two-tone Input
(Ampl. Loop BW reduced to 200KHz)

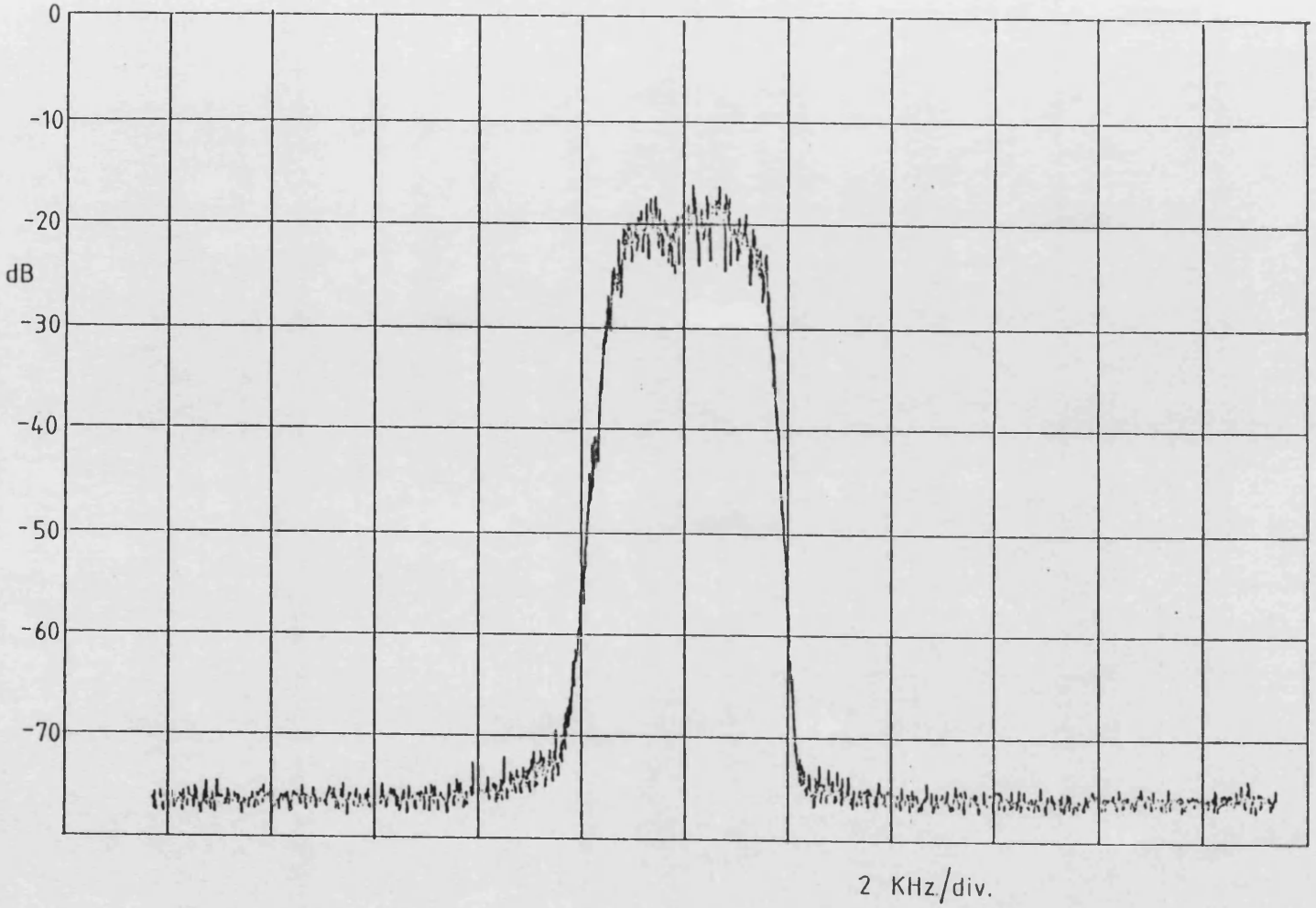

Figure 6.14 : 950MHz Transmitter Output with White Noise Input
(Ampl. Loop BW reduced to 200KHz)

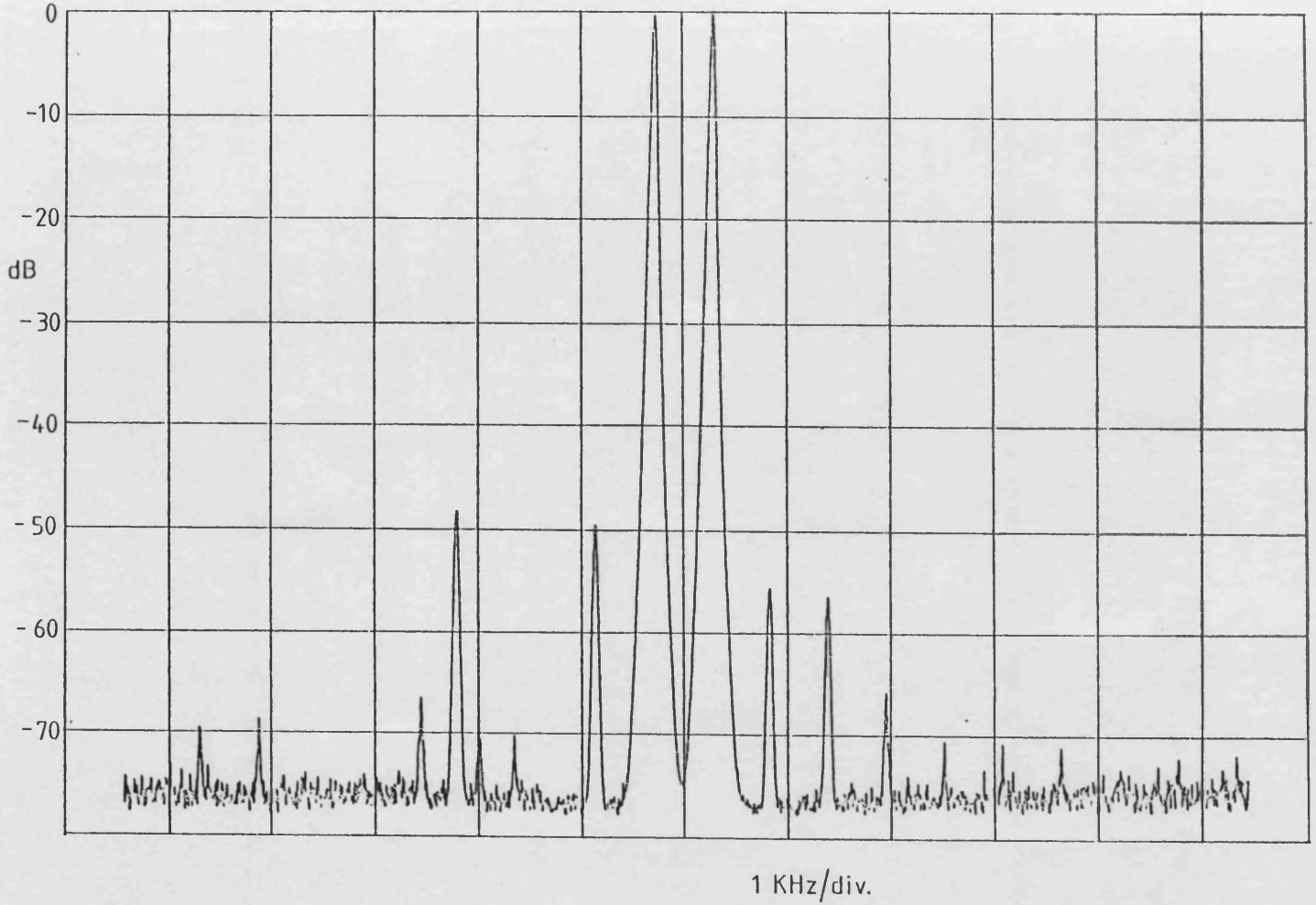

Figure 6.15 : 950MHz Transmitter Output with Two-tone Input
(Ampl. Loop BW reduced to 100KHz)

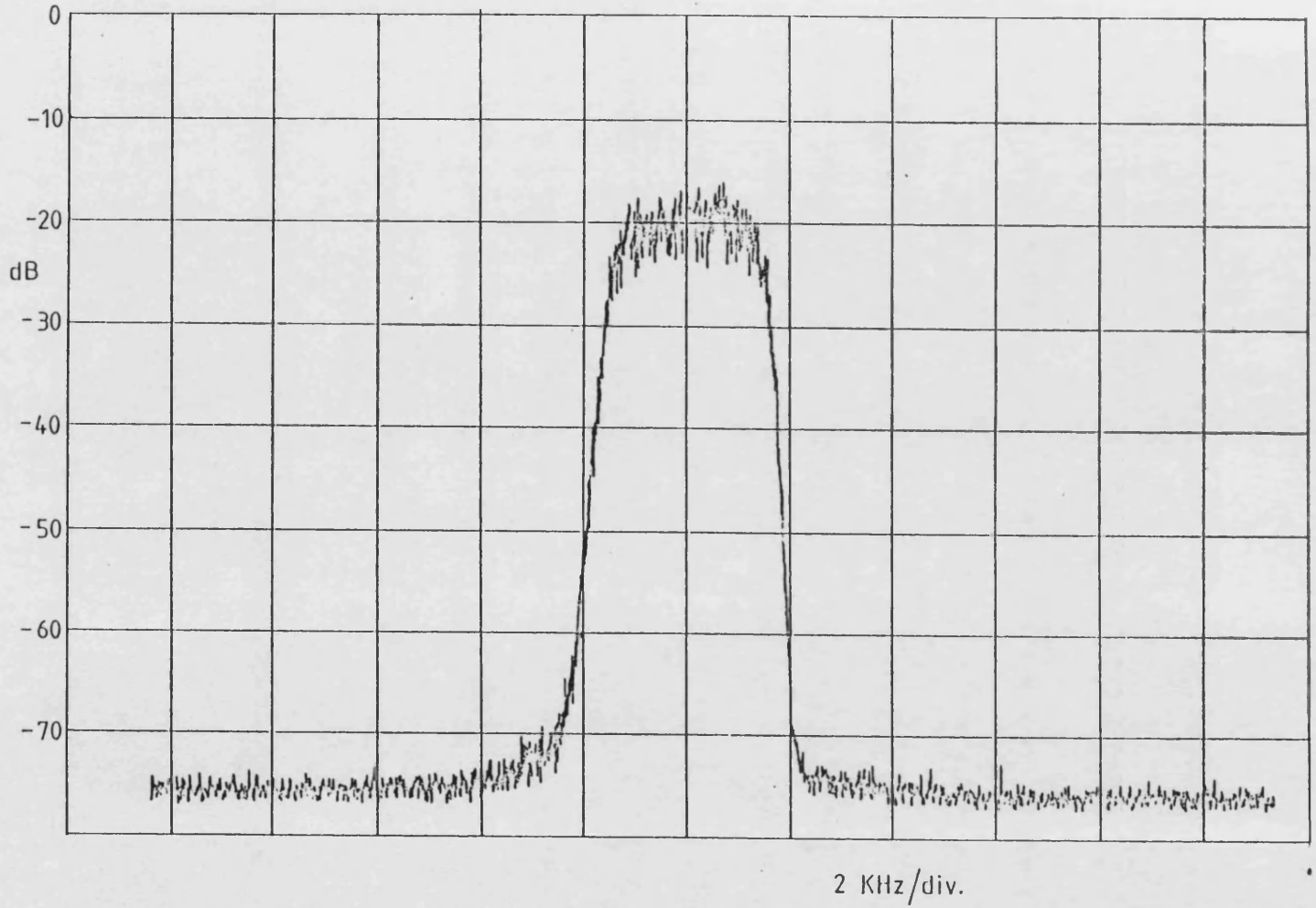

Figure 6.16 : 950MHz Transmitter Output with White Noise Input
(Ampl. Loop BW reduced to 100KHz)

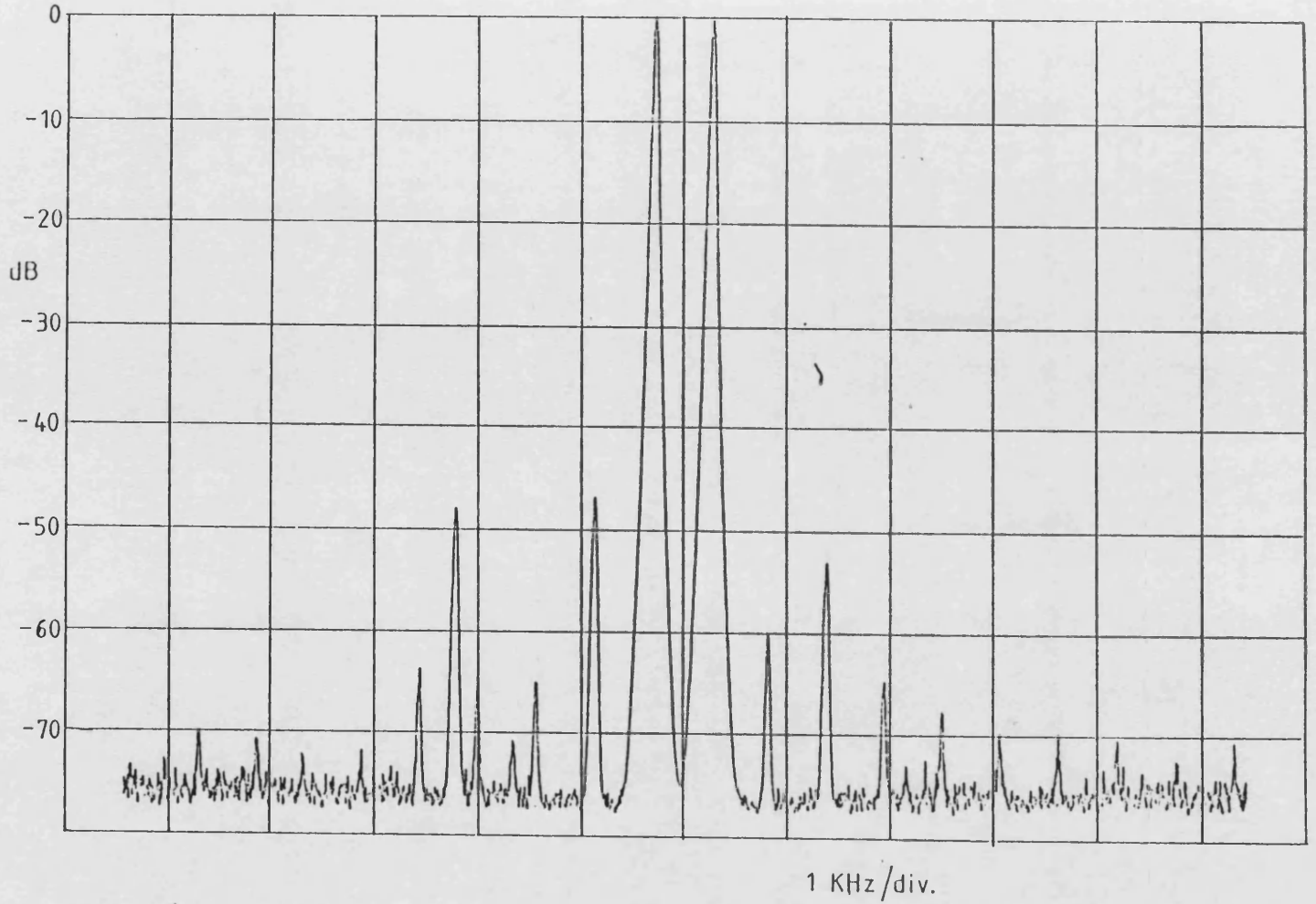

Figure 6.17 : 950MHz Transmitter Output with Two-tone Input
(Ampl. Loop BW reduced to 50KHz)

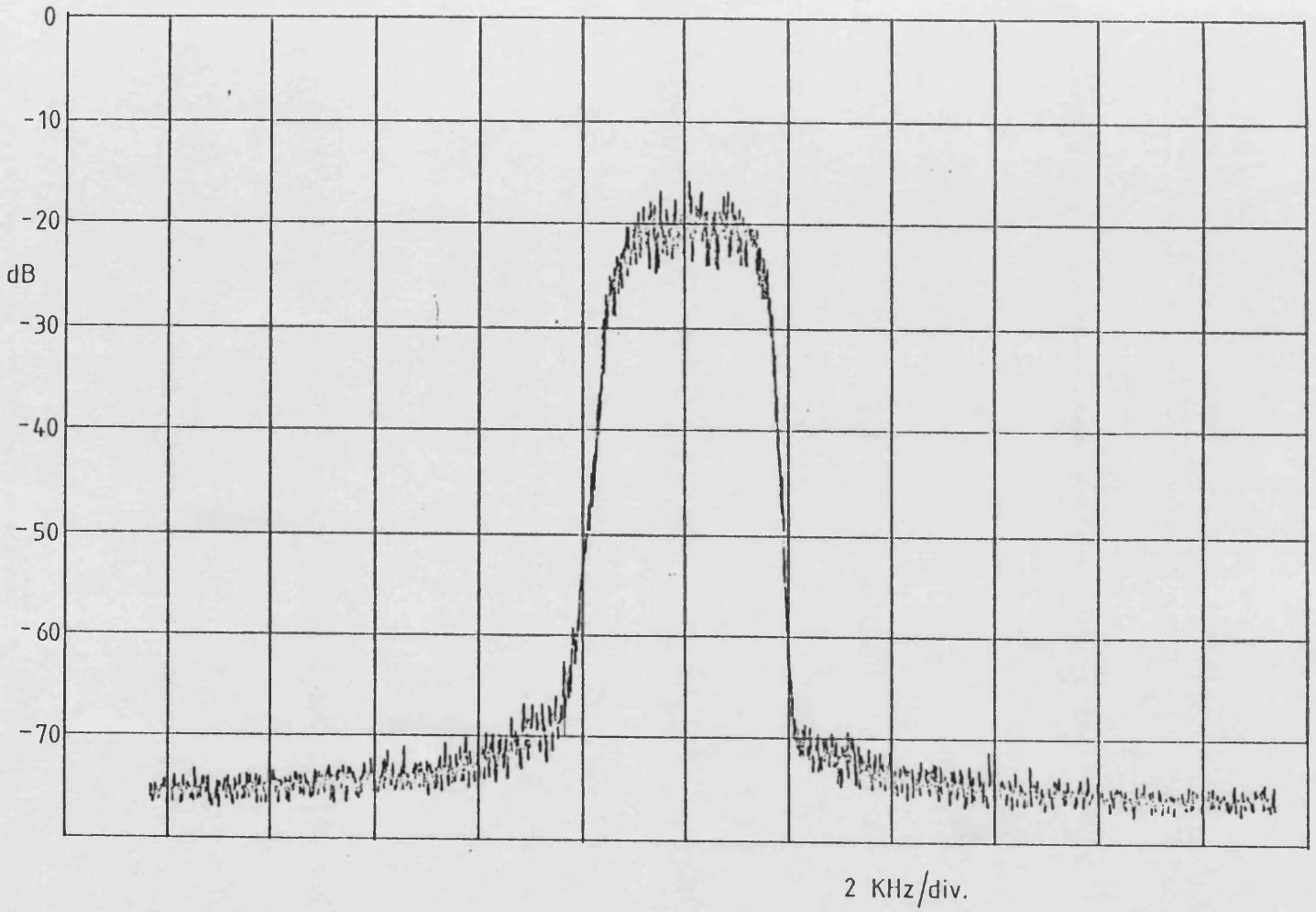

Figure 6.18 : 950MHz Transmitter Output with White Noise Input
(Ampl. Loop BW reduced to 50KHz)

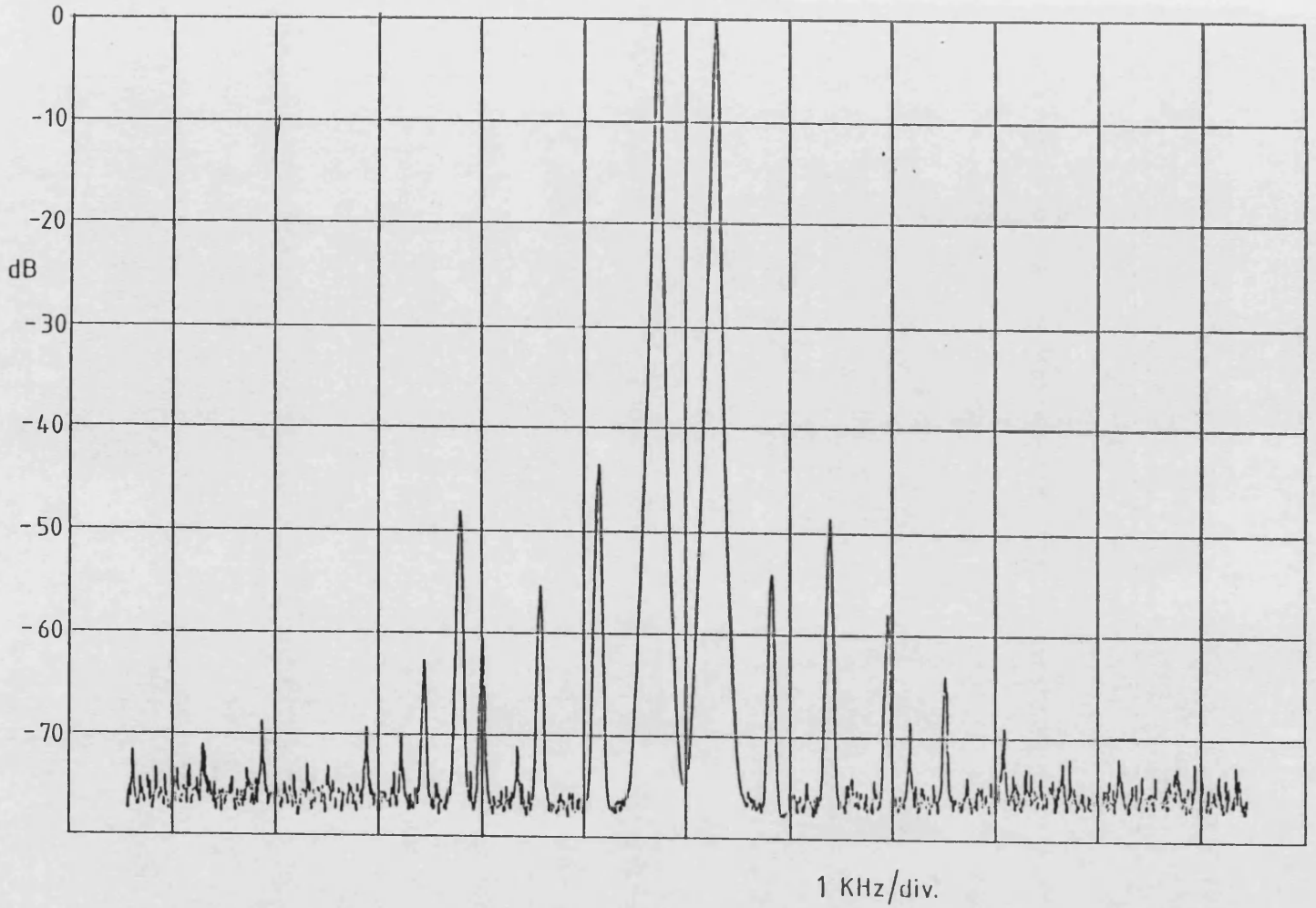

Figure 6.19 : 950MHz Transmitter Output with Two-tone Input
(Ampl. Loop BW reduced to 25KHz)

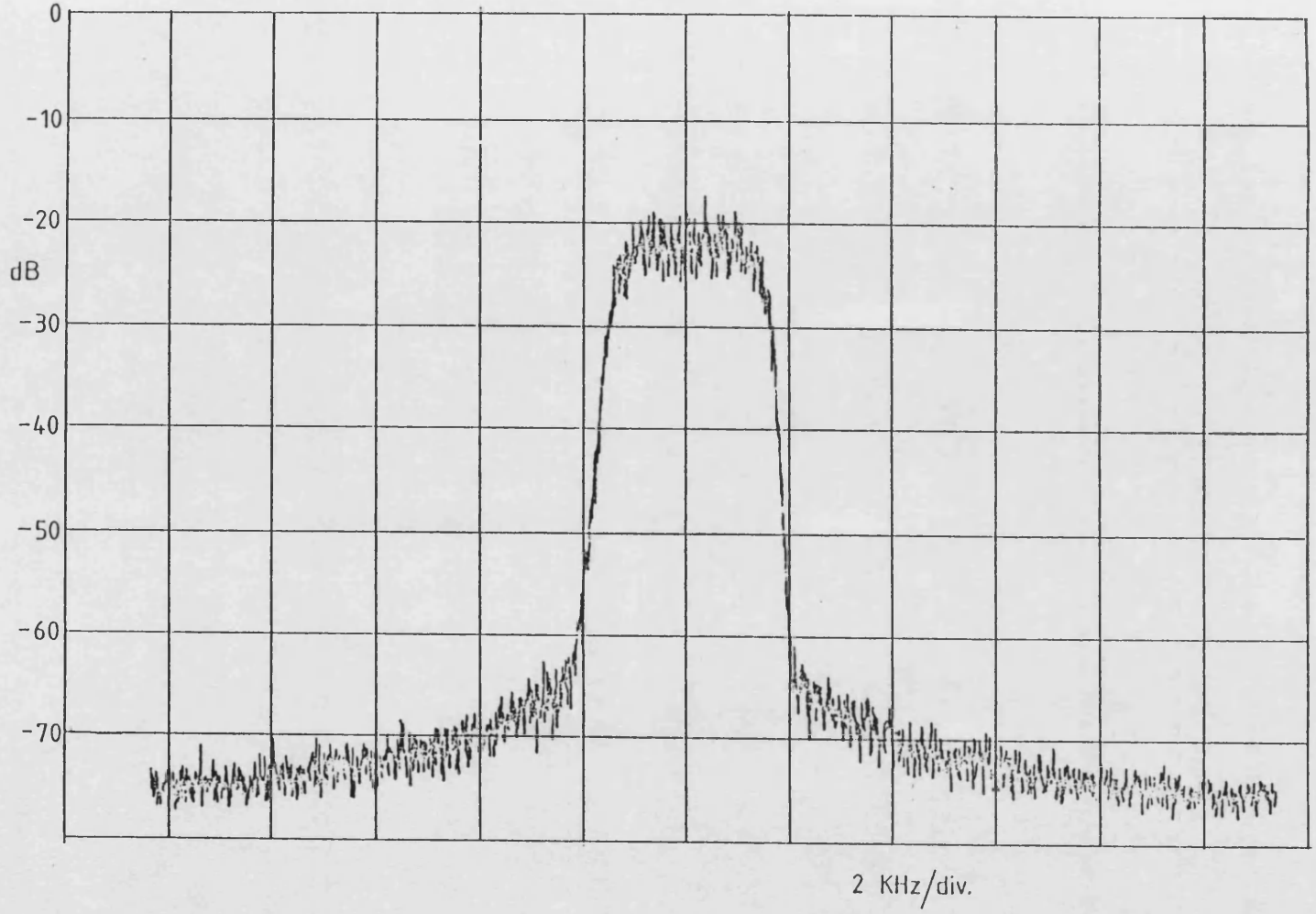

Figure 6.20 : 950MHz Transmitter Output with White Noise Input
(Ampl. Loop BW reduced to 25KHz)

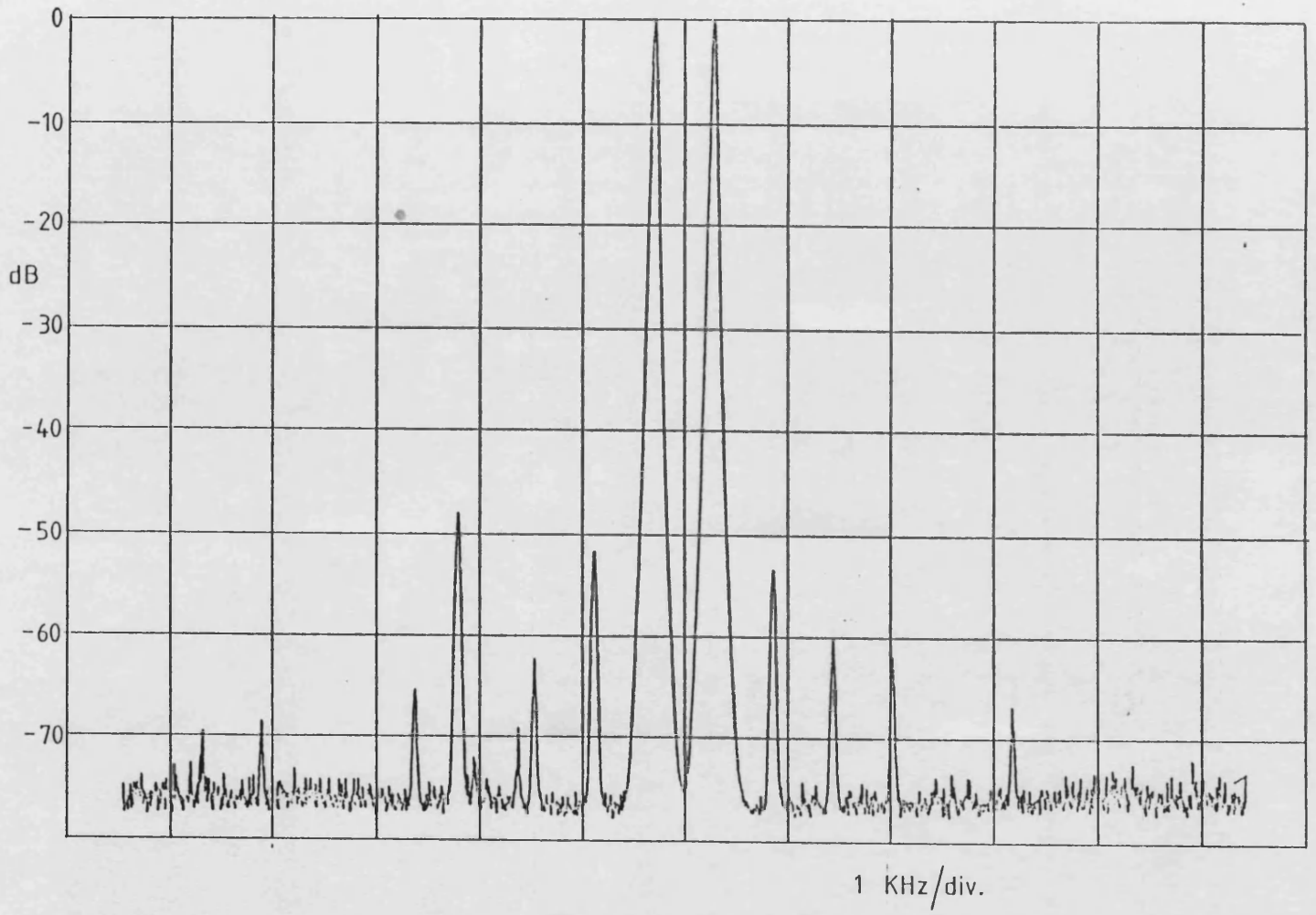

Figure 6.21 : 950MHz Transmitter Output with Two-tone Input
(PLL BW reduced to 200KHz)

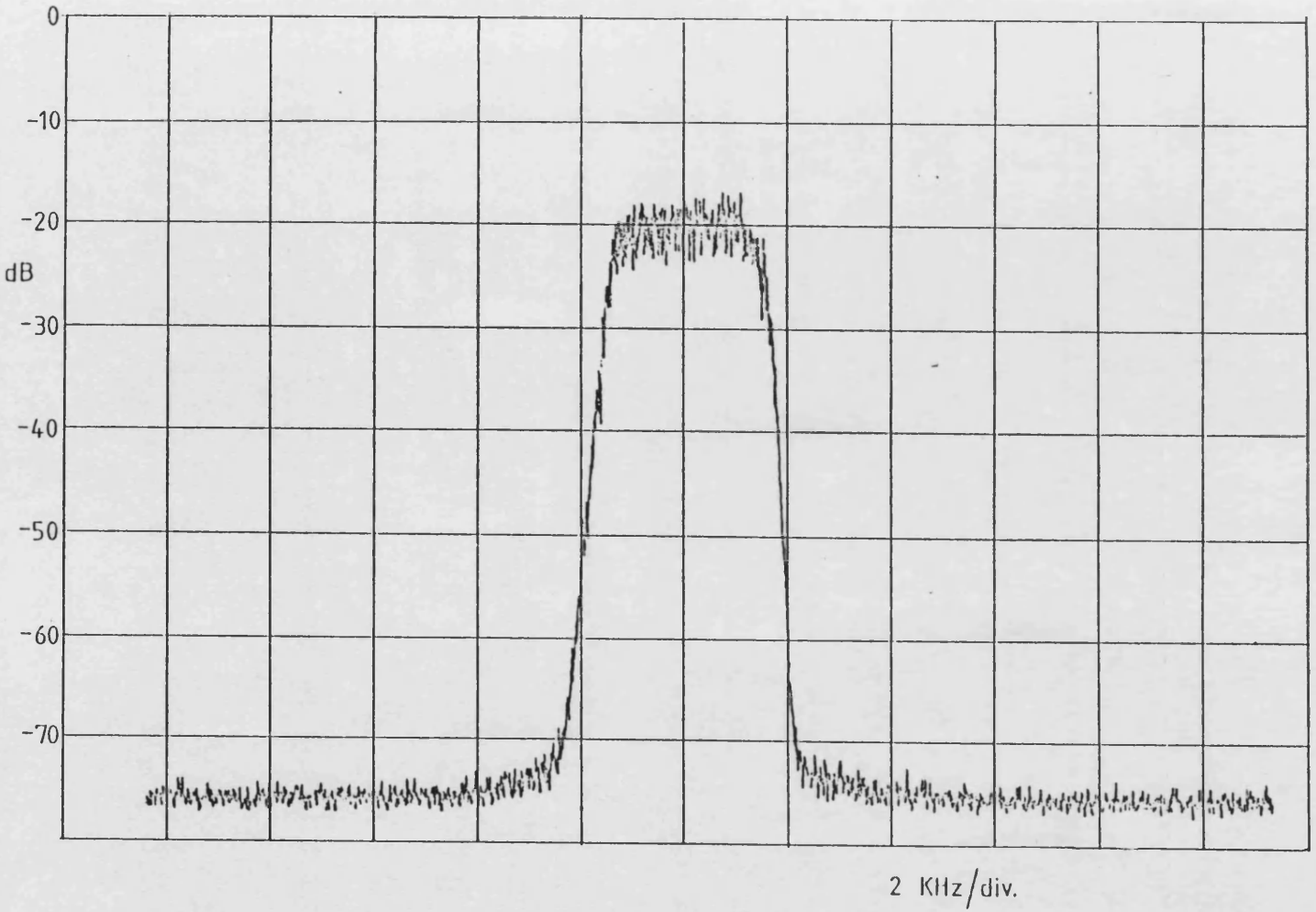

Figure 6.22 : 950MHz Transmitter Output with White Noise Input
(PLL BW reduced to 200KHz)

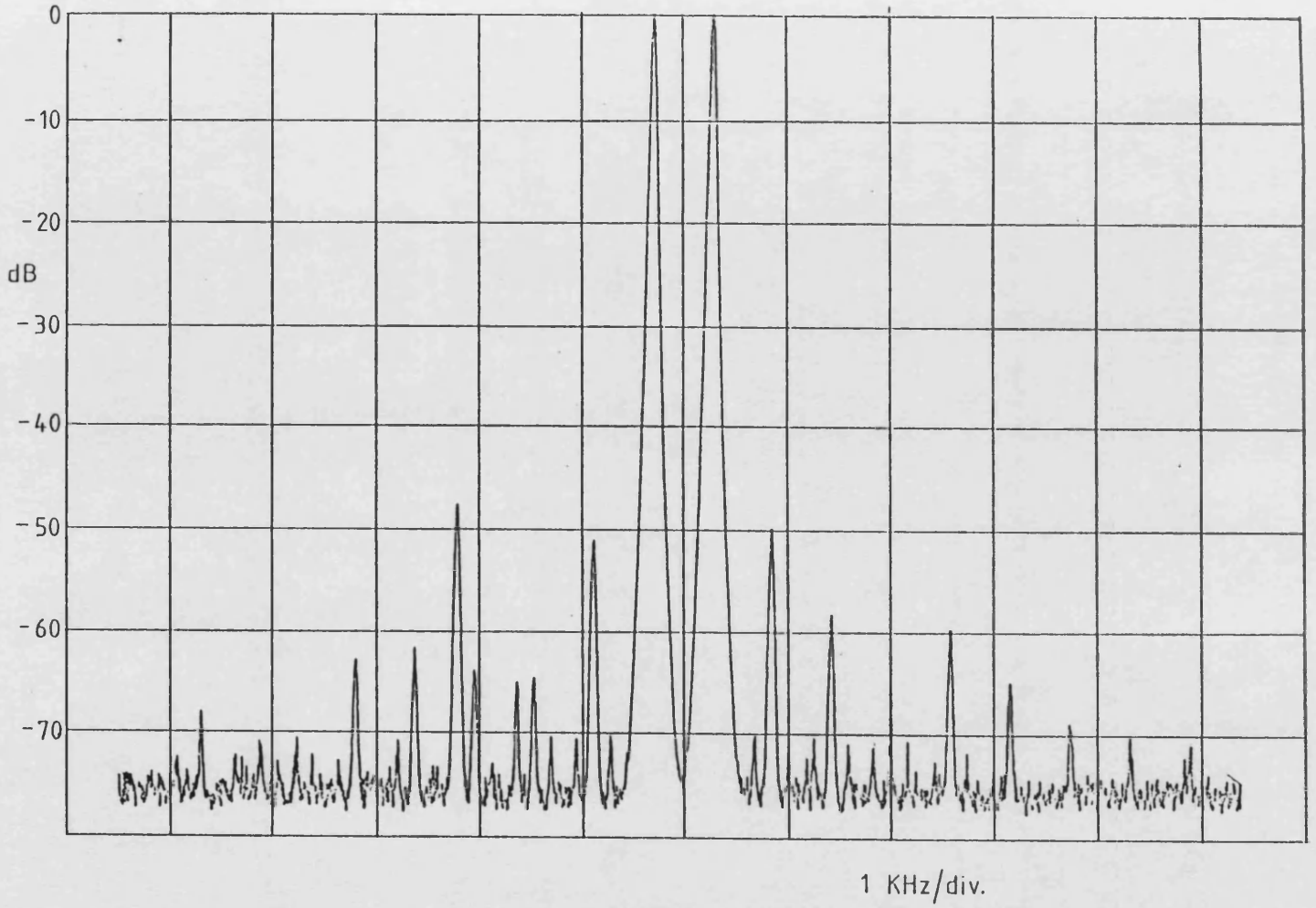

Figure 6.23 : 950MHz Transmitter Output with Two-tone Input
(PLL BW reduced to 100KHz)

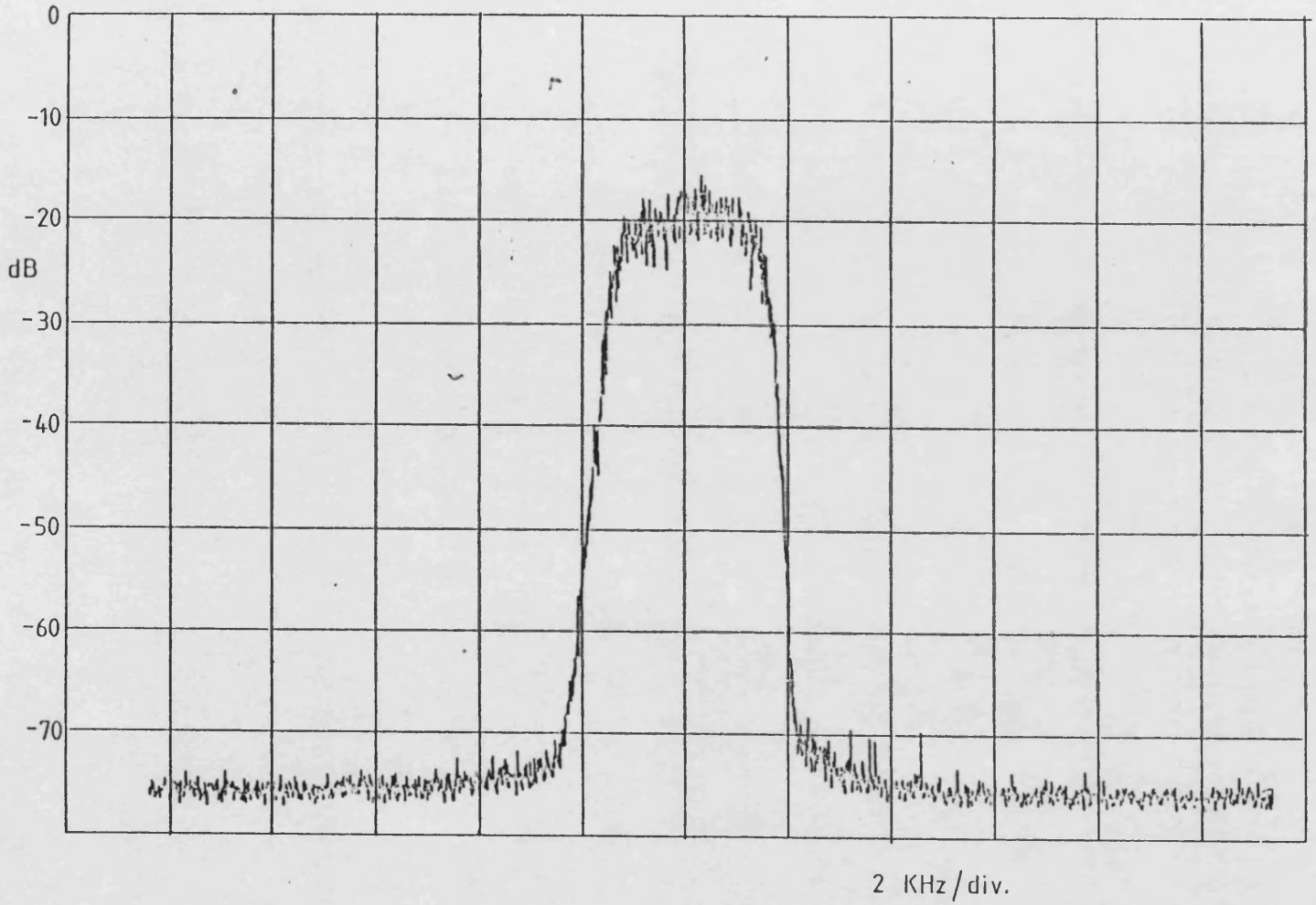

Figure 6.24 : 950MHz Transmitter Output with White Noise Input
(PLL BW reduced to 100KHz)

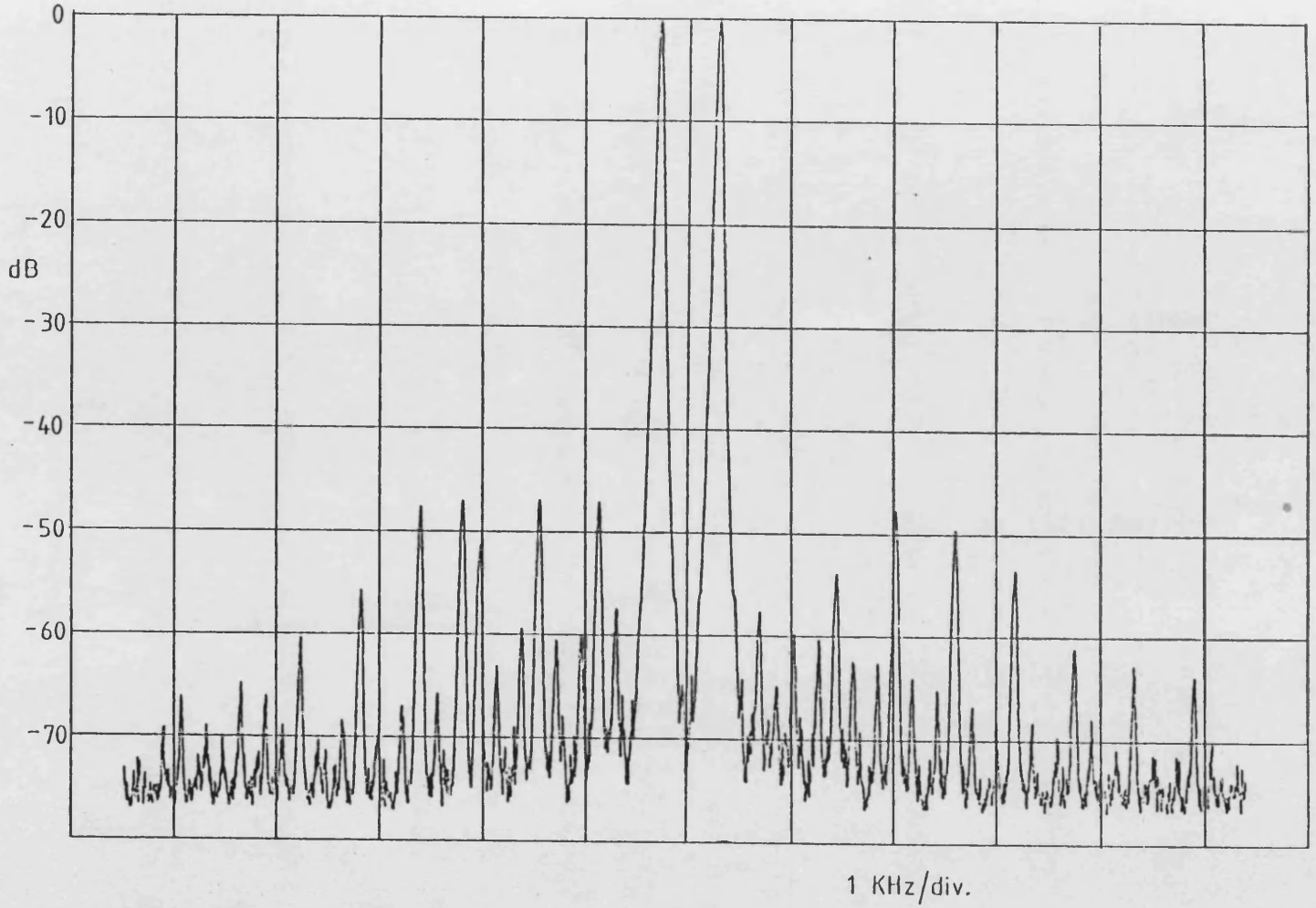

Figure 6.25 : 950MHz Transmitter Output with Two-tone Input
(PLL BW reduced to 50KHz)

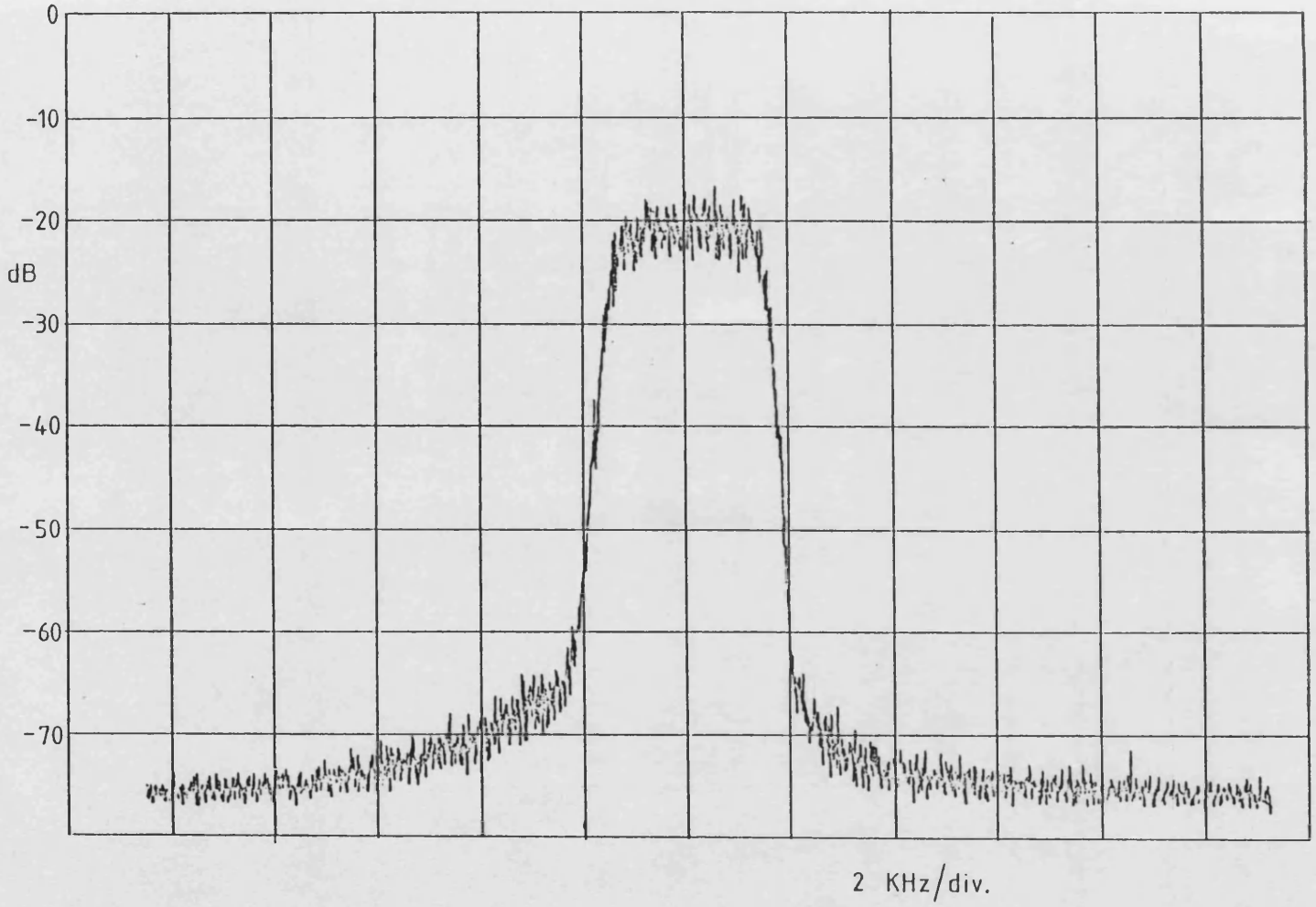

Figure 6.26 : 950MHz Transmitter Output with White Noise Input
(PLL BW reduced to 50KHz)

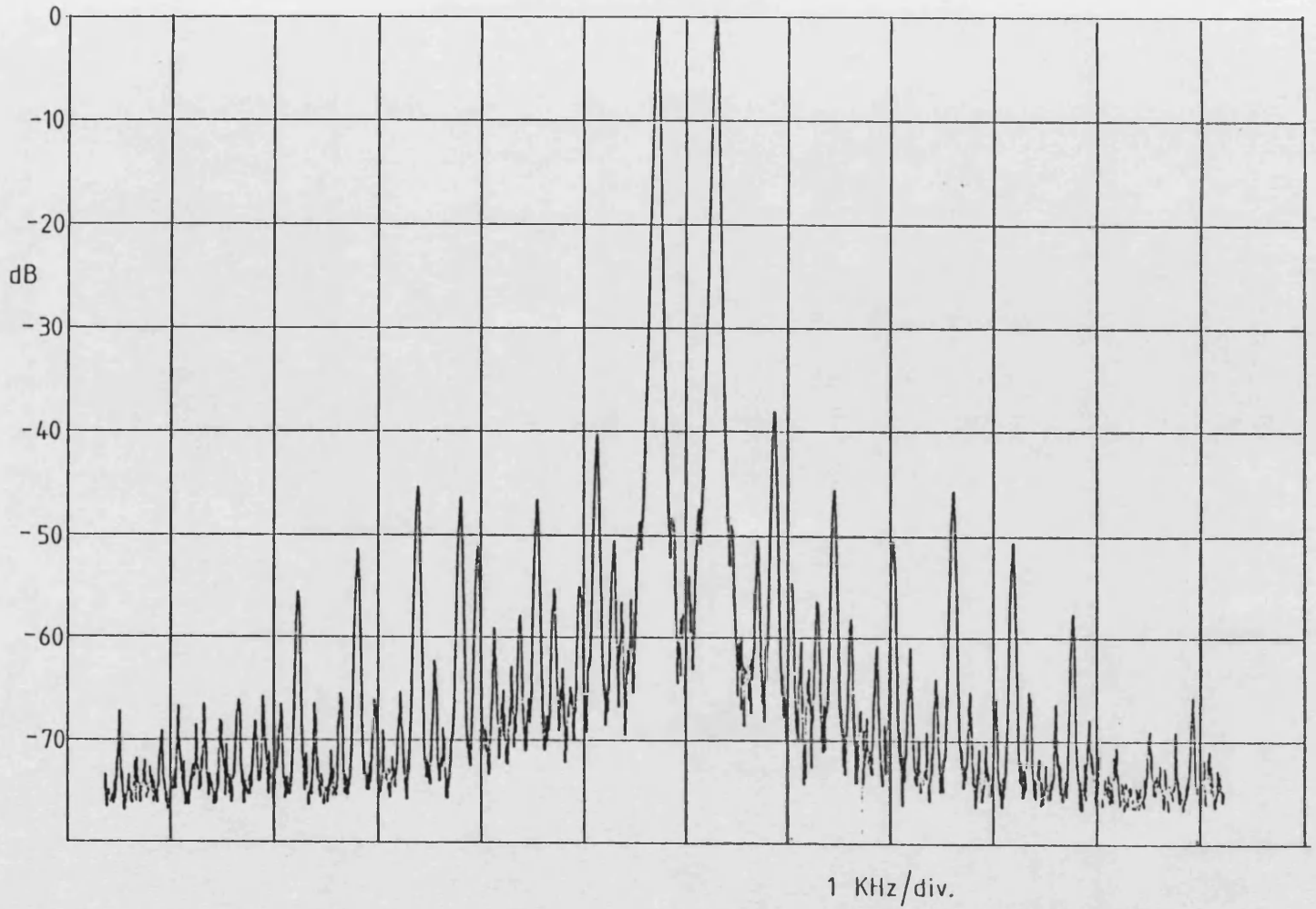

Figure 6.27 : 950MHz Transmitter Output with Two-tone Input
(PLL BW reduced to 25KHz)

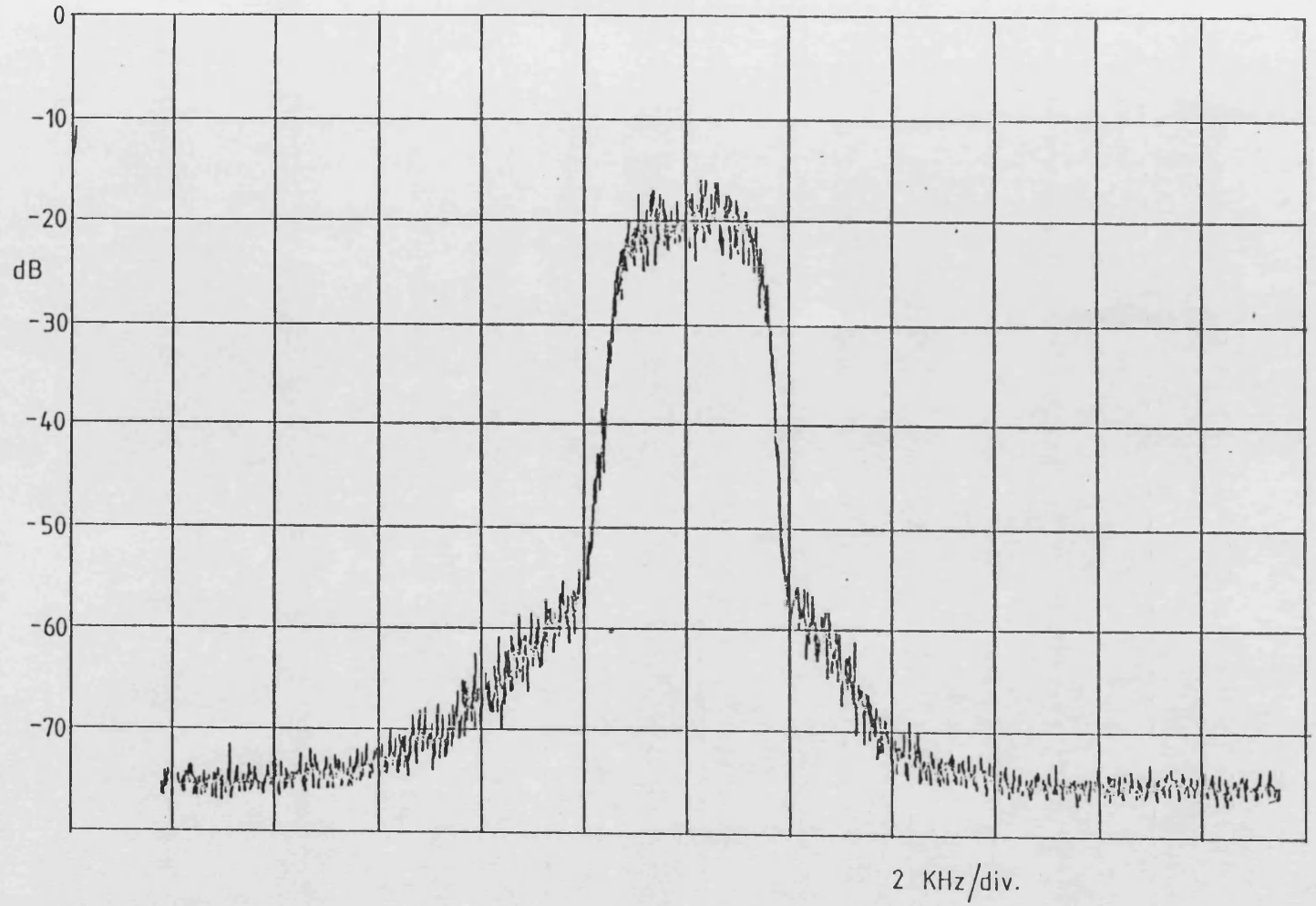

Figure 6.28 : 950MHz Transmitter Output with White Noise Input
(PLL BW reduced to 25KHz)

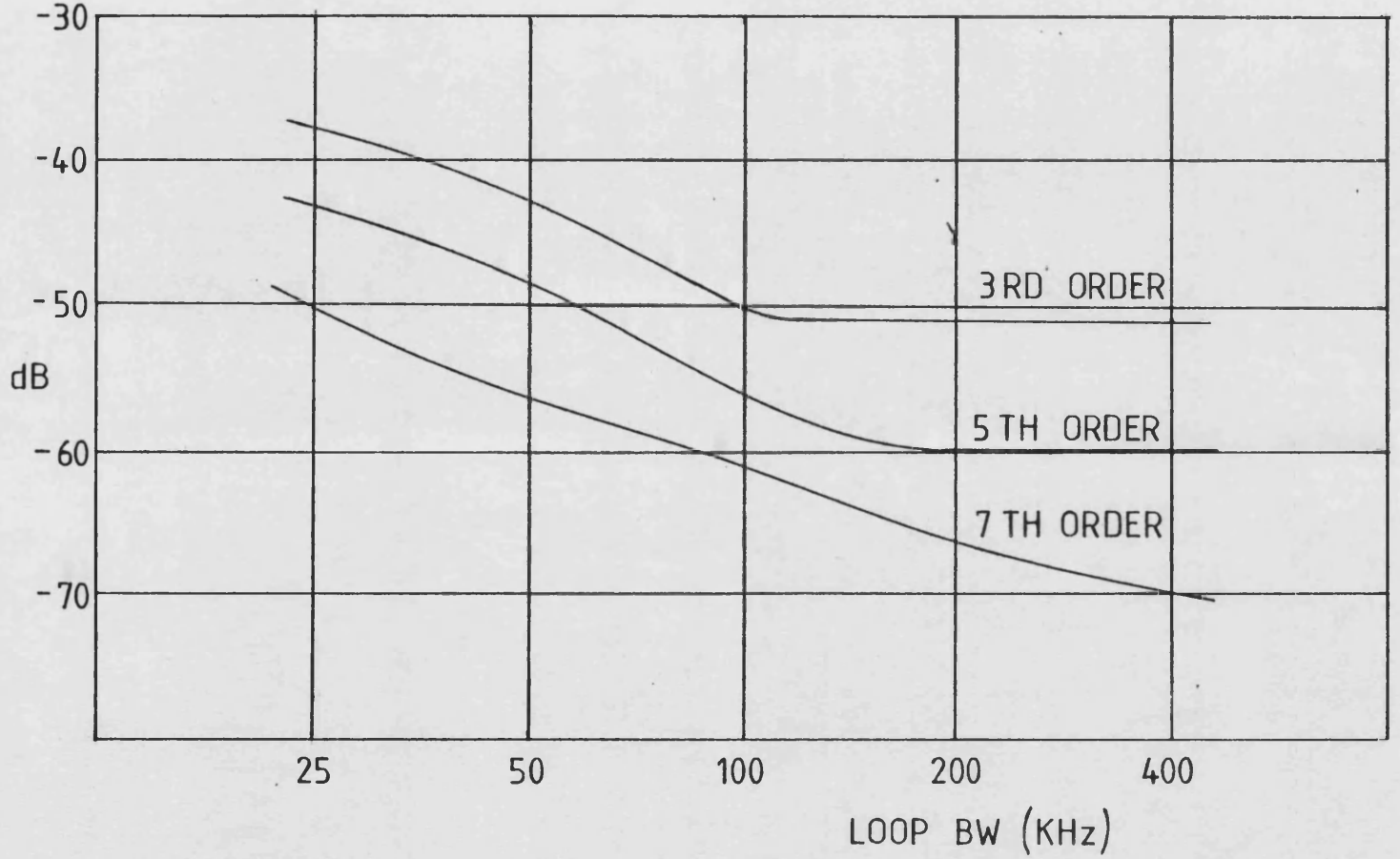

Figure 6.29 : Intermodulation Distortion versus Loop Bandwidth (Both Loops Varied)

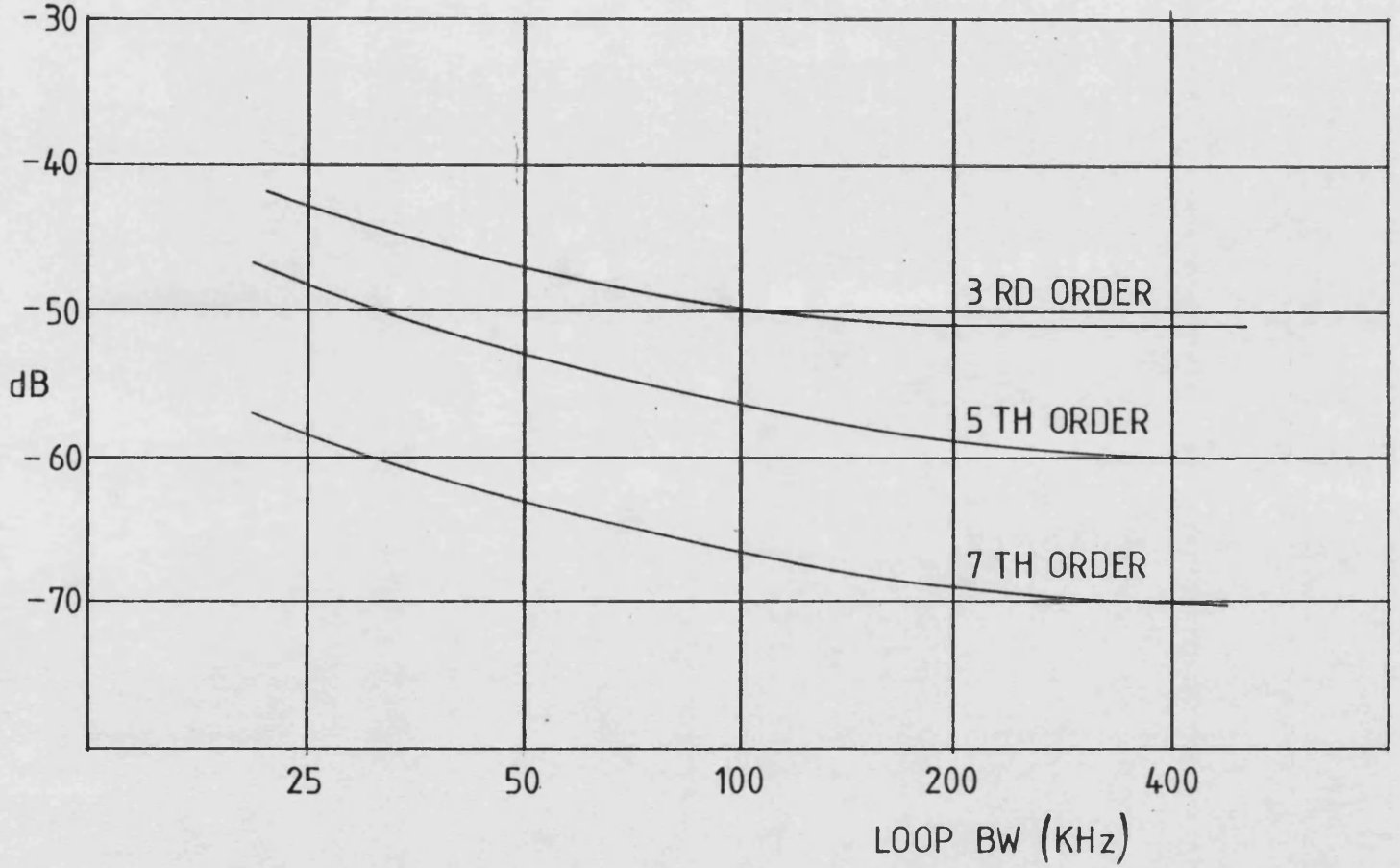

Figure 6.30 : Intermodulation Distortion versus Amplitude Loop Bandwidth
(PLL Bandwidth fixed at 400KHz)

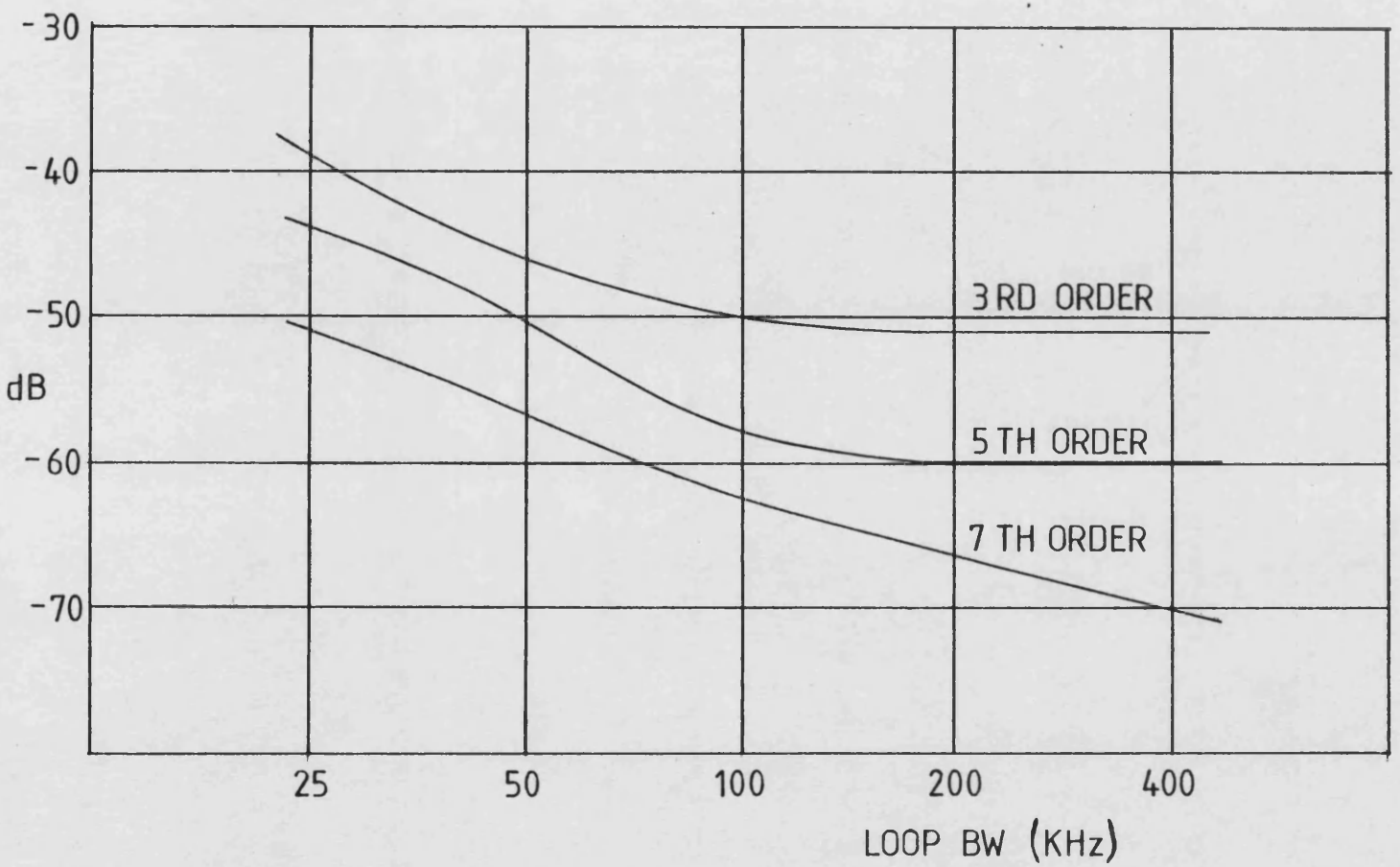

Figure 6.31 : Intermodulation Distortion versus PLL Loop Bandwidth
(Amp. Loop Bandwidth fixed at 400KHz)

noticeable for the 3rd order products, for bandwidths of greater than 100KHz, when their level drifted between -50 and -54dB. The 450MHz transmitter, which had its bandwidths fixed at 240 and 400 KHz, exhibited the same drift problem but to a lesser extent. The spectra of Figures 6.1 and 6.2 were the best achieved.

6.2.2 Amplitude Distortion

To measure the total amplitude distortion, a two tone SSB signal was applied to the transmitter input, and the spectrum of the amplitude modulator control voltage observed. If all the elements of the transmitter were perfectly linear, the control voltage would be a full-wave rectified sine-wave. However, due to the distortion generated by the modulator, power amplifier and polar resolver, this waveform will be modified by the total distortion present. The spectrum of the control voltage is shown in Figure 6.32, and with a wider frequency scan, in Figure 6.33. By subtracting the known spectrum of a full wave rectified sine-wave, the residual distortion spectrum is obtained. This is shown in Figure 6.34, where the 0dB reference corresponds to the tone level of the output signal. Also shown in Figure 6.34 is the theoretical suppression of this distortion by the feedback loop (assuming ideal behaviour), for several loop bandwidths.

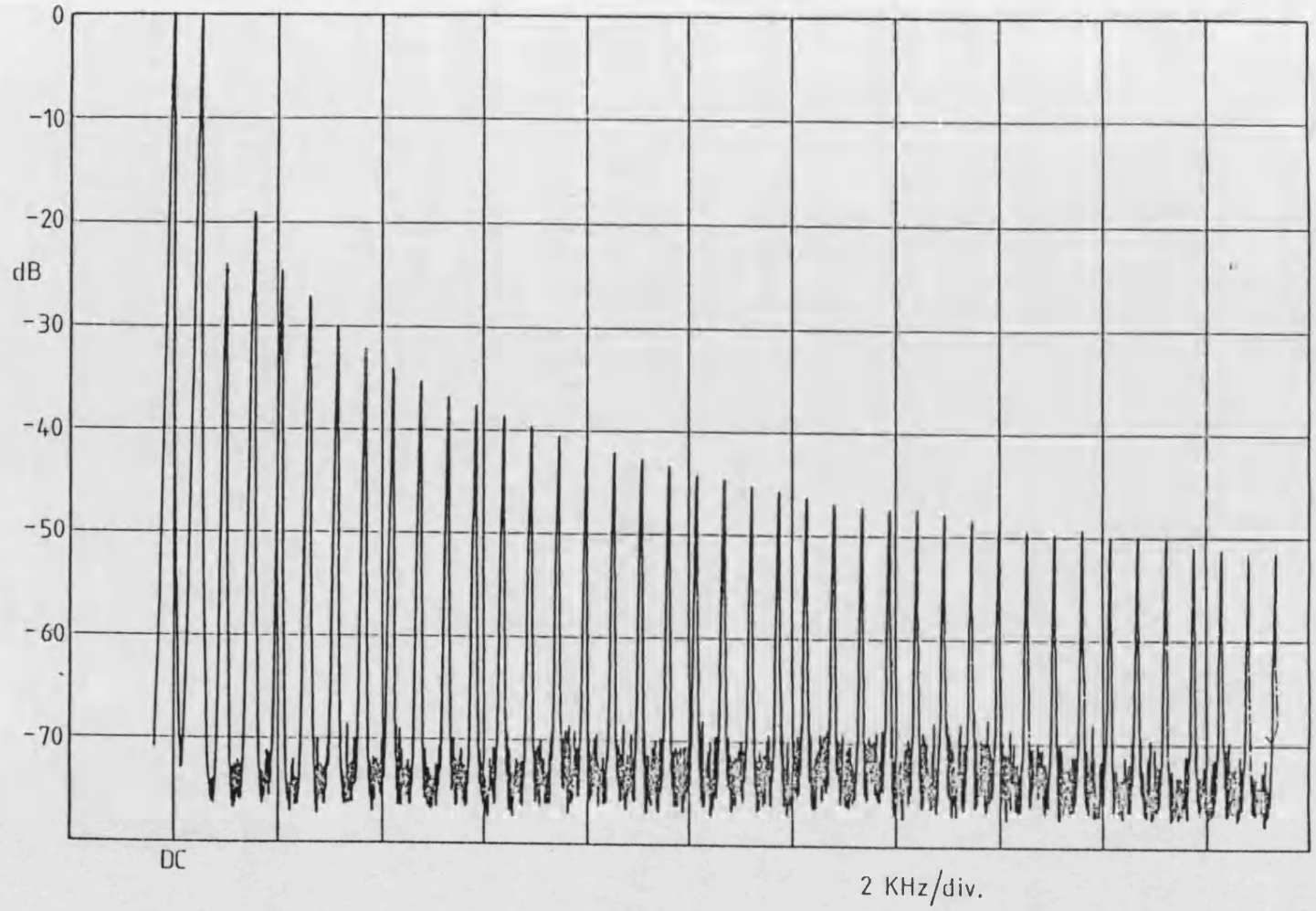

Figure 6.32 : Amplitude Modulator Control Voltage when Transmitter is producing Two Tones

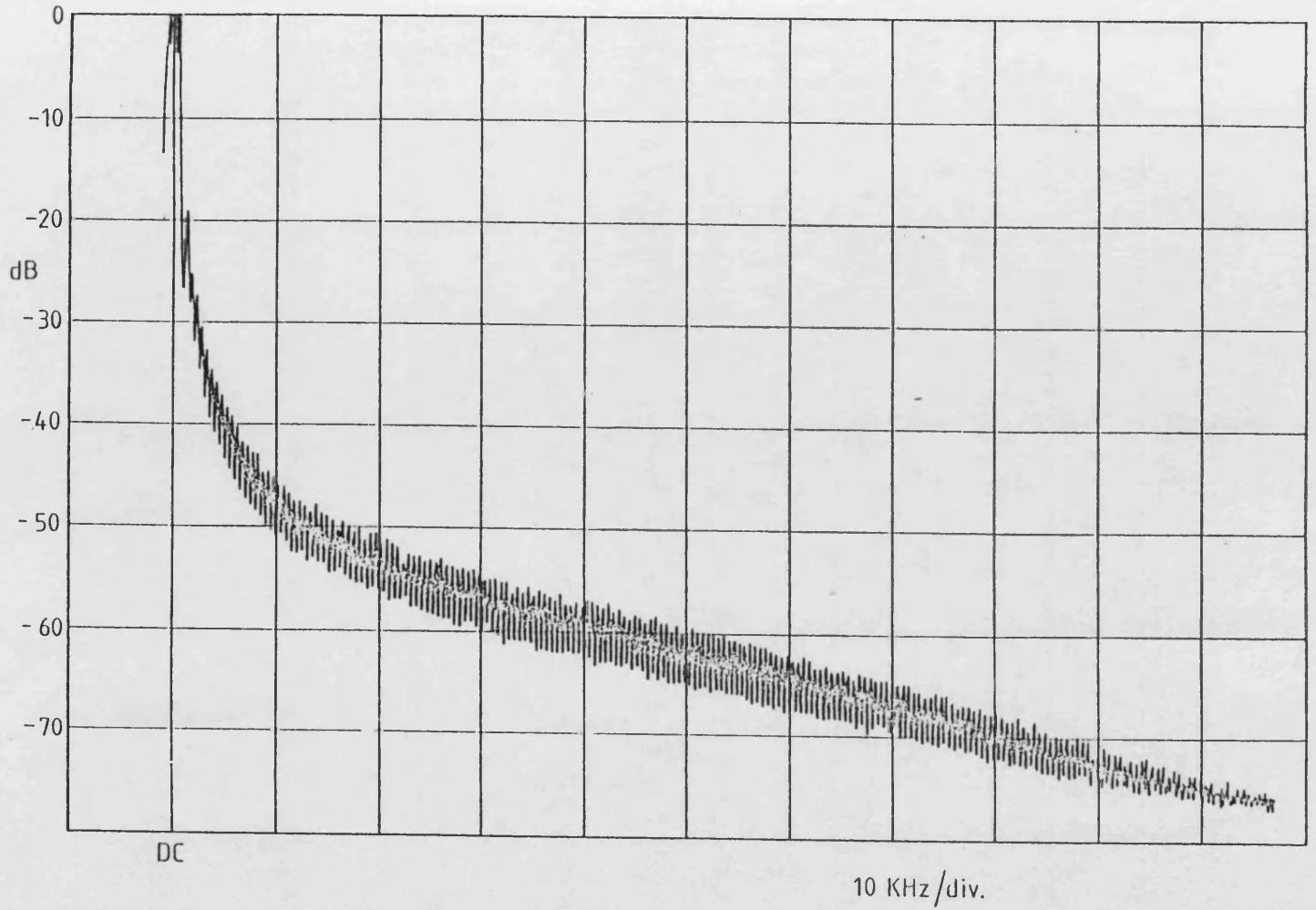

Figure 6.33 : Amplitude Modulator Control Voltage when Transmitter is producing Two Tones (Wider Scan)

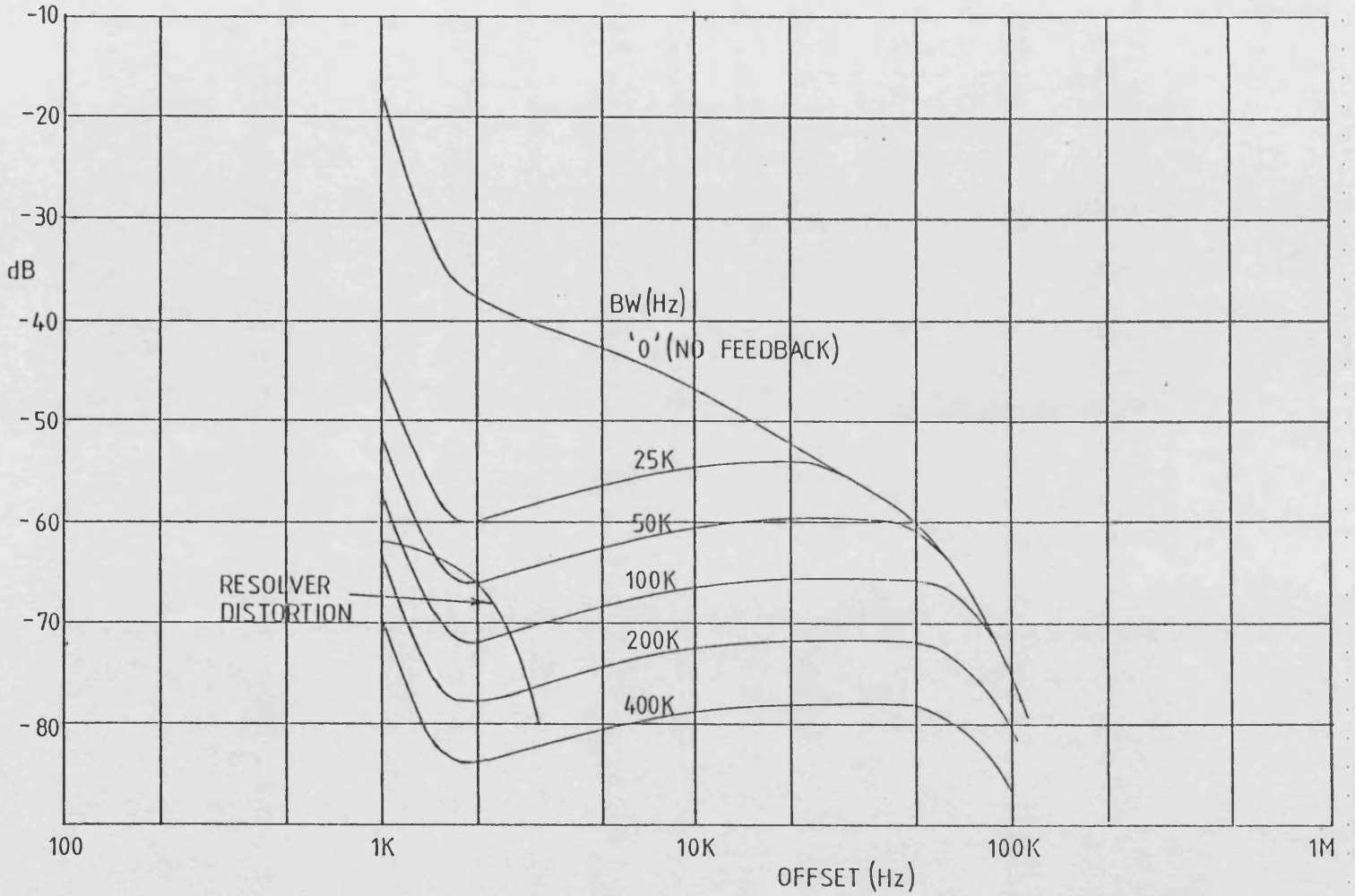

Figure 6.34 : Amplitude Distortion Spectra

6.2.3 Phase Distortion

Measurement of the total transmitter phase distortion, requires a different approach to that used for the amplitude distortion. As the PSD is positioned before all of the loop gain, its output is too low to obtain a useful spectrum when the transmitter is operating normally. To overcome this, the loop bandwidth was set at a very low value (900Hz), and an AM input signal applied, where the modulating signal was a full-wave rectified sine-wave. This signal has the envelope of a two-tone SSB signal, but a constant phase. Thus, if the transmitter was perfect, the PSD output would be a d.c. level. Any phase distortion present (due to AM to PM conversion) will therefore appear at the PSD output uncorrected by the loop, provided it is above the loop bandwidth. The spectrum of the PSD output under these conditions is shown in Figure 6.35. The 0dB reference corresponds to a phase deviation of 1 radian rms. Since the magnitude of the distortion components corresponds to a phase deviation, $\beta \ll 1$, the resulting phase modulated signal at the transmitter output will be 'narrowband' PM. There is therefore only one significant pair of sidebands (at $\beta/2$) for each component. The phase distortion spectrum is therefore simply plotted, as shown in Figure 6.36. In this case, the 0dB reference corresponds to the tone level, for a two-tone SSB input. As in the case of the amplitude distortion, the theoretical distortion reduction due to the PLL is also shown, for various bandwidths.

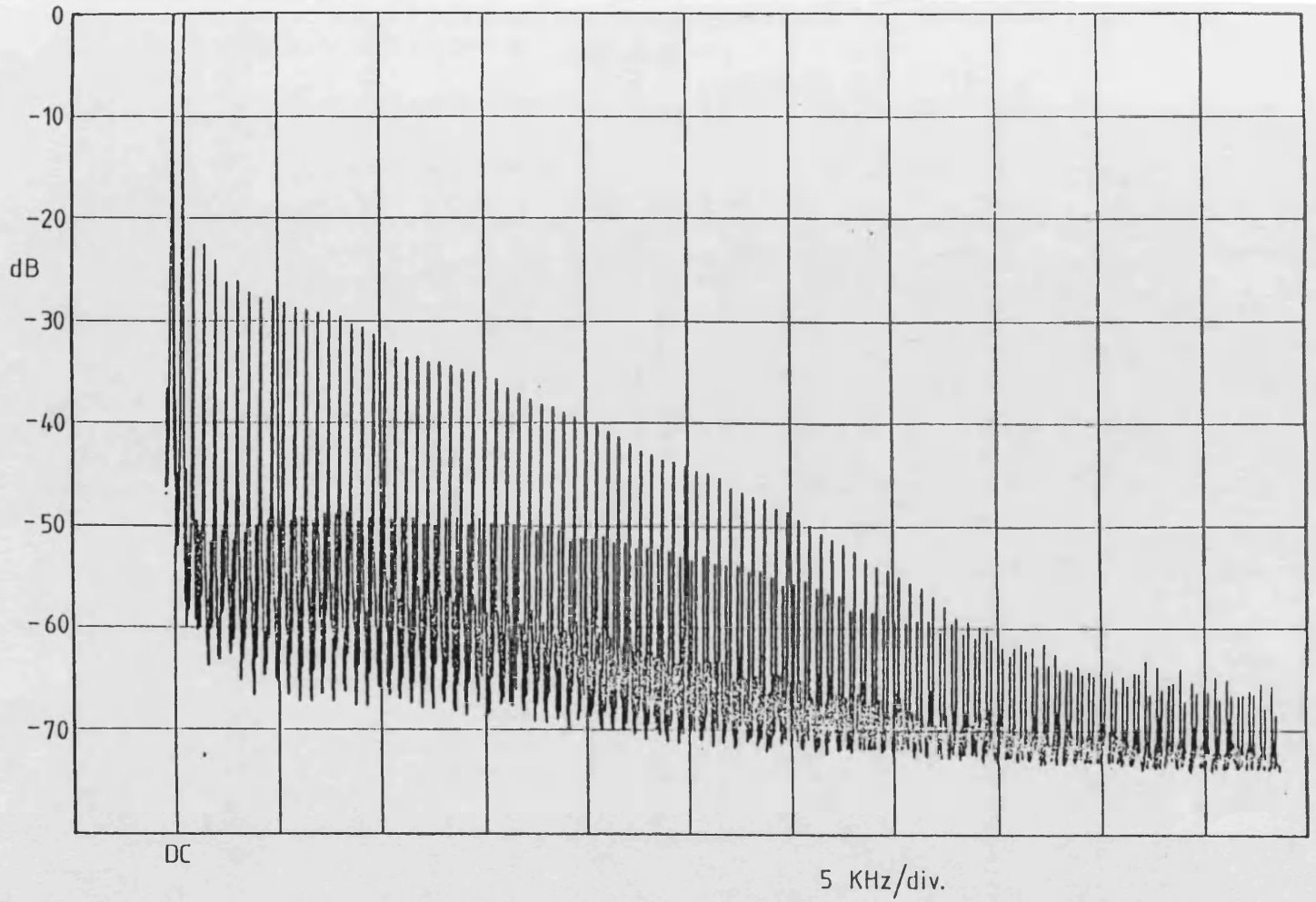

Figure 6.35 : PSD Output Spectrum with Transmitter Producing AM Output with Envelope of Two-tone SSB

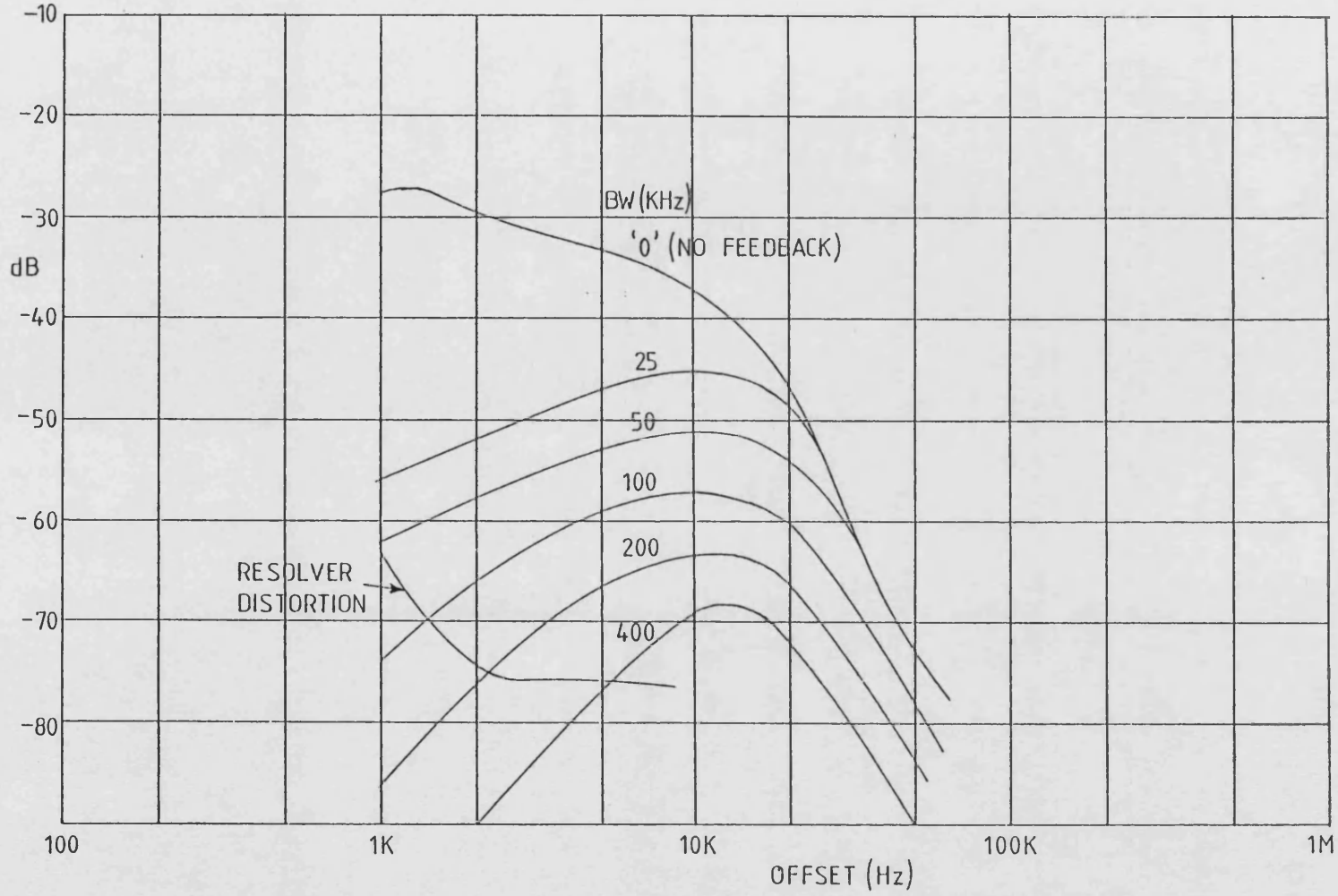

Figure 6.36 : Phase Distortion Spectra

6.3 LINEARITY OF THE POLAR RESOLVER

6.3.1 Amplitude Distortion

To measure the amplitude distortion produced by the polar resolver, an identical modulated signal must be applied to each resolver input. The residual, differential, demodulated envelope signal appearing at the cross-coupled demodulator outputs then provides a measure of the distortion. Figure 6.37 shows the spectrum of this output when one input is a two-tone SSB signal, and the other is an unmodulated carrier. The spectrum is that of a full-wave rectified sine-wave. When the other input is also a two-tone SSB signal, the difference output collapses to that shown in Figure 6.38. It can be seen that the amplitude imbalance in the polar resolver is less than -60dB relative to the wanted signal. If the same test is carried out with a 100% sinusoidally modulated AM signal, the spectra of Figures 6.39 and 6.40 are obtained. Figure 6.39 shows that each half of the resolver produces 2nd harmonic distortion at -35dB, even though the demodulator sections are linear to -70dB. This implies that the resolver amplitude imbalance is entirely due to imbalance between the AM to PM conversion levels of the two limiters.

The amplitude distortion spectrum produced by the polar resolver is included in the spectra of Figure 6.34 for comparison purposes.

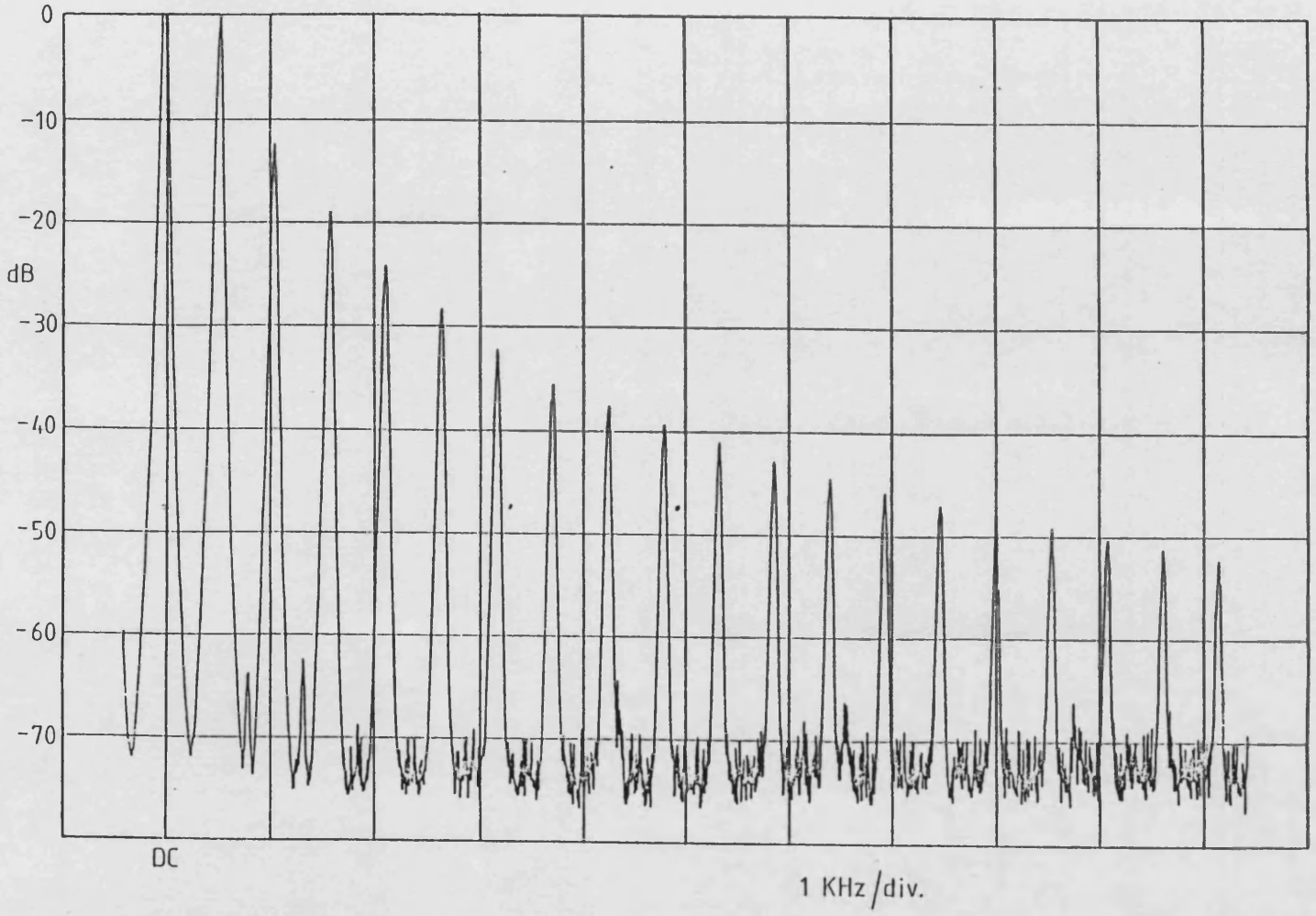

Figure 6.37 : Resolver Output Envelope Spectrum when one Input is Two-tone SSB and the other is an unmodulated carrier

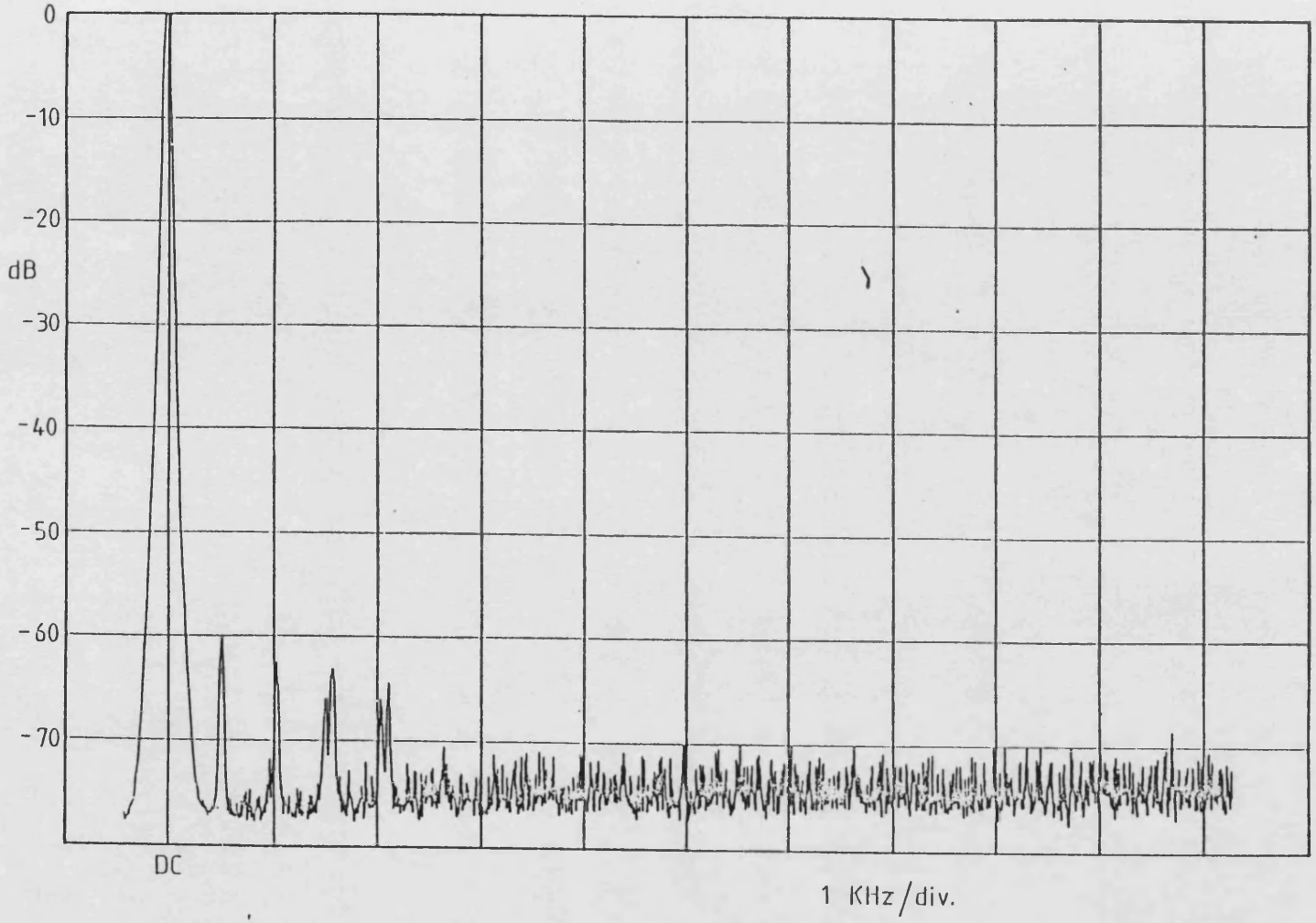

Figure 6.38 : Resolver Output Envelope Spectrum when both Inputs are Identical Two-tone SSB Signals

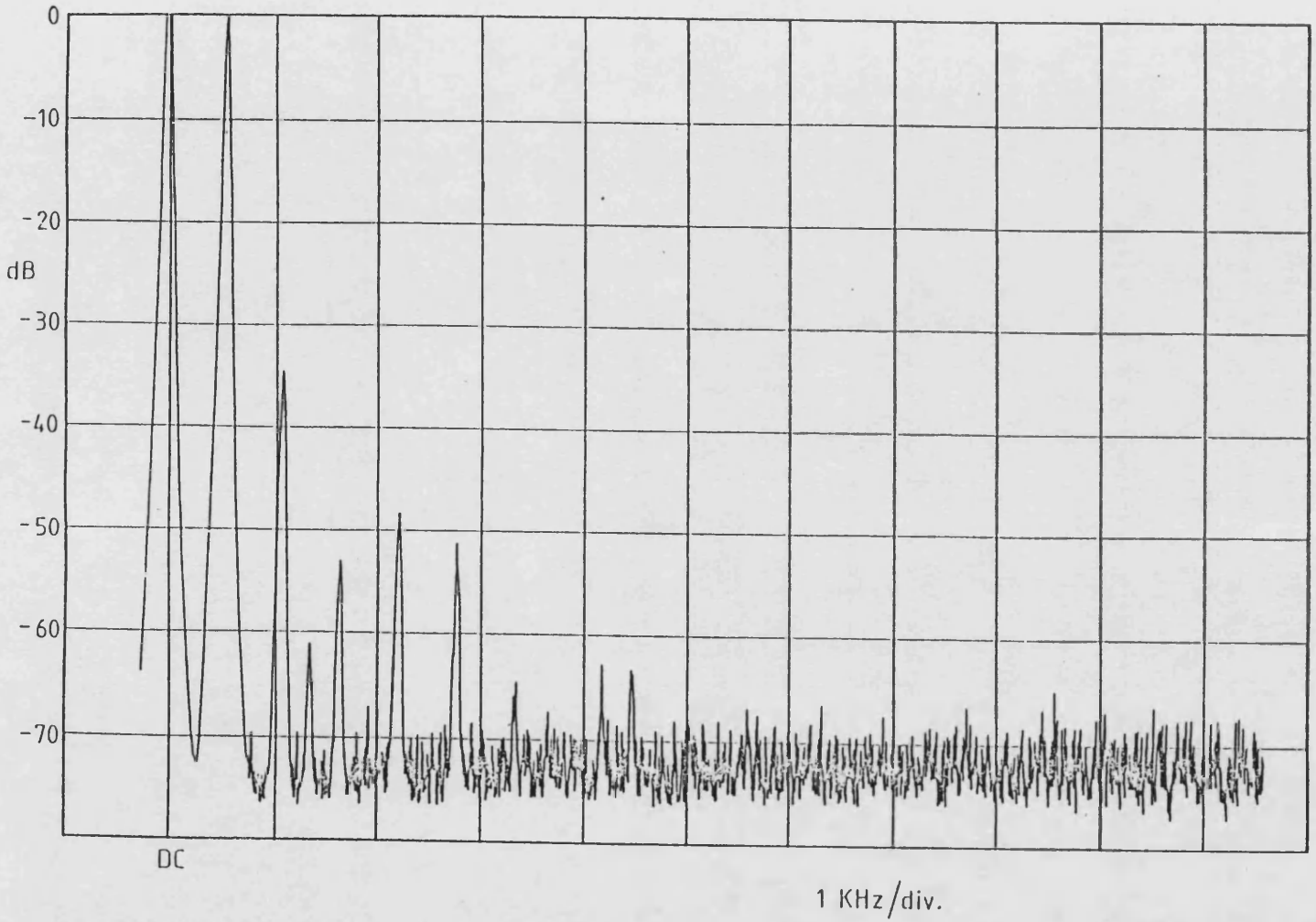

Figure 6.39 : Resolver Output Envelope Spectrum when one Input is Sinewave Modulated AM and the other is an Unmodulated Carrier

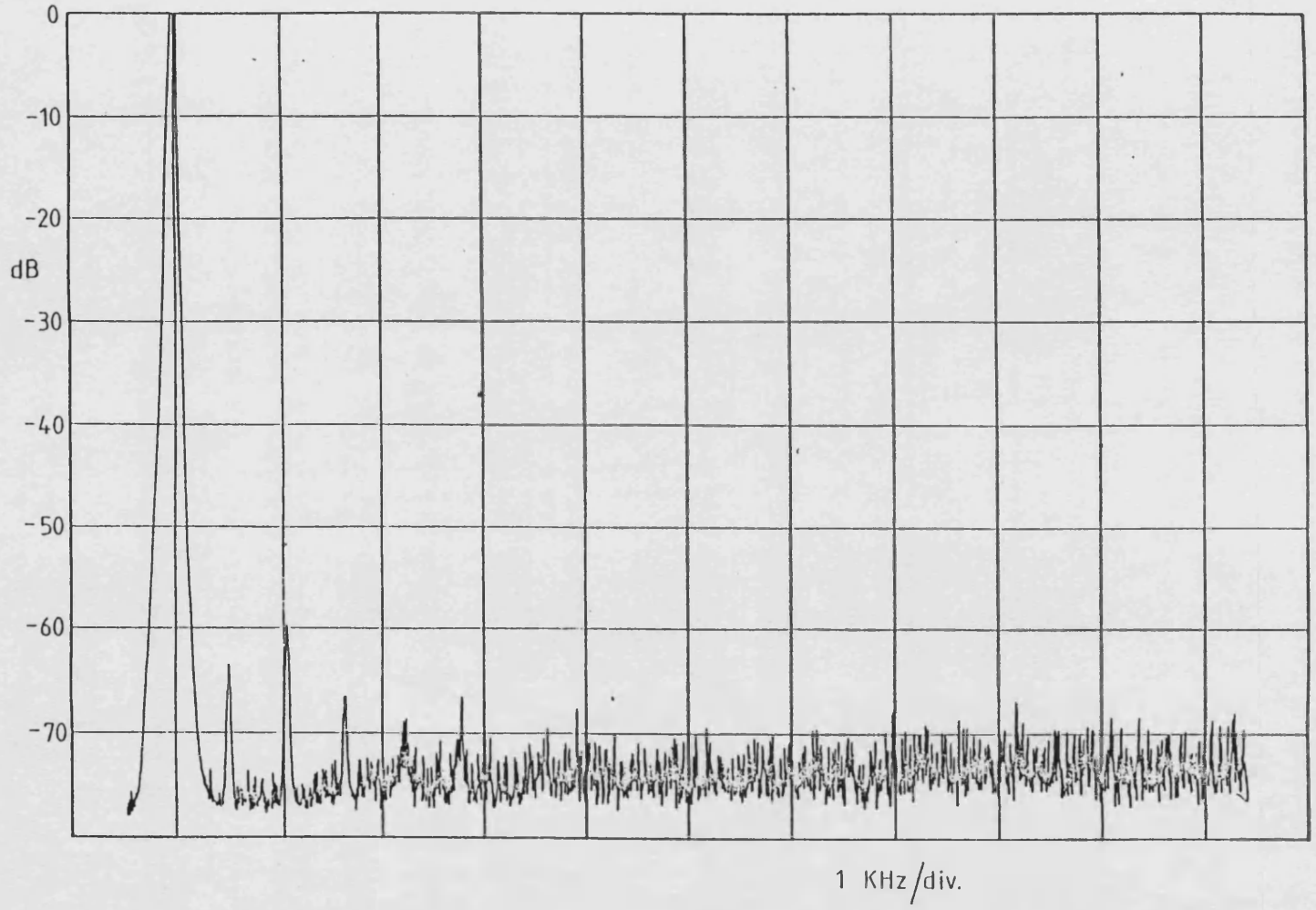

Figure 6.40 : Resolver Output Envelope Spectrum when both Inputs are identical Sinewave Modulated AM Signals

6.3.2 Phase Distortion

The measurement of the phase distortion produced by the polar resolver can follow the same procedure as for the amplitude distortion, with the exception that the output is taken from the PSD. Figure 6.41 shows the PSD output spectrum when a two-tone SSB signal is applied to both sides of the resolver. The reference level is 1 rad rms, as before. This spectrum is included in the transmitter phase distortion spectra of Figure 6.36, scaled to the same reference level. For completeness, the phase distortion produced by one side of the resolver was also measured. In this case the full-wave rectified sine-wave modulated AM signal was applied to one resolver input, and an unmodulated carrier to the other. The resulting spectrum is shown in Figure 6.42. It can be seen that the largest distortion component is 27dB larger than that in Figure 6.41.

6.4 TRANSMITTER NOISE LEVEL

The level of the noise sidebands appearing at the transmitter output were measured using the test set-up of Figure 6.43. The transmitter output is attenuated, and mixed down to 10.7MHz by a low noise signal generator. After amplification, the signal is passed through an 8-pole crystal filter and then to the spectrum analyser. With the transmitter producing a single tone, at a level equal to the nominal peak envelope power, the signal generator was

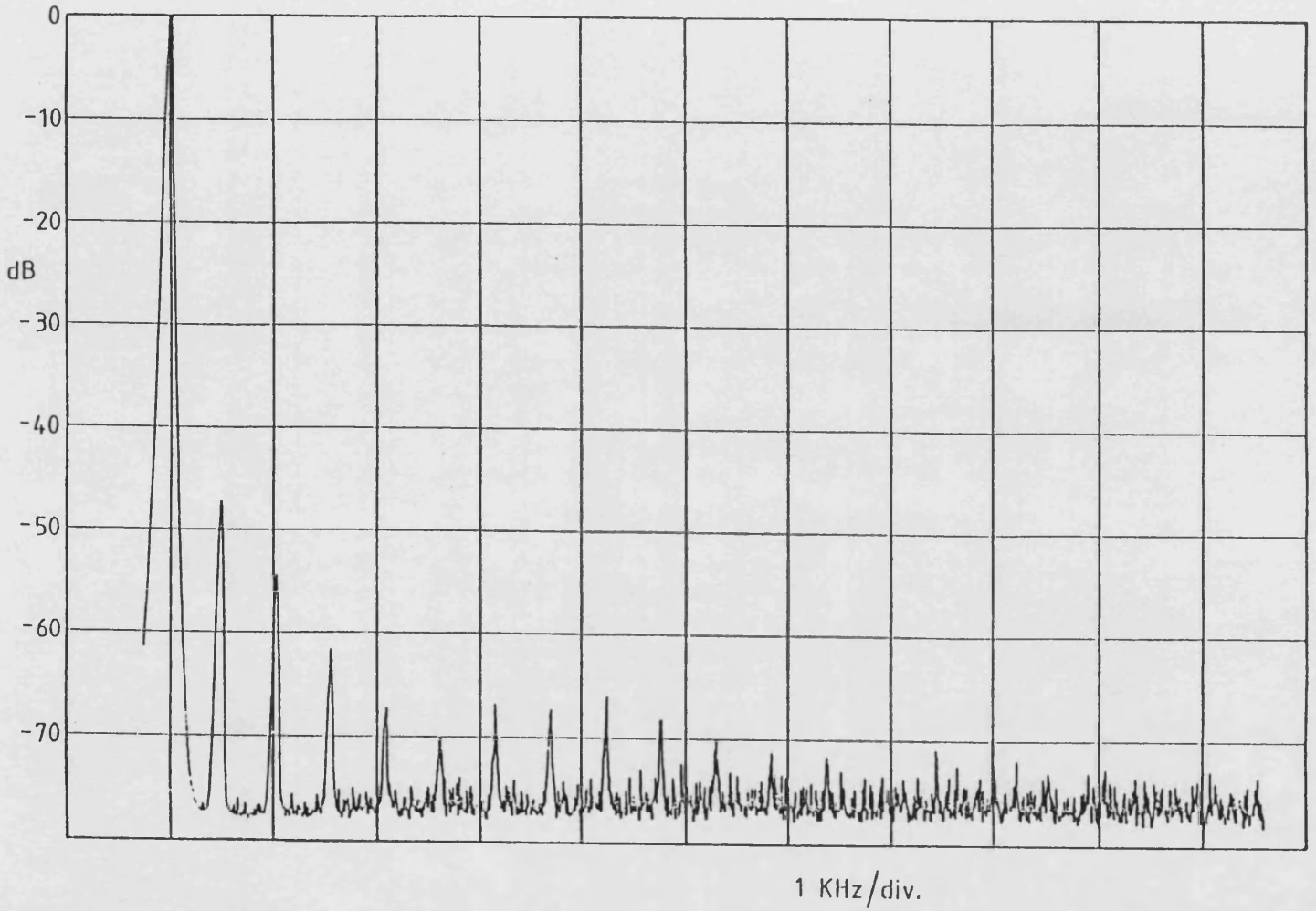

Figure 6.41 : PSD Output Spectrum with Two-tone SSB applied to both Inputs

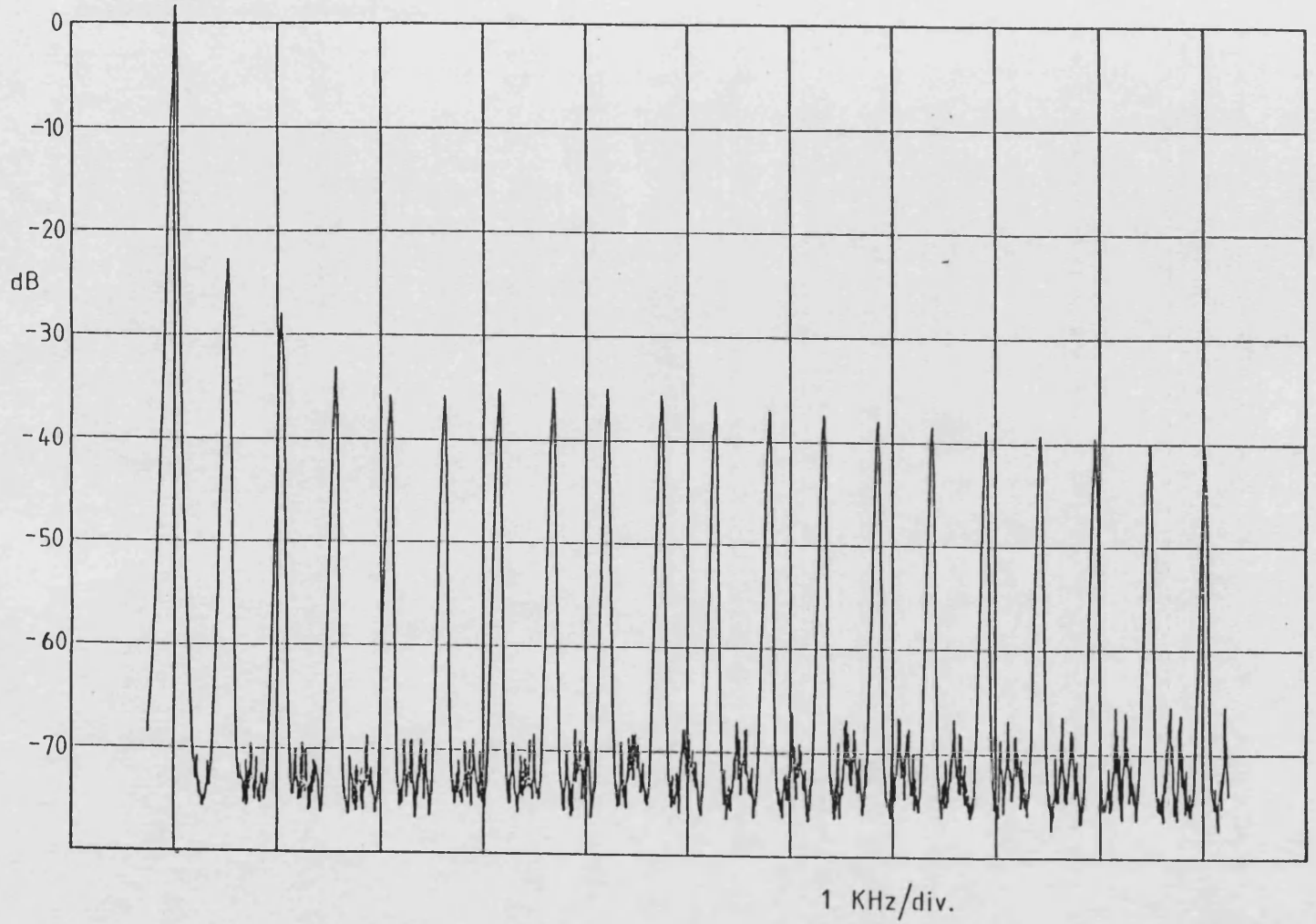

Figure 6.42 : PSD Output Spectrum with Full-Wave Rectified Sinewave Modulated AM Signal applied to one Input and Unmodulated Carrier to the other

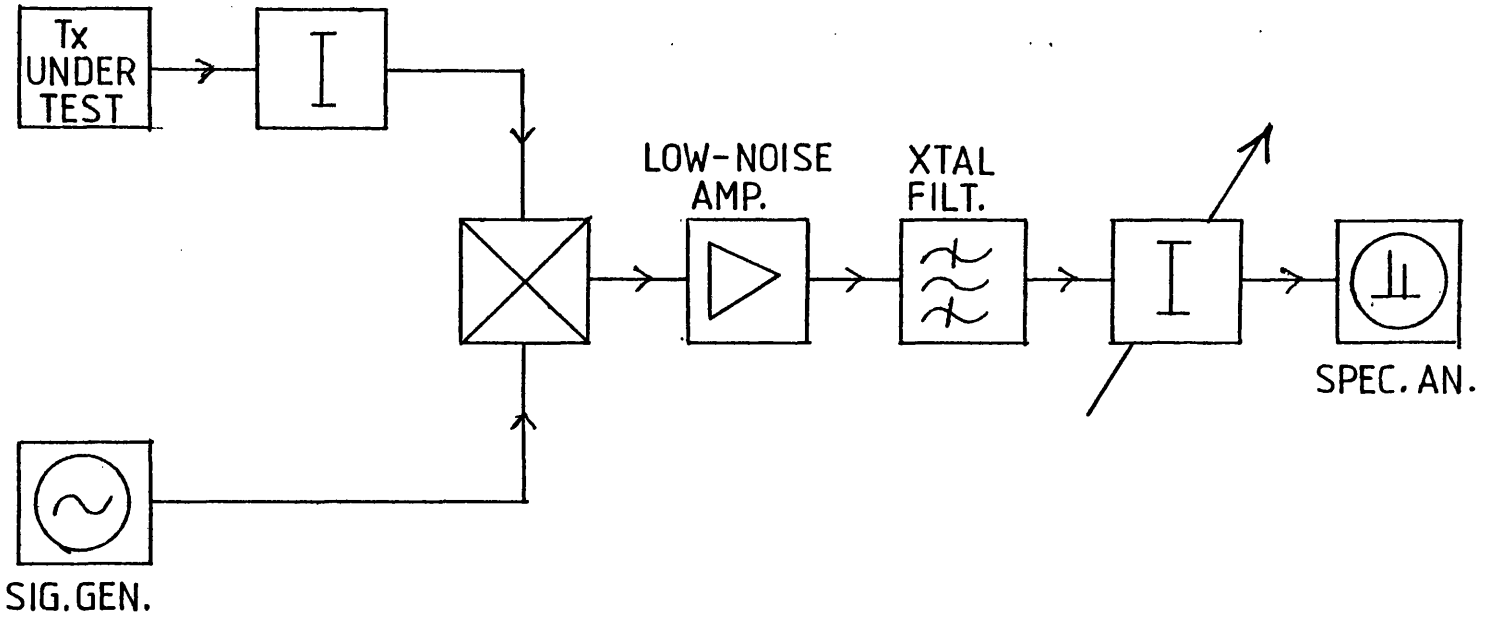

Figure 6.43 : Transmitter Noise Level Test Set-up

initially adjusted to be exactly 10.7MHz offset from the transmitter frequency. The 10.7MHz tone appearing at the mixer output passes through the filter, and can be used to set the spectrum analyser reference level with the attenuator at maximum (50dB). With the signal generator then displaced from the 10.7MHz offset point, the filter rejects the downconverted tone and passes only the noise sidebands. Removal of the attenuation effectively lowers the noise floor of the spectrum analyser at -73dB to -123dB. By measuring in a 100Hz bandwidth, the system noise floor is therefore -143dB/Hz.

This arrangement measures both amplitude and phase noise sidebands. The two are not separable using this technique.

The results of the noise level measurements on the 950MHz transmitter are shown in Figures 6.44, 6.45 and 6.46. These spectra show the effect on the noise levels of reducing the loop bandwidths in the same manner as for the distortion measurements. Firstly, both loops are reduced in bandwidth simultaneously, secondly, the amplitude loop only, and finally the phase locked loop only.

It can be seen that if the amplitude loop is narrowed, the noise level does not reduce appreciably. The spectrum follows the synthesiser noise to 20KHz, then levels off into a 'plateau' at approximately -130dB/Hz, before rolling off at 500KHz. This is in excellent agreement with the prediction in Section 5.5.3.4.

If the PLL is reduced in bandwidth, there is little

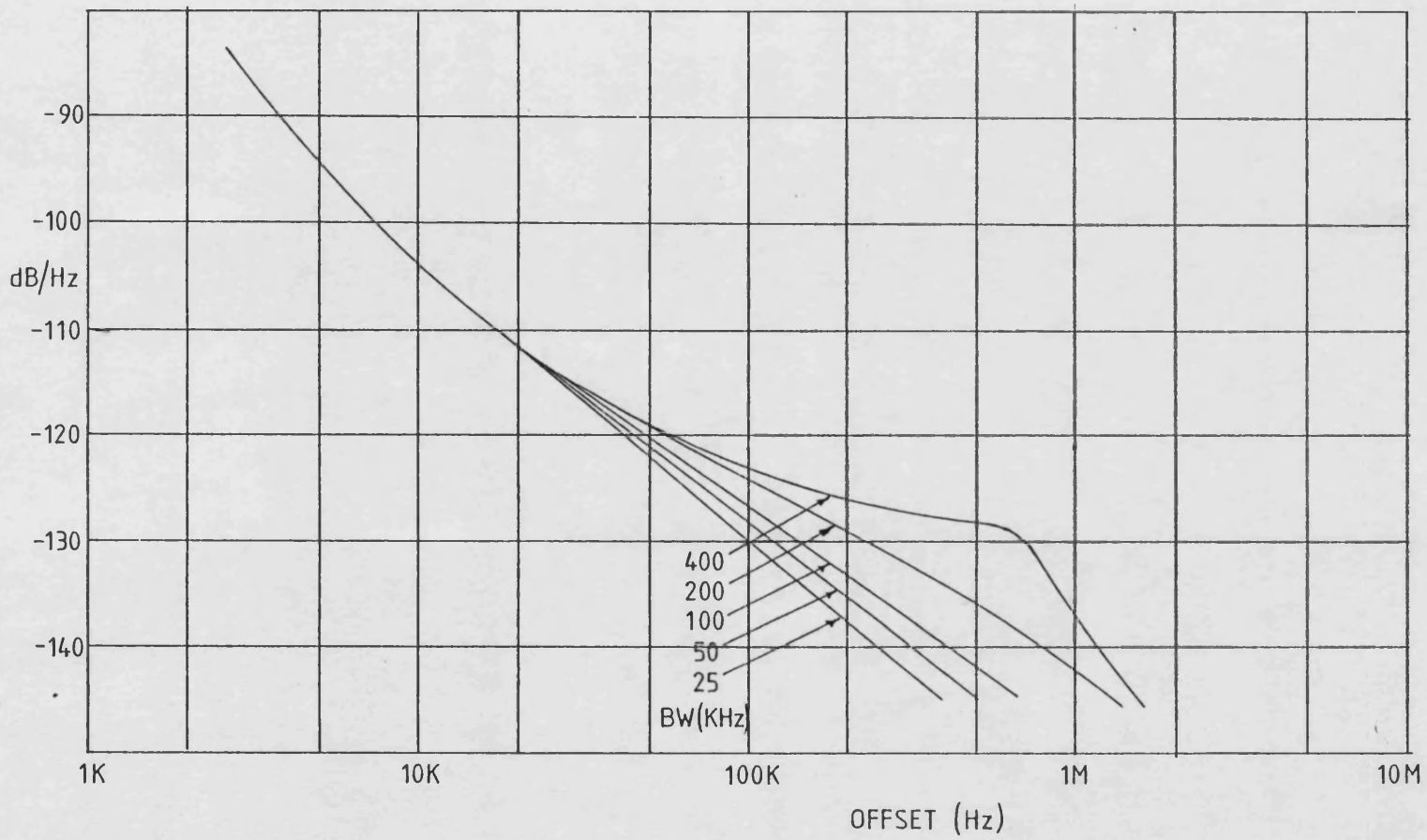

Figure 6.44 : 950MHz Transmitter Noise Sideband Spectra for several values of Loop BW

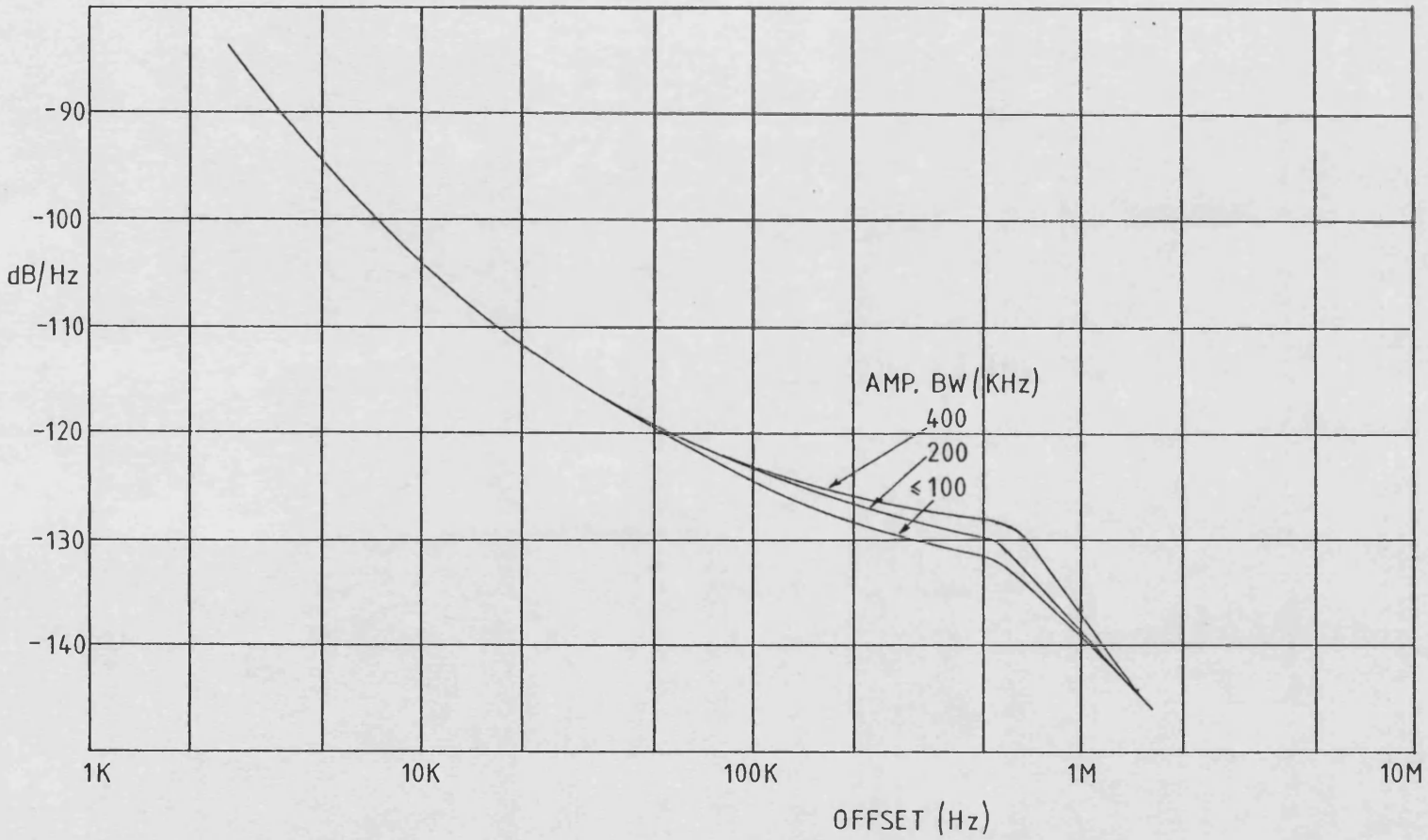

Figure 6.45 : 950MHz Transmitter Noise Sideband Spectra for several values of Ampl. BW (PLL BW fixed at 400KHz)

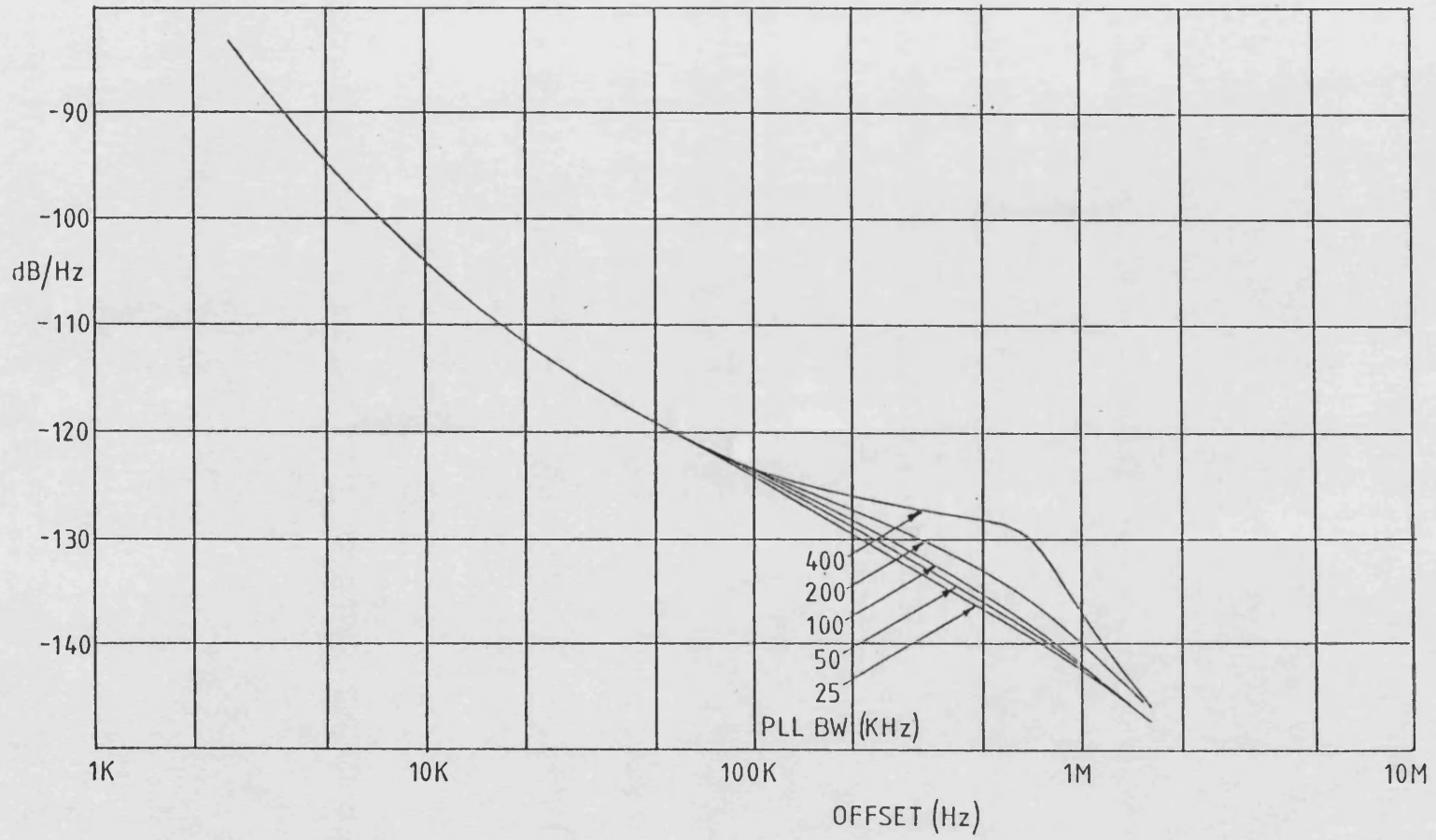

Figure 6.46 : 950MHz Transmitter Noise Sideband Spectra for several values of PLL BW (Ampl. BW fixed at 400KHz)

further improvement in noise level for PLL bandwidths less than 100KHz. In this case, the amplitude noise is dominant. The noise level does not fall below -134dB/Hz, for offsets below 400KHz, as predicted in Section 5.5.2.3.

Although the phase noise is the largest contributor to the output noise, the amplitude noise is only 4dB less, at large offsets. The biggest improvement is therefore obtained when both loops are reduced in bandwidth. This is shown in Figure 6.44, where reducing both loops to 100KHz, lowers the noise level by 20dB at 500KHz. Reducing the bandwidths still further, produces less improvement, since the VCO noise is then making a significant contribution.

The noise level produced by the 450MHz transmitter was also measured, but for only one set of loop bandwidths, 240KHz for the PLL and 500KHz for the amplitude loop. This is shown in the spectrum of Figure 6.47. The noise performance is much poorer than that of the 950MHz transmitter, as expected, due to the higher noise levels in the limiters, PSD and to a lesser extent, the SSB generator and downconverter.

6.5 EFFICIENCY

The efficiency of a transmitter is defined as the ratio of the mean RF output power to the mean d.c. power taken by the power amplifier.

For the 450MHz transmitter this was 28%, when the output was a two-tone signal. Although, apparently a poor figure,

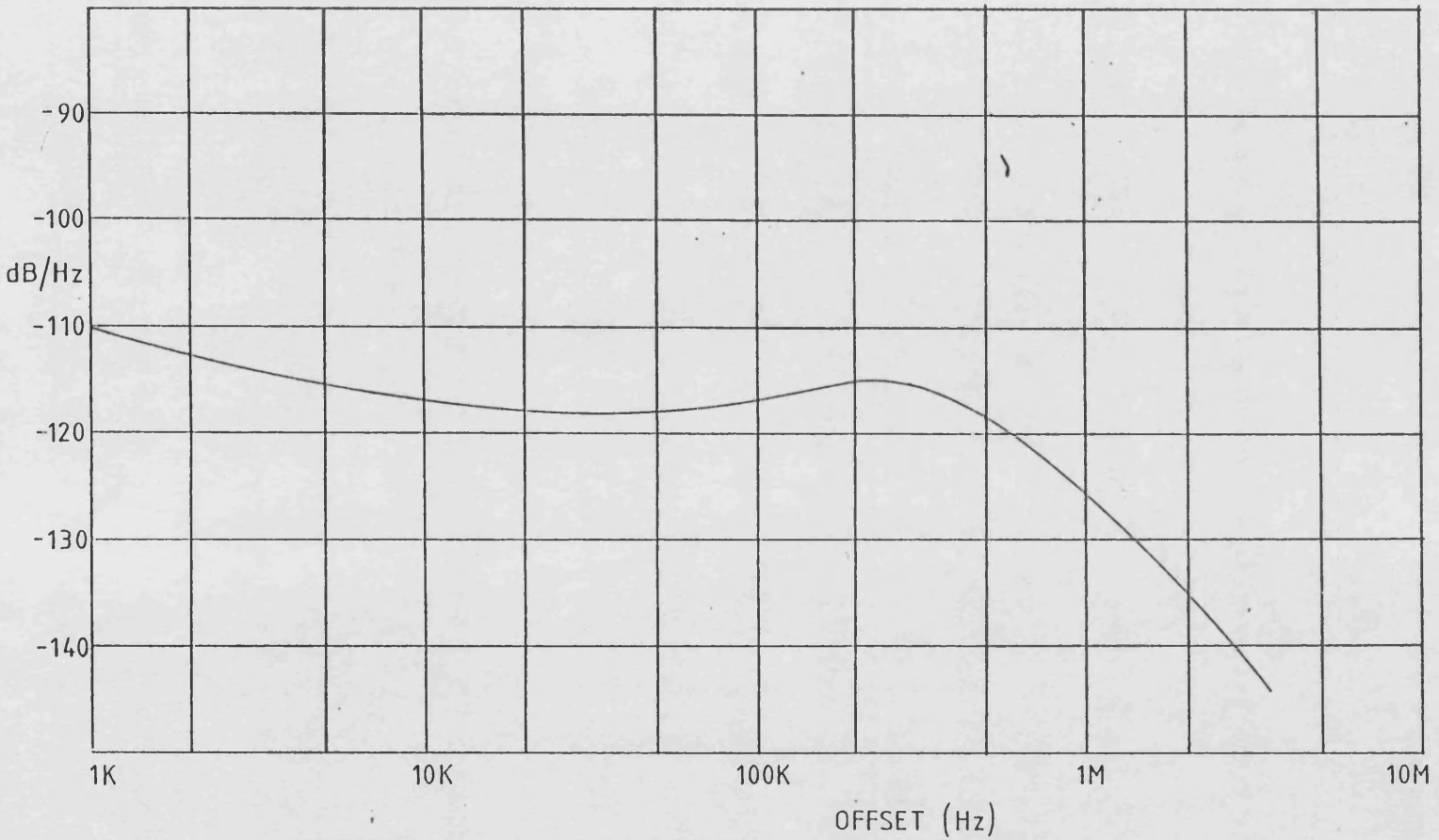

Figure 6.47 : 450MHz Transmitter Noise Sideband Spectrum

this must be compared with the efficiency of the power amplifier module in CW mode, of 35%. Thus, the use of a polar loop SSB transmitter results in little loss of efficiency compared to a conventional FM transmitter. If the power taken by the control circuits is included, the efficiency drops to 21%. It must be pointed out however, that none of the transmitter circuits were designed with low power consumption in mind, and so this figure could undoubtedly be improved upon.

For the 950MHz transmitter, the figures are 41% for the power amplifier, and 32% including the control circuits.

6.6 SUMMARY AND ANALYSIS OF RESULTS

Measurements made on the 450MHz and 950MHz UHF polar loop transmitters have shown that they are both capable of excellent linearity. On a two-tone test, the 450MHz transmitter gave third order intermodulation products -56dB relative to the tone level. For the 950MHz transmitter, the distortion products were typically at -51dB.

Investigation into the sources of the distortion has shown that for loop bandwidths in excess of 100KHz, the polar resolver is the dominant cause, with phase distortion making the largest contribution. Both amplitude and phase distortion in the polar resolver is now known to be caused entirely by imbalance in the AM to PM conversion levels in the two limiters. For loop bandwidths below 100KHz, the distortion due to the amplitude modulator, power amplifier

and unwanted 'pulling' of the VCO, exceed that due to the resolver, and consequently a degradation of the output spectrum occurs. The drift in the distortion levels, noted mainly on the 950MHz transmitter, occurred only for wide loop bandwidths, when the spectrum is resolver limited. Hence, this effect must be due to drift in the resolver imbalance with temperature. The fact that the 450MHz transmitter was less prone to this effect, despite the inferior limiters, is an indication of the better matching and thermal tracking of the two halves of the dual SL624 resolver.

The output spectra taken using a bandlimited noise input (to simulate speech), confirmed the excellent linearity achievable. Even with the loop bandwidths reduced to 50KHz, the adjacent channel spurious output was in excess of 70dB below the peak envelope power.

The measured noise sideband levels for the 950MHz transmitter have shown excellent correlation with the predicted values. The output noise was found to comprise both amplitude and phase noise, with the latter being the most significant. For offsets below 20KHz, the synthesiser noise is dominant, but for larger offsets, the limiters and PSD make the largest contribution. Although the lowest noise level would be achieved with loop bandwidths of 25KHz or less, in accordance with the theoretical analysis, a degradation of under 10dB results from increasing the bandwidths to 100KHz. In view of the linearity performance obtained at 100KHz bandwidths, this would appear to be a good compromise.

CHAPTER SEVEN

CONCLUSIONS AND SUGGESTIONS FOR FURTHER WORK

7.1 CONCLUSIONS

The Polar Loop Technique has been successfully applied to the UHF frequency bands of 450MHz and 950MHz. Practical polar loop SSB transmitters have been designed, constructed and evaluated for both of these bands, and have given excellent performance. The levels of the spurious outputs and noise sidebands achieved, exceed the likely specifications which would need to be met, if SSB were adopted at UHF in the mobile radio service.

In Chapter 1, the problems associated with using SSB modulation at VHF and UHF for mobile radio, were examined. Most of the potential difficulties, such as local oscillator frequency stability, Doppler shift due to relative motion between transmitter and receiver, and rapid multipath fading, would appear to have been largely solved. The transmission of a reference, or pilot component with the sideband, provides the receiver with a means for correction of both amplitude and frequency fluctuation, in the form of fast acting AGC and AFC. However the problem area which still needed to be solved was the implementation of a transmitter which had high efficiency, yet also had good spectral purity.

A review into the various means of improving the linearity of RF amplifiers for this application was carried out in Chapter 2. This showed that open-loop techniques such as predistortion and feedforward have limited value, since

only small improvements in linearity would be practicable, with unchanged or poorer efficiency. Similarly, feedback cannot provide a significant reduction in distortion due to stability problems. However, by applying feedback to the modulation rather than directly to the RF signal, much larger improvements are possible, particularly when the feedback is applied to both the amplitude and phase modulation. This technique is used in the Polar Loop Transmitter, which also employs the high efficiency RF amplification arrangement known as Envelope Elimination and Restoration (EER).

In Chapter 3, the Polar Loop Technique was examined in detail. It was shown that non ideal behaviour in the transmitter, such as finite loop bandwidths, threshold effects in the limiters or time delay between the feedback loops, would have the effect of producing spurious components at the output. However, the analysis showed that the magnitude of such spurii would be much less than the components due to power amplifier distortion.

The sources of amplitude and phase noise sidebands were identified, and the effect of the feedback loops on their levels was evaluated. It was shown that there is an optimum PLL bandwidth which results in minimum phase noise, but also that this may conflict with the bandwidth required for lowest distortion.

In Chapter 4, an investigation into the effects of implementing the polar loop at UHF was made. This showed that the distortion levels likely to be encountered would

be higher than those at lower frequencies, but also that the amount of feedback available should be sufficient to reduce this to acceptable levels. It was also realised that achieving adequate isolation of the VCO and within the amplitude modulator would be a major problem at UHF. A review of the potential devices to meet this requirement showed that only the dual-gate MOSFET could provide sufficient isolation. Consideration of the theoretical transmitter phase noise, showed that the inherent degradation due to increasing the operating frequency would have to be countered by an improved Q-factor in the VCO. This led to the conclusion that the best option was to use microstrip technology for the oscillator.

Construction of practical UHF transmitters, and design of the feedback loops was covered in Chapter 5. The LC oscillators employing microstrip inductors proved to be a highly effective means of implementing a low noise VCO. A phase noise level of -94dB/Hz at a 5KHz offset was achieved.

Measurements made on the transmitters, and documented in Chapter 6, showed them to have outstanding linearity. On a two-tone test, third order intermodulation products were over 50dB below the wanted sideband, despite the use of RF amplifiers which operated purely in class C. Similar performance was obtained using a white noise input to simulate speech. For both types of signal, the adjacent channel spurious output was less than -70dB relative to the wanted output, yet the efficiency was little worse than when the transmitters were used in CW mode (as they would do for FM

transmission). The limiting factor in the linearity performance was found to be the residual imbalance in the polar resolving circuits. In particular, the difference in the levels of AM to PM conversion in the two limiters was entirely responsible for this imbalance. Fabrication of the resolver circuits on a single chip may help to alleviate this problem.

The measured noise sideband levels at the transmitter outputs were in excellent agreement with the theoretical predictions, being determined mainly by the VCO noise level, provided loop bandwidths were kept below 100KHz. An adjacent channel noise level of -94dB/Hz at a 5KHz offset was recorded. This corresponds to -60dB in a 2.4KHz bandwidth (the standard SSB filter bandwidth). Although higher than the transmitter spurious output, this is still well below the spurious level from a conventional transmitter. Improvement in this area would require a lower noise VCO, such as those based on SAW devices. At large frequency offsets, the 450MHz transmitter had considerably worse noise performance than the 950MHz transmitter. However, this was due entirely to the excessive noise level found to be present in the first generation of IF and control circuits.

In the light of the results obtained on the UHF polar loop transmitters, and the work that has been carried out on SSB receivers at UHF, it is believed that UHF SSB is entirely practicable for the land mobile radio service.

7.2 SUGGESTIONS FOR FURTHER WORK

The main limitation to the linearity performance of the polar loop transmitter is the differential resolver distortion, due to AM to PM conversion imbalance between the two limiters. It would be valuable therefore, to make a thorough investigation into the mechanism of this effect, and how it can be reduced. One would intuitively expect that two limiters fabricated on the same chip of silicon would be extremely well matched. There are already ECL devices available which contain several nominally identical amplifiers on one chip, and these could form a useful starting point in this respect.

On a different aspect, the need to amplitude modulate the output signal results in a loss of efficiency. A possible means of improving this would be to use the Chireix (outphasing) method of amplification (115). This combines the output of two power amplifiers each operating at constant amplitude, but varies the phase difference between them so that the overall output is amplitude modulated. The individual amplifiers thus always operate at maximum efficiency. The RF stages of a polar loop transmitter using this idea would therefore take the form of Figure 7.1. Phase modulating the two channels in opposition would give amplitude modulation at the output, whereas the same phase shift applied to both would produce phase modulation. Further work would be necessary to establish whether this is feasible in practice.

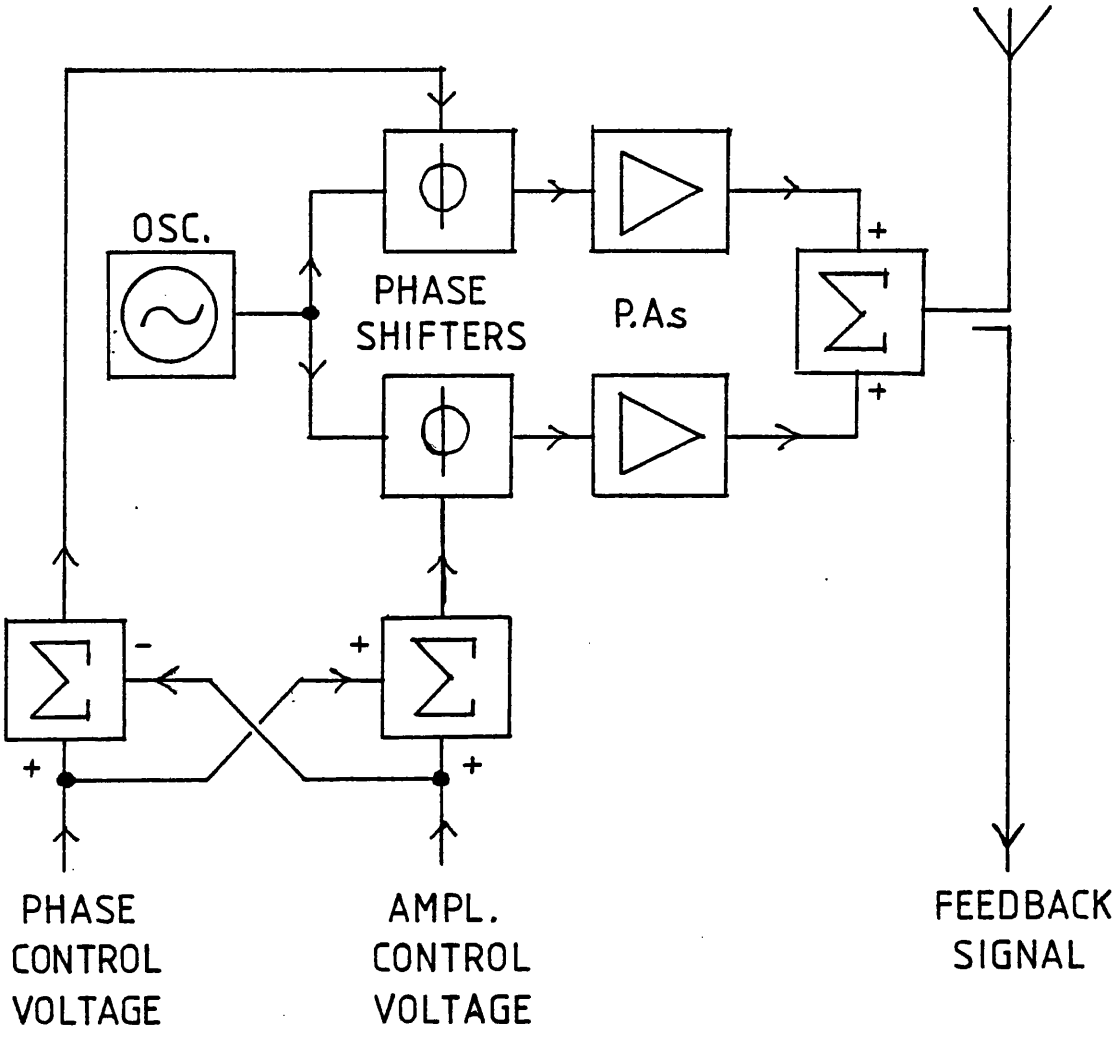

Figure 7.1 : RF Stages of a Polar-Loop Transmitter using the Chireix (Outphasing) Method of Amplification

Since handportable equipments would be an important requirement for any new radio system, the feasibility of implementing a handportable polar loop transmitter should be investigated. The problems which may be envisaged would arise due to the use of a low voltage supply of limited capacity. This would adversely affect the VCO stability and may require alternative realisation of the polar resolving circuit.

An alternative approach to amplifier linearisation to the polar loop technique would be to rearrange the modulation feedback such that it is applied in cartesian, rather than polar coordinate form. This arrangement, invented by Smith and Petrovic (118), is known as the Cartesian Loop Transmitter and is shown in the block diagram of Figure 7.2. The input signal, which may have any form of modulation, and which may be generated at any frequency, is frequency translated to baseband by quadrature carrier signals. These carriers would normally be centred on the input spectrum. The two baseband signals, which may be termed the cartesian coordinates of the input, completely define the input modulation, both amplitude and phase. At the transmitter output, a similar resolving process is carried out but with carriers centred on the desired channel frequency. The cartesian coordinates so obtained, are fed back and compared with the input coordinates in high gain differential amplifiers. These amplifiers remodulate the same carriers to reconstitute at the output an RF signal with the same modulation as the input signal, but which is

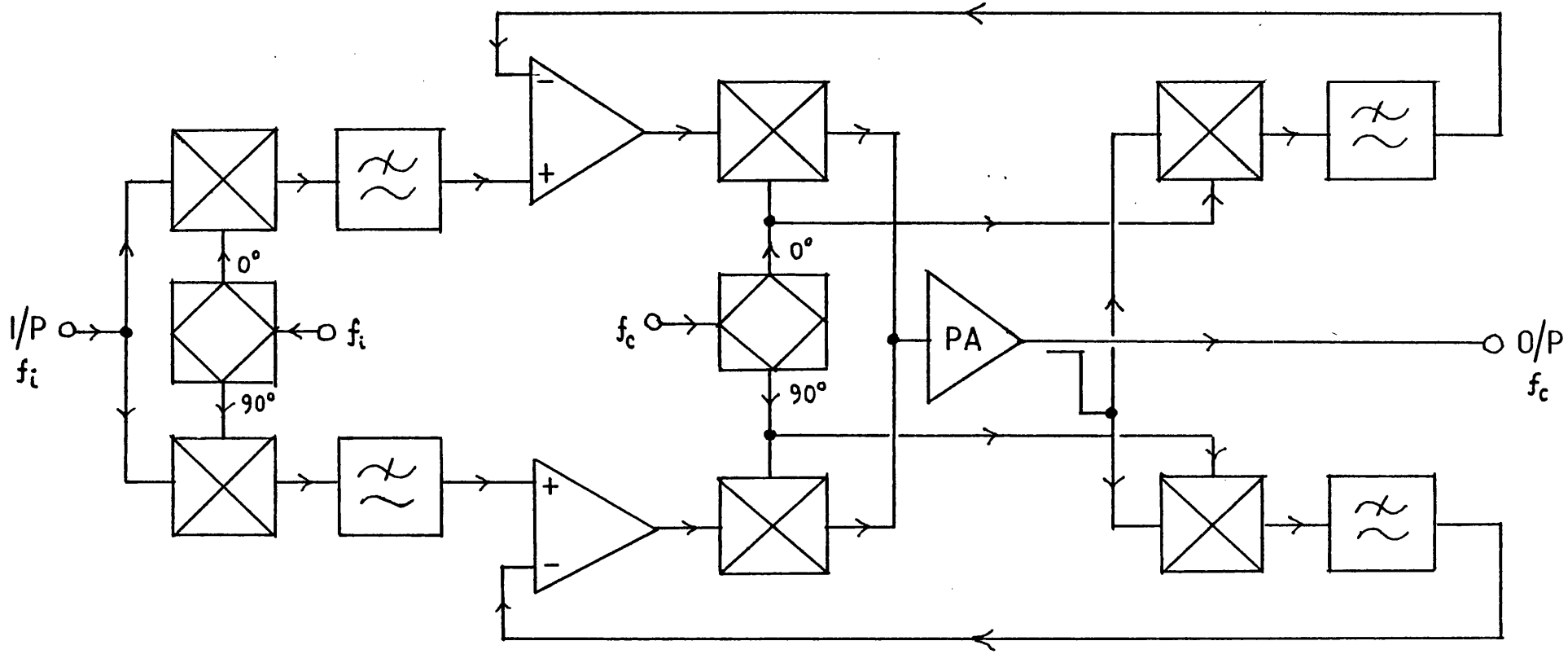

Figure 7.2 : The Cartesian-Loop Transmitter

frequency translated. As in the case of the Polar Loop, the system thus forms two orthogonal feedback loops.

The main benefit of the Cartesian Loop is that its resolving is simply carried out using balanced mixers, which may be made almost arbitrarily linear. The resolver matching problem experienced with the Polar Loop, is therefore avoided.

Although work is at an early stage, a VHF implementation of a Cartesian Loop Transmitter has achieved excellent results, with third order intermodulation levels of -65dB on a two-tone test.

Further work should be carried out to examine the factors affecting linearity and noise levels, and to investigate the application of the technique at HF and UHF.

APPENDICES

APPENDIX A

APPROXIMATE EXPRESSION FOR THE PHASE SHIFT IN A TUNED CIRCUIT AS A FUNCTION OF CAPACITANCE

The phase response of a tuned circuit is as shown below:-

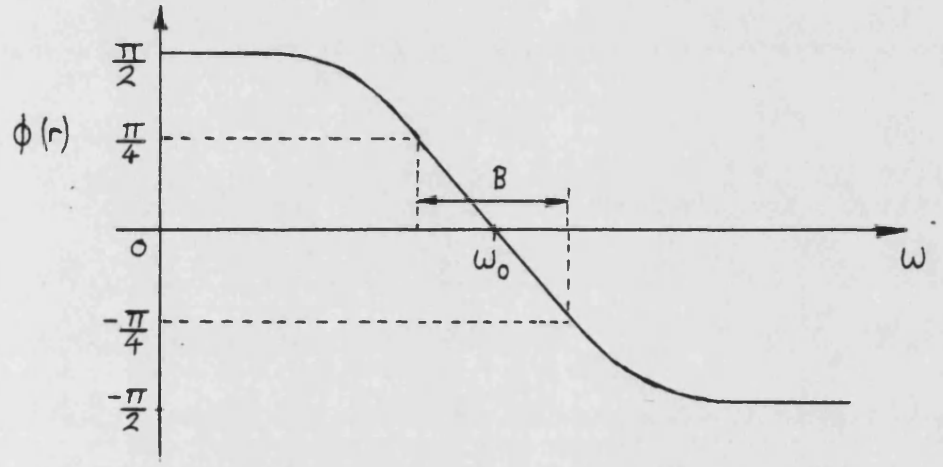

Within the bandwidth of the tuned circuit, B, the phase response is approximately linear, with a slope:-

$$\frac{d\phi}{d\omega} \approx \frac{\left[\frac{\pi}{2}\right]}{B} = \frac{\pi Q}{2\omega_o} \quad , \quad \text{at } \omega_o \qquad \text{(A.1)}$$

Since $\omega_o = (LC)^{-\frac{1}{2}}$

$$\Rightarrow \frac{d\omega}{dC} = -\frac{1}{2}(LC)^{-\frac{3}{2}} \cdot L$$

$$= -\frac{1}{2}\omega_o(LC)^{-1} \cdot L$$

$$= -\frac{\omega_o}{2C} \qquad \text{(A.2)}$$

Hence the phase change with capacitance is given by:-

$$\frac{d\phi}{dC} = \frac{d\phi}{d\omega} \cdot \frac{d\omega}{dC} \qquad (A.3)$$

$$= \frac{\pi Q}{2\omega_o} \quad \frac{-\omega_o}{2C}$$

$$= \frac{-\pi Q}{4C} \text{ rad/F.} \qquad (A.4)$$

APPENDIX B

APPLICATION OF OVERALL NEGATIVE FEEDBACK TO A THREE STAGE AMPLIFIER

Assume each stage has the response:-

$$A = \frac{k}{1 + j\omega\tau} \tag{B.1}$$

where k = low frequency gain

$1/\tau$ = -3dB bandwidth of stage

For three identical stages:-

$$A_T = \frac{k^3}{(1 + j\omega\tau)^3} \tag{B.2}$$

$$= \frac{k^3}{1 - 3(\omega\tau)^2 + j[3\omega\tau - (\omega\tau)^3]} \tag{B.3}$$

$$\text{and, } |A_T| = \frac{k^3}{\sqrt{[1 - 3(\omega\tau)^2]^2 + [3\omega\tau - (\omega\tau)^3]^2}} \tag{B.4}$$

Normalising w.r.t. 3dB bandwidth of single stage, $1/\tau = \omega_B$

$$|A_T| = \frac{k^3}{\sqrt{\left[1 - 3\left(\frac{\omega}{\omega_B}\right)^2\right]^2 + \left[3\frac{\omega}{\omega_B} - \left(\frac{\omega}{\omega_B}\right)^3\right]^2}} \tag{B.5}$$

Assuming 10dB of feedback:

$1 + \beta A_T = 3.16$, at low frequency.

$$\text{Hence, } \beta = \frac{2.16}{A_T} = \frac{2.16}{k^3}$$

Thus, the closed loop gain A_C will be:

$$A_C = \frac{A_T}{1 + \beta A_T}$$

$$= \frac{\left\{ \frac{k^3}{\left[1 - 3\left(\frac{\omega}{\omega_B}\right)^2\right] + j\left[3\frac{\omega}{\omega_B} - \left(\frac{\omega}{\omega_B}\right)^3\right]} \right\}}{1 + \frac{2.16}{k^3}\left\{ \frac{k^3}{\left[1 - 3\left(\frac{\omega}{\omega_B}\right)^2\right] + j\left[3\frac{\omega}{\omega_B} - \left(\frac{\omega}{\omega_B}\right)^3\right]^2} \right\}} \qquad \text{(B.6)}$$

$$= \frac{k^3}{\left[1 - 3\left(\frac{\omega}{\omega_B}\right)^2 + 2.16\right] + j\left[3\left(\frac{\omega}{\omega_B}\right) - \left(\frac{\omega}{\omega_B}\right)^3\right]} \qquad \text{(B.7)}$$

$$A_C = \frac{k^3}{\sqrt{\left[3 - 16 - 3\left(\frac{\omega}{\omega_B}\right)^2\right]^2 + \left[3\left(\frac{\omega}{\omega_B}\right) - \left(\frac{\omega}{\omega_B}\right)^3\right]^2}} \qquad \text{(B.8)}$$

This function is plotted in Figure B.1, along with the open loop gain and phase. It can be seen that the phase margin is 40^o, and that the closed loop response peaks 4dB when the loop gain equals unity.

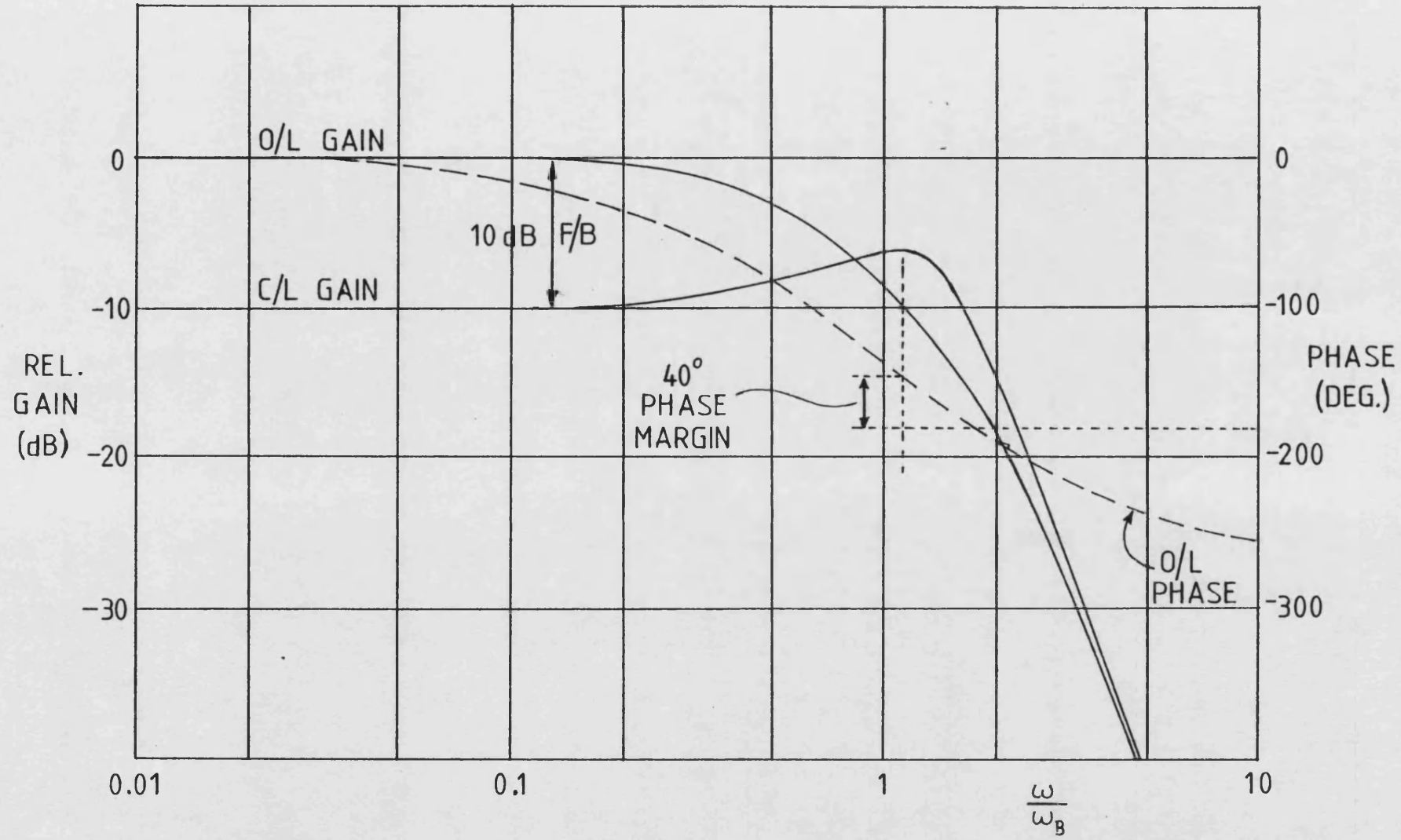

Figure B.1 : Frequency Responses for 3 Stage Amplifier with 10dB Overall Feedback

APPENDIX C

DERIVATION OF THE CLOSED LOOP RESPONSE OF A SECOND ORDER PLL POSSESSING FIRST ORDER CHARACTERISTICS

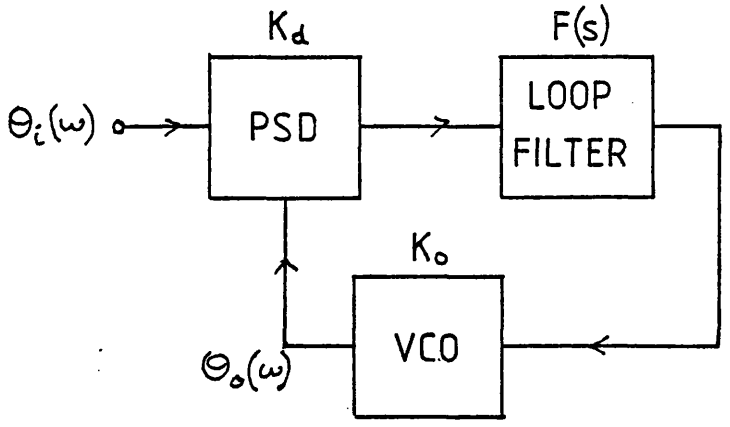

According to (113) the transfer function of a PLL is given by:-

$$\frac{\theta_o(\omega)}{\theta_i(\omega)} = \frac{k_o\, k_d\, F(\omega)}{j\omega + k_o\, k_d\, F(\omega)} \qquad (C.1)$$

If the loop filter, $F(\omega)$, is the active integrate/phase lead form, its transfer function is:-

$$F(\omega) = \frac{1 + j\omega\, R_2\, C_2}{j\omega\, R_1\, C_2} \qquad (C.2)$$

Hence:

$$\frac{\theta_o(\omega)}{\theta_i(\omega)} = \frac{\left[k_o\, k_d\, \frac{(1 + j\omega\, R_2\, C_2)}{j\omega\, R_1\, C_2}\right]}{j\omega + \left[k_o\, k_d\, \frac{(1 + j\omega\, R_2\, C_2)}{j\omega\, R_1\, C_2}\right]} \qquad (C.3)$$

Rearranging:-

$$\frac{\theta_o(\omega)}{\theta_i(\omega)} = \frac{1}{1 + \frac{j\omega}{\left[k_o\, k_d \frac{(1 + j\omega\, R_2\, C_2)}{j\omega\, R_1\, C_2}\right]}}$$

$$= \frac{1}{1 + \frac{j\omega}{k_o\, k_d \frac{R_2}{R_1}} \cdot \left[\frac{j\omega\, C_2\, R_2}{1 + j\omega\, C_2\, R_2}\right]} \qquad (C.4)$$

When:- $\omega \ll k_o\, k_d \frac{R_2}{R_1}$

and, $\omega \ll \frac{1}{R_2\, C_2}$

$$\frac{\theta_o}{\theta_i}(\omega) \to 1$$

When:- $\omega \gg k_o\, k_d \frac{R_2}{R_1}$

$$\omega \gg \frac{1}{R_2\, C_2}$$

$$\frac{\theta_o}{\theta_i}(\omega) \to \frac{k_o\, k_d \frac{R_2}{R_1}}{j\omega}$$

When:- $\omega \to k_o\, k_d \frac{R_2}{R_1}$

$$\frac{\theta_o}{\theta_i}(\omega) \to \frac{1}{1 + j.1}$$

provided that the function $\left[\frac{j\omega\, C_2\, R_2}{1 + j\omega\, C_2\, R_2}\right] \to 1$

For this to be true:-

$$\left(k_o\ k_d\ \frac{R_2}{R_1}\right) \cdot C_2\ R_2 \gg 1$$

i.e. $k_o\ k_d\ \frac{R_2}{R_1} \gg \frac{1}{C_2\ R_2}$

Thus it can be seen that the PLL transfer function $\theta_o/\theta_i(\omega)$ is a first order lowpass filter with a bandwidth of $k_o\ k_d$.R2/R1, provided that this bandwidth is much greater than the loop filter phase lead break point, $1/R_2\ C_2$.

APPENDIX D

MEASUREMENT OF THE CLOSED LOOP RESPONSE OF THE PLL

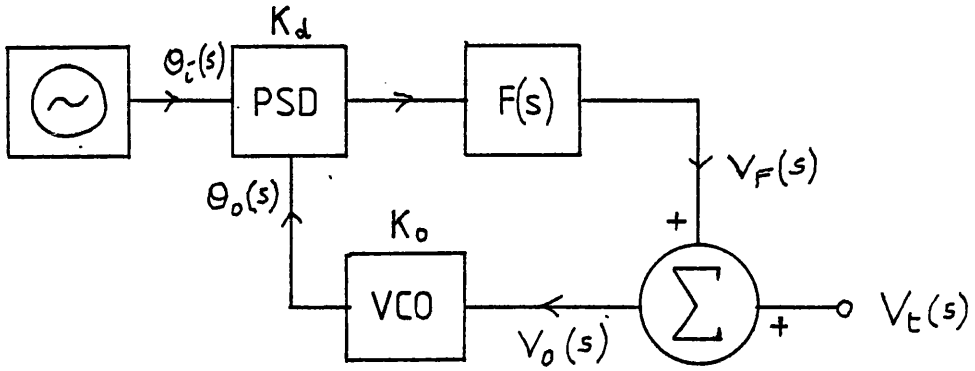

Since the input frequency is fixed:

$$\theta_i(s) = 0,$$

and:- $$V_f(s) = -k_d\, \theta_o(s)\, F(s)$$

$$= -k_d \frac{k_o}{s} V_o(s)\, F(s)$$

$$= \frac{-k_d\, k_o\, F(s)}{s} \left(V_f(s) + V_t(s)\right)$$

Hence:

$$V_f(s) \left[1 + \frac{k_d\, k_o\, F(s)}{s}\right] = - \frac{k_d\, k_o\, F(s)}{s} V_t(s)$$

and

$$\frac{V_f(s)}{V_t(s)} = - \frac{k_d\, k_o\, F(s)}{s + k_d\, k_o\, F(s)} = - \frac{\theta_o(s)}{\theta_i(s)}$$

Thus $\dfrac{V_f(s)}{V_t(s)}$ is the desired closed loop response.

APPENDIX E

FOURIER SERIES EXPANSION OF THE ERROR FUNCTION $\Delta(t)$, WHEN A TIMING ERROR EXISTS BETWEEN THE AMPLITUDE AND PHASE COMPONENTS

The amplitude error function $\Delta(t)$, is as shown in Figure E.1(c). Its Fourier series expansion is given by:-

$$\Delta(t) = \frac{1}{2} a_o + \sum_{n=1}^{\infty} (a_n \cos n\omega t + b_n \sin n\omega t) \qquad (E.1)$$

where $a_o = 0$, by inspection dc component is zero.

$$a_n = \frac{1}{\pi} \int_o^{2\pi} \Delta(t) \cos n\omega t \, d(\omega t)$$

$$b_n = \frac{1}{\pi} \int_o^{2\pi} \Delta(t) \sin n\omega t \, d(\omega t)$$

Since:- $\Delta(t) = 0$, for $\quad 0 < \omega t < \frac{\pi}{2}$

$$\text{and } \frac{\pi}{2} + \theta < \omega t < \frac{3\pi}{2}$$

$$\text{and } \frac{3\pi}{2} + \theta < \omega t < 2\pi$$

and, $\Delta(t) = \frac{V}{\theta} \left[\omega t - \frac{\pi}{2} \right]$ for $\frac{\pi}{2} < \omega t < \frac{\pi}{2} + \theta$

and, $\Delta(t) = \frac{-V}{\theta} \left[\omega t - \frac{3\pi}{2} \right]$ for $\frac{3\pi}{2} < \omega t < \frac{3\pi}{2} + \theta$

- assuming θ is small ($< 5^o$) then a_n and b_n can be evaluated as follows:-

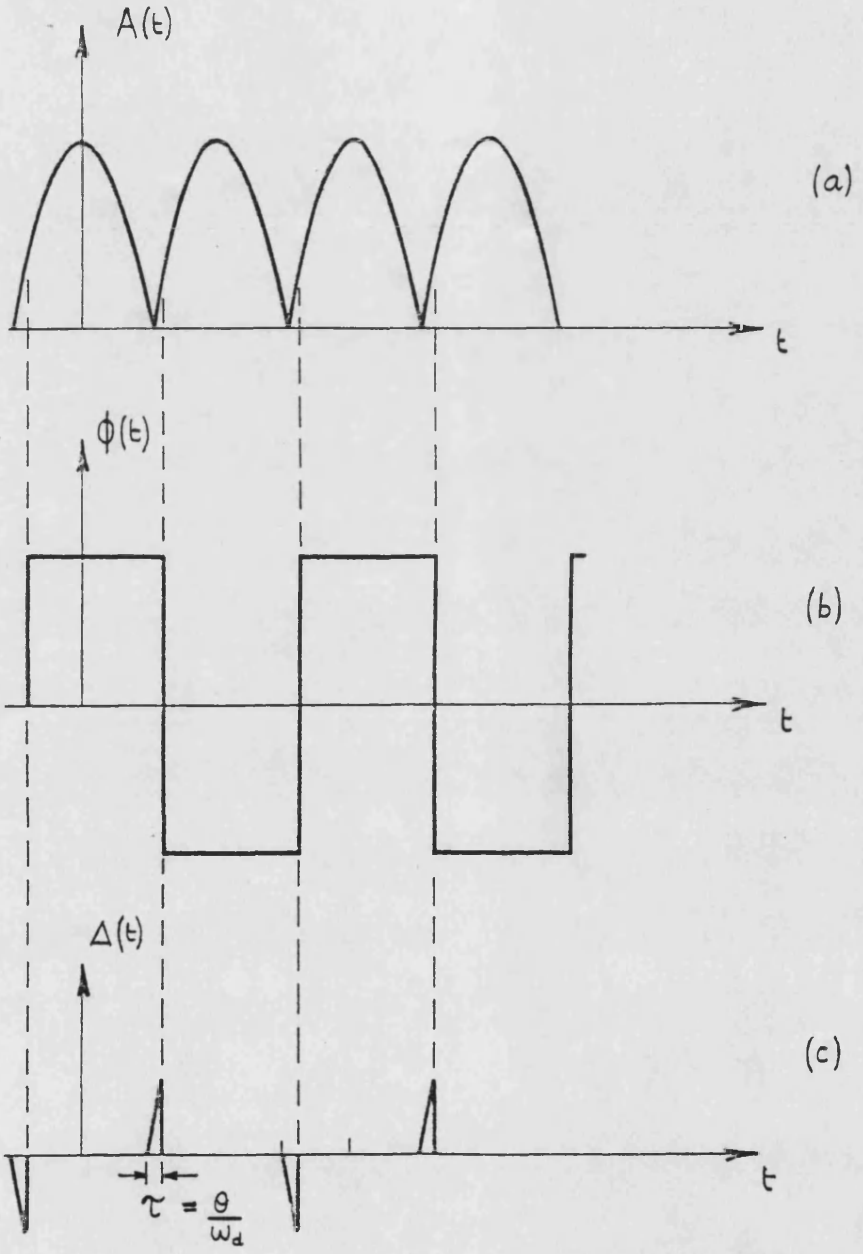

Figure E.1 : Timing Error between Amplitude and Phase Components

$$a_n = \frac{1}{\pi}\int_{\frac{\pi}{2}}^{\frac{\pi}{2}+\theta} \frac{V}{\theta}\left(\omega t - \frac{\pi}{2}\right) \cos n\omega t \, d(\omega t)$$

$$+ \frac{1}{\pi}\int_{\frac{3\pi}{2}}^{\frac{3\pi}{2}+\theta} -\frac{V}{\theta}\left(\omega t - \frac{3\pi}{2}\right) \cos n\omega t \, d(\omega t) \qquad \text{(E.2)}$$

$$= \frac{V}{\pi\theta}\left[\frac{1}{n}\left(\omega t - \frac{\pi}{2}\right) \sin n\omega t + \frac{1}{n^2}\cos n\omega t\right]_{\frac{\pi}{2}}^{\frac{\pi}{2}+\theta}$$

$$- \frac{V}{\pi\theta}\left[\frac{1}{n}\left(\omega t - \frac{3\pi}{2}\right) \sin n\omega t + \frac{1}{n^2}\cos n\omega t\right]_{\frac{3\pi}{2}}^{\frac{3\pi}{2}+\theta} \qquad \text{(E.3)}$$

$$= \frac{V}{\pi\theta}\left\{\left[\frac{1}{n}\left(\frac{\pi}{2} + \theta - \frac{\pi}{2}\right) \sin n\left(\frac{\pi}{2} + \theta\right) + \frac{1}{n^2}\cos n\left(\frac{\pi}{2} + \theta\right)\right]\right.$$

$$\left. -\left[\frac{1}{n}\,\frac{3\pi}{2} - \frac{3\pi}{2} \sin n\,\frac{3\pi}{2} + \frac{1}{n^2}\cos n\,\frac{3\pi}{2}\right]\right\} \qquad \text{(E.4)}$$

$$= \frac{V}{\pi\theta}\left[\frac{1}{n}\,\theta \sin n\left(\frac{\pi}{2} + \theta\right) + \frac{1}{n^2}\cos n\left(\frac{\pi}{2} + \theta\right) - \frac{1}{n^2}\cos n\,\frac{\pi}{2}\right]$$

$$- \frac{V}{\pi\theta}\left[\frac{1}{n} \sin n\left(\frac{3\pi}{2} + \theta\right) + \frac{1}{n^2}\cos n\left(\frac{3\pi}{2} + \theta\right) - \frac{1}{n^2}\cos n\,\frac{3\pi}{2}\right] \qquad \text{(E.5)}$$

$$= \frac{V}{n^2\pi\theta}\left[n\,\theta \sin n\left(\frac{\pi}{2} + \theta\right) - n\,\theta \sin n\left(\frac{3\pi}{2} + \theta\right)\right.$$

$$\left. + \cos n\left(\frac{\pi}{2} + \theta\right) - \cos n\left(\frac{3\pi}{2} + \theta\right)\right] \qquad \text{(E.6)}$$

$$= \frac{V}{n^2\pi\theta}\left[n\ \theta\ \sin n\left(\frac{\pi}{2}+\theta\right) + n\ \theta\ \sin n\left(\frac{\pi}{2}-\theta\right) + \cos n\left(\frac{\pi}{2}+\theta\right) - \cos n\left(\frac{\pi}{2}-\theta\right)\right] \qquad (E.7)$$

$$= \frac{2V}{n^2\pi\theta}\left[n\ \theta\ \sin n\frac{\pi}{2}\cos n\ \theta - \sin n\frac{\pi}{2}\sin n\ \theta\right] \qquad (E.8)$$

$$= \frac{2V}{n^2\pi\theta}\left[\sin n\frac{\pi}{2}\left(n\ \theta\ \cos n\ \theta - \sin n\ \theta\right)\right] \qquad (E.9)$$

$$b_n = \frac{1}{\pi}\int_{\frac{\pi}{2}}^{\frac{\pi}{2}+\theta}\frac{V}{\pi}\left(\omega t - \frac{\pi}{2}\right)\sin n\omega t\ d(\omega t) + \frac{1}{\pi}\int_{\frac{3\pi}{2}}^{\frac{3\pi}{2}+\theta} -\frac{V}{\theta}\left(\omega t - \frac{3\pi}{2}\right)\sin n\omega t\ d(\omega t) \qquad (E.10)$$

$$= \frac{V}{\pi\theta}\left[-\frac{1}{n}\left(\omega t - \frac{\pi}{2}\right)\cos n\omega t + \frac{1}{n^2}\sin n\omega t\right]_{\frac{\pi}{2}}^{\frac{\pi}{2}+\theta}$$

$$-\frac{V}{\pi\theta}\left[-\frac{1}{n}\left(\omega t - \frac{3\pi}{2}\right)\cos n\omega t + \frac{1}{n^2}\sin n\omega t\right]_{\frac{3\pi}{2}}^{\frac{3\pi}{2}+\theta} \qquad (E.11)$$

$$= \frac{V}{\pi\theta}\left\{\left[-\frac{1}{n}\left(\frac{\pi}{2}+\theta-\frac{\pi}{2}\right)\cos n\left(\frac{\pi}{2}+\theta\right) + \frac{1}{n^2}\sin n\left(\frac{\pi}{2}+\theta\right)\right]\right.$$

$$-\left[-\frac{1}{n}\left(\frac{\pi}{2}-\frac{\pi}{2}\right)\cos n\frac{\pi}{2}+\frac{1}{n^2}\sin n\frac{\pi}{2}\right]\Bigg\}$$

$$-\frac{V}{\pi\theta}\Bigg\{\left[-\frac{1}{n}\left(\frac{3\pi}{2}+\theta-\frac{3\pi}{2}\right)\cos n\left(\frac{3\pi}{2}+\theta\right)+\frac{1}{n^2}\sin n\left(\frac{3\pi}{2}+\theta\right)\right]$$

$$-\left[-\frac{1}{n}\left(\frac{3\pi}{2}-\frac{3\pi}{2}\right)\cos n\frac{3\pi}{2}+\frac{1}{n^2}\sin n\frac{3\pi}{2}\right]\Bigg\} \qquad \text{(E.12)}$$

$$=\frac{V}{\pi\theta}\left[-\frac{\theta}{n}\cos n\left(\frac{\pi}{2}+\theta\right)+\frac{1}{n^2}\sin n\left(\frac{\pi}{2}+\theta\right)-\frac{1}{n^2}\sin n\frac{\pi}{2}\right]$$

$$-\frac{V}{\pi\theta}\left[-\frac{\theta}{n}\cos n\left(\frac{3\pi}{2}+\theta\right)+\frac{1}{n^2}\sin n\left(\frac{3\pi}{2}+\theta\right)-\frac{1}{n^2}\sin n\frac{3\pi}{2}\right]$$

(E.13)

$$=\frac{V}{n^2\pi\theta}\Bigg[-n\theta\cos n\left(\frac{\pi}{2}+\theta\right)+n\theta\cos n\left(\frac{3\pi}{2}+\theta\right)$$

$$+\sin n\left(\frac{\pi}{2}+\theta\right)-\sin n\left(\frac{3\pi}{2}+\theta\right)$$

$$-\sin n\frac{\pi}{2}+\sin n\frac{3\pi}{2}\Bigg] \qquad \text{(E.14)}$$

$$=\frac{V}{n^2\pi\theta}\Bigg[-n\theta\cos n\left(\frac{\pi}{2}+\theta\right)+n\theta\cos n\left(\frac{\pi}{2}-\theta\right)$$

$$+\sin n\left(\frac{\pi}{2}+\theta\right)+\sin n\left(\frac{\pi}{2}-\theta\right)$$

$$-\sin n\frac{\pi}{2}-\sin n\frac{\pi}{2}\Bigg] \qquad \text{(E.15)}$$

$$= \frac{2V}{n^2\pi\theta}\left[n\ \theta\ \sin n\frac{\pi}{2}\sin n\ \theta + \sin n\frac{\pi}{2}\cos n\ \theta - \sin n\frac{\pi}{2}\right]$$

(E.16)

$$= \frac{2V}{n^2\pi\theta}\left[\sin n\frac{\pi}{2}\left(n\ \theta\ \sin n\ \theta + \cos n\ \theta - 1\right)\right] \qquad \text{(E.17)}$$

The error function $\Delta(t)$ may now be written as:-

$$\Delta(t) = \frac{2V}{\pi\theta}\sum_{n=1}^{\infty}\frac{\sin n\frac{\pi}{2}}{n^2}\left[\left(n\ \theta\ \cos n\ \theta - \sin n\ \theta\right)\cos n\frac{\omega_d t}{2} + \left(n\ \theta\ \sin n\ \theta + \cos n\ \theta - 1\right)\sin n\frac{\omega_d t}{2}\right] \qquad \text{(E.18)}$$

Writing, $X = n\ \theta\ \cos n\ \theta - \sin n\ \theta$

and, $Y = n\ \theta\ \sin\theta + \cos n\ \theta - 1$

$\Delta(t)$ becomes:-

$$\Delta(t) = \frac{2V}{\pi\theta}\sum_{n=1}^{\infty}\frac{\sin n\frac{\pi}{2}}{n^2}\left(X\cos n\frac{\omega_d t}{2} + Y\sin n\frac{\omega_d t}{2}\right) \qquad \text{(E.19)}$$

The amplitude of $\Delta(t)$ may be expressed in terms of the amplitude component $A(t)$. Referring to Figure E.1:-

$$V = 2 \times 2\ A\sin\theta$$

$$\doteq 4\ A\sin\theta \qquad \text{(E.20)}$$

Hence:-

$$\Delta(t) = \frac{8A\sin\theta}{\pi\theta}\sum_{n=1}^{\infty}\frac{\sin n\frac{\pi}{2}}{n^2}\left(X\cos n\frac{\omega_d t}{2} + Y\sin n\frac{\omega_d t}{2}\right)$$

(E.21)

APPENDIX F

FOURIER SERIES EXPANSION OF THE ERROR FUNCTION $\ell(t)$ REPRESENTING A LOSS OF SIGNAL DUE TO LIMITER THRESHOLD

The limiter threshold error function $\ell(t)$ is shown in Figure F.1. It may be expanded as a Fourier series as follows:-

By inspection, the d.c. component is zero, and since the function is odd, it contains sine terms only. Hence:-

$$\ell(t) = \sum_{n=1}^{\infty} b_n \sin n\omega t \qquad \text{(F.1)}$$

and, $$b_n = \frac{1}{\pi} \int_{-\pi}^{\pi} \ell(t) \sin n\omega t \, d(\omega t)$$

$$= \frac{2}{\pi} \int_{0}^{\pi} \ell(t) \sin n\omega t \, d(\omega t) \qquad \text{(F.2)}$$

$$= \frac{2}{\pi} \int_{0}^{\theta} -\frac{V_t}{\theta} \omega t \sin n\omega t \, d(\omega t) + \frac{2}{\pi} \int_{\pi-\theta}^{\pi} -\frac{V_t}{\theta}(\pi-\omega t) \sin n\omega t \, d(\omega t) \qquad \text{(F.3)}$$

$$= \frac{-2V_t}{\pi\theta} \int_{0}^{\theta} \omega t \sin n\omega t \, d(\omega t) - \int_{\pi-\theta}^{\theta} (\omega t-\pi) \sin n\omega t \, d(\omega t) \qquad \text{(F.4)}$$

$$= \frac{-2V_t}{\pi\theta} \left\{ \left[-\frac{\omega t \cos n\omega t}{n} + \frac{\sin n\omega t}{n^2} \right]_0^{\theta} - \left[-\frac{(\omega t-\pi) \cos n\omega t}{n} + \frac{\sin n\omega t}{n^2} \right]_{\pi-\theta}^{\pi} \right\} \qquad \text{(F.5)}$$

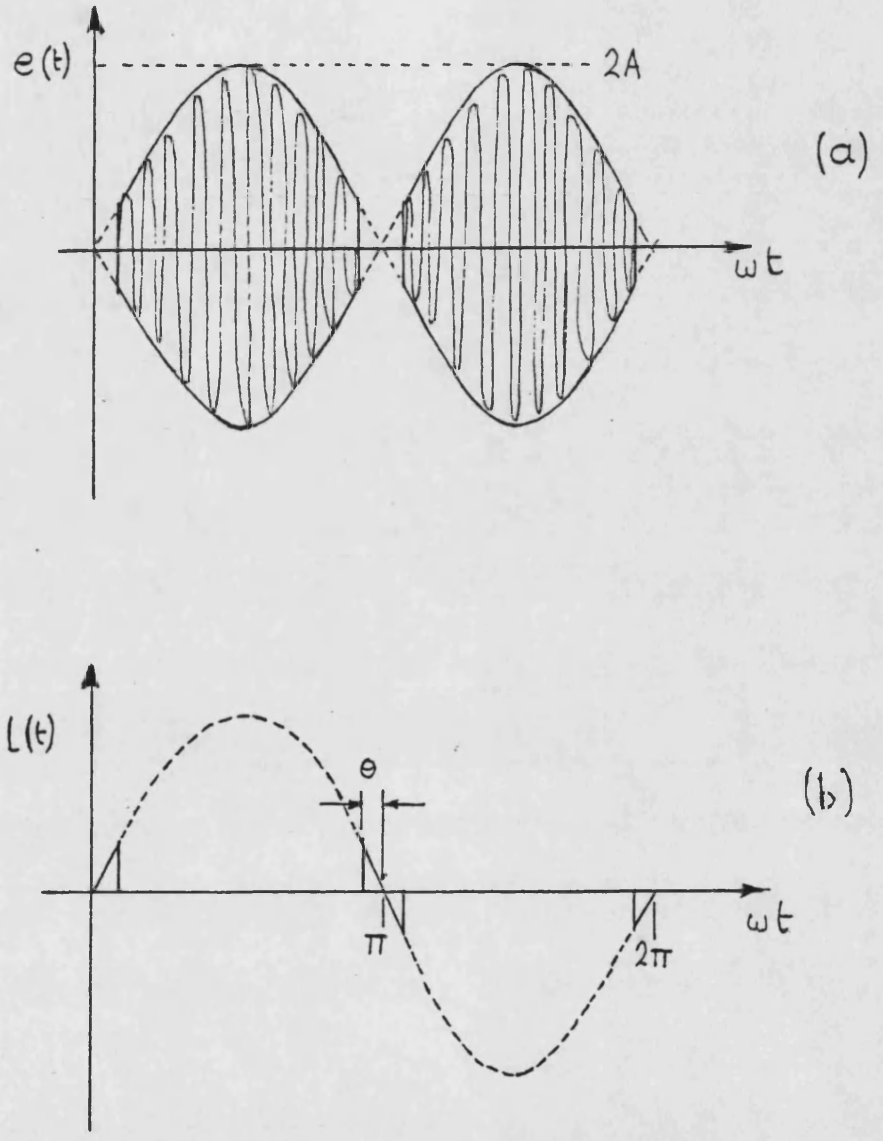

Figure F.1 : Effect of Limiter Threshold showing Error Function

$$= \frac{2V_t}{\pi\theta}\left\{\left[-\frac{\theta\cos n\theta}{n} + \frac{\sin n\theta}{n^2}\right] + \left[\frac{\theta\cos n(\pi-\theta)}{n} + \frac{\sin n(\pi-\theta)}{n^2}\right]\right\} \quad \text{(F.6)}$$

$$= \frac{2V_t}{\pi\theta n^2}\left\{-n\theta\cos n\theta + \sin n\theta + n\theta\cos n(\pi-\theta) + \sin n(\pi-\theta)\right\} \quad \text{(F.7)}$$

$$= \frac{2V_t}{\pi\theta n^2}(-n\theta\cos n\theta + \sin n\theta + n\theta\cos n\theta\cos n\pi - \sin n\theta\cos n\pi) \quad \text{(F.8)}$$

$$= \frac{2V_t}{\pi\theta n^2}(1-\cos n\pi)(\sin n\theta - n\theta\cos n\theta) \quad \text{(F.9)}$$

$$= \frac{4V_t}{\pi\theta n^2}(\sin n\theta - n\theta\cos n\theta),\ n \text{ odd}$$

$$= 0,\ n \text{ even.} \quad \text{(F.10)}$$

Since $V_t = 2A\sin\theta$, then:-

$$b_n = \frac{8A\sin\theta}{\pi\theta n^2}(\sin n\theta - n\theta\cos n\theta) \quad \text{(F.11)}$$

and:-

$$\ell(t) = \frac{8A\sin\theta}{\pi\theta n^2}\sum_{n=1}^{\infty}(\sin n\theta - n\theta\cos n\theta)\sin n\frac{\omega_d t}{2} \quad \text{(F.12)}$$

APPENDIX G

EFFECT OF LOAD IMPEDANCE CHANGE ON THE FREQUENCY OF A COLPITTS OSCILLATOR

A grounded gate Colpitts oscillator may be represented by the equivalent circuit shown below:-

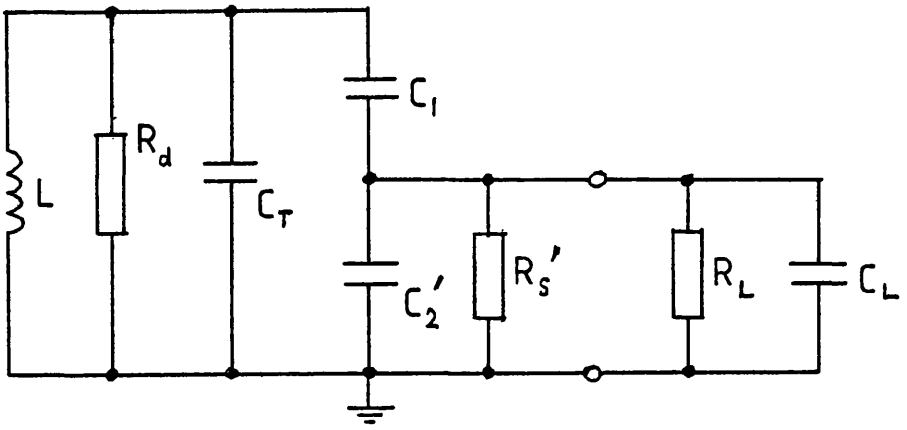

Let $R_s = R_s' // R_L$

and $C_2 = C_2' // C_L$

The admittance connected in parallel with the inductance is given by:-

$$G + j\omega C_{TOT} = \frac{1}{R_d} + j\omega C_T + \frac{1}{\left(\frac{1}{j\omega C_1} + \frac{R_s}{1 + j\omega C_2 R_s}\right)} \qquad (G.1)$$

$$= \frac{1}{R_d} + j\omega C_T + \frac{j\omega C_1(1 + j\omega C_2 R_s)}{1 + j\omega(C_1 + C_2)R_s} \qquad (G.2)$$

Rationalising gives the capacitive part as:

$$C_{TOT} = C_T + \frac{C_1[1 + \omega^2 C_2(C_1 + C_2)R_s^2]}{1 + \omega^2(C_1 + C_2)^2 R_s^2} \qquad (G.3)$$

Differentiating with respect to C_2 gives:-

$$\frac{dC_{TOT}}{dC_2} = \frac{\left\{\begin{array}{l}[1 + \omega^2(C_1 + C_2)^2R_s^2]C_1\omega^2R_s^2(C_1 + 2C_2) \\ - C_1[1 + \omega^2C_2(C_1 + C_2)R_s^2]\omega^2R_s2(C_1 + C_2)\end{array}\right\}}{[1 + \omega^2(C_1 + C_2)^2R_s^2]^2} \qquad (G.4)$$

$$= \frac{\omega^2R_s^2C_1^2[\omega^2R_s^2(C_1 + C_2)^2 - 1]}{[1 + \omega^2(C_1 + C_2)^2R_s^2]^2} \qquad (G.5)$$

Differentiating with respect to R_s gives:-

$$\frac{dC_{TOT}}{dR_s} = \frac{\left\{\begin{array}{l}[1 + \omega^2(C_1 + C_2)^2R_s^2]\omega^2C_2(C_1 + C_2)2R_sC_1 \\ - C_1[1 + \omega^2C_2(C_1 + C_2)R_s^2]\omega^2(C_1 + C_2)^2 2R_s\end{array}\right\}}{[1 + \omega^2(C_1 + C_2)^2R_s^2]^2} \qquad (G.6)$$

$$= \frac{-2\omega^2R_sC_1^2(C_1 + C_2)}{[1 + \omega^2(C_1 + C_2)^2R_s^2]^2} \qquad (G.7)$$

Since $C_2 = C_2' + C_L$

$$\Rightarrow \frac{dC_2}{dC_L} = 1$$

And since $R_s = \frac{R_s'R_L}{R_s' + R_L}$ (G.8)

$$\Rightarrow \frac{dR_s}{dR_L} = \left[\frac{R_s'}{R_s' + R_L}\right]^2 \qquad (G.9)$$

Hence:-

$$\frac{dC_{TOT}}{dC_L} = \frac{\omega^2 R_s^2 C_1^2 [\omega^2 R_s^2 (C_1 + C_2)^2 - 1]}{[1 + \omega^2 (C_1 + C_2)^2 R_s^2]^2} \qquad (G.10)$$

and

$$\frac{dC_{TOT}}{dR_L} = \left[\frac{R_s'}{R_s' + R_L}\right]^2 \cdot \left[\frac{-2\omega^2 R_s C_1^2 (C_1 + C_2)}{[1 + \omega^2 (C_1 + C_2)^2 R_s^2]^2}\right] \qquad (G.11)$$

The resonant frequency of the tuned circuit is given by:-

$$\omega_o = \frac{1}{\sqrt{LC_{TOT}}} = (LC_{TOT})^{-\frac{1}{2}} \qquad (G.12)$$

Hence:- $$\frac{d\omega_o}{dC_{TOT}} = L^{-\frac{1}{2}} \cdot \frac{-1}{2} C_{TOT}^{-\frac{3}{2}} = \frac{-\omega_o}{C_{TOT}} \qquad (G.13)$$

Thus the change in resonant frequency with load capacitance or load resistance change can be written:-

$$\frac{d\omega_o}{dC_L} = \frac{-\omega_o^3 R_s^2 C_1^2 [\omega_o^2 R_s^2 (C_1 + C_2)^2 - 1]}{2C_{TOT}[1 + \omega_o^2 (C_1 + C_2)^2 R_s^2]^2} \qquad (G.14)$$

and

$$\frac{d\omega_o}{dR_L} = \frac{\omega_o^3 R_s (R_s')^2 C_1^2 (C_1 + C_2)}{C_{TOT}(R_s' + R_L)^2 [1 + \omega_o^2 (C_1 + C_2)^2 R_s^2]^2} \qquad (G.15)$$

For a typical UHF Colpitts oscillator operating at 450MHz, the component values in the above expressions would be:-

ω_o = $2 \cdot 9.10^9$ r/s

R_s' = 63Ω

R_L = 300Ω

R_s = 52Ω

C_1 = 12pF

C_2 = 12pF

C_{TOT} = 12pF

Which gives:-

$$\frac{d\omega_o}{dC_L} = 2{\cdot}4.10^{19} \text{ r/s/F} \quad = \quad 3{\cdot}8\text{MHz/pF}$$

$$\frac{d\omega_o}{dR_L} = 5{\cdot}5.10^{4} \text{ r/s/}\Omega \quad = \quad 8{\cdot}8\text{KHz/}\Omega$$

REFERENCES

1. Brinkley, J.R., '12.5KHz Channel Spacing for Mobile Communications in the UHF band between 420 and 512MHz', The Radio and Electronic Engineer, June 1971.
2. Pinches, M.C., King, R.D., 'The potential for further reduction in channel spacing in the VHF band', IEE Conf. Proc. Communications, 76.
3. Cooper, G.R., Nettleton, R.W., 'Cellular mobile technology : the great multiplier', IEEE Spectrum, June 1983.
4. PACTEL and PATS CENTRE International, 'Future Mobile Communications Services in Europe', Report to the Eurodata Foundation on Systems and Opportunities for Services to the Year 2000, Sept. 1981.
5. Carson, J.R., U.S. Patents: 1449382, 1343306, 1343307, 1915.
6. White, I.F., 'Single Sideband Telephony on the VHF and UHF Amateur Bands', Proc. IERE Conf. on Land Mobile Radio, Lancaster, Sept. 1979.
7. Oswald, A.A., 'A Short Wave Single Sideband Radio Telephone System', Proc. IRE, Dec. 1938.
8. Wells, R., 'SSB for VHF Mobile Radio at 5KHz Channel Spacing', Communications, Dec. 1978.
9. Gosling, W. *et al*, 'Receiver for the Wolfson SSB/VHF Land Mobile System', IERE Conf. Proc. Radio Receivers and Associated Systems, July 1978.
10. Lusignan, B., 'The Use of Amplitude Compandored SSB in the Mobile Radio Bands', FCC Tech. Report, No.29, July 1980.

11. Wells, R., 'The Application of Single Sideband Modulation in the 450MHz and 960MHz Land Mobile Bands', IERE Conf. Proc. on Radio Receivers and Associated Systems, 1979.

12. Gosling, W., 'Synchronous SSB in Land Mobile Radio', Communications International, May 1979.

13. Garner, P.J., 'Co-channel and Quasi-synchronous Characteristics of SSB relative to FM in Mobile Radio Communications', IEE Conf. Proc. Comms., 1980.

14. Magnuski, H., Firestone, W., 'Comparison of SSB and FM for the VHF Mobile Service', Proc. IRE, Dec. 1956.

15. Richardson, R., Eness, O., Dronsuth, R., 'Experience with SSB Mobile Equipment', Proc. IRE, June 1957.

16. Gibson, R.W., Wells, R., 'The Potential of SSB for Land Mobile Radio', Proc. 29th IEEE Vehicular Technology Conf., March 1979.

17. Wells, R., 'SSB Modulation for VHF Mobile and Handportable Transeivers', Electronics and Power, Sept. 1981.

18. Flett, A., 'Adjacent Channel Performance of FM, AM and SSB at VHF', IEE Conf. Proc. Comms., 1978.

19. Bruene, W.B., 'Linear Power Amplifier Design', Proc. IRE, Dec. 1956.

20. Bennet, T.J., Clements, R.F., 'Feedforward - An Alternative Approach to Amplifier Linearisation', Radio and Electronic Engineer, May 1974.

21. Petrovic, V., 'A High Efficiency VHF SSB Transmitter', IERE Conf. on Civil Land Mobile Radio, Teddington, Nov. 1975.

22. Lubell, P.D., Denniston, W.B., Hertz, R.F., 'Linearising

Amplifiers for Multi-Signal Use', Microwaves, April 1974.

23. Recommendations and Reports of the CCIR, 1978, Volume 1, Spectrum Utilisation and Monitoring (p.327).

24. Dept. of Trade and Industry, Radio Regulatory Dept., Performance Spec., Angle Modulated VHF and UHF radio equipment for use at base and mobile stations in the Private Mobile Radio Service, MPT 1301.

25. Dept. of Trade and Industry, Radio Regulatory Dept., Performance Spec., Amplitude Modulated VHF radio equipment for use at base and mobile stations in the Private Mobile Radio Service.

26. Rockwell, W.E., 'Reduction of Intermodulation Products in Single Sideband Transmitters', M.Eng. Thesis, Nova Scotia Tech. Coll., Feb. 1969.

27. Kurokawa, T., Matsuzaki, O., Doi, M., 'Intermodulation Interference Compensation', NEC Res. and Dev. (Japan), April 1980.

28. Hecker, R.P., Heidt, R.C., 'Predistortion linearisation of the AR6A transmitter', IEEE Conf. Proc. ICC 80.

29. Nojima, T., Okamoto, Y., 'Predistortion Non-linear Compensator for microwave SSB-AM System', IEEE Conf. Proc. ICC 80.

30. Sato, G., 'A lineariser for satellite communications', IEEE Conf. Proc. ICC 80.

31. Gray, L.F., 'Application of broadband linearisers to satellite transponders', IEEE Conf. Proc. ICC 80.

32. Welti, G.R., 'Application of predistortion linearisers to satellite transponders', IEEE Conf. Proc. ICC 80.

33. Holbrook, G.W., 'Reducing amplifier distortion', Electronic Technology, Jan. 1960.

34. Behrend, W.L., 'Pre-Phase Modulation to Compensate for Incidental PM in an AM transmitter', RCA Tech. Note 1256, Sept. 1980.

35. Black, H.S., 'Translating System', U.S. Patent No.1686792, Oct. 1928.

36. Seidel, H., Beurrier, H.R., Friedman, A.N., 'Error controlled High Power Linear Amplifiers at VHF', Bell System Tech. Jnl., May and June 1968.

37. Seidel, H., 'A Feedforward Experiment applied to an L-4 Carrier System Amplifier', IEEE Trans. Comm. Tech., June 1971.

38. Meyer, R.G., Eschenbach, R., Edgerley, W.M., 'A wideband feedforward amplifier', IEEE Jnl. Solid State Ccts., Dec. 1974.

39. Black, H.S., 'Wave Translation System', U.S. Patent 2102671, Dec. 1937.

40. Black, H.S., 'Stabilised Feedback Amplifiers', Bell Sys. Tech. Jnl., Jan. 1934.

41. U.K. Patent No.323823, 'Improvements in or relating to Arrangements of Amplifying Electrical Oscillations', Jan. 1930.

42. Nyquist, H., 'Regneration Theory', Bell Sys. Tech. Jnl., July 1932.

43. Bruene, W.B., 'Distortion Reducing means for SSB Transmitters', Proc. IRE, Dec. 1956.

44. Bruene, W.B., 'Linear power amplifier for SSB transmitters',

Electronics, Aug. 1955.

45. Mitchell, A.F., 'A 135MHz feedback amplifier', IEE Colloq. Broadband high frequency amplifiers, Nov. 1979.

46. Leypold, D., Leyseiffer, H., Grunow, H.K., 'Development problems of radio relay systems using SSB modulation', NTZ Journal, 1965, No.2

47. Schelleng, J.C., 'Method and Means for Electric Energy Translation', U.S. Patent No.1534287, April 1925.

48. Heising, R.A., U.S. Patent No.1442146, Jan. 1923.

49. Poppele, J.R., Cunningham, F.W., Kishpaugh, A.W., 'Design and Equipment of a 50KW Broadcast Station for WOR', Proc. IRE, Aug. 1936.

50. Terman, F.E., Buss, R.R., 'Some notes on linear and grid modulated radio frequency amplifiers', Proc. IRE, March 1941.

51. Arthanayake, T., Wood, H.B., 'Linear amplification using envelope feedback', Elec. Lett., 8th April 1971.

52. Warren, G., 'Application of the Polar Loop Technique to HF SSB Transmitters', Ph.D. Thesis, University of Bath, 1983.

53. Bradshaw, D.B., 'Improvements in or relating to high frequency power amplifier arrangements', U.K. Patent No. 1246209, Sept. 1971.

54. Raob, F.H., 'High efficiency amplification techniques', IEEE Ccts and Systems Jnl., Dec. 1975.

55. Petrovic, V., Gosling, W., 'Polar Loop Transmitter', Elec. Lett., 10th May 1979.

56. Kahn, L.R., 'SSB transmission by envelope elimination and

restoration', Proc. IRE, July 1952.

57. Kahn, L.R., 'Comparison of linear SSB transmitters with envelope elimination and restoration SSB transmitters', Proc. IRE, Dec. 1956.

58. Warren, G., Petrovic, V., Gosling, W., 'Application of the polar loop technique to HF SSB transmitters', Proc. IEE Conf. Radio transmitters and modulation techniques, 1980.

59. Petrovic, V., Gosling, W., 'A radically new approach to SSB transmitter design', Proc. IEE Conf. Radio transmitters and modulation techniques, 1980.

60. Petrovic, V., Smith, C.N., 'The design of VHF SSB polar loop transmitters', IEE Conf. Proc. Comms. 1982.

61. Kaya, E., 'Computer Modelling of the Polar Loop Transmitter', Ph.D. Thesis, University of Bath, to be published.

62. Petrovic, V., Gosling, W., 'Design of a High Efficiency VHF Double Sideband Diminished Carrier Transmitter having Low Spurious Emission', Proc. IEE, 1974, 121, (2).

63. Utsi, Y., 'Phase noise in phase locked loops', Proc. IEE Colloq. on Phase Locked Techniques, March 1980.

64. Barnett, R.J., Long, T.J., Windram, M.D., 'Synthesiser phase noise and its effects in broadcasting systems', IERE Conf., Radio Receivers and Associated Systems, July 1981.

65. Manassewitsch, V., 'Frequency Synthesisers, Theory and Design', John Wiley, 1976.

66. Egan, W.F., 'Frequency Synthesis by Phase Lock', John Wiley, 1981.

67. Alley, G.D., Wang, H.C., 'An Ultra low noise Microwave Synthesiser', IEEE Trans. MTT, Dec. 1979.

68. Mospower FET Databook, Siliconix.

69. Gardner, F.M., 'Angle Modulation limits of a noise free phase locked loop', IEEE Trans. Comm, Aug. 1978.

70. Surana, D.C., Gardiner, J.G., 'Gain and Distortion properties of FET Mixers and Modulators', IEEE Trans. Electromag. Compat. Feb. 1974.

71. Surana, D.C., Gardiner, J.G., 'Calculation of Intermodulation distortion levels in FET Mixers and Modulators', Elec. Lett., 22nd April 1971.

72. Cheung, W.N., 'Analysis of an FET Amplitude Modulator', Elec. Eng., July 1969.

73. Cheung, W.N., 'Design and performance of an FET balanced modulator', Int. Jnl. Electronics, April 1979.

74. Kim, L.T., 'Design of a transistor modulator', Telecomm. and Radio Eng., Part 1, Sept. 1969.

75. Venkateswarlu, V., Sonde, B.S., 'A micropower amplitude modulator', Proc. IEEE, July 1971.

76. Matsushita, I., Namura, H., 'Broadband transistor modulators', Fuyitsu Sci. and Tech. Jnl., March 1969.

77. Petrovic, V., Gosling, W., 'VHF/AM transmitter using VMOS technology', Elec. Eng., June 1978.

78. H.P. Application Note 922 'Application of PIN Diodes'.

79. Grivet, P., Blaquiere, A., 'Nonlinear effects of noise in electronic clocks', Proc. IEEE, Nov. 1963.

80. Lindsey, W.C., Chei, C.M., 'Theory of oscillator instability based upon structure functions', Proc. IEEE, Dec. 1976.

81. Johnson, S.L., Smith, B.H., Calder, D.A., 'Noise spectrum characteristics of low noise microwave tubes and solid state devices', Proc. IEEE, Feb. 1966.

82. Baghdady, E.J., Lincoln, R.N., Nelin, B.D., 'Short term frequency stability : Characterisation, Theory and Measurements', Proc. IEEE, July 1965.

83. Edson, W.A., 'Noise in oscillators', Proc. IRE, Aug. 1960.

84. Malling, L.R., 'Phase stable oscillators for space communications', Proc. IRE, July 1962.

85. Leeson, D.B., 'A simple model of a feedback oscillator spectrum', Proc. IEEE, Feb. 1966.

86. Leeson, D.B., 'Short term stable microwave sources', Mic. Jnl., June 1970.

87. Frerking, M.E., 'Crystal oscillator design and temperature compensation', Van Nostrand Reinhold.

88. Stanesby, H., Fryer, P.W., 'Variable frequency crystal oscillators', Jnl. IEE, Part IIIa, 1947.

89. Garner, P.J., 'Voltage controlled crystal oscillators', Proc. IERE Conf., Radio Receivers and Associated Systems, 1978.

90. Rayleigh, Lord, 'On waves propagated along the plane surface of an elastic solid', Proc. London Math. Soc., 1885, pp.4-11.

91. White, R.M., Voltmer, F.W., 'Direct piezoelectric coupling to surface elastic waves', Applied Physics Lett., 15th Dec. 1965.

92. Joseph, T.R., 'Saw oscillators for phase locked applications, Proc. 31st Annual Freq. Control Symp., June 1977.

93. Gratze, S.C., 'The development of surface acoustic wave oscillators', Elec. Eng., April 1977.

94. Underhill, M.J., 'Comparison of the noise performance of some oscillators for tuneable receivers', Proc. IERE Conf., Radio Receivers and Ass. Sys., 1978.

95. Slobodnik, A.J., 'Surface acoustic waves and SAW materials', Proc. IEEE, May 1976.

96. Bell, D.J., Li, R.C.M., 'Surface acoustic wave resonators', Proc. IEEE, May 1976.

97. Ragan, L.H., 'Voltage controlled surface wave resonator oscillators', 1976 Ultrasonics Symposium (IEEE).

98. Vandewege, J., *et al*, 'Acoustic surface wave resonators for broadband applications', 8th Eur. Mic. Conf., 1978.

99. Cross, P.S., Haydl, W.H., Smith, R.S., 'Design and applications of 2-port SAW resonators on YZ-Lithium Niobate', Proc. IEEE, May 1976.

100. Harvey, A.F., 'Microwave Engineering', Academic Press, 1963, London and N.Y.

101. Helszajn, J., 'Principles of Microwave Ferrite Engineering', John Wiley, 1969.

102. Liao, S.Y., 'Microwave Devices and Circuits', Prentice-Hall, 1980.

103. Argence, E., Kahan, T., 'Theory of waveguides and cavity resonators', Blackie, 1967.

104. Muchmore, R.B., 'Essentials of microwaves', John Wiley, 1960.

105. Okaya, A., Barash, L.F., 'The dielectric microwave resonator', Proc. IRE, Oct. 1962.

106. Verplanken, M., Van Bladell, J., 'Resonances of a pillar-box dielectric resonator', 8th Eur. Mic. Conf., 1978.

107. Suter, W.A., 'Squaring off with dielectric resonators', Microwaves, Aug. 1981.

108. Pate, G., Roberts, R., 'Say hello to the DSO', Microwaves, May 1981.

109. Wheeler, H.A., 'Transmission line properties of parallel strips separated by a dielectric sheet', IEEE Trans. MTT, June 1968.

110. Sobol, H., 'Extending IC technology to microwave equipment', Electronics, March 1967.

111. Pucel, R.A., Masse, D.J., Harting, C.P., 'Losses in microstrip', IEEE Trans. MTT, June 1968.

112. Lampkin, G.F., 'An improvement in constant frequency oscillators', Proc. IRE, March 1939.

113. Gardner, F.M., 'Phaselock Techniques', John Wiley, 1979.

114. Stewart, J.L., 'Frequency modulation noise in oscillators', Proc. IRE, March 1956.

115. Chireix, H., 'High power outphasing modulation', Proc. IRE, Nov. 1935.

116. Gardner, F.M., 'Hang-up in PLLs', IEEE Trans, COMM, Oct. 1977.

117. Corrington, M.S., 'Frequency Modulation Distortion caused by Common and Adjacent Channel Interference, RCA Review, Vol.7, Dec. 1946.

118. Petrovic, V., Smith, C.N., 'Reduction of intermodulation distortion by means of modulation feedback', IEE Colloq., Intermodulation - Causes, Effects and Mitigation, April 1984.